UNIVERSITY OF OKLAHOMA

GRADUATE COLLEGE

EXPLORING THE CELLULAR EFFECTS OF SMALL MOLECULE INHIBITORS OF OXYSTEROL-BINDING PROTEIN

A DISSERTATION

SUBMITTED TO THE GRADUATE FACULTY

in partial fulfillment of the requirements for the

Degree of

DOCTOR OF PHILOSOPHY

By

BRETT ROBERTS
Norman, Oklahoma
2018

EXPLORING THE CELLULAR EFFECTS OF SMALL MOLECULE INHIBITORS OF

OXYSTEROL-BINDING PROTEIN

A DISSERTATION APPROVED FOR THE
DEPARTMENT OF CHEMISTRY AND BIOCHEMISTRY

BY

Dr. Anthony Burgett, Chair

Dr. Christina Bourne

Dr. Shaorong Liu

Dr. John P. Masly

Dr. Susan Schroeder

To my loving fiancé, you have been the glue that has held us together throughout this entire experience. Without your sturdiness, none of this would have been possible. I dedicate this dissertation to you, and promise it will bring us closer to the dream we both hold in our hearts. So let us look forward to better birds, bugs, and beer.

Acknowledgements

I would like to thank the Burgett research group for their various contributions to the work outlined in this dissertation. Many thanks to Zachary Severance and Ryan Bensen for your research contributions throughout Chapters 2-4. To Ahn McClain and Cori Malinky, thank you for your contributions in synthesizing some of the molecules used within this work. Thanks to Dr. Juan Nuñez for his contribution in the further development of the radioactive binding assay used in our research. I would also like to extend much thanks to Dr. Naga Rama Kothapalli for her guidance throughout the years.

Thanks are needed for Hongyan Ma in Dr. Si Wu's lab and Shawna Standke in Dr. Zhibo Yang's lab for their work on the analytic mass spectrometry aspect of the projects. Thanks to Dr. Tingting Gu of the Samuel Roberts Noble Microscopy Laboratory for teaching me how to acquire and analyze micrographs. To Jarrod King, thank you for your help in acquiring the Operetta images. I would also like to thank Dr. Earl Blewett for his work in conducting the viral experiments outlined in this work and for teaching me various virology techniques.

Thanks are also needed to the various professors that have allowed the use of their equipment to me throughout the course of my degree: Dr. Christina Bourne, Dr. Robert Cichewicz, Dr. Adam Duerfeldt, Dr. Shaorong Liu, Dr. Paul Sims, Dr. Ann West, and Dr. Si Wu.

Finally, I would like to thank my committee for their support.

Table of Contents

Acknowledgements v

List of Tables xiii

List of Figures xiv

Abstract xviii

Chapter 1: Introduction to the Oxysterol-binding Proteins 1

1.1 Overview 1

1.2 Oxysterols as ligands for the OSBP/ORPs 1

1.3 OSBP/ORP biology 7

1.3.1 OSBP 7

1.3.2 ORP4 11

1.3.3 Subfamily II: ORP1 and ORP2 15

1.3.4 Subfamily III: ORP3, ORP6, and ORP7 16

1.3.5 Subfamily IV: ORP5 and ORP8 17

1.3.6 Subfamily V: ORP9 18

1.3.7 Subfamily VI: ORP10 and ORP11 18

1.4 OSBP/ORP Disease Relevance 19

1.4.1 OSBP Function in Virus Replication 19

1.4.2 Cancer Cell Survival and Proliferation 24

1.5 ORPphillins and OSBP/ORP4 25

1.5.1 OSW-1 25

1.5.2 Schweinfurthins 26

1.5.3 Cephalostatin 1 and Ritterazine B 28
1.5.4 Itraconazole 29
1.5.5 Minor Enviroxime-like Compounds 30
1.6 Small Molecule Drug Targets 32
1.6.1 Proteasome Overview 32
1.6.2 Proteasome Inhibitors 34
1.6.3 Proteasomal Degradation induced by compounds 36
1.6.4 Autophagy Overview 36
1.6.5 Autophagy Induces and Inhibitors 37
1.6.6 Cycloheximide 38
Chapter 2: Persistent Reduction of Oxysterol-binding Protein Caused by Compound Treatment Induces Prophylactic Anti-Viral Activity 40
2.1 Abstract 40
2.2 Introduction 41
2.3 Results 42
2.3.1 Constant OSW-1 compound treatment leads to a differential time dependent reduction of OSBP and ORP4 protein levels. 42
2.3.2 Short, non-toxic doses of OSW-1 compound leads to prolonged OSBP loss in multiple cell lines up to 72 hours after compound has been removed 44
2.3.3 Loss of OSBP due to OSW-1 washout is not an artifact 46
2.3.4 Cellular localization of OSBP confirms OSBP loss in vivo during washout recovery 47

2.3.5 OSW-1 compound washout cells show no signs of cytotoxicity, cell growth arrest, or morphological changes. 50
2.3.6 The long-term reduction of OSBP levels upon OSW-1 compound washout treatment occurs in multiple cell lines and with as little as 1 hour of exposure. 51
2.3.7 OSW-1 compound washout prolonged reduction of OSBP is not due to residual compound 54
2.3.8 OSW-1 compound washout induces prophylactic antiviral response to two clinical isolates of Enteroviruses. 56
2.4 Discussion 58
2.5 Conclusion 59
2.6 Methods 60
2.6.1 Cell Lines and Viruses 60
2.6.2 General Cell Culture 61
2.6.3 OSW-1 Compound 62
2.6.4 Cell Lysis 62
2.6.5 Western Blotting 64
2.6.6 Washout Experiments 65
2.6.7 Immunofluorescence 65
2.6.8 Trypan Blue Staining 66
2.6.9 Calcein AM and Hoechst Staining 66
2.6.10 Intracellular OSW-1 Quantification Using LC-MS and Single Cell MS Methods 67

2.6.11 Single Cell Mass Spectrometry 67
2.6.12 Mass Spec label-free 2D OSBP quantification 68
2.6.13 Anti-Viral Experiments 69
2.6.14 Plasmid and Cloning 70
2.6.15 ([3H]-25-OHC) Charcoal/Dextran Binding Assay 71
2.6.16 Statistical Analysis 71
Chapter 3: OSW-1 compound treatment induced OSBP loss occurs through an unknown mechanism 72
3.1 Abstract 72
3.2 Introduction 73
3.3 Results 74
3.3.1 OSW-1 “washout effect” is not due to prolonged proteasomal degradation 74
3.3.2 OSW-1 “washout effect” induces autophagy, but autophagy is not the cause of long-term OSBP repression. 77
3.3.3 Sustained OSBP loss is not due to rapid protein turnover 79
3.3.4 OSBP mRNA transcript remains stable throughout washout recovery. . 80
3.3.5 OSW-1 Compound Triggered Long-term Reduction of OSBP Levels is Specific for OSBP and Not a General Proteome Reduction 81
3.4 Discussion 83
3.5 Conclusion 85
3.6 Methods 86
3.6.1 Cell Culture 86
3.6.2 General Cell Culture 86

3.6.3 OSW-1 Compound 87
3.6.4 Cell Lysis 87
3.6.5 Western Blotting 88
3.6.6 Cycloheximide Chase Experiments 89
3.6.7 Proteasome Inhibitor Assays 89
3.6.8 Calpain Anaysis 90
3.6.9 RT-PCR Analysis 90
3.6.10 Autophagy Experiments 92
3.6.11 iTRAQ Experiments 92
3.6.12 LC-MS/MS analysis of labeled peptides 93
3.6.13 Cell Splitting and Density Experiment 94
3.6.14 Statistical Analysis 94
Chapter 4: The compound OSW-1 is a unique ORPphillin that has prophylactic anti-viral capabilities 96
4.1 Abstract 96
4.2 Introduction 97
4.3 Results 98
4.3.1 OSW-1, but no other ORPphillin, affects cell growth or OSBP protein expression 98
4.3.2 ORPphillins show differential localization patterns of OSBP 98
4.3.3 Co-incubation with THEV2 or ITZ, but not oxysterols, can rescue OSBP loss induced by OSW-1 102

4.3.4 THEV2 binds OSBP competitively and suppresses OSW-1 cytotoxic activity. 103
4.3.5 OSW-1 exerts anti-viral activity 24 hours after compound has been removed 107
4.4 Discussion 109
4.5 Conclusion 111
4.6 Methods 112
4.6.1 Plasmids and Cloning 112
4.6.2 Cell Lines and Viruses 113
4.6.3 General Cell Culture 113
4.6.4 Compounds 114
4.6.5 Cell Lysis 115
4.6.6 Western Blotting 116
4.6.7 ORPphillin Compound Treatments and Cell Viability Assay 116
4.6.8 Sterol Treatments 117
4.6.9 Immunofluorescence 117
4.6.10 Cytotoxicity Assay 118
4.6.11 ([3H]-25-OHC) Charcoal/Dextran Binding Assay 119
4.6.12 Antiviral Experiments 119
4.6.13 Statistical Analysis 121
Chapter 5: Conclusions and Future Outlook 122
References 127
Appendix 1: Chapter 2 Supplemental 158

Appendix 2: Chapter 3 Supplemental 178

Appendix 3: Chapter 4 Supplemental 187

Appendix 4: Chapter 5 Supplemental 192

List of Tables

Table 1 3

List of Figures

Chapter 1: Introduction to the Oxysterol-binding Proteins

Figure 1. 2

Figure 2. 3

Figure 3 5

Figure 4. 6

Figure 5. 8

Figure 6 10

Figure 7. 11

Figure 8 15

Figure 9 26

Figure 10 28

Figure 11 29

Figure 12 30

Figure 13 32

Figure 14 34

Figure 15 38

Figure 16. 39

Chapter 2: Persistent Reduction of Oxysterol-binding Protein Caused by Compound Treatment Induces Prophylactic Anti-Viral Activity

Figure 17 44

Figure 18 45

Figure 19 47

Figure 20. 49

Figure 21 51

Figure 22 53

Figure 23 55

Figure 24 57

Chapter 3: OSW-1 compound treatment induced OSBP loss occurs through an unknown mechanism

Figure 25. 76

Figure 26 78

Figure 27 80

Figure 28. 82

Chapter 4: The compound OSW-1 is a unique ORPphillin that has prophylactic anti-viral capabilities

Figure 29 100

Figure 30 101

Figure 31 103

Figure 32. 106

Figure 33 108

Appendix 1: Chapter 2 Supplemental

Figure 34. 158

Figure 35 159

Figure 36 160

Figure 37 161

Figure 38 162
Figure 39 163
Figure 40. 164
Figure 41 165
Figure 42 166
Figure 43 167
Figure 44. 168
Figure 45. 169
Figure 46 170
Figure 47 171
Figure 48 172
Figure 49. 173
Figure 50 174
Figure 51 175
Figure 52 176
Figure 53 176
Figure 54 177

Appendix 2: Chapter 3 Supplemental

Figure 55. 178
Figure 56 179
Figure 57 180
Figure 58: 181
Figure 59 182

Figure 60 183

Figure 61 184

Figure 62 185

Figure 63 186

Appendix 3: Chapter 4 Supplemental

Figure 64 187

Figure 65 188

Figure 66 189

Figure 67. 190

Figure 68 191

Appendix 4: Chapter 5 Supplemental

Figure 69. 192

Figure 70 193

Abstract

Oxysterol-binding protein (OSBP) is the founding member of a conserved protein family found among eukaryotes that functions as a lipid transporter between the ER and Golgi. OSBP is ubiquitously expressed in all tissues and is an essential host protein in the viral replication of many public health menaces, especially the *Enteroviruses*. Over the past decade, many broad-spectrum anti-viral small molecules have been identified as OSBP inhibitors. The anti-cancer and anti-viral natural product, OSW-1, is of interest due to its high affinity for OSBP and its ability to cause proteasomal degradation of OSBP. The work outlined in this dissertation details the unique ability of the OSW-1 compound to induce persistent OSBP repression in cells through multiple days without affecting cell viability. Even in the absence of the OSW-1 compound, the reduced OSBP levels confers a prophylactic anti-viral activity against clinical isolates of *Enterovirus* viruses. This long-term reduction is specific for OSBP in the proteasome, and reduction occurs through an unknown mechanism that does not involve OSBP proteolysis or transcriptional repression. Of the known OSBP small molecule inhibitors with anti-viral activity, only OSW-1 triggered the long-term repression of OSBP. The OSBP inhibitor compound T-00127-HEV2 was the only compound tested able to protect OSBP levels from the OSW-1-induced repression of the protein. Of the OSBP inhibitor compounds, only the OSW-1 compound was able to induce the prophylactic anti-viral response against two clinical isolates of Enterovirus viruses. The results produced will be beneficial in future research that seeks to define OSBP cellular regulation, especially upon OSW-1 treatment, and to potentially develop prophylactic anti-viral therapeutics through targeting OSBP.

Chapter 1: Introduction to the Oxysterol-binding Proteins

1.1 Overview

Oxysterol-binding protein (OSBP) and OSBP-related proteins (ORPs) are a highly conserved family of proteins found in almost all eukaryotes spanning from yeast to humans(1, 2). This family of proteins contains a conserved ligand binding domain with the function of binding various forms of sterols and phospholipids (1–4). Despite the conserved domains and overlapping function, each member of the family seems to have its own role within the cell that appears to be involved with membrane lipid homeostasis(2, 5). With these specific roles, each family member has been implicated in various forms of cancer as well as other lipid based human diseases(2). The true roles that each member of the family plays within the cell is not fully known and the regulation of the proteins is unknown. This chapter will outline the basic structure of OSBP/ORPs and their specific cellular binding ligands and the known biological role of each family member. OSBP and its closest homolog ORP4 will be preferentially highlighted due to their focus in this dissertation. This chapter will look at their clinical relevance and the various small molecule ligands that each bind while briefly addressing some of the cellular effects that these molecules induce.

1.2 Oxysterols as ligands for the OSBP/ORPs

Oxysterols are 27-carbon oxidized forms of cholesterol that are generated through the cholesterol biosynthetic pathway and are involved in multiple activities in the body(6, 7). Numerous oxysterols are generated by the ER or mitochondria of hepatic cells by cytochrome P450 enzymes, *in vivo*, and also through food processing during cholesterol autoxidation(6, 7) (**Figure 1**). Once produced, these oxysterols serve as major signaling molecules with a variety of functions such as development, differentiation, immune functions, apoptosis, etc.(6, 7) (**Figure**

2). Like any other cellular signaling molecule, there are specific receptors for oxysterols, one of which is OSBP/ORPs(6) (

Table 1).

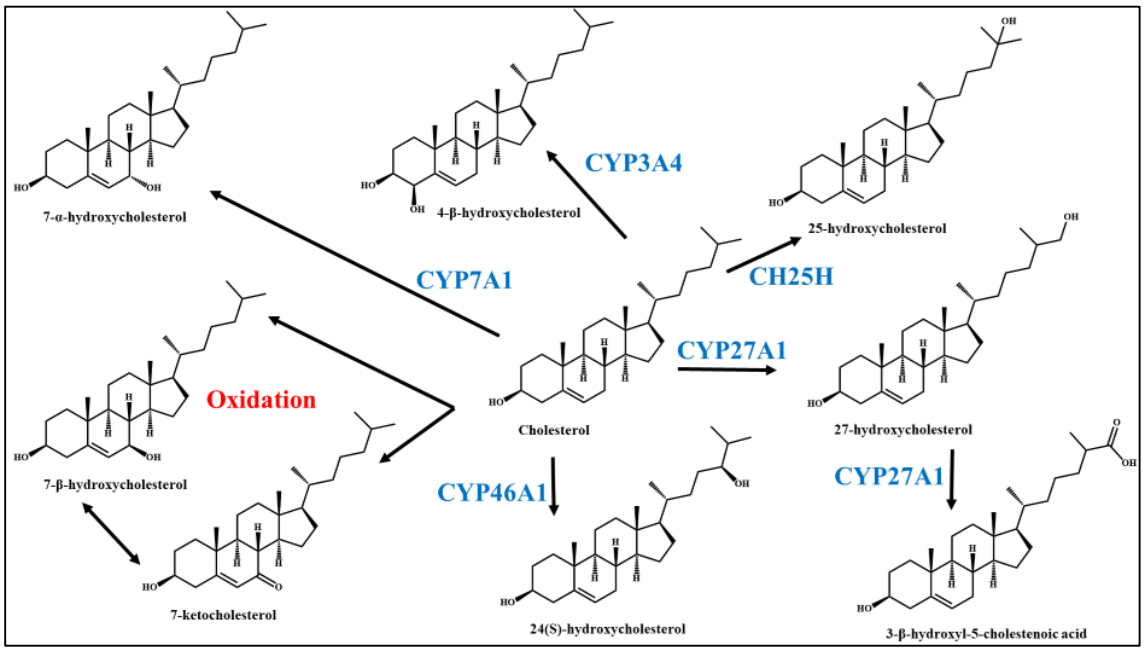

Figure 1: Fates of Cholesterol when processed by CYP450's. When cholesterol is processed by various CYP450 enzymes or oxidation, a variety of oxysterols are produced that contain very similar structures but very different effects.

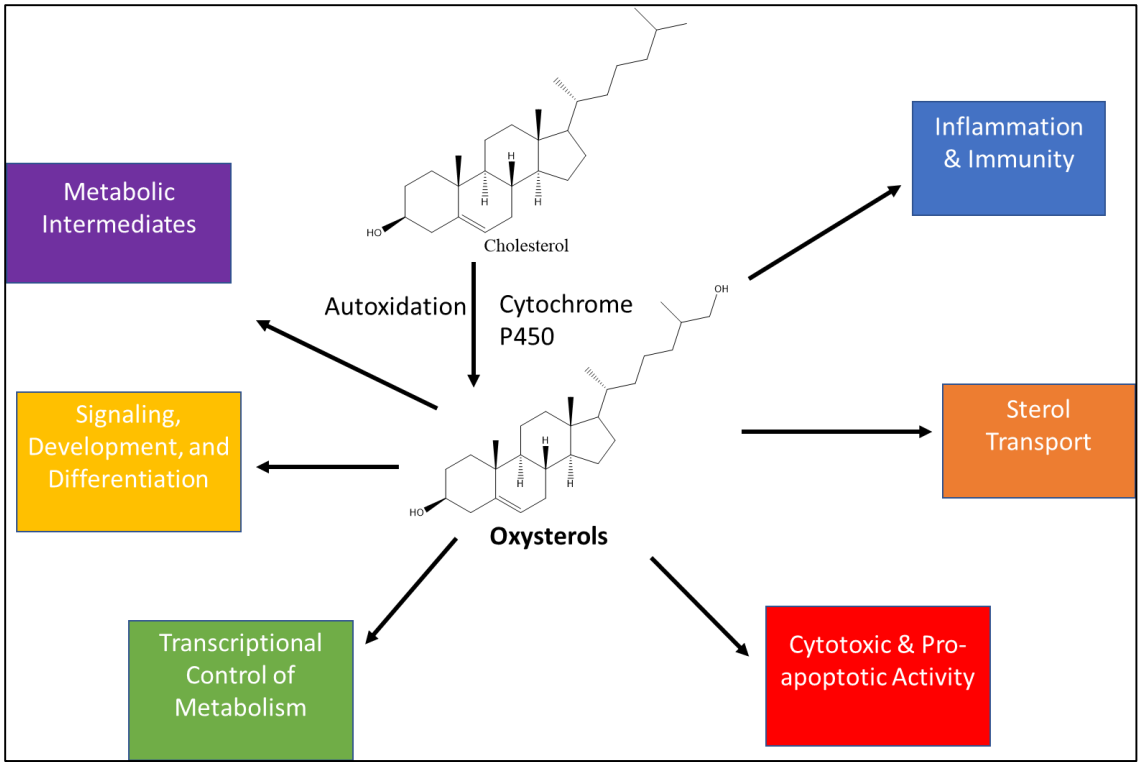

Figure 2: Cellular signaling of oxysterols. Cholesterol is processed into various oxysterols and these oxysterols have cellular signaling for developmental processes, differentiation abilities, and transcriptional control. They also have inflammation, immunity and apoptotic abilities alongside normal metabolic processes of sterols.

Table 1: List of oxysterol receptors and the various functions. Table adapted from Olkkonen et al. 2012.

Receptor (or rec. Family)	**Function**
LXRα, LXRβ	Transcriptional regulation of cholesterol adsorption and cellular efflux, cholesterol and bile acid synthesis, neutral lipid secretion into bile, inflammation and immune response
OSBP/ORPs	Regulation of lipid homeostasis, vesicle transport and cell signaling
Insig	Regulation of SREBP maturation: cholesterol and fatty acid biosynthesis and LDL receptor expression
StarD5	Cellular cholesterol metabolism and transport; up-regulated upon ER stress
NPC1	Egress of endocytosed cholesterol out of late endocytic compartments
RORα, RORγ	Transcriptional regulation of genes involved in development, metabolism, and immunity
EB12/GRP183	Control of B-cell migration
Smoothened	Hedgehog signaling

OSBP/ORPs functions are thought to be sterol sensing molecules and the binding of oxysterols over cholesterol leads to sterol transport that helps maintain lipid homeostasis of various membranes as well as specific signaling events based on the ligand(3, 4, 6, 8, 9). The sensing ability of OSBP/ORPs is due to their ability to complex cholesterol and oxysterols(10–17) as well as various phosphatidylinositol phosphates (PIPs)(13, 17–19) in their conserved ligand binding domain (LBD). There are no protein crystal structures of mammalian OSBP/ORPs, but based on the protein crystal structures of the yeast OSBP/ORP homologs, the conserved LBD is a beta barrel comprised of 19 anti-parallel beta sheets(20). The OSBP/ORP homolog with the most extensive protein structure is the yeast protein Osh4, which has been co-crystallized with various sterols and oxysterols bound(20). The ligand binding pocket contains a hydrophobic tunnel and a flexible lid capable of shielding the bound ligand sterol from the aqueous environment(20) (**Figure 3B**). After transport, the lid opens and has a flat surface allowing for contact with the cell membrane and possible sterol targeting to the membrane(20). In addition to sterols and oxysterols being ligands for OSBP/ORPs, crystal structures of Osh4 have also been generated with PI4P bound in the LBD(21). The acyl chains of PI4P are stuck down in to the hydrophobic tunnel while the polar head group makes specific contact with the entrance and lid region(21).

In order to bind both sterols and PI4P, OSBP/ORPs have various targeting domains besides their conserved LBD. OSBP/ORPs have an endoplasmic reticulum (ER) targeting domain (FFAT) that interacts with vesicle-associated membrane protein-associated proteins (VAPs)(22) and/or a pleckstrin homology (PH) domain that may interact with PIPs on various membranes(16, 23–26) (Figure 3**A**). ORPs can associate with two membranes through the binding of PIPs where the ORP will bind a ligand sterol, go through a conformational change, and deliver the sterol to the opposite membrane (**Figure 4A**). ORPs can also bind both PIPs and sterols in the same binding pocket,

creating an exchange of the two in opposite directions to modulate lipid compositions (**Figure 4B**). Endocytosis is controlled by ORPs through binding PIP, blocking transport factors and sending signals for metabolic regulation, and binding of sterols releases the ORPs and decreases the activity (**Figure 4D**). Longer ORPs associate with the ER through peptide motifs where oxysterol binding activates a PH domain to bind PIPs on a non-ER membrane contact site and recruit effector molecules of various functions, while binding of sterols can dissociate this complex (**Figure 4C&E**).

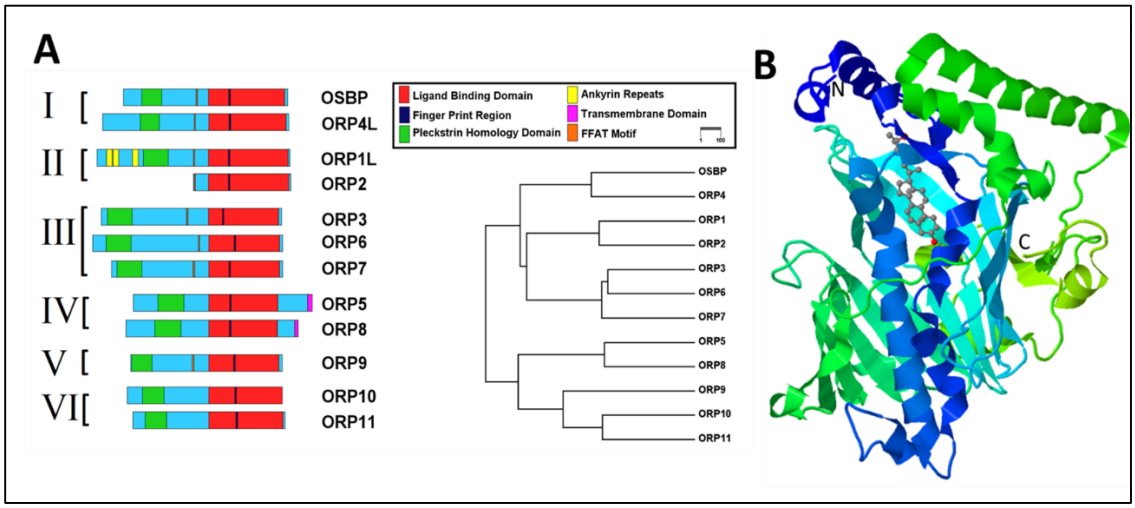

Figure 3: Homology and Basic Structure of Human ORPs. A) Protein domain homology graph showing the different OSBP/ORP families B) Structure model showing the beta-barrel of the ORP domain with the N-terminus lid interaction with 25-hydroxycholesterol shown. **Figure**s A was created by Juan Nuñez & B is a screen shot from the yeast oxysterol binding protein Osh4 in complex with 25-hydroxycholesterol (PDB number 1ZHX)

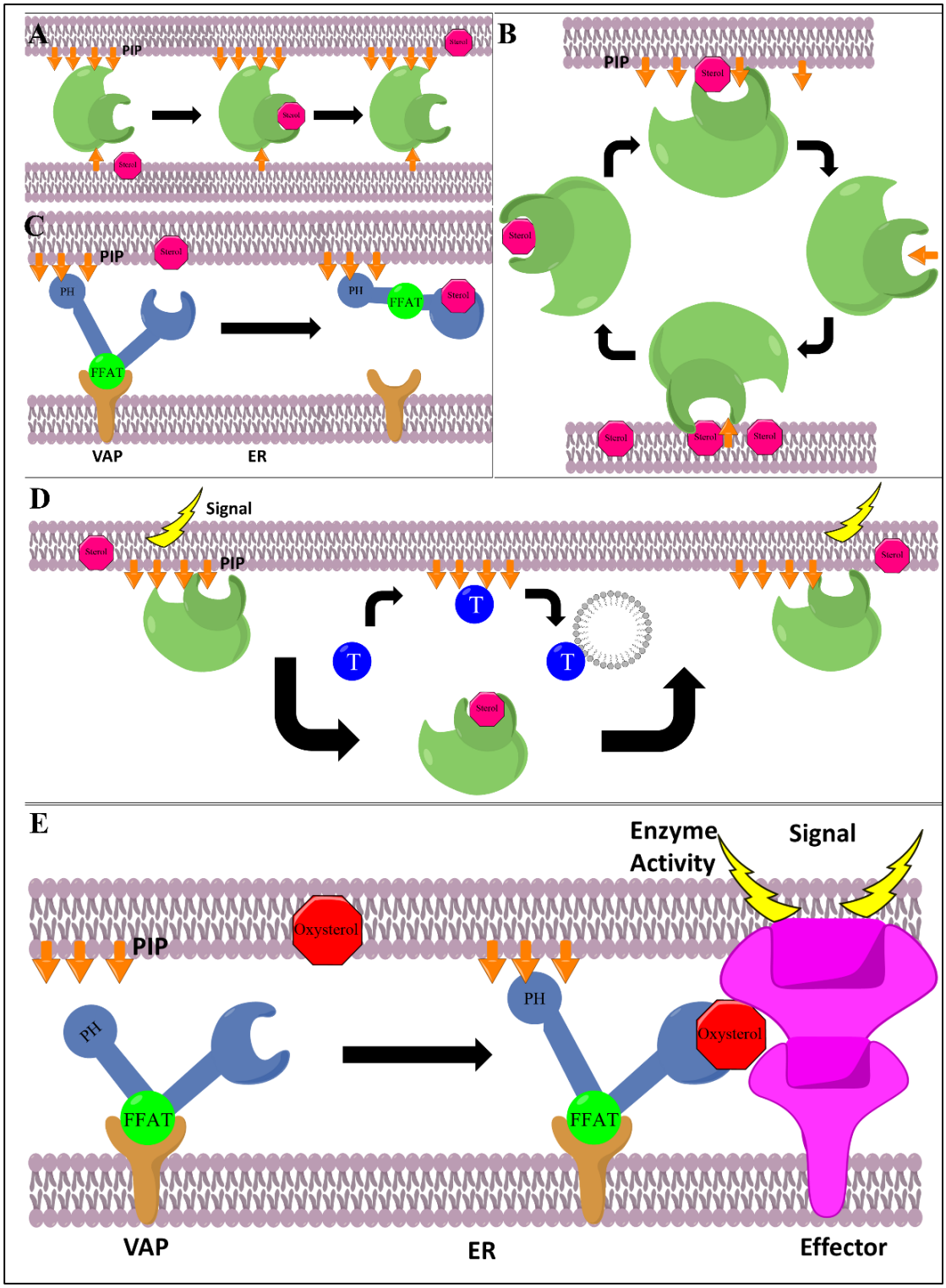

Figure 4: Schematics of ORP/OSBP cellular pathway interactions. (A) Sterol transport between membranes using PIP's as a docking site. (B) Binding sterols and PIPs in the same pocket in an exchange-like fashion. (C) Disassembly of ER complex with sterol binding. (D) Modulating endocytosis by blocking transport factors. (E) Binding to ER to activate effector proteins for signal transduction with oxysterol binding.

1.3 OSBP/ORP biology

1.3.1 OSBP

Oxysterol-binding protein (OSBP) was first described by its ability to bind oxysterols *in* vitro(27–29). In the early 1990s, OSBP gene was cloned and the OSBP protein was determined to be an 809 amino acid (~89 kDa) protein(10, 30). In the early 2000s, OSBP was recognized as being a member of a conserved protein family present in all eukaryotic cells(31, 32). The OSBP-related proteins (ORPs) were identified based on the shared presence of a C-terminus ligand binding domain (LBD)(31). In addition to the LBD, OSBP also contains a PH domain located near the N-terminus that interacts with PI4P and ARF1 for trans-Golgi localization and a FFAT domain that interacts with VAPA on the ER membrane(33, 34). It was shown that upon ligand binding, the mostly cytocyolic OSBP would shift localization to membrane contact sites (MCS) consistent with trans-Golgi and ER staining(11).

Multiple *in vitro* assays have shown the ability of OSBP to tether between the ER and Golgi membranes to counter transport cholesterol and PI4P(35, 36) (**Figure 5**). Use of a high affinity ligand of OSBP, 25-hydroxycholsterol, has also been shown to stop the counter transport and lead to aggregation of OSBP tethered particles, further confirming the ability of OSBP to bind to MCSs(35). Through these *in vitro* assays it was suggested that OSBP uses PI4P as a fuel source due to SAC1 hydrolysis of PI4P on the ER membrane, keeping the concentration gradient intact(35). Further studies in cells suggest that the major role of OSBP in cells is to control cholesterol transport through interacting with the kinase PI4KIIIβ(36). This kinase, which is responsible for making PI4P, and thereby OSBP can consume large quantities of PI4P in order to transport cholesterol to regulate the lipid compositions of various cellular membranes(36). In

addition to its cholesterol transport ability, OSBP is also able to recruit CERT to the Golgi for ceramide transport and SM production(37). This recruitment of CERT is presumably through OSBP's association with ARF1 that leads to PI4KIIIβ stimulation of PI4P production, allowing inactive CERT to localize to the Golgi(38). This adds another level of OSBP's ability to control overall lipid composition of cell membranes.

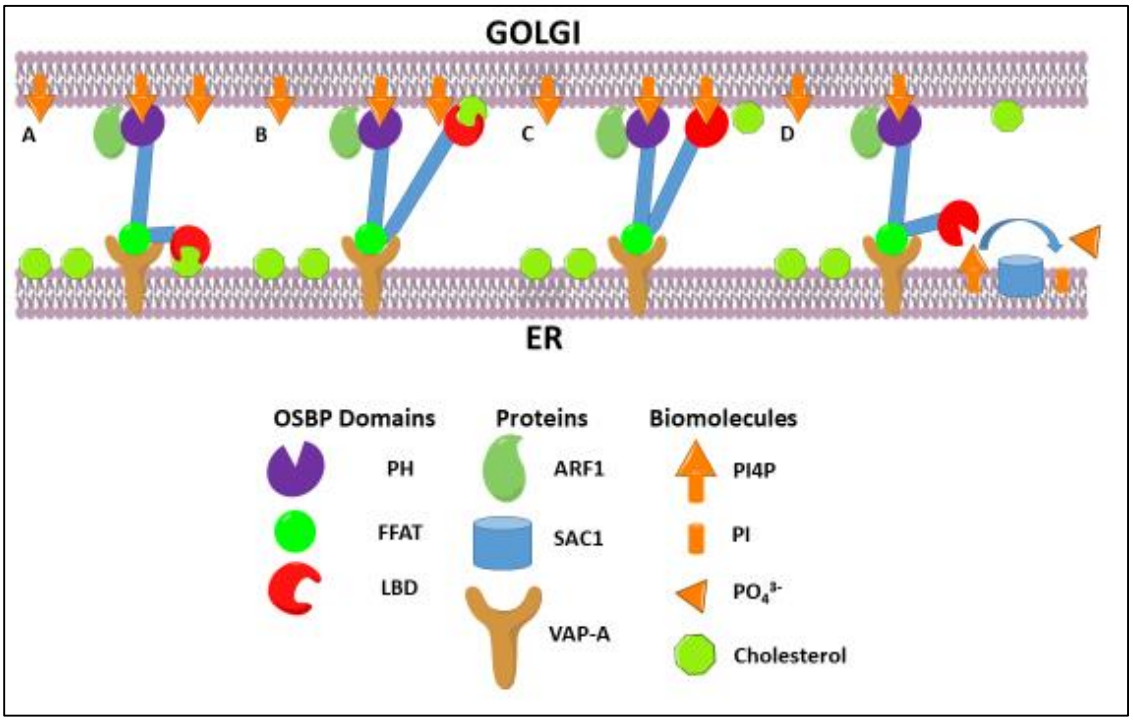

Figure 5: OSBP Counter-transport schematic. (A) OSBP binds to PI4P at the Golgi using its PH domain which is stabilized by ARF1 and interacts with the ER using its FFAT domain that binds VAP-A. The LBD domain of OSBP binds cholesterol at the ER and (B) transports it to the Golgi membrane. (C) OSBP releases cholesterol into the Golgi membrane and the LBD then binds PI4P. (D) OSBP counter-transports PI4P from the Golgi to the ER membrane where it is then hydrolyzed by the ER-resident SAC1.

1.3.1.1 Cell Signaling Role

As mentioned before, OSBP/ORPs can take place in various cell signaling pathways through the binding of sterols(3, 4, 6, 8, 9). OSBP can be regulated by a cellular kinase or act as a scaffold for either kinases or phosphatases(37, 39, 40). OSBP activity has also been shown to be regulated by phosphorylation at Ser242 by PKD. A phospo-metic version of OSBP was shown to

have impaired Golgi localization and induced Golgi fragmentation(37). This is consistent with the mechanism of action of brefeldin A, which inactivates ARF-1 and leads to Golgi fragmentation(41). This phosphorylation leads to the masking of the PH domain and possibly the interaction with ARF1, which is essential for Golgi localization(37). This leads to an inactivated form of OSBP and disassociation from the MCS. PKD's substrates also include PI4KIIIβ and CERT, leading to activation of the former and deactivation of the later(42, 43). These results support an OSBP mechanism of action in which PKD first phosphorylates PI4KIIIβ, leading to activation and production of PI4P. This production of PI4P then leads to recruitment of OSBP through its PH domain, which interacts with ARF1 in its active form. This in turn leads to more production of PI4P, allowing for the recruitment of CERT to the MCS. OSBP transports cholesterol for PI4P while CERT shuttles ceramide to make SM, and this activity is then controlled by PKD phosphorylation to preserve lipid raft formation and lipid homeostasis(37).

One study found that OSBP is also involved in regulating the activity of the ERK1/2 signaling pathway(39). This study suggested that cytosolic OSBP acts as a sterol sensor that under normal conditions when cholesterol is bound, the PH domain is masked and the conformation of the protein changes to associate with HePTP and PP2A, which are tyrosine and serine/threonine phosphatases(39). This complex is then able to deactivate ERK1/2 and will only dissociate when cholesterol levels are low or oxysterols bind to OSBP. Under these conditions the conformation

changes, opening the PH domain and the phosphatases are removed, allowing for localization to the Golgi where cholesterol can be replenished (**Figure 6**).

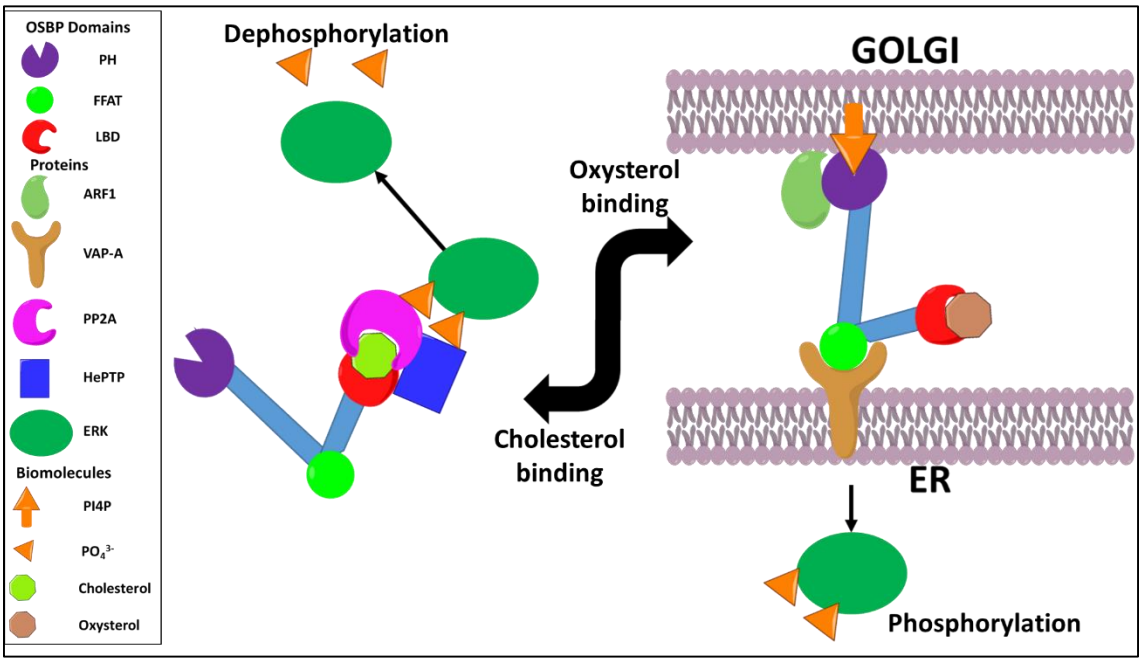

Figure 6: OSBP in ERK signaling. When cholesterol is bound to OSBP it allows for the phosphatases PP2A and HePTP to complex with OSBP and dephosphorylate ERK. When cholesterol levels are low and oxysterol levels rise, oxysterol binding to OSBP allows for the complex to dissociate and OSBP then localizes between the ER and Golgi, allowing for ERK phosphorylation to occur.

OSBP also has interactions with the JAK2/STAT3 pathway to lead to gene expression of profilin-1. 7-ketocholesterol levels were shown to lead to an up-regulation of profilin-1 transcription due to increased STAT3 activation, through JAK2 and OSBP(40). When the oxysterol binds, OSBP interacts with JAK2 and is phosphorylated at position 394, which leads to a conformational change that allows for STAT3 to interact with the OSBP/JAK2 complex and also becomes activated by JAK2 phosphorylation(40). Once activated, STAT3 can translocate to the nucleus and induce transcription of profilin-1 by binding to the gene promoter. This provides more evidence that OSBP maintains lipid homeostasis by acting as a sterol/lipid sensor, and through this sensing can modulate cell signaling in response to various ligand levels (**Figure 7**)

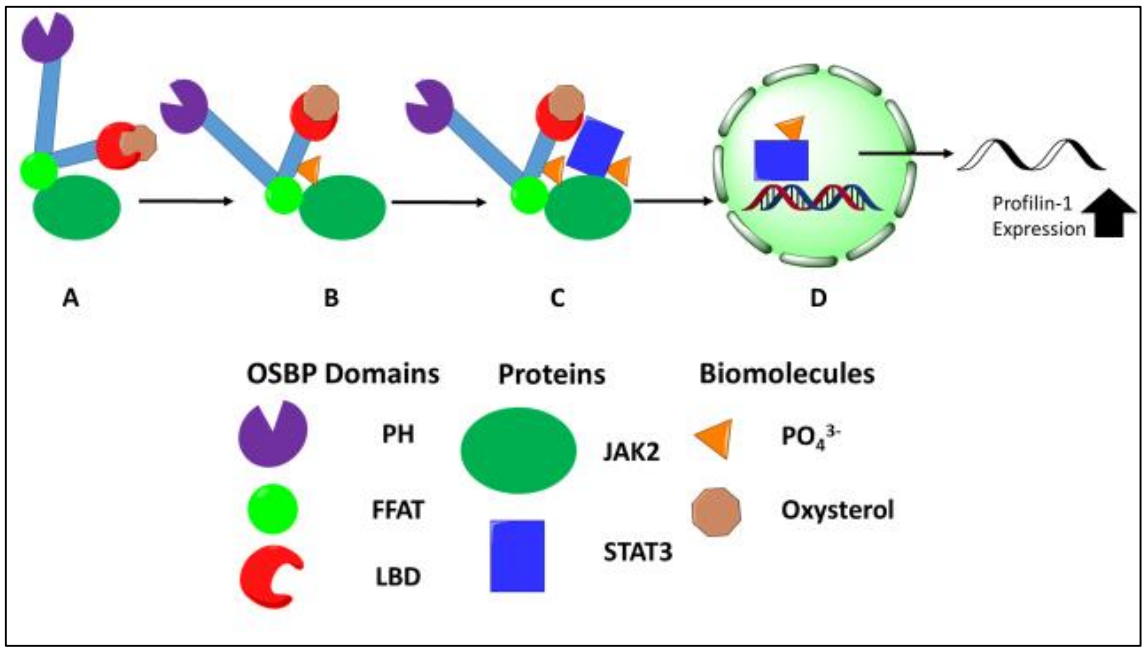

Figure 7: OSBP in JAK/STAT signaling. (A) OSBP binds an oxysterol which allows for JAK2 interactions leading to (B) OSBP phosphorylation and conformational change. (C) The new OSBP conformation allows for STAT3 to interact with the OSBP/JAK2 complex leading to STAT3 phosphorylation. (D) Activated STAT3 is then able to translocate into the nucleus and increase the transcription of profilin-1.

1.3.2 ORP4

1.3.2.1 Variants and Tissue Specificity

ORP4 is a protein of 916 amino acids that consists of an N-terminus PH and FFAT domain with a C-terminus ligand binding domain. OSBP shares the closest sequence similarity to ORP4 than any other human ORP with 58% sequence identity on the DNA level and 64% on the protein level(44). Despite this high similarity in sequence, the two proteins are different in biological function. Unlike OSBP, ORP4 has three difference splice variants named: ORP4L, ORP4M, and ORP4S(12, 17). ORP4L is the longest splice variant with all 916 amino acids and targeting domains(12, 17, 44). ORP4M has a truncated PH domain that is predicted to be nonfunctional in binding PI4P(17). ORP4S is lacking the N-terminus PH domain altogether and a portion of the

ligand binding domain(12, 17). Whereas OSBP is ubiquitously expressed, ORP4 seems to be tissue specific with the highest levels being in brain, retina, heart, and kidney tissues(12, 44). ORP4 was also shown to be overexpressed in patients with chronic leukemia as well as various cancer cell lines(17, 45, 46). Like OSBP, ORP4L was shown to have high affinity for cholesterol and 25-OHC, as well as bind PI4P and VAPA(12, 47).

1.3.2.2 Ligand Binding and Cellular Localization

Unlike OSBP, which is mainly cytosolic unless ligand bound(11), immunostaining has shown that ORP4L is loosely associated with vimentin intermediate filaments while ORP4S causes aggregation of the vimentin network(12).

ORP4S induced aggregation is due to the loss of leucine repeats near the N-terminus of the protein based on mutational experiments with ORP4L and OSBP(47). Mutated OSBP proteins revealed that loss of the leucine repeats caused vimentin collapses like ORP4L, but the localization of OSBP was mostly cytosolic(47). Due to this cytosolic staining of OSBP, it was thought that OSBP does not directly interact with the vimentin network, but with ORP4L through its similar dimerization domain. Yeast-two hybrid analysis revealed that mutations in the dimerization domain of OSBP lead to loss of interaction with ORP4L while mutations in the leucine repeat region did not have a loss of interaction while mutating both regions on OSBP lead to rescuing of the vimentin network(47). These results suggest that ORP4L can interact with OSBP in a regulatory fashion.

Despite the ability to bind cholesterol, oxysterols, and PI4P, ORP4L was not originally thought to localize to the Golgi or change localization at all upon treatment with these compounds(12, 17, 48). A recent study has shown that using a C-terminal tagged protein, that ORP4L does in fact translocate to the Golgi upon 25-OHC treatment or cholesterol depletion(49). ORP4L was shown to have perinuclear structures after 25-OHC treatment or cholesterol depletion

that were ligand independent as tested through mutations of ORP4L(49). This localization of ORP4L to the Golgi was OSBP and Golgi localized PI4P dependent and loss of ORP4L lead to loss of Golgi structure (49). These results suggest that OSBP localization to the MCS, which leads to increased PI4P production could lead to the recruitment of ORP4L either through direct interactions through the dimerization domain or through ORP4L's PH domain targeting the increased PI4P pool.

1.3.2.3 Vimentin Binding

Vimentin has been shown to be involved with the recycling of LDL-derived cholesterol and recycling of glycosphingolipids from endosomes to the Golgi(50–52). Studies have shown that cells lacking vimentin have increased cholesterol synthesis and decreased cholesterol esterification, suggesting that vimentin plays a role in the transport of LDL-derived cholesterol from the endosomes(50). One of the ways that this might occur is through ORP4 binding to the vimentin network. Studies have shown that overexpression of ORP4S causes an aggregation of this network and results in a 40% reduction of LDL-derived cholesterol esterification(12). ORP4M was also shown to cause vimentin aggregation due to the non-functional PH domain, implying that the PH domain of ORP4L plays a role in preventing vimentin collapse(17).

The sterol binding domain of ORP4L was shown to be capable of binding vimentin regardless of cholesterol or 25-OHC being bound to the protein. Cholesterol and 25-OHC binding was lost with the deletion of the α-helical lid and the first β-strand in the sterol binding region (residues 501-505), but vimentin binding was still retained(47). This suggests that ORP4L can interact with vimentin in either a ligand bound or free state. This provides evidence that ORP4 interaction can regulate the transport of LDL-derived cholesterol from the endosomal compartments to the ER via the vimentin network. Consistent with the idea that ORP4 interacts

with vimentin to modulate cholesterol localization is that ORP4 knockdown in mice leads to male sterility(53). Knockout of ORP4 causes a condition known as oligo-astheno-teratozoospermia, which leads to low sperm count, low motility and abnormal morphology(53). Loss of ORP4 leads to mislocalization of the oocyte activation factor MN13, which needs to translocate from the sterol rich region of the sperm head to an almost sterol free location(53). The formation of the sperm head under normal ORP4 conditions shows significant ORP4 localization in the equatorial region, which also contains rich vimentin intermediate filaments and is a sterol rich region(53). These results suggest that functional ORP4 needs to interact with vimentin within the regions of the sperm head in order to translocate MN13 for efficient spermatogenesis.

1.3.2.4 Role in Cellular Proliferation

ORP4 has also been shown to be linked to cell survival and proliferation(17). Knockdown of all ORP4 variants, but not OSBP, was shown to cause growth arrest in HEK293 and HeLa cells, while overexpression of any one of the knockdown resistant variants partially prevented this arrest(17). Silencing ORP4L and not the ORP4M and ORP4S variants, also caused a partial growth arrest in HeLa cells(17). These results suggest that ORP4 is required for cell line viability and proliferation. Knocking down of ORP4 in non-malignant IEC-18 cell lines lead to apoptosis through conventional pathways, and RAS transformations of IEC-18 cells had more total ORP4 and did not go through cell death(17). This suggests that ORP4 may be overexpressed during the transformation of cells in order to make them immortalized.

Another line of evidence that ORP4 is used for proliferation is its ability to promote oxidative phosphorylation in the mitochondria, driving cellular metabolism(48, 54). A recent study in T-ALL has shown that ORP4L acts as a scaffold/adaptor allowing for the assembly of CD3β, $G\alpha_{q/11}$, and PLCβ3(54). This ORP4L-mediated complex activates PLCβ3 to process IP_3 into

signaling molecules to induce the Ca^{2+} release from the ER used in oxidative phosphorylation(54) (**Figure 8**). This complex was also found to be active in macrophages, and in macrophages, the complex sustains cell viability through the ER Ca^{2+} release leading to c-AMP responsive element binding protein activation and upregulation of transcription of the anti-apoptotic factor Bcl-XL(48). Disruption of this complex through ORP4L binding to 25-OHC leads to increased apoptosis due to the decrease in Bcl-XL transcription(48).

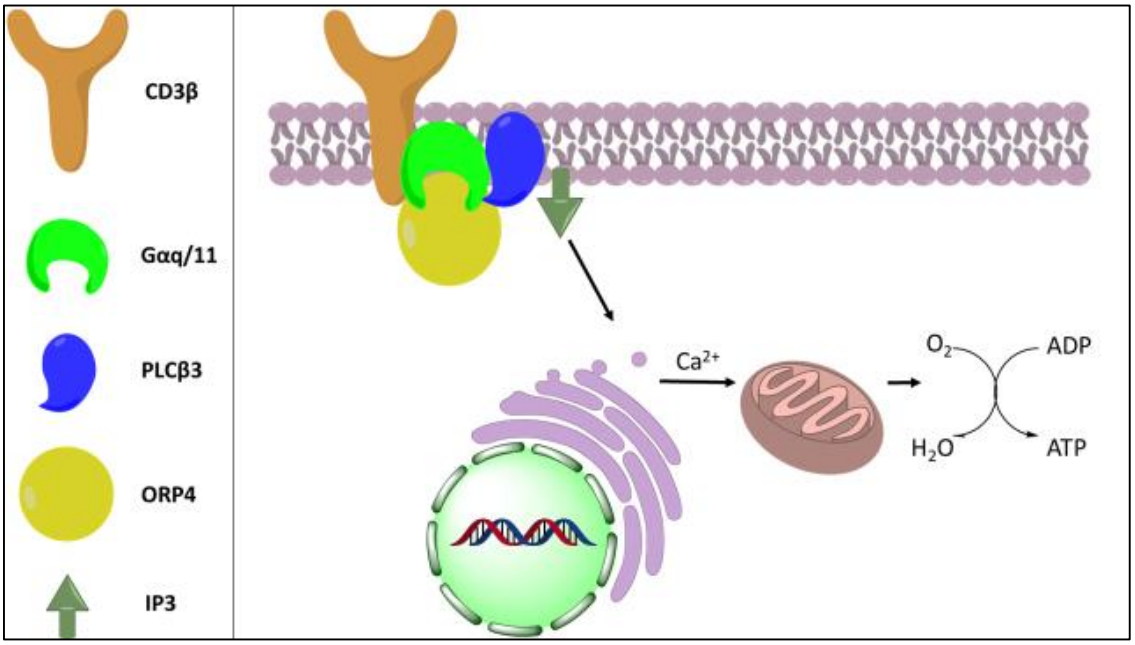

Figure 8: Schematic of ORP4's role in oxidative phosphorylation. ORP4 complexed with CD3β, Gαq/11, and PLCβ3. This complex leads to the activation of PLCβ3, which cleaves IP3 into signaling molecules. These signaling molecules are then able to release Ca^{2+} from the ER into the mitochondria allowing for increased oxidative phosphorylation.

1.3.3 Subfamily II: ORP1 and ORP2

Unlike OSBP and ORP4, the subfamily II member ORP1 has two variants (ORP1L & ORP1S) which have very different expression patterns. The long form variant has been shown to found in brain, lung, and macrophages while the short form has highest expression in skeletal muscles and the heart(55). Similar to OSBP/ORP4, ORP1L has an FFAT domain that is able to bind to VAP proteins on the ER(13). ORP1L also has a PH domain that can bind PI4P(13). These

targeting domains allow it to carry out its function of removing cholesterol from late endosomes with the aid of Niemann-Pick C1 protein and PI4P and placing it into the ER membrane(13). In contrast, ORP1S has the ability to translocate into the nucleus upon ligand stimulation and bind to LXR, which promotes binding to LXR-responsive elements and leads to production of LXR-dependent gene transcription, specifically the apoE gene(56).

Like OSBP, ORP2 is ubiquitously expressed in all cell typess(57), but ORP2 is unique in the OSBP/ORP family in that only a short version of the protein is encoded(3). ORP2 binds neutral lipid membranes and has a possible cholesterol-mediated role in triglyceride metabolism(58). ORP2 has a FFAT domain that allows it to target the ER and was shown to be localized at lipid droplets (LD), suggesting it has a potential mediation effect in ER-LD association that allows for coordination of neutral lipid metabolism(59). ORP2 shares sequence similarity to ORP1S, and like-wise also binds LXR and promotes transcription of LXR target genes(60).

1.3.4 Subfamily III: ORP3, ORP6, and ORP7

ORP3, ORP6, andORP7 comprise subfamily III of the OSBP/ORPs. Similar to OSBP and ORP4, all of subfamily III have PH and FFAT domains(61). All of subfamily III have detectable expression in all cell types but ORP3 is highly expressed in kidneys, lymph nodes, and thymus(61). ORP3 interacts with R-Ras proteins to control cell adhesion and becomes phosphorylated when cells become un-adhered suggesting an outside-in feedback signals(62, 63). Hyper-phosphorylation of ORP3 leads to multiple VAPA interactions at the ER and it is then able to contact the plasma membrane (PM) through its PH domain(63). This allows ORP3 to activate R-Ras proteins giving rise to the idea that ORP3 plays a role in ER-PM communication(3, 63).

ORP6 shows high expression in the brain and skeletal muscle tissue(61) and has been shown to be involved with regulation of cholesterol efflux and trafficking by affecting the early

lysosomal network(64). Similar to ORP3, ORP6 was shown to localize to the ER and ER-PM contact sites in cerebellar granule neurons(65). ORP6 is transcriptionally regulated by LXR in order to respond to intracellular cholesterol and is tightly controlled by cellular sterol levels(64).

ORP7 expression is abundant in the gastrointestinal tract and has also been shown to localize to ER/PM(61) to interact with R-Ras proteins(3). ORP7 is involved in autophagy through sterol-ligand induced interactions with GATE-16, which induces degradation of the Golgi SNARE protein GS28 and subsequent addition of ORP7/GATE-16 complexes to autophagosomes(66). ORP7 was also identified as the only OSBP/ORP family protein that could associate with serum lipids and therefore ORP7 could have a role in gastrointestinal lipid absorption(67).

1.3.5 Subfamily IV: ORP5 and ORP8

Subfamily IV, consisting of ORP5 and ORP8, is unique to the rest of the OSBP/ORP family due to the presence of transmembrane domains. The transmembrane domains anchor the proteins directly to the ER without the need of the FFAT domains interacting with VAPA(15, 22). ORP5 and ORP8 possess a PH domain and were shown to bridge the ER and PM by binding PI4P with their PH domain(68). This allows for the transport of phosphatidylserine (PS) from the ER to the PM with PI4P being counter-transported and hydrolyzed by SAC1 at the ER(68). This lipid shuttling system is similar to the OSBP counter-transport of cholesterol and PI4P(68). ORP5 and ORP8 are also able to utilize phosphatidylinositol-4, 5-biphosphate ($PI(4,5)P_2$) for counter-transport of PS at ER/PM(18). ORP5 and ORP8 have the ability to deliver PS from the ER to the mitochondria, which appears to be crucial to mitochondria function(69). ORP5 and ORP8 RNAi silencing leads to mitochondria dysfunction(69).

Besides the overlapping functions exhibited by both proteins, ORP5 can extract cholesterol from LE(15) and also localize mTOR to lysosomes which is associated with cell proliferation and

migration(70). ORP8 on the other hand has implications in controlling lipid homeostasis and SREBP activity(71). ORP8 was shown to interact and localize with the nuclear membrane by binding with nuclear pore protein Nup62 and is thought to possibly dismantle the pore preventing SREBP entry into the nucleus(71).

1.3.6 Subfamily V: ORP9

ORP9 is expressed as both a long form (ORP9L) and short (ORP9S) form(72). Both ORP9L and ORP9S contain the FFAT domains that bind VAP proteins at the ER, but only the ORP9L possess the PH domain(72). ORP9L, like OSBP, has the ability to connect the Golgi and ER at the MCS using PI4P, and ORP9L can counter-transport cholesterol in a PI4P dependent manner(16). Silencing of ORP9L or overexpression of ORP9S leads to Golgi fragmentation, which parallels the destructive effect of expression of the phosphorylated-mimetic version of OSBP(73, 74). Similar to OSBP, ORP9 is also a substrate for PKD phosphorylation and regulates activation of AKT, and through AKT, mTOR activation(75). Further support for the fact that ORP9 plays a role in the Golgi secretory pathway is the ability of ORP9S to phenocopy the OSBP yeast homolog Osh4P and mediate Golgi-derived vesicular trafficking(76).

1.3.7 Subfamily VI: ORP10 and ORP11

Subfamily VI is unique among the family in the fact that they do not contain an ER targeting FFAT sequence but do contain PH domains(3). ORP10 has a PH domain that interacts with PI4P and a LBD domain that binds cholesterol and several acidic phospholipids(23). ORP10 is implicated in having a role in lipid metabolism(23). ORP10 localizes to microtubules presumably through its interaction with microtubule effector protein DIAPH1(23, 77). The PH domain of ORP10 has the ability to localize to the Golgi due to PI4P binding, and the protein plays a role in the secretion of apolipoproteinB-100(23).

ORP11 has been shown to reside at the Golgi complex and LE, which is presumably due to its ability to dimerize with ORP9(78). Along with ORP11, ORP10 can also dimerize with ORP9, which with its FFAT domain, might compensate for the lack of an ER targeting domain in subfamily VI(23). This information suggests that there is a possible crosstalk between two or more ORPs that allows for communication between the ER, Golgi, LE, and microtubules(23, 76, 78).

1.4 OSBP/ORP Disease Relevance

1.4.1 OSBP Function in Virus Replication

OSBP has been implicated as an essential host protein in a wide variety of viral infections(79–84). The cholesterol shuttling ability of OSBP is hijacked by these viruses in order to carry out efficient replication within the host cell(79–84). To date OSBP function has been shown to be important in the replication of Hepatitis C, *Enterovirus* genus, Encephalomyocarditis, and Dengue viruses(79–84).

1.4.1.1 Hepatitis C Virus

Hepatitis C (HCV) virus is a member of the Flaviviridae family that has no preventable treatment other than host behavior changes. HCV currently infects about 3% of the world population(85). HCV was one of the first viruses that was linked to OSBP's ability to shuttle cholesterol(79). HCV is a positive-sense strand RNA virus that forms a protrusion replication organelle (RO), where the donor membrane is bent into the cytoplasm(86). These ROs can be single or double membraned structures that are dynamic and form membranous webs with their integrity based on cholesterol and PI4P(87, 88). Viral protein NS5A recruits and activates PI4KIIIα at the RO membrane, which leads to the upregulation of PI4P production(89, 90). This increase in PI4P then leads to recruitment of OSBP and CERT to the membrane for cholesterol and sphingomyelin efflux to the RO membrane(79, 91, 92). Disruption of the PI4K/PI4P/OSBP

pathway through means of chemical or translational inhibition leads to reduction of viral replication.

PI4KIIIβ has also been shown to be involved with OSBP recruitment to ROs in other variants of HCV, but it is suggested that its role is more essential for secretion of viral partials(93). Inhibition of PI4KIIIβ has been shown to inhibit egress of virion particles without affecting virion replication(94). Depletion of cholesterol or sphingomyelin from HCV virions has been shown to decrease infectivity of the viral particles, suggesting these two molecules may play a role in efficient entry of the virus into cells(95). OSBP's ability to interact with PI4KIIIβ and stimulate sphingomyelin synthesis via CERT, provides evidence of OSBP having multiple roles in virus life cycle.

HCV egress from the cell has been linked to the host secretory pathway, specifically the utilization of very low density lipoprotein (VLDL) to form lipoviroparticles (LVPs)(96). The LVPs have been shown to bind to low density lipoprotein receptors (LDLRs) on the cell surface, facilitating viral entry into the host(97). HCV's usage of the LDLRs provides not only efficient entry, but also sustained viral replication(98). HCV increases LDLR expression through stimulation of sterol-regulatory binding proteins (SREBPs), which results in increased LDL particle uptake from the bloodstream(98). Overexpression of OSBP in hepatocytes has been shown to increase SREBP-1c expression, which in turn increased VLDL production(99). This information provides further evidence that OSBP may have a broader effect in the HCV life cycle beyond just viral replication.

1.4.1.2 Enteroviruses

The genus *Enterovirus* are positive-sense strand RNA viruses in the family Picornaviridae and encompasses a variety of important human pathogens. The most famous member of the genus

is poliovirus (PV) due to its historical notoriety as the causative agent of poliomyelitis. In 1988 the World Health Organization (WHO) started the Global Polio Eradication Initiative and in 2017 there were only 22 cases reported worldwide compared to ~350,000 cases when the initiative started(100). The eradication of polio is due to the development of an oral PV vaccine (OPV) that is feasible to administer but has drawbacks due to the ability of the OPV to revert back to vaccine derived PV (VDPV)(101). In areas where the community is under vaccinated, this VDPV can spread from person to person and is then considered chronic VDVP (cVDVP) and is as severe as wild PV(101). While there were only 22 cases of wild PV reported in 2017, there were 96 cases of cVDPV(100). This suggests the need for antiviral therapies to help control cVDPV to help in the eradication of PV. Recently, OSBP was shown to have a role in the replication cycle of PV and disruption of OSBP function through protein knockdown or small molecule inhibitors lead to a decrease in PV replication(80). Targeting OSBP could be a potential strategy to control cVDPV.

Other *Enterovirus* species include Human Rhino Virus (HRV), numbered enteroviruses (eg. EV71, EV68), Coxsackievirus (CV), and Echovirus. These viruses affect millions of individuals each year and include illnesses that range in severity such as the common cold and viral conjunctivitis to more serious diseases such as viral meningitis/encephalitis and acute flaccid paralysis(102). HRV infections cause over 50% of cold-like and flu-like illnesses, and are an enormous economic burden, costing billions of dollars annually(103, 104). Infections can be linked to asthma in children and is a significant cause of acute respiratory illness in immune compromised patients(103, 104). Within the past two decades, outbreaks of EV71 and EV68 have become public health concerns, especially for infants and young children(105–107). Both serotypes of the virus have been shown to cause acute flaccid myelitis and other severe neurological conditions(105–107). EV71 and CV are some of the most causative agents of hand, foot, and mouth disease and a

recent outbreak in China between 2008-2012 resulted in over 7 million cases with over 2500 deaths(105, 106). Echoviruses are among the most common cause of meningitis and can also cause myocarditis and development of type 1 diabetes(108). Unlike PV, due to the large number of serotypes, the non-polio enteroviruses do not have a vaccine and there currently are no approved antiviral treatments.

Enterovirus species encode a single protein of about 250kDa that is processed by viral proteases to make structural and non-structural proteins. Like HCV, these viruses also induce a protrusion-type RO which are thought to shield the RNA in the cytoplasm from host defenses and support replication(109). The virus needs to modulate the lipid composition of the membrane to retain integrity of the membrane to sustain efficient replication, and to do this it hijacks host proteins involved in lipid metabolism(110). Viral protein 3A has been shown to play a role in the RO formation by recruiting host factors ARF1 and GFB1 to the membrane, which in turn recruits PI4KIIIβ to increase PI4P production at the RO(111–113). OSBP can localize to these ROs through its normal interactions with ARF1 and PI4P targeting and disruption of OSBP function leads to broad enteroviral inhibition due to OSBP's role in cholesterol shuttling in response to PI4KIIIβ derived PI4P accumulation at ROs(81, 114). The viral RNA-dependent RNA-polymerase, $3D^{pol}$, was shown to have specificity in binding PI4P *in vitro* which suggests that PI4P may act as a scaffold at ROs for viral protein localization for assembly of genome replication machinery(112). Another component of RO generation is the accumulation of cholesterol from various host membranes(114). *Enteroviruses* have been shown to extract cholesterol from the ER, lipid droplets, and recycling endosomes from increased endocytosis, and disruption of cholesterol homeostasis leads to decreased viral replication(114–116). The dependence of these viruses on cholesterol suggests that OSBP would be a favorable host target for antiviral therapies.

1.4.1.3 Role of OSBP in the Replication of Other Viruses

Encephalomyocarditis virus (EMCV) is a positive-sense strand RNA virus belonging to the genus *Cardiovirus* that is responsible for fatal myocarditis and encephalitis in various animals with no current treatment. The main reservoir for EMCV is thought to be rodents, and although EMCV infects a variety of animals, pigs seem to be the most susceptible(117). EMCV infection is thought to be fairly common in humans with up to 17% of various town populations being seropositive to EMCV, but despite the common exposure there are rarely any symptoms reported(117). One potential human health issue that could arise is the use of pig heart tissue for xenografts in humans. The common occurrence of the virus and its specificity for pig heart tissue could destroy the xenograft tissue quickly leading to patient complications.

Recent studies have shown that EMCV utilizes the same pathway as HCV for viral replication(83). EMCV hijacks PI4KIIIα, which associates with viral protein 3A at the RO to recruit OSBP. OSBP is recruited to counter transport PI4P for cholesterol at the RO(114). Disruption of the function of either OSBP or PI4KIIIα prevent viral replication(114). Interestingly, single point mutations in 3A that lead to resistance to PI4KIIIα small molecule inhibitors did not confer resistance to OSBP inhibitors(118). This suggests an uncoupled function of PI4KIIIα and OSBP in the virus replication(118).

Dengue virus (DV) is a positive-sense strand RNA virus in the Flaviviridae family that is transferred by an arthropod vector to humans. DV causes dengue hemorrhagic fever and dengue shock syndrome(119). DV has four closely related serotypes and infection with one serotype can make reinfection with a different serotype more dangerous(120, 121). More than two fifths of the world's population is at risk for possible dengue infection and the development of a vaccine to cover all the serotypes is a slow process with many challenges(119). Unlike the other viruses

mentioned earlier, DV makes an invagination RO into the ER which is PI4KIII independent(122). Despite the lack of PI4KIII dependency, inhibition of cholesterol biosynthesis or cholesterol depletion was shown to be antiviral towards DV(123). A recent study has shown that OSBP is involved in DV replication. Knockdown of OSBP and use of OSBP inhibitors was shown to inhibit DV replication and cause a redistribution of cellular cholesterol(84). This new study solidifies the role that OSBP plays in a broad spectrum of viral infections and signifies the potential therapy OSBP targeting could provide.

1.4.2 Cancer Cell Survival and Proliferation

ORP4 and OSBP were originally identified as the target of various natural product compounds that showed anti-cancer activity in various cultured human cancer cell lines(46). This study showed that overexpression of either protein resulted in an increased resistance to the compounds and that loss of OSBP resulted in increased sensitivity of the compounds(46). ORP4 was originally identified as a potential molecular marker for solid state tumors due to its mRNA overexpression in patient blood and tissue samples of lung and breast cancer(124). In a subsequent study ORP4 was shown to be overexpressed in chronic myeloid leukemia from patient samples as well as several cultured cell lines derived from various forms of leukemia(45). Knockdown of ORP4 resulted in cellular growth arrest in cancerous and immortalized cultured cell lines and apoptosis of non-transformed cells(17). Consistent with the finding that ORP4 is utilized in the oncogenesis/transformation of cells was the finding that ORP4 mRNA expression was increased when the human papilloma virus proteins E6 and E7, which can immortalize cell lines *in vitro*, were transfected into cells(124). A recent study has shown that ORP4L is expressed in T-cell acute lymphoblastic leukemia (T-ALL) but not normal T-cells(54). ORP4L in the T-ALL cancer cell was linked with an increase in oxidative phosphorylation through calcium signaling(54). ORP4's

link with various forms of cancer and cell survival provide an attractive target for anti-cancer strategies due to its limited tissue expression as previously mentioned.

1.5 ORPphillins and OSBP/ORP4

A variety of small molecule inhibitors of OSBP and ORP4, termed ORPphillins, have been identified through the screening of these compounds as anti-cancer and antiviral agents(46, 80, 81, 125). These compounds range from steroidal based natural products to synthetic triazoles(46, 80, 81, 125). Despite the diversity of structures, most of the compounds exhibit the ability to inhibit OSBP function *in vitro*, but many of the cellular effects on OSBP and ORP4 remain unknown for these compounds(46, 80, 81, 125).

1.5.1 OSW-1

The natural product OSW-1 (**Figure 9**), (3β,16β)-3,17-Dihydroxy-22-oxocholest-5-en-16-yl-2-O-acetyl-3-O-[2-O-(4-methoxybenzoyl)-β-D-xylopyranosyl]-α-L-arabinopyranoside, was originally extracted from bulbs of *Ornithogalum saundersiae*, a Star-of-Bethlehem plant found in South Africa, in 1992 and was shown to have considerable activity against cyclic AMP phosphodiesterase(126). It was later shown that OSW-1 had significant anti-proliferative effects against various tumor derived cell lines and had a mean IC_{50} of 0.78 nM in the National Cancer Institute 60-cell *in vitro* screen (NCI60)(127). The target of OSW-1 was identified to be OSBP and ORP4(46). OSW-1 was shown to cause proteasome dependent degradation of OSBP in a time dependent manner(128). OSW-1 has been shown to cause disruption of intracellular calcium leading to mitochondria membrane disruption and calcium dependent apoptosis(129). Further research has also shown that OSW-1 causes a disruption of cellular calcium homeostasis which affected the mitochondria and the survival factor GRP78 which lead to apoptosis in leukemia cells(130). This mechanism of action coupled with the idea that increased ORP4L is tied to

oxidative phosphorylation through intracellular calcium signaling in T-ALL cells(54) suggests that ORP4 is the anticancer target of OSW-1.

OSW-1 has been shown to have antiviral activity(81, 82). OSW-1 was first shown to have antiviral activity against HCV due to the disruption of OSBP function and the resulting loss of cholesterol to ROs(92). It has also been shown to be a broad spectrum antiviral against *Enteroviruses* through the disruption of OSBP shuttling cholesterol to ROs which affected genome replication of the viruses(81, 82). OSW-1 treatment was also recently shown to reduce DV replication presumably through the disruption of cellular cholesterol homeostasis due to impaired OSBP function(84). These findings suggest that OSBP is the antiviral target of OSW-1, while the anti-cancer target is ORP4.

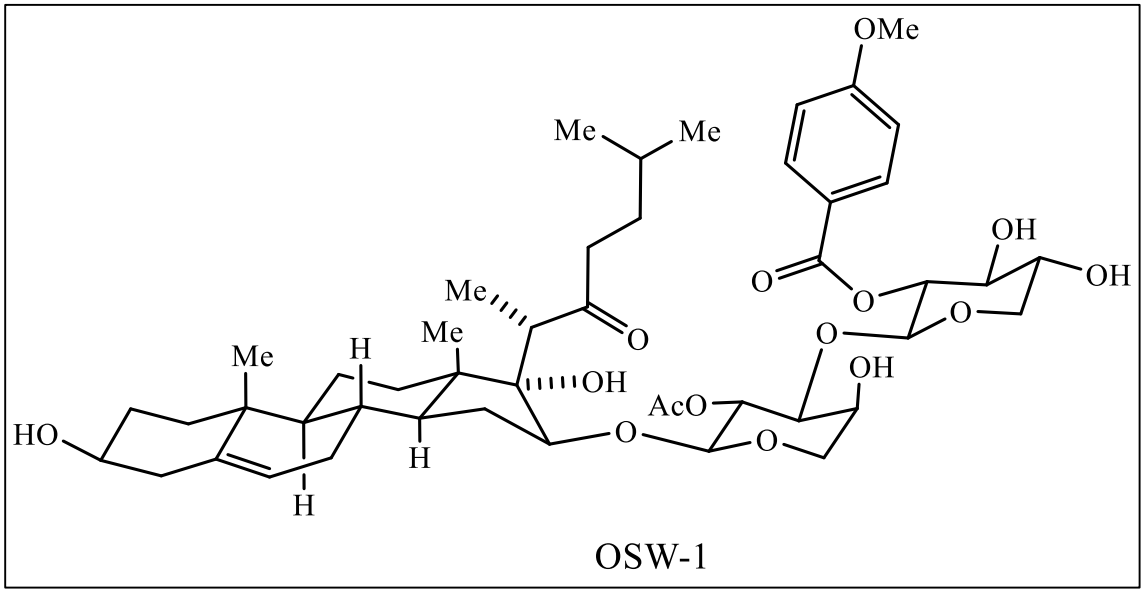

OSW-1

Figure 9: Structure of OSW-1

1.5.2 Schweinfurthins

Schweinfurthins (A-C) were originally isolated from *Macaranga schweinfurthii*, a flowering tree in the spurge family found in Cameroon, in 1998 and A (**Figure 10**) and B were

shown to have cytotoxic activity with a mean NCI60 IC_{50} value of 360 nM and 810 nM respectively(131). Further isolations from *M. schweinfurthii* revealed Schweinfurthin (D, I, and J) while isolations from two other species in the *Macaranga* genus yielded 11 other Schweinfurthins lettered to Q with Schweinfurthin F having the lowest mean NCI60 IC_{50} value of 130 nM(132–134). Schweinfurthin A was shown to bind to OSBP in the low nanomolar range while ORP4 binding was in the low micromolar range(46). Unlike OSW-1, Schweinfurthin A does not cause OSBP protein degradation(46). A recent study has shown that Schweinfurthin G (**Figure 10**) inhibits mTOR/AKT cancer cell proliferation through disruption of the trans-Golgi network (TGN)(135). Schweinfurthin G was shown to bind with OSBP and increase its affinity for PI4P, suggesting that the interaction might lead to sequestration of PI4P trafficking that leads to TGN disruption(135). Schweinfurthin A presents as an interesting candidate for an antiviral drug due its selectivity for OSBP over ORP4 but the limited availability due to supply issues presents an obstacle to overcome(136).

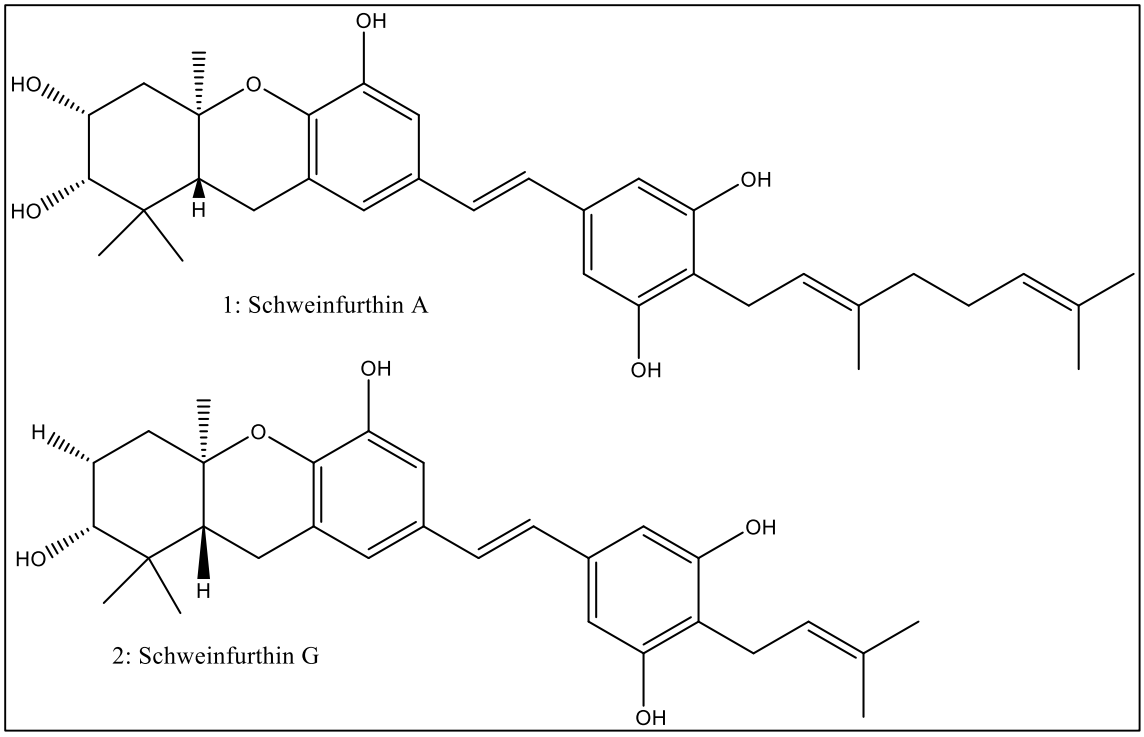

Figure 10: Structures of Schweinfurthins that bind OSBP. Schweinfurthin A (1) and G (2).

1.5.3 Cephalostatin 1 and Ritterazine B

Cephalostain 1 (**Figure 11**) was originally collected in extracts from the marine worm *Cephalodiscus gilchristi* off the coast of Southeast Africa in 1972 and was not fully characterized until 1987(137). Cephalostatin 1 has a mean NCI60 IC_{50} value of 2.2 nM(137, 138). Another marine extracted natural product with a structure related to cephalostatin 1 and possessing potent cytotoxicity is ritterazine B (**Figure 11**) (139). Ritterazine B was isolated from the tunicate *Ritterella tokioka* collected off the coast of Japan in 1995(139). Ritterazine B has a mean NCI60 IC_{50} value of 3.2 nM which is comparable to that of Cephalostatin 1(140). Both of these compounds were shown to bind OSBP with low nanomolar affinity(46). Cephalostatin 1 also has low nanomolar affinity for ORP4(46). Ritterazine B did not bind ORP4L as well as cephalostatin 1, but a inhibition binding value could not be determined due to lack of sufficient compound(46). Interestingly, cephalostatin 1 was also able to induce OSBP degradation upon treatment similar to

OSW-1(46). Neither of these compounds has been tested for antiviral activity and do not seem feasible to pursue due to their limited availability and time intensive synthesis(141).

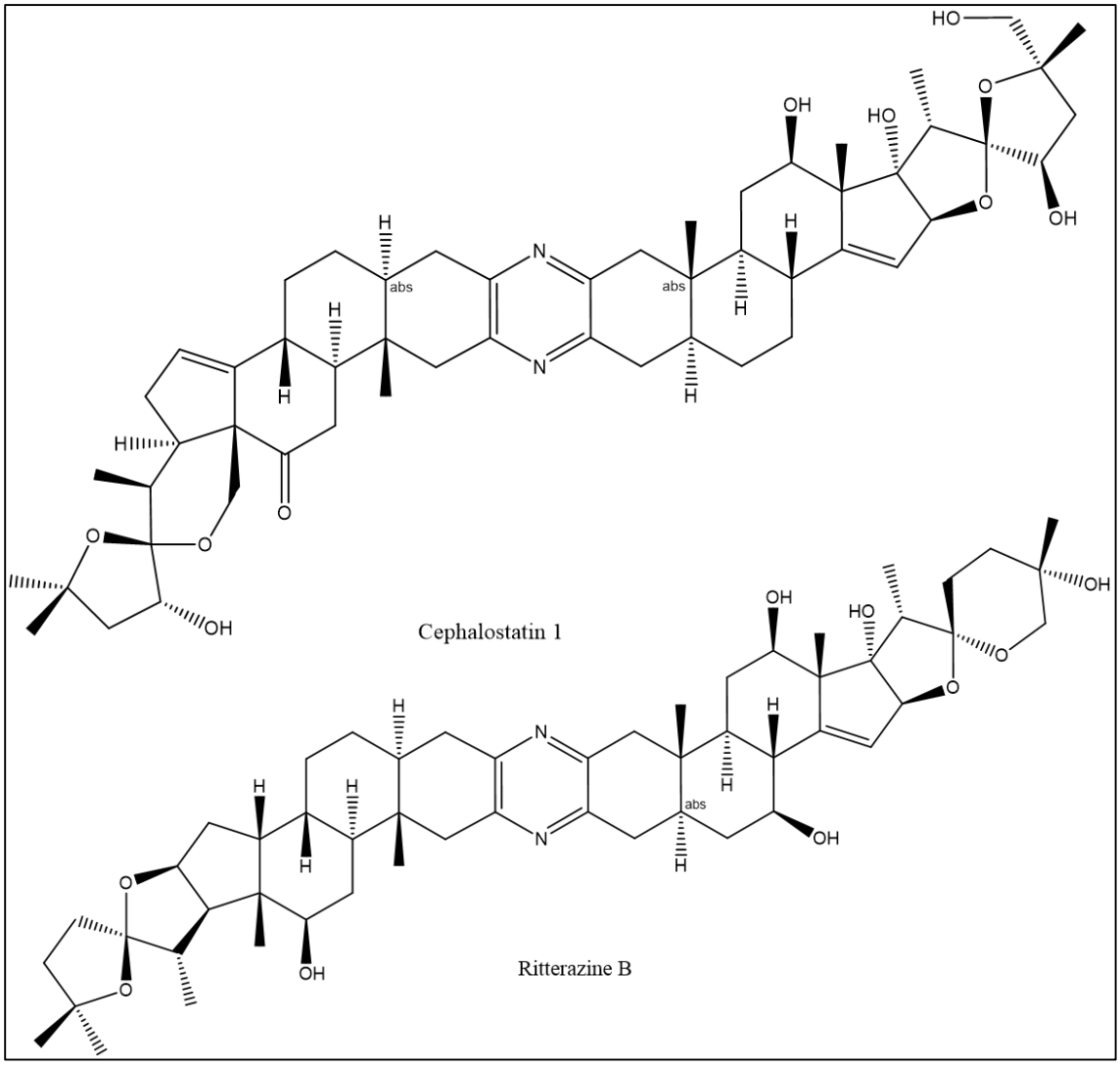

Figure 11: Structures of Cephalostatin 1 and Ritterazine B.

1.5.4 Itraconazole

Itraconazole (ITZ) (**Figure 12**) is a synthetic triazole created in 1983 by a division at Janssen Pharmaceutica in Belgium as a broad spectrum anti-fungal agent(142, 143). The anti-fungal mechanism of action of ITZ is by inhibiting the cytochrome P450 34A enzyme responsible for synthesizing ergosterol, which is an essential fungal sterol (144). ITZ gained FDA approval for

anti-fungal use in 2001(145). ITZ has been identified as a hit in drug repurposing screens for anti-cancer and antiviral compounds(146, 147). The anti-cancer activity of ITZ, which is separate from its anti-fungal activity, stems from its ability to inhibit both angiogenesis through the process of disruption of mTOR signaling and vascular endothelial growth factor receptor 2 trafficking, and also through effecting the hedgehog pathway signaling(148–150). ITZ's ability to broadly inhibit virus replication is independent of its anti-fungal and anti-cancer activities, and it occurs through inhibiting OSBP and possibly ORP4(81). ITZ was shown to bind OSBP with a Kd of 430 nM(81). ITZ treatment of cells alters OSBP localization patterns, and like OSW-1, ITZ treatment of cells inhibits the cholesterol and PI4P counter transport that is necessary to fuel RO viral replication(81). Pursuing ITZ as an OSBP inhibitor seems feasible due to its established FDA approval, but the lack of specificity due to the multiplicity of targets and the extremely poor water solubility of the compound are potentially limiting(151).

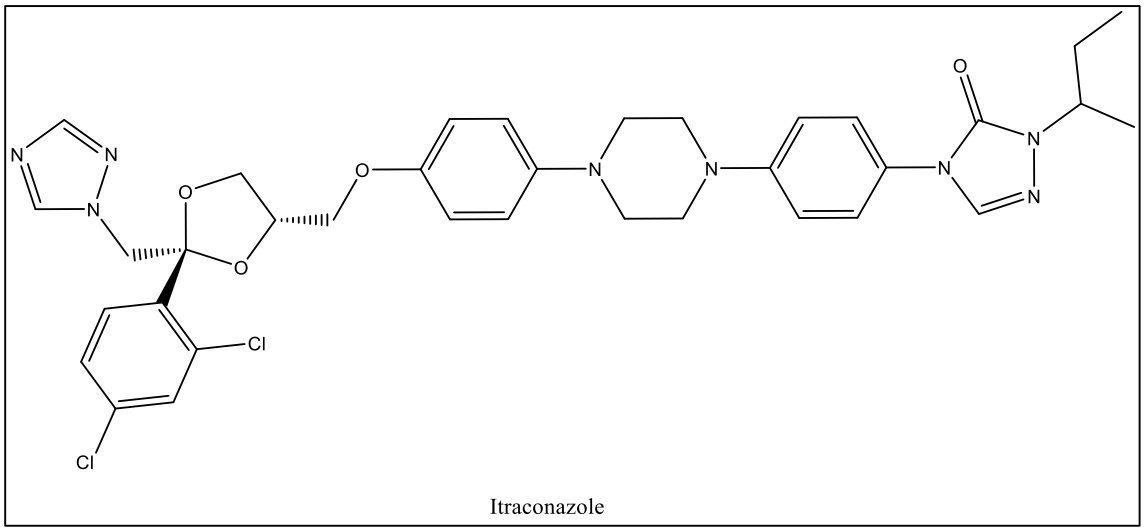

Itraconazole

Figure 12: Structure of Itraconazole.

1.5.5 Minor Enviroxime-like Compounds

Enviroxime is a compound that inhibits positive-strand RNA viral synthesis by indirectly targeting viral proteins 3A and/or 3AB(152, 153). This interaction prevents the replication

complex from forming properly(152, 153). Mutations in the viral 3A and/or 3AB proteins leads to resistance to the compound(152, 153). Enviroxime-like compounds are compounds with anti-viral activity that are structurally-unrelated to enviroxime, but the same mutations that confer resistence to enviroxime also confer resistance to the enviroxime-like compounds(154). The enviroxime-like compounds can be further classified as major or minor compounds, with major compounds being PI4KIIIβ inhibitors and the minor compounds being non- PI4KIIIβ inhibitors(155). The minor enviroxime-like compound T-00127-HEV2 (**Figure 13**) (THEV2) was shown to have increased anti-poliovirus activity when OSBP was knocked down(155). Further, cellular treatment with THEV2 led to OSBP localization to the Golgi, similar to 25-OHC treatment, and a corresponding decrease of PI4P at the Golgi(155). Similarly, the minor compound TTP-8307 (**Figure 13**) (TTP) was also shown to exert its anti-viral activity through the targeting of OSBP(156). TTP was shown to inhibit the *in vitro* cholesterol transferring ability of OSBP and to cause localization of the protein to the Golgi similar to other known OSBP interacting compounds(156). Interestingly, overexpression of OSBP in infected cells did not lead to viral resistance to the TTP compound, suggesting this compound might also interact with other components in the viral replication pathway beyond OSBP(156). Further analysis of these THEV2 and TTP compounds biological activity is required to define their interaction with OSBP and evaluate their potential efficacy as antiviral lead compounds.

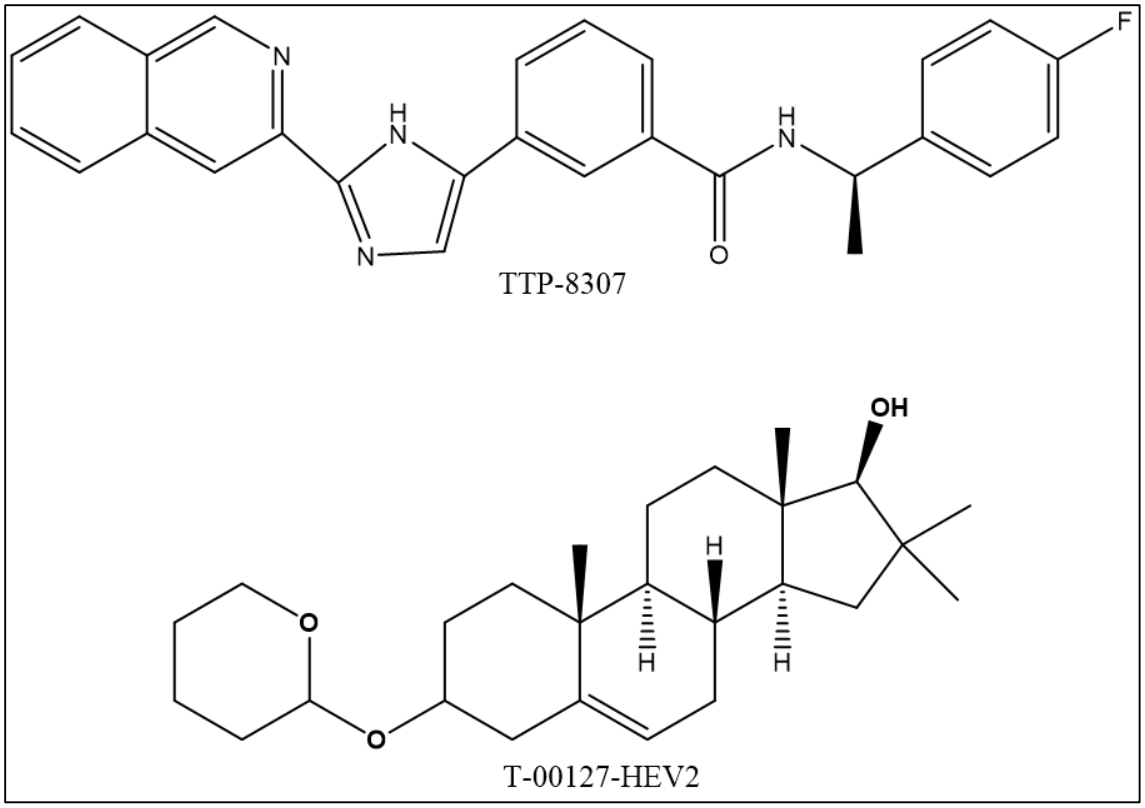

Figure 13: Structures of minor enviroxime-like compounds that target OSBP.

1.6 Small Molecule Drug Targets

There are currently over 2300 FDA approved small molecule drugs(157) for a variety of targets and diseases, which can be utilized as chemical probes to understand functions of proteins and various biological processes(158). The latter chapters of this dissertation explore the cellular effects of ORPphilin inhibition of OSBP. Small molecule inhibitors to key cellular pathways, such as the proteasome and autophagy, are utilized to determine the fate of OSBP inhibited by these ORPphillins. The cellular processes, and their small molecule inhibitors, that are explored in the subsequent chapters are briefly outlined in the following section.

1.6.1 Proteasome Overview

The proteasome is a large protein complex that is responsible for degradation of cellular proteins tagged by the ubiquitin post translational modification(159, 160). Addition of

polymerized ubiquitin on a protein serves as a degradation signal to target the protein to the proteasome(159, 160). Ubiquitination is performed by a network of proteins: E1, E2, and E3(159, 160). E1 proteins are ubiquitin activators that obtain ubiquitin and transfer it to the E2 ubiquitin-conjugating enzymes(159, 160). The E2 enzymes complex with the E3 ubiquitin-ligating enzymes and the protein substrate (159, 160). E3 proteins are substrate selective and there are more than 500 different E3 proteins to accommodate the cellular protein substrates in need of polyubiquitination(161). Once polyubiquitination has occurred, the protein substrate is released and is then targeted to the proteasome complex. This complex consists of one or two 19S regulatory particles (RP) that serve to remove the ubiquitin tags and unfold the protein(161). The unfolded protein is fed into the 20S catalytic unit of the proteasome which degrades the protein into peptides of 3-15 amino acids, which are further degraded by oligopeptidases and/or amino-carboxyl peptidases to generate amino acids(161). The proteasome complex degrades ~80% of intracellular proteins, and the proteasome plays a vital role in major cellular processes such as in the cell cycle, cellular stress response, protein quality control, immune system functions, and apoptosis(162–164). In recent years, proteasome inhibition has been shown to have anti-cancer activity(165) and be a potential anti-inflammatory therapy(166). Inhibition of the proteasome has also advance basic cell biology through knowledge gained about the cell cycle, transcriptional response, metabolic regulation,etc(167).

1.6.2 Proteasome Inhibitors

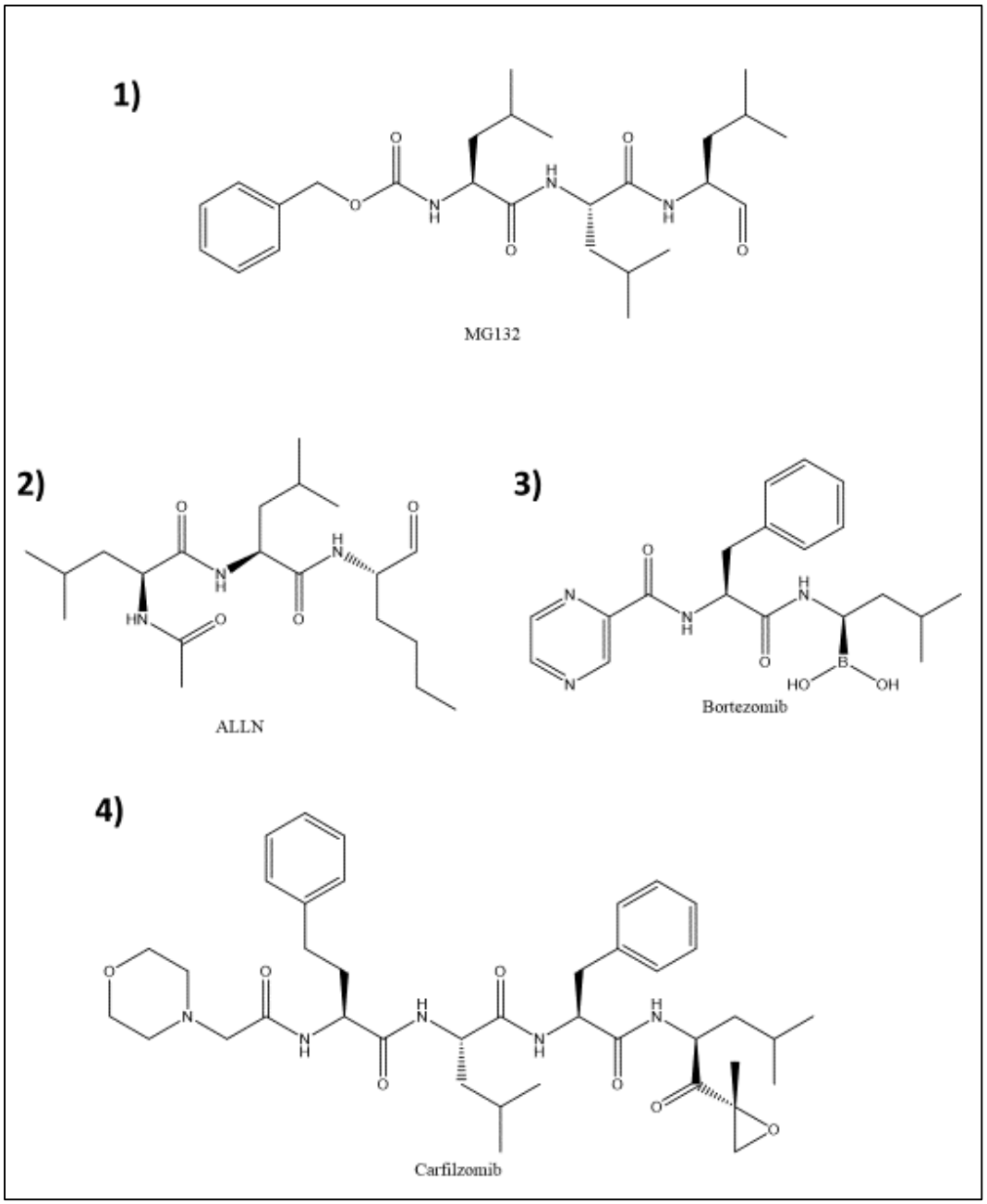

Figure 14: Structures of Various Proteasome Inhibitors.

1.6.2.1 Peptide aldehydes: MG132 & ALLN

Peptide aldehydes were the first class of proteasome inhibitors to be developed, and these compounds are widely used as research agents to inhibit the proteasome (168). In general, these inhibitors rapidly enter the cell, but have slow and reversible binding to the proteasome(169, 170). Peptide aldehydes are subject to rapid oxidation into inactive forms in the cells, and this means that proteasome inhibition can be rapidly reversed by removing the inhibitor from the cell media (169, 170). ALLN (**Figure 14**, [2]), was first described as an inhibitor of the calcium-dependent proteases known as calpains(171), but ALLN was also shown to have proteasome inhibitor activity, albeit with ~25-fold less selectivity for the proteasome to the calpains(168, 172). In contrast, MG132 (**Figure 14**, [1]), is more potent and selective for the proteasome than ALLN(173, 174). Ten-fold higher concentrations of MG132 are required to inhibit calpains than the proteasome(173, 174). Due its potency, commercial availability, and low cost, MG132 is a primary reagent used to study proteasomal involvement on cellular activity(168).

1.6.2.2 Peptide boronates and epoxyketones: Bortezomib and Carfilzomib

Unlike the peptide aldehydes, peptide boronates are more selective for the proteasome compared to other cellular proteases, take longer to dissociate from the proteasome, and are less prone to metabolic inactivation in cells(168). Bortezomib (**Figure 14**, [3]) was the first approved proteasome inhibitor for use as an anti-cancer treatment(175). Bortezomib binds reversibly to the proteasome but the drug-receptor complex remains stable for several hours(176, 177).

Peptide epoxyketones are the most selective proteasome inhibitors due to their selective irreversible binding to only the proteasome(168, 177). The covalent modification of the proteasome requires the generation of new proteasome subunits in order to regain function(168, 177). Carfilzomib (**Figure 14**, [4]), which has also been approved for anti-cancer treatment, is a

second generation proteasome inhibitor that is a modified version of an early naturally occurring epoxyketone that has been shown to bind irreversibly to only the proteasome and not target any other cellular proteases(177, 178). These more selective proteasome inhibitors are utilized to confirm the role of a suspected proteasome target identified by MG132.

1.6.3 Proteasomal Degradation induced by compounds

Bioactive small molecules can induce the proteasomal degradation of cellular proteins through both direct and indirect interactions(46, 130, 179–183). Small molecule binding to the Hsp90 family of chaperone proteins leads to degradation of various proteins due to their inability to fold properly, including signaling proteins (183). Small molecule binding of targets that induce proteasomal degradation of that specific target usually target enzymes or receptors. The FTY720 small molecule compound both inhibits and induces the proteasomal degradation of sphingosine kinase 1 (SK1)(181, 182). Chimeric small molecules have been developed that are capable of inducing the proteasomal degradation of select targets(179, 184). These compounds interact with the protein target but also contain a structural domains capable of recruiting specific E3 ligases for polyubiquitination(179, 184). The natural product compound OSW-1 induces the proteasomal degradation of the OSBP protein(46). This is a unique instance of a small molecule inducing the proteasomal degradation of a non-enzymatic receptor through a direct interaction(46).

1.6.4 Autophagy Overview

Autophagy is a cellular mechanism that is designed for degradation and recycling of cellular components(185). Autophagy is a highly conserved process in eukaryotes which(185). There are three distinct types of autophagy but macroautophagy is the most well studied form due to its involvement with in nutrient regulation and cell survival(186). The basic progression of autophagy occurs through induction and the formation of a phagosome to engulf the cargo

designated for recycling(187). The process of phagosome formation goes through an elongation step to form an autophagosome before eventually fusing with the lysosome(187).

Initiation of autophagy occurs when the kinase mTORC1 dissociates from the unc-51-like kinase 1 (ULK1) induction complex(188). Once dissociated, ULK1 becomes activated, translocating to autophagy initiation sites, and recruits the vacuolar protein sorting 34 (VPS34) complex consisting of Beclin-1, ATG14, and class III phosphatidylinositol 3-kinase(187). This new complex of ULK1 and recruits the ATG12-5-16 and ATG8-LC3 ubiquitin-like complexes to expand the phagophore until it fully matures(187). At this point, the autophagoasome closes and fuses with the lysosome(187).

1.6.5 Autophagy Induces and Inhibitors

Rapamycin (**Figure 15**) is an anti-fungal(189) and immunosuppressive(190) natural product compound originally from a soil sample bacterium in 1972(191). Identifying the cellular target of rapamycin lead to the discovery of the mammalian target of rapamycin (mTOR) proteins(191). mTOR forms two complexes in cells (TORC1 and TORC2)(191). As stated above, autophagy is induced when the mTORC1 complex dissociates from the initiation complex(191). Rapamycin is used to induce autophagy in cellular experiments(192, 193). In order to monitor the induction of autophagy and the autophagic flux triggered by rapamycin, the conversion of LC3-I to LC3-II and the subsequent degradation of LC3-II are cellular markers of autophagy(192, 194). In addition to LC3 monitoring, which is an indicator of early autophagy, the protein p62 is selectively degraded during autophagy, and p62 degradation is a marker of autophagic flux(192). Another common reagent used to measure autophagic flux is the inhibitor compound chloroquine (CQ) (**Figure 15**) (192). CQ blocks the fusion of the autophagasome with the lysosome and this

prevents the autophagocytic degradation of proteins, including the proteins used as markers of induction of autophagy (195).

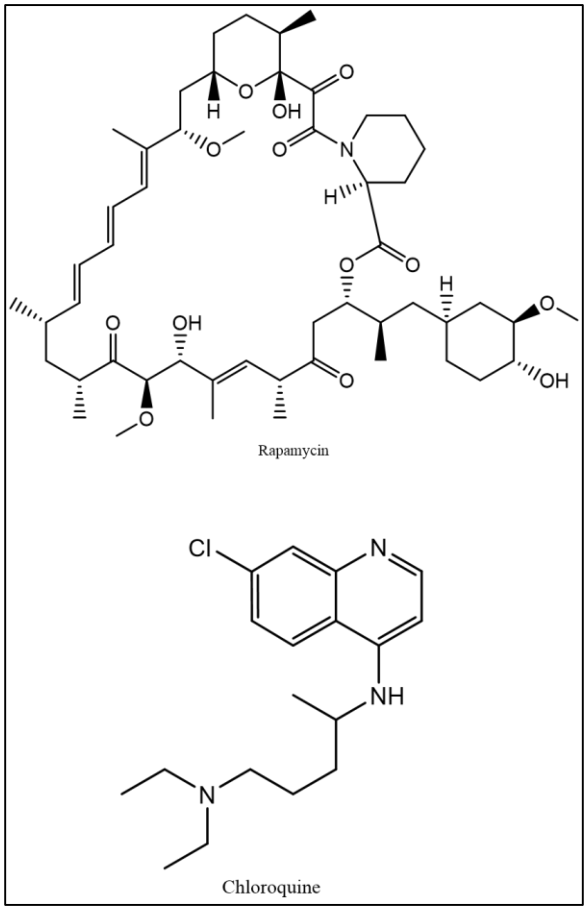

Figure 15: Structures of an Autophagy Induce and Inhibitor.

1.6.6 Cycloheximide

Cycloheximide (**Figure 16**) (CHX), originally isolated from bacteria, is an inhibitor of eukaryotic protein synthesis(196). CHX has blocks the elongation phase of translation by binding to the ribosome and inhibits the eEF2-mediated translocation step from the A to the P site(196, 197). The exact mechanism of CHX translation inhibition is still unknown, but it is thought that CHX requires a deacylated tRNA bound to the E site of the ribosome in order to exert its effects(196, 198). Due to this ability to inhibit protein synthesis, CHX is used as a cellular reagent to determine the half-life of proteins in cells(199).

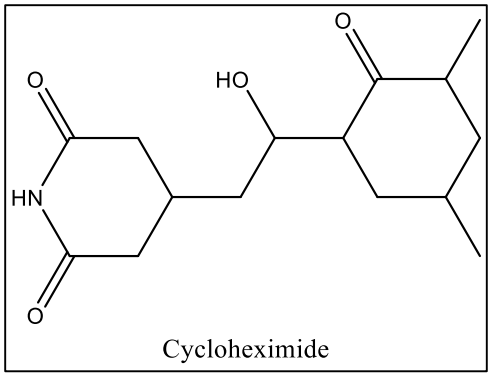

Figure 16: Structure of Cycloheximide.

Chapter 2: Persistent Reduction of Oxysterol-binding Protein Caused by Compound Treatment Induces Prophylactic Anti-Viral Activity

The following chapter is partially taken from the publication in ACS Chemical Biology by the author of this dissertation: Persistent, Multi-Generational Reduction of Oxysterol-Binding Protein Caused by Compound Treatment Induces Prophylactic Anti-Viral Activity. This was a collaborative work that consists of the following authors: Brett L. Roberts, Zachary C. Severance, Ryan C. Bensen, Anh T. Le, Naga Rama Kothapalli, Juan I. Nuñez, Hongyan Ma, Si Wu, Shawna J. Standke, Zhibo Yang, William J. Reddig, Earl L. Blewett, Anthony W. G. Burgett.

Mr. Zachary Severance conducted the experiments in **Figure 17**, **Figure 18**, **Figure 19** and **Figure 22** using the HEK293 and HeLa cell lines.

Mr. Ryan Bensen conducted the experiments in **Figure 17**, **Figure 18**, **Figure 22** and **Figure 23** using the HCT116 cell line.

Ms. Hongyan Ma conducted the bottom up proteomic MS experiment in **Figure 19**

Ms. Shawna Standke conducted the LCMS and SCMS experiments in **Figure 23.**

Dr. Earl Blewett conducted the anti-viral experiments in **Figure 24.**

2.1 Abstract

Oyxsterol-binding protein (OSBP) is the founding member of a highly conserved protein family found among eukaryotes that transports cholesterol and lipids among cellular membranes to maintain lipid homeostasis. OSBP has been implicated as a necessary host factor for viral replication among a wide variety of viruses, especially enteroviruses. The natural product OSW-1 has anti-viral properties due to its selective inhibition of OSBP function. We have discovered that short-non lethal doses of OSW-1 followed by removal of the compound can induce ~90% reduction of OSBP protein levels for multiple days in a variety of cell lines. We have termed these

experiments “washouts” and have shown that the persistent effect of the initial treatment is not due to residual compound lingering in the cells. The “washout effect” occurs in all cell lines tested, and can occur within as little as 45 minutes of exposure at near sub nanomolar doses. As expected, continual treatment of cells with OSW-1 leads to lowered viral titers of two clinically isolated enteroviruses. Surprisingly, washout treated cells showed anti-viral activity towards the viruses, despite the compound being removed from the cells 24 hours prior to infection. Our results show that OSW-1 could be a powerful new prophylactic anti-enteroviral by repressing the host protein, OSBP, for multiple days without noted toxicity.

2.2 Introduction

OSBP is a lipid transport protein that is able to bridge the ER and Golgi using its various targeting domains in order to exchange cholesterol for PI4P(35, 36) (see section 1.3.1 **OSBP**). The closest homolog of OSBP, ORP4, shares significant sequence similarity (**Figure 34**) but has select tissue expression and performs different biological functions(44, 54) (see section 1.3.2 **ORP4**). OSBP is known to be involved with various cellular signaling pathways(39, 40) (see section 1.3.1.1 **Cell Signaling Role**) while ORP4 has roles in cellular proliferation(17) (see section 1.3.2.3 **Role in Cellular Proliferation**). Despite the knowledge of OSBP/ORP4s role in specific cellular functions, close to nothing is known about their regulation within cells.

The natural product OSW-1 is a selective inhibitor of both OSBP and ORP4, which can induce proteasomal dependent degradation of OSBP over time(46) (see section 1.5.1 **OSW-1**). The effect of OSW-1 on ORP4 is not known, but it can be speculated that ORP4 is also degraded in a similar manner due to OSBP and ORP4 having dimerization domains(12) (see section 1.3.2.2 **Ligand Binding and Cellular Localization**). The mechanism of how OSW-1 induces the degradation of OSBP, and the duration of the degradation remains a mystery.

OSBP, and to a lesser extent ORP4, have been implicated as a necessary host protein required for viral replication(81) (see section 1.4.1 **OSBP Function in Virus Replication**). OSBP has been shown to be essential for *Enterovirus* replication, which are major public health menace(81, 82) (see section 1.4.1.2 **Enteroviruses**). OSW-1 has been confirmed as an anti-viral compounds through its inhibition of OSBP(82) (see section 1.5.1 **OSW-1**). This suggests that OSW-1 could be a potential therapeutic for *Enterovirus* species due to the degradation of a host protein that has been shown not to influence cell survival.

Herein we describe the discovery that the treatment of mammalian cells with a single, non-toxic dose of the OSW-1 compound induces a significant reduction of OSBP protein levels that lasts for several days after the brief exposure to the compound. The reduction of OSBP levels remains even after the intracellular soluble OSW-1 compound concentrations have dropped to undetectable levels, and these cells have undergone multiple rounds of cell division. Triggering the persistent reduction of OSBP levels with the OSW-1 compound reduces the replication of two Enterovirus pathogens 24 hours after the compound is removed from the cell media. The inhibition of viral replication by triggering the reduction of a required host protein through small molecule treatment could be a new modality of anti-viral prophylaxis and potential therapeutic development.

2.3 Results

2.3.1 Constant OSW-1 compound treatment leads to a differential time dependent reduction of OSBP and ORP4 protein levels.

The OSW-1 compound binds to both OSBP and ORP4 with similar affinity(46). Additionally, OSW-1 compound treatment of cells is reported to cause a loss of OSBP in a time dependent manner(46), but effects of OSW-1 treatment on the pro-proliferation protein ORP4 are unknown. 1 nM OSW-1 compound treatment showed >90% reduction of OSBP levels after 24

hours while also showing an average of ~50% reduction of ORP4 levels during the same time frame (**Figure 17A**). This result, as far as we are aware, is not only the first instance where cellular levels of ORP4 protein have been analyzed after treatment with OSW-1 compound, but also the first to show ORP4 is lost in a similar manner as OSBP. Although novel, this event is not surprising since prolong exposure to the OSW-1 compound has been reported to lead to apoptosis(200, 201), mitochondrial dysfunction(130), and intracellular calcium release(130), which are consistent with ORP4 functions(48, 54) and suggests the anti-cancer activity of the OSW-1 compound is through ORP4 targeting and degradation rather than OSBP disruption.

Since knockdown of ORP4 was shown to cause cell growth arrest in multiple cells that were used in the initial experiment(17), continual treatment with OSW-1 compound was not desirable. Our results indicated that the degree to which both OSBP and ORP4 are affected by the compound after 24 hours is vastly different (**Figure 17A**), so we determined if there was a differential loss of the proteins over time. We found that treatment with 1 nM of the OSW-1 compound led to significant loss of OSBP in all cell lines tested at 6 hours, with levels continuing to drop up until the 24-hour time point (**Figure 17B**). In contrast, ORP4 levels are more variable overall, but do not show significant loss in most of the cell lines tested until the 24-hour point (**Figure 17B**).

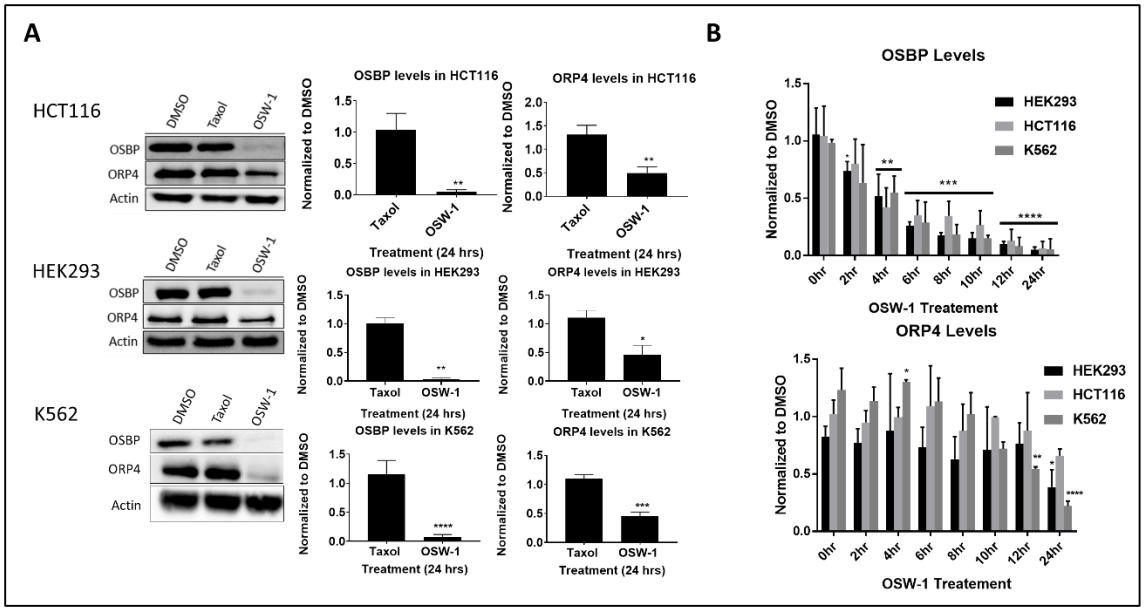

Figure 17: Continual OSW-1 compound treatment leads to differential loss of OSBP and ORP4. (A) 1 nM of OSW-1 for 24 hours shows significant loss of both OSBP and ORP4. (B) 1 nM of OSW-1 shows significant loss of OSBP after 4 hrs of treatment with continuing loss up to 24 hrs while ORP4 does not show significant loss until after 12 hrs. All values are mean ± SD (n=3). HCT116 and HEK293 treatments and analysis were done by Mr. Ryan Bensen and Mr. Zach Severance. (Full blots in **Figure 35, Figure 36 & Figure 37**)

2.3.2 Short, non-toxic doses of OSW-1 compound leads to prolonged OSBP loss in multiple cell lines up to 72 hours after compound has been removed

Following up on the differential loss of OSBP over ORP4 (**Figure 17B**), we determined the persistence of OSBP loss after 6 hours of OSW-1 compound treatment, which led to an unexpected discovery. Initial results showed that 6-hour treatment followed by removal of the compound led to lower OSBP protein levels with diminishing signal up to 4 hours post removal at which point OSBP protein was below 10% of the DMSO control in HEK293 cells (**Figure 39A**). A more prolonged recovery time tracking experiment (0-24 hours post compound removal) showed no recovery of the protein (**Figure 39B**). To rule out any possibility of remaining OSW-1 compound, a standard procedure was implemented which is termed washout experiments. In the

OSW-1 compound washout experiments: 1) media containing OSW-1 compound is added to cells; 2) at the specified time, the compound-containing media is removed; 3) the cells are gently washed three times in complete media to remove any residual OSW-1 compound; and, 4) the cells are reincubated and recover from treatment in compound-free media for the indicated period of times post-washout (pWO). Using the OSW-1 washout experiments, we found that 1 nM OSW-1 compound treatment for 6 hours followed by washout led to 90% reduced OSBP levels for multiple days (48-72 hrs) after the compound has been removed in multiple cell lines (**Figure 18**). In contrast, the taxol control treatment had no effect on OSBP protein levels (**Figure 18**).

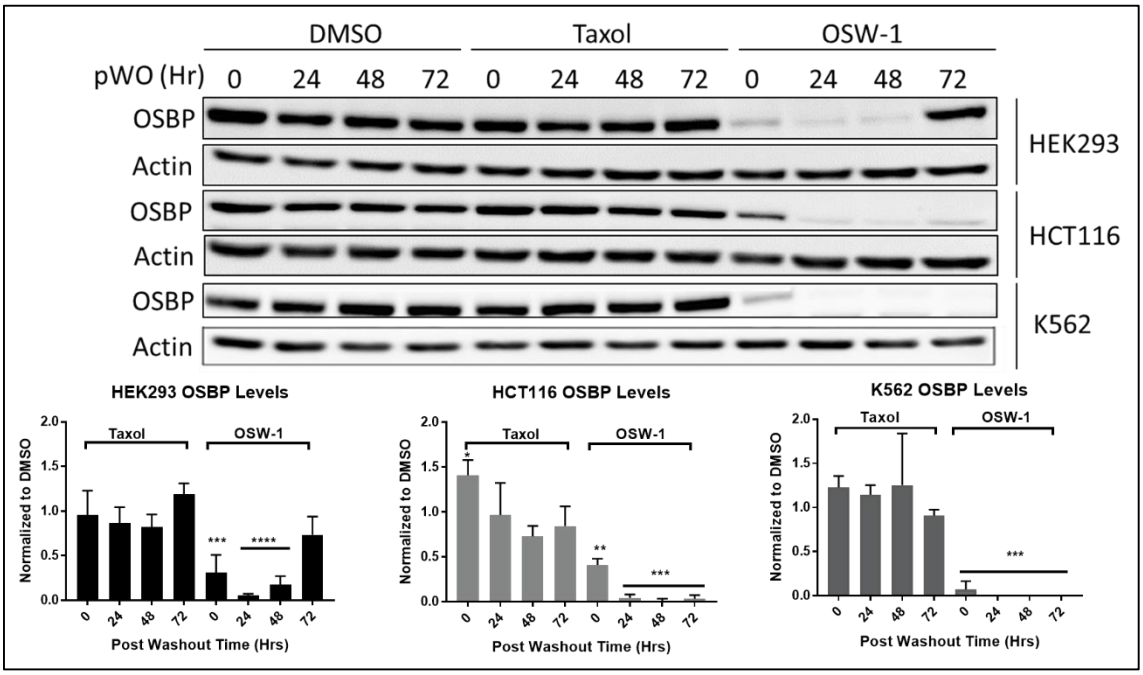

Figure 18: Short, non-lethal doses of OSW-1 compound leads to prolonged OSBP loss in multiple cell lines up to 72 hours after compound has been removed. All cells tested were subjected to 1 nM OSW-1 compound, 1 nM Taxol, or DMSO treatment for 6 hours followed by washout and lysed at the indicated pWO time. All values are mean ± SD (n=3). HCT116 and HEK293 treatments and analysis were done by Mr. Ryan Bensen and Mr. Zachary Severance. (Full blots in **Figure 38**)

2.3.3 Loss of OSBP due to OSW-1 washout is not an artifact

To confirm that OSBP levels were reduced due to cellular mechanisms, we performed a series of experiments to eliminate possible artifacts. First, to make sure that loss of OSBP was not due to the freeze thaw (AC) lysis procedure, a chemical lysis with mammalian protein extraction reagent (Mper) lysis method was used due to its ability to extract ~25% more protein(202) (**Figure 19A**). Both lysis methods confirm the loss of OSBP to similar levels in multiple cell lines. We utilized multiple antibodies recognizing different OSBP epitopes to confirm the reduction of OSBP (**Figure 40**). The two additional antibodies used show similar OSBP levels in both DMSO and OSW-1 compound treated cells. In addition to Western blot confirmation of OSBP loss, we employed bottom-up proteomic mass spectrometry to confirm the reduction of OSBP levels. A two-dimensional low/high pH HPLC separation of the trypsin-digested lysates was employed to allow for the detection of the low abundance OSBP-peptides without enrichment or purification(203). The proteomic mass spectrometry analysis was done by the research group of Professor Si Wu in the Department of Chemistry and Biochemistry at the University of Oklahoma. This analysis shows a significant reduction in the detected OSBP peptides in the OSW-1 washout cells as compared to DMSO washout cells (**Figure 19B & C**), which confirms the reduction of OSBP levels detected by Western blotting (**Figure 18**).

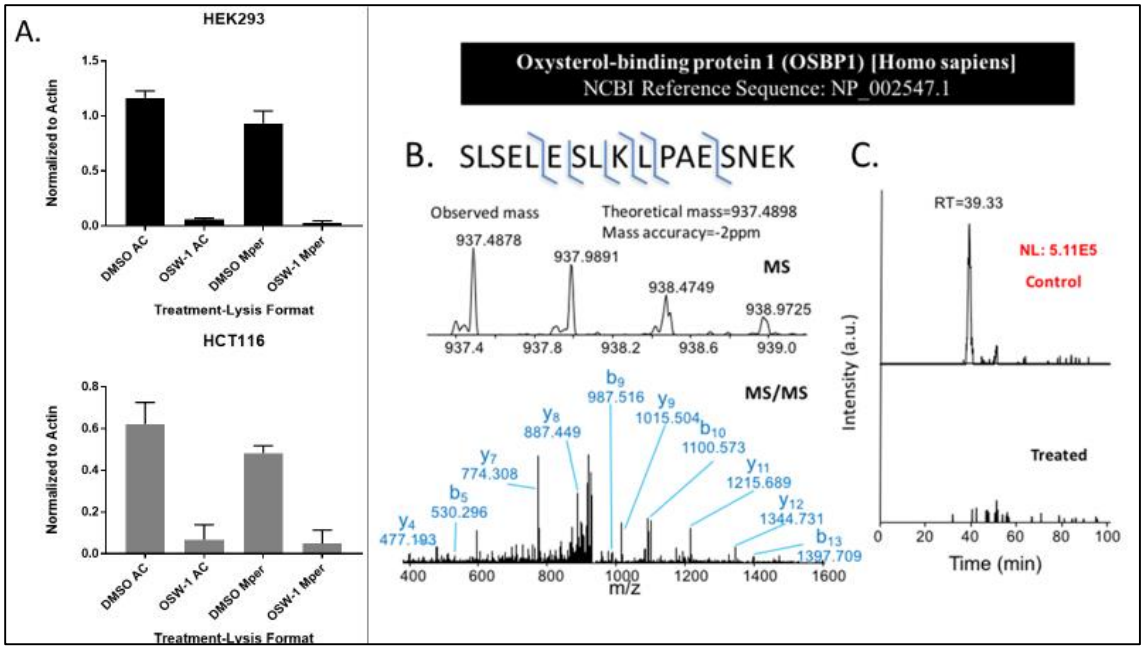

Figure 19: Loss of OSBP due to OSW-1 compound washout is not an artifact. (A) Freeze thaw (AC) and mammalian protein extraction reagent (Mper) lysis methods show similar OSBP loss in 1 nM OSW-1 compound washout treated cells 24 hours pWO as quantified by Western blot analysis. (B) Bottom up proteomic mass spectrometry analysis of vehicle control or 1 nM OSW-1 compound treated for 6 hours followed by washout and a 24-hour recovery period. (C) Shows loss of detectable OSBP peptide (i.e. peak with retention time of 39.33 min) in HEK293 washout cells as compared vehicle control. (B) and (C) lysates and analysis performed by Mr. Zachary Severance and Ms. Hongyan Ma; Ms. Ma is a graduate student in the lab of Dr. Si Wu, Department of Chemistry and Biochemistry, Univ. of Oklahoma. (Full blots in **Figure 41**). The author had no contribution to producing the bottom up MS results.

2.3.4 Cellular localization of OSBP confirms OSBP loss in vivo during washout recovery.

To verify the loss of OSBP other than by Western blotting, we utilized immunofluorescence microscopy in HCT116 cells. OSBP is predominately located at ER/Golgi membrane contact sites(35, 36, 128, 204) Cellular treatment with the OSW-1 compound is known to alter the OSBP localization in the cell(46). The imagining experiments used the OSBP antibody and an antibody recognizing the trans Golgi marker TGN46, as well as a nuclear stain. Both continual treatment and washout treatment showed reduced OSBP levels (**Figure 20**). DMSO treated cells showed OSBP localized to the TGN46 marker in a perinuclear fashion and treatment

with OSW-1 compound led to relocalization into a punctate cluster (**Figure 20**). Continual treatment with the OSW-1 compound showed OSBP clustering within 2 hours followed by diminishing OSBP signal. Very little OSBP signal is evident at 24 hours (**Figure 20A**), which is consistent with the Western blot OSBP levels upon continuous OSW-1 compound treatment (**Figure 17B**). The TGN46 Golgi signal also decreased and became dissociated from some of the OSBP starting at 12 hours of continuous OSW-1 compound treatment. Similarly, the OSW-1 compound washout cells showed a similar clustering pattern at 0-hour post-washout recovery (6-hour straight treatment) (**Figure 20B**). The OSBP signal remains substantially reduced 24 hours post-washout. The localization of the TGN46 signal changed from the DMSO-treated pattern at 0-4 hours post-washout, but the TGN46 signal returns to a perinuclear pattern staining starting at 8 hours post-washout. The low OSBP signal also returns to a perinuclear colocalization pattern with TGN46 at 12 and 24 hours post compound removal (**Figure 20B**). These results suggest that the

Golgi has returned to a normal localization pattern post-washout of the OSW-1 compound

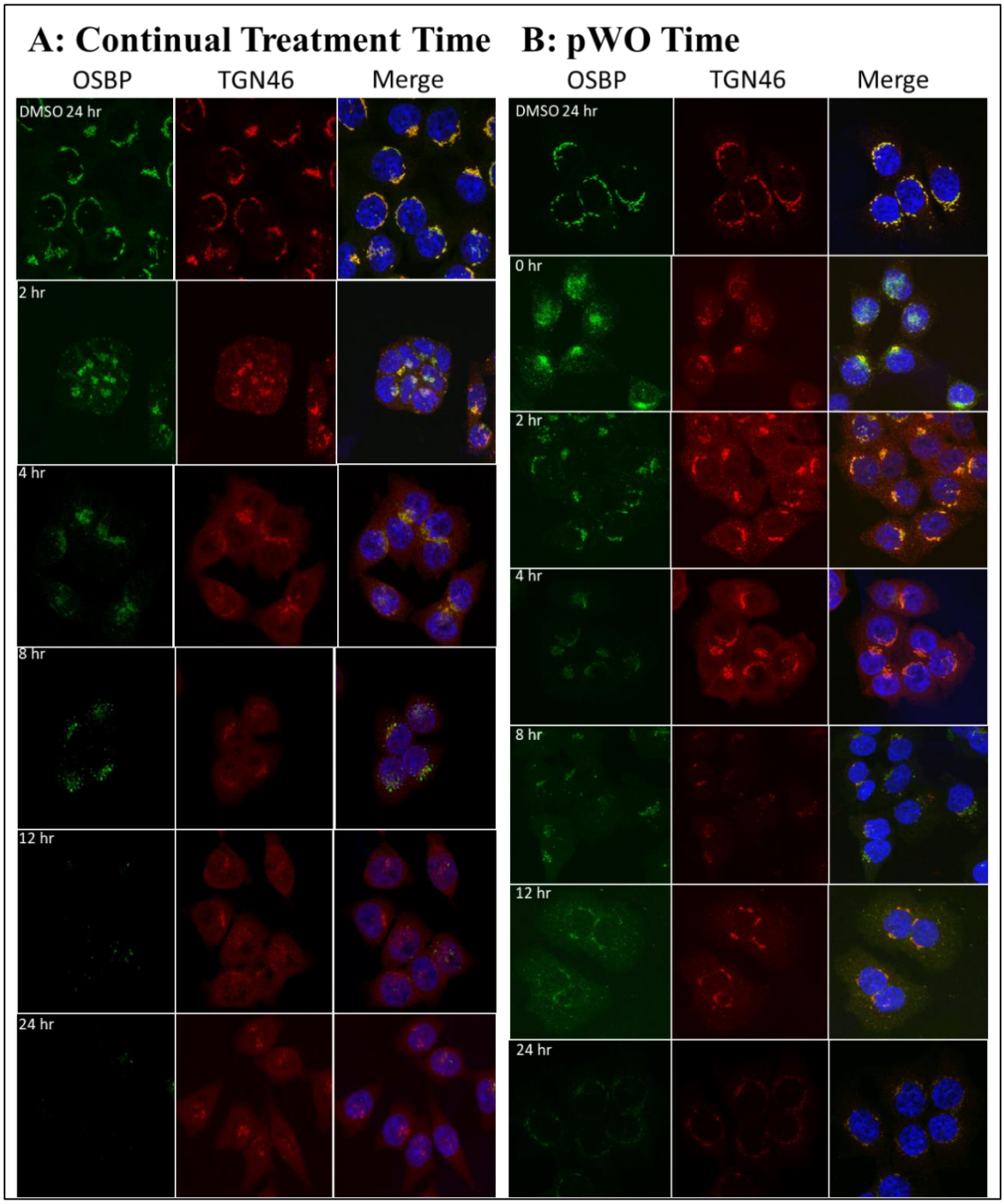

Figure 20: Cellular localization of OSBP confirms OSBP loss in vivo during washout recovery. (A) Continuous 1 nM OSW-1 compound treatment in HCT116 cells shows localization of OSBP to the Golgi followed by loss of both OSBP and Golgi signals. (B) OSW-1 washout treatment (i.e., 1 nM for 6 hours, then recovery post-washout for the indicated times) reduces OSBP and Golgi signals but the reduced OSBP and Golgi signal localization patterns are similar to DMSO-treated by 24-hour recovery.

2.3.5 OSW-1 compound washout cells show no signs of cytotoxicity, cell growth arrest, or morphological changes.

The effect of short-term, transient and low dose OSW-1 treatment on cellular viability and morphology was determined. The cellular viability of washout cells was tracked using Trypan blue staining over the 72-hour recovery course in HCT116 and HEK293 cell lines (**Figure 21A**). The viability of both cell lines showed no change in comparison to vehicle control washout cells. As a second confirmation that the washout cells were not affected by long-term OSBP loss, we utilized cellular viability imaging using Calcein AM and Hoechst 33342 staining of HEK293 cells (**Figure 21B**). There was no apparent cytotoxicity based on the staining patterns and overall cellular growth/morphology between DMSO and OSW-1 compound washout cells was similar. In contrast, continual treatment of OSW-1 compound over 72 hours showed apparent cytotoxicity after 24 hours of treatment with most of the cells dead by the 72-hour mark (**Figure 42A**). This evidence shows that cells continue to function normally despite long-term OSBP loss and that OSBP loss is sustained through 2-3 rounds of cellular division.

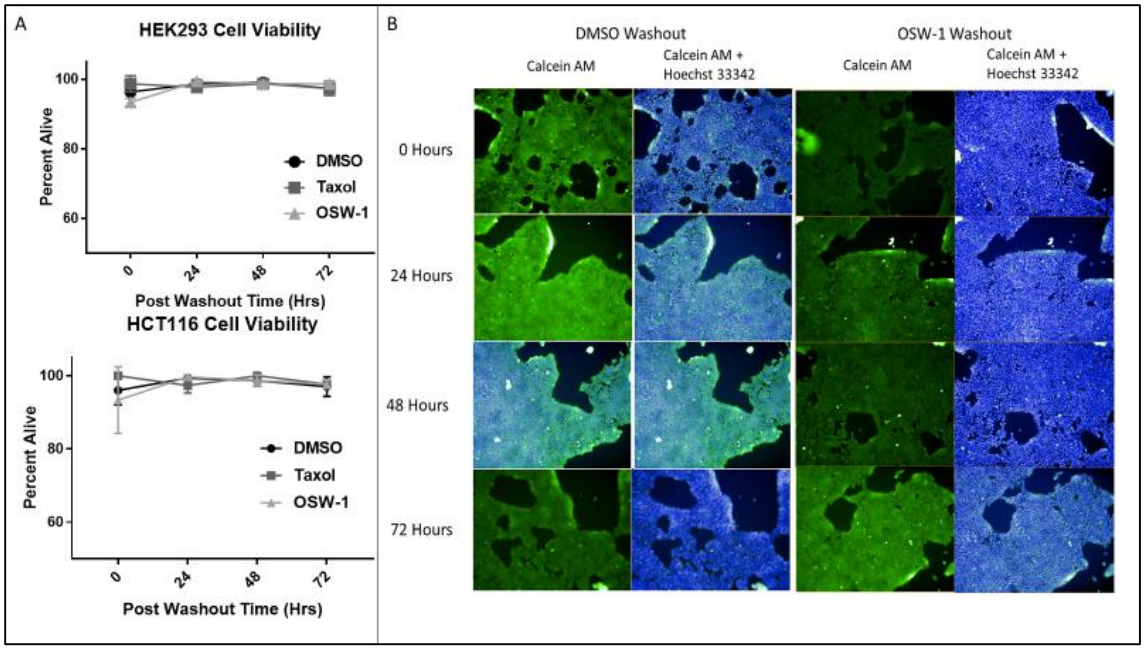

Figure 21: OSW-1 compound washout cells show no signs of cytotoxicity, cell growth arrest, or morphological changes. (A) Trypan blue staining of HEK293 and HCT116 0-72 hours pWO of 1 nM OSW-1, 1 nM taxol, or DMSO. (B) Calcein AM and Hoechst 33342 staining of 0-72 pWO of 1 nM OSW-1 or DMSO in HEK293 cells using Operetta High-Content Imaging System.

2.3.6 The long-term reduction of OSBP levels upon OSW-1 compound washout treatment occurs in multiple cell lines and with as little as 1 hour of exposure.

The effect on OSBP levels of OSW-1 washout treatment in other human cultured cell lines from various tissue types was determined. The cancer cell lines (HCT116, HeLa, K562, and MCF-7) as well as the normal cell lines (HEK293 and MRC5) tested showed significant loss of OSBP signal after 24 hours pWO with an initial 1 nM, 6-hour OSW-1 compound treatment (**Figure 22A**). The cell line that showed the least sensitivity to the washout, but was still significantly reduced, was the diploid lung-fibroblast MRC5 line which has a finite passaging of 42-46 replications(205).

Interestingly, no ORP4 signal could be detected by Western blotting in the MRC5 cell line, which could explain the finite replication ability of these cells.

Having established the OSBP reduction upon OSW-1 compound treatment in multiple cell lines, the minimal time and concentration of OSW-1 washout treatment to induce the OSBP reduction was determined. A 1 hour treatment of 1 nM OSW-1 compound, followed by the compound's washout removal, was sufficient to induce significant OSBP reduction 24 hours pWO in all cell lines tested (**Figure 22B**). Following this result, the time was reduced to check the exposure on the minute scale. We found that 45 minutes of exposure with 1 nM OSW-1 compound led to significant reduction of OSBP 24 hours pWO in all cell lines tested (**Figure 22C**). Additionally, 15 minute exposure in two of the cell lines was sufficient to cause ~50% reduction of OSBP 24 hours pWO. Additionally, compound concentration was tested at 6 hours of exposure and it was determined that 0.5 nM concentration could significantly lower OSBP levels similar to 1 nM, but lower concentrations failed to induce the response (**Figure 46**). These experiments show

that the OSW-1 compound "washout effect" is triggered by very low and very brief OSW-1 compound exposures.

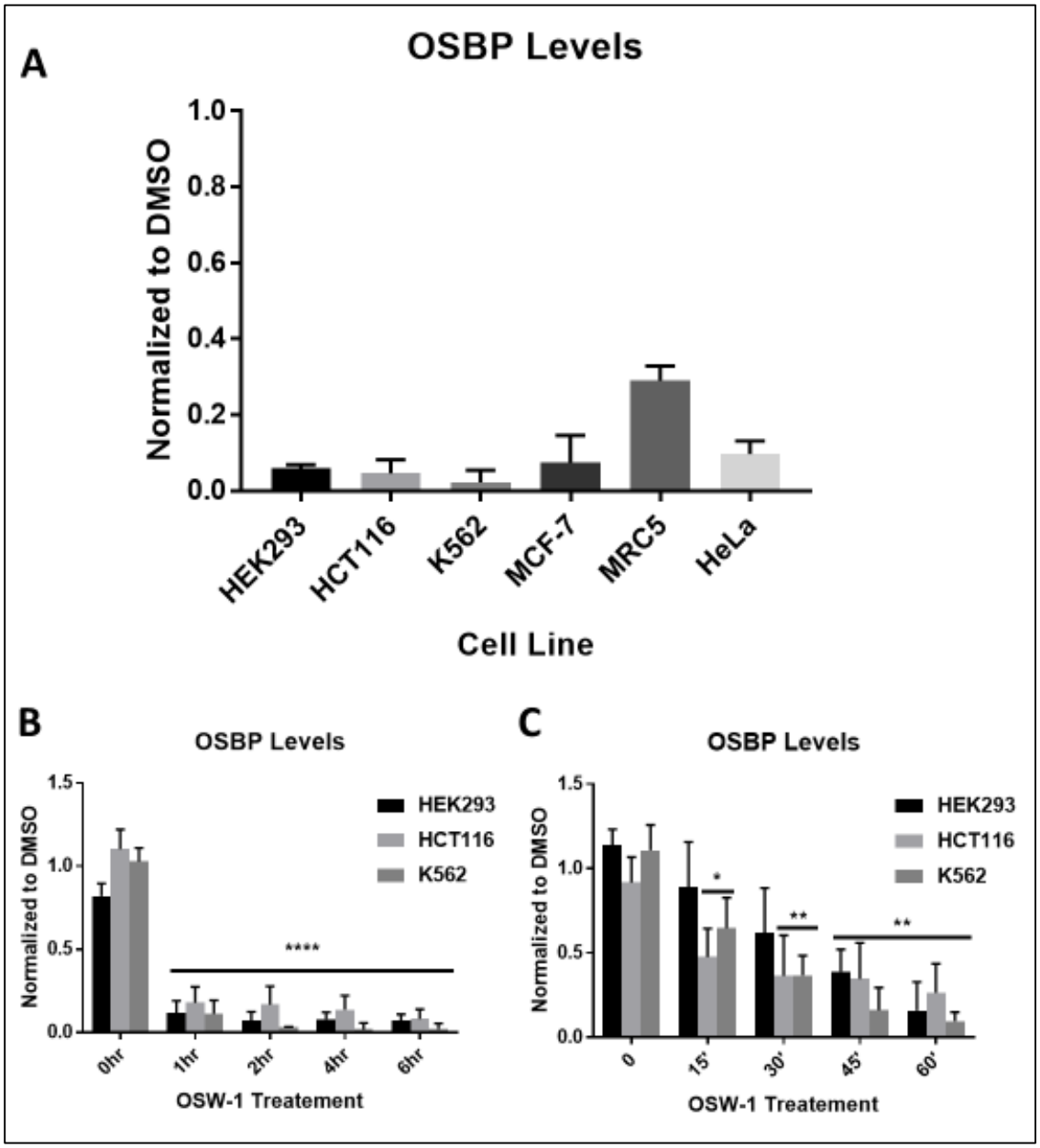

Figure 22: The long-term reduction of OSBP levels upon OSW-1 compound washout treatment occurs in multiple cell lines and with as little as 1 hour of exposure. (A) All cell lines tested with 1 nM OSW-1 compound followed by 24-hour recovery show significant OSBP loss. (B&C) 1 nM treatment of OSW-1 for the indicated times, followed by 24-hour recovery shows significant loss of OSBP with as little as 30 minutes of treatment in various cell lines. HCT116, HEK293 and HeLa treatments and analysis were done by Mr. Ryan Bensen and Mr. Zachary Severance. (Full blots in **Figure 43, Figure 44** & **Figure 45**).

2.3.7 OSW-1 compound washout prolonged reduction of OSBP is not due to residual compound

We reasoned that the observed OSBP reduction caused by the OSW-1 compound washout was not likely caused by residual compound present in the cell media or cell culture plastic. However, to verify this we utilized the suspension cell line K562, following OSW-1 treatment, allowed for complete transfer of cells to new plasticware devoid of any OSW-1 as part of the washout condition. Further, to determine if the OSW-1 compound remained in cells at biologically relevant concentrations following the washout condition, we used two complementary mass spectrometry analytical techniques to measure intracellular OSW-1 levels. We first used quantitative LCMS measurements using a deuterated OSW-1 compound as an internal standard to measure OSW-1 compound from HCT116 cell lysates (**Figure 23A** & **Figure 47**). The intracellular soluble non-protein bound OSW-1 compound concentration of HCT116 cells treated for 1 hr with 100 nM of the compound was 1.74 ± 0.74 μM (**Figure 23C**). Post-washout, followed by a 24-hour recovery, the intracellular OSW-1 compound concentration was below the measurable threshold of ~100 pM (**Figure 23A** & **Figure 48**).

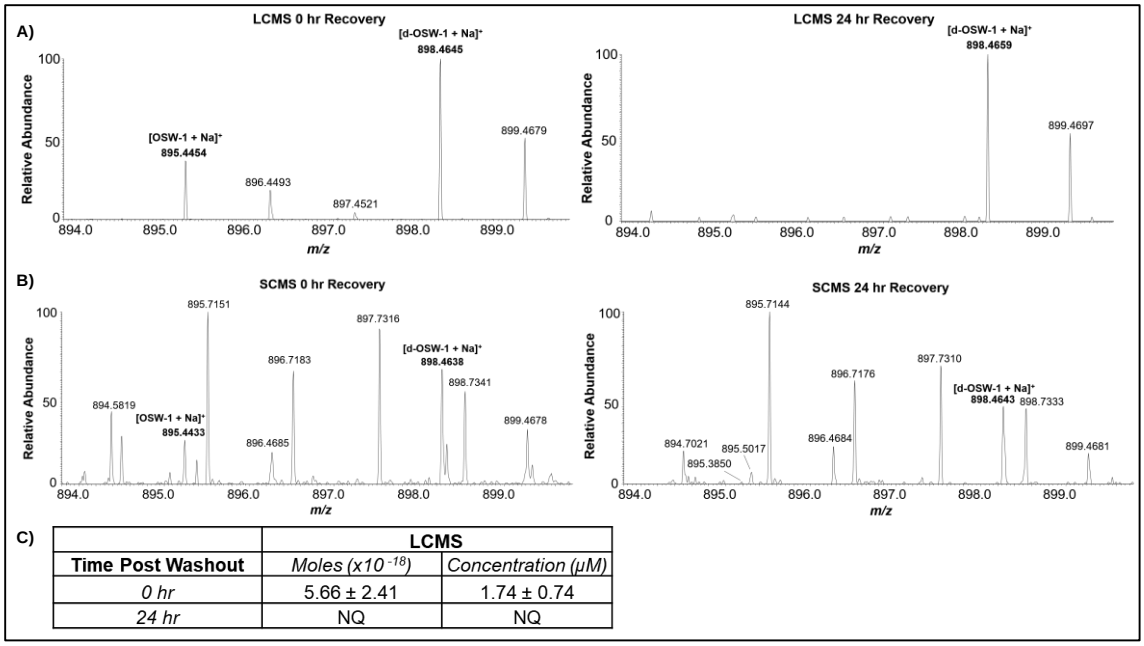

C)

	LCMS	
Time Post Washout	*Moles (x10 $^{-18}$)*	*Concentration (μM)*
0 hr	5.66 ± 2.41	1.74 ± 0.74
24 hr	NQ	NQ

Figure 23: Mass spectrometry quantification shows intracellular OSW-1 concentrations are reduced to non-detectable levels 24 hours post washout (pWO). (A) Liquid Chromatography Mass Spectrometry (LCMS) quantification of OSW-1 at 0 and 24 hours pWO of a 100 nM treatment of HCT116 cells for 1 hour. 50 nM of the deuterated OSW-1 analog is used as an internal standard to allow for LCMS compound quantification. (B) Single Cell Mass Spectrometry quantification (SCMS) spectra of intracellular OSW-1 detection in HCT116 cells following the 1 hour, 100 nM OSW-1 treatment at 0 and 24 hours pWO. A minimum of 30 cells were analyzed for each of the experimental conditions. (C) LCMS single cell intracellular quantification of the amount of OSW-1 (moles) and estimated concentration utilizing the total cell count and averaged cellular volume. Average of three independent biological replicates reported (n=3). NQ= Not Quantifiable. Experiments and analysis were conducted by Mr. Ryan Bensen and Ms. Shawna Standke. The author had no contribution to producing the results.

Single cell mass spectrometry (SCMS) is a method that can quantify intracellular concentrations of compounds in a similar manner as LCMS but does not require any sample preparation that could lead to loss of analytes due to cell lysis(206–209). Using this semi-quantitative technique, we confirmed the loss of detectable intracellular OSW-1 compound after the washout conditions (**Figure 23B**, **Figure 49** & **Figure 50**). These results showed that no OSW-1 compound is present at biologically-active concentrations to induce the cellular changes seen during the washout

experiments (**Figure 19** & **Figure 22**), but that a persistent cellular mechanism triggered by OSW-1 treatment is responsible for the long-term reduction of OSBP levels.

2.3.8 OSW-1 compound washout induces prophylactic antiviral response to two clinical isolates of Enteroviruses.

As stated before, OSBP is required for the cellular replication of viruses belonging to the *Enterovirus* genus, which includes many human pathogens (1.4.1.2 **Enteroviruses**). OSW-1, as well as other OSBP binding compounds, has been shown to inhibit the replication of multiple Enterovirus viruses in cells (1.5 **ORPphillins and OSBP/ORP4)**. Consistent with published results, continuous treatment of OSW-1 compound inhibits the viral replication of two clinical isolates of pathogenic *Enterovirus* viruses, Coxsackievirus A9 and Echo2, in HeLa cells in a concentration-dependent manner (**Figure 24A**). Continual OSW-1 compound treatment reduced the viral titer of 10-hour viral infection in HeLa cells approximately ~10,000 fold (**Figure 24A**). HeLa cells subjected to a 6-hour OSW-1 compound treatment followed by the washout protocol and a 24 hour recovery in compound-free media showed a reduction of viral titers of approximately 100-fold for the Echo2 virus and ~1000-fold for the Coxsackievirus 9A virus (**Figure 24B**). Based on the quantitative mass spectrometry of intracellular OSW-1 compound levels 24 hours pWO (**Figure 23**), this observed prophylactic anti-viral activity in the OSW-1 compound washout experiment is not likely due to residual OSW-1 compound. Instead, the anti-viral activity is likely due to a sustained reduction of OSBP levels pWO as seen in HeLa cells where 1 nM OSW-1 compound washout reduced OSBP levels by ~90% 24 hours pWO (**Figure 22A**).

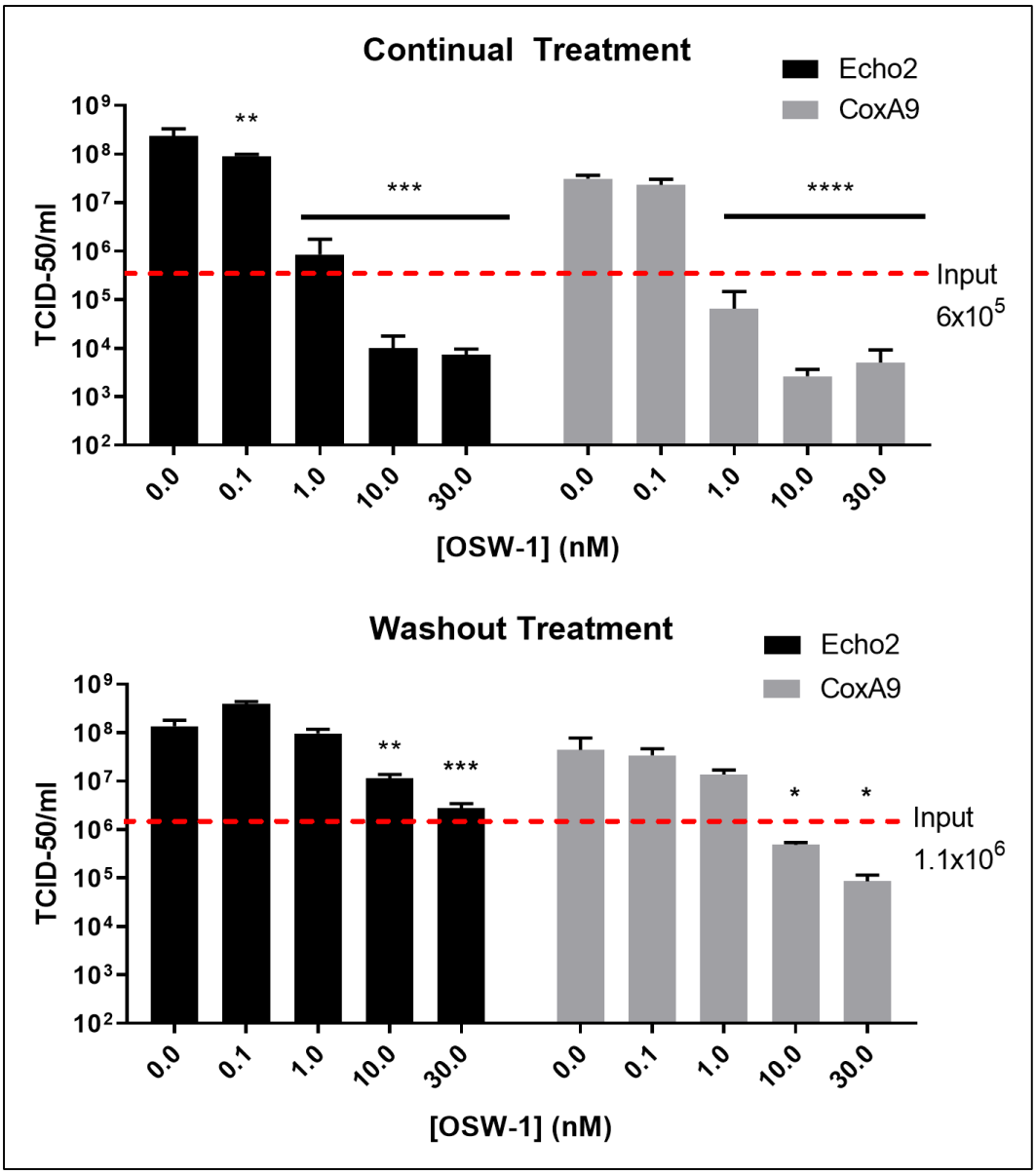

Figure 24: OSW-1 compound washout induces prophylactic antiviral response to two clinical isolates of Enteroviruses. (A)Viral titers of infected HeLa cells incubated in the presence of the OSW-1 compound. Cells were treated with the indicated concentrations of OSW-1 compound for 6 hours, followed by viral infection for 30 min (MOI of 1.0), followed by re-incubation for 10 hours with OSW-1 compound (B) Viral titers in OSW-1 compound washout HeLa cells. Cell were treated with the indicated concentrations of OSW-1 compound for 6 hours, compound was removed, cells were allowed to recovery for 24 hours in compound-free media. Then, cells were infected for 30 min with virus (M.O.I.=1.0) followed by 10-hour incubation in compound-free media. All viral results were collected by Dr. Earl Blewett. The author had no contribution to producing the results

2.4 Discussion

The results show that the OSW-1 compound cellular treatment induces the reduction of both OSBP and ORP4 in a similar manner, but on different time frames and to different amounts (**Figure 17**). OSBP is degraded much faster and to a much more pronounced degree than ORP4; ORP4 levels only decrease after 24 hours of continuous treatment (**Figure 17B**). Importantly, the reduction of ORP4 levels at 24 with 1 nM continuous OSW-1 treatment is consistent with observed cytotoxicity in HEK293 cells (**Figure 42A**). Given that we and others show loss of OSBP does not result in cytotoxicity(46) (**Figure 21**), these results would suggest that OSBP could act to absorb the OSW-1 compound preventing the compound from interacting with ORP4. As the OSBP levels rapidly drop due to OSW-1 compound, the compound could then interact with ORP4 causing the cytotoxicity.

Our results show that short non-toxic cellular treatment with the OSW-1 compound followed by removal of the compound from the cells, leads to a sustained loss of OSBP (~90%) lasting 48-72 hours after the compound treatment stopped. This OSBP reduction upon the OSW-1 washout happens in multiple cell lines and persists through multiple cell divisions (**Figure 19**). The OSW-1 compound washout cells do not show any signs of growth arrest, cytotoxicity or changes in cellular morphology (**Figure 21**). The OSW-1 compound interacts with OSBP and ORP4 with comparable affinities, as measured through *in vitro* competitive binding of 25-hydroxycholsterol (**Figure 51**). ORP4 protein levels do not change significantly upon the OSW-1 washout conditions, and this is consistent with the lack of induced cytotoxicity (**Figure 42B**). Additionally, morphology of the Golgi network returns to a normal pattern 12 hours post-washout during the washout recovery and the trans Golgi network appears to recover 12 hours pWO (**Figure 20**).

The lack of cytotoxicity in the OSW-1 compound after washout from cells, despite the sustained loss of OSBP suggests either OSBP is not necessary in cellular growth or that there is a compensatory mechanism that possibly works through the functional redundancy of the OSBP/ORP family. In contrast to this, OSBP function is necessary for the replication of various human pathogens across different viral families (1.4.1 **OSBP Function in Virus Replication**). OSW-1 treatment has been shown to cause inhibition of *Enterovirus* replication(81, 82) and we have shown that continuous treatment of cells with OSW-1 inhibits two clinical isolates of *Enteroviruses* (**Figure 24A**). We also show that the OSW-1 compound "washout effect" induces a prophylactic antiviral response to two clinically isolated *Enterovirus* species (**Figure 24B**). This is the first time a broad-spectrum, prophylactic anti-viral response is reported through targeting a host protein. This suggests that OSW-1-derived compounds triggering the long-term reduction of OSBP levels is a discovery that has clear therapeutic potential.

2.5 Conclusion

The discovery that brief, transient OSW-1 compound treatment induces a long-term reduction of OSBP levels is a novel and potentially significant discovery. The compound induced OSBP reduction prevents *Enterovirus* replication in cells. This novel prophylactic, broad-spectrum anti-viral activity presents a new approach to potentially preventing and treating infections against a wide range of important human viral pathogens that currently have no approved preventable or direct treatment. New classes of OSW-1-derived compounds capable of selectively binding OSBP and not ORP4 would be critical chemical probes in defining the regulation and anti-viral therapeutic potential of compound-induced OSBP repression. Such OSBP-specific, noncytotoxic, small molecule effectors could be potentially developed to inhibit a broad spectrum of severe human pathogenic viruses that currently cannot be prevented or directly treated.

2.6 Methods

2.6.1 Cell Lines and Viruses

HEK293 STF (ATCC CRL-3249) and HeLa (ATCC CCL-2) were cultured in DMEM (Thermo 11995073) supplemented with 10% Hyclone (Fisher Sci SH3006603) and 1% penicillin-streptomycin (Thermo 15140122). HCT116 (ATCC CCL-247) was cultured in McCoy 5A media (Thermo 16600108) supplemented with 10% Hyclone and 1% penicillin streptomycin. K-562 (ATCC CCL-243) was cultured in RPMI 1640 (Thermo 22400105) media supplemented with 10% Hyclone and 1% penicillin streptomycin. MCF-7 cells were a gift from R. Cichewicz (University of Oklahoma, Norman) and cultured in MEM (Thermo 11095114) media 10% Hyclone, 1% penicillin streptomycin and 0.2 mg/mL insulin (A11382II). MRC-5 cells were a gift from E. Blewett (Oklahoma State University- Center for Health Sciences, Tulsa) and cultured in MEM media supplemented with 10% Hyclone and 1% penicillin streptomycin. RD, (rhabdomyosarcoma) cells (ATCC-CCL-136) were cultured in DMEM (Fisher Sci SH30081.0) with 10% FBS (Atlanta Biological S11550) and 1% penicillin-streptomycin (Gibco 15140-122). Coxsackievirus A9 (strain CoxA9-01) and Echovirus 2 (strain Echo2-01) were obtained from the Oklahoma State Department of Health Laboratory. They are clinical isolates, obtained from OK residents and typed by the OK State Department of Health and/or the Center for Disease Control and Prevention. All other identifiers have been stripped off. These viruses were passaged twice in RD cells, aliquoted in 1.0 mL amounts and stored in complete medium at -80 ºC. Each virus was titered on RD cells using a 50% tissue culture infective dose (TCID-50) assay(210). To allow a multiplicity of infection (M.O.I.) to be determined, a conversion factor of 0.7 was used to change TCID-50 to plaque forming units (pfu)/ml.

2.6.2 General Cell Culture

All mammalian cell lines were cultured at 37 ºC in 5% CO2. All handling of the mammalian cell culture was performed in a standard tissue culture hood using standard aseptic technique. Cell lines were cultured in the complete media described above. Cell culture stocks were aliquoted in complete media with 10% DMSO in 2 mL cryogenic vials (Corning 430659) and stored in liquid nitrogen vapor phase. Before beginning a new culture, the freezer stocks were thawed, diluted in 9 mL complete media and plated in Nunclon Delta 10 cm^3 dishes (VWR 10171744) or T25 flask (CellStar 690160) for

suspension cell lines. After allowing ~16 hours for the revived cells to attach, the DMSO containing media was replaced with DMSO free complete media. All revived cultures were split at least twice prior to use in an experiment. Cell cultures were restarted approximately every 3-4 weeks. All cell based experiments reported used multiple restarted cell cultures in the independent experiments that make up the replicate results. For experiments, cell cultures were used with a confluency of ~70%. The cell cultures were not allowed to ever become superconfluent, and the cellular morphology and proliferation rate of the cell culture was carefully tracked to identify any abnormalities; any cell culture showing the abnormalities were discarded and the cell line restarted from frozen stocks. For experiments, cells were allowed to recover from splitting and replating a minimum of 16 hours prior to the start of an experiment.

The adherent mammalian cell lines are split every ~3 days with the following general procedure: the complete media is removed via aspiration and the cells are gently washed with 5 mL of 1X PBS. TrypLE^{TM} trypsin reagent (2.5 mL for 10 cm2 plate) is added and incubated for approximately 10 min at 37 ºC. After 10 mins 7.5 mL of the complete culture media is added to

inactivate the TrypLE™ reagent. Cells were counted using a TC20™ Automated Cell Counter (BioRad), by combining 10 µL of cell solution with 10 µL Trypan Blue stain (Thermo 15250061).

The K562 leukemia suspension cell line was handled as described for the adherent cell lines except for the splitting and seeding procedure. For K562 cells, the cells were centrifuged at 200 x g for 5 minutes and the media was aspirated from the cell culture using care so as not to disturb the cell pellet and replaced with 10 mL of complete media. The cell pellet was then resuspended and diluted to the desired seeding density using complete media.

2.6.3 OSW-1 Compound

The OSW-1 compound used was obtained through total synthesis in the Burgett lab or from isolation from the natural source. OSW-1 used in the experiments was of >95% purity as determined with ^{1}H-NMR and LCMS analysis. Solid OSW-1 compound was dissolved in analytical grade DMSO solution to produce 10mM stocks for experimentation. The 10 mM OSW-1 stock solution was aliquoted into Eppendorf brand 1.5 mL centrifuge tubes; Each individual 10 mM OSW-1 aliquot was thawed no more than three times. Additional cycles of freeze/thaws caused partial loss of OSW-1 compound in the aliquots.

2.6.4 Cell Lysis

Cell Lysis Method 1 (AC Freeze/Thaw Lysis): Adherent cells were cultured in Nunclon Delta 10 cm^3 dishes (VWR 10171744) and lysate preparation began by removing the media, washing with 1X PBS, followed by addition of 1 mL PBS and scraping. Cells were collected in a 1.5 mL Eppendorf brand centrifuge tubes and spun down at 14,000 x g for 45 seconds. Supernatant was removed, and the cells were resuspended in 50 µL of AC Lysis buffer (150 mM NaCl, 1.5 mM $MgCl_2$, 5% glycerol, 0.8% NP40, 1mM DTT, 50 mM HEPES, 25 mM NaF, 1 mM Na_3PO_4) with 3X HALT/EDTA protease inhibitor (Thermo 78438) and 0.2 mM

phenylmethanesulfonylfluoride (Goldbio). Cell lysis was performed by freezing in liquid nitrogen and thawing in a 37°C bead bath three times, followed by a 14,000 x g centrifugation for 15 minutes. Supernatant was transferred to a new tube and a portion was taken for protein quantification using a Bradford assay (Bio-Rad Protein Assay Dye Reagent Concentrate #5000006, BSA-Santa Cruz sc-2323). After protein quantification, the lysates were diluted to the desired concentration using AC lysis buffer and a final concentration of 1X Laemmli buffer (1 M Tris pH 6.8, 8% SDS, 40% glycerol, 20% β-mercaptoethanol, and 0.2% bromophenol blue), followed by dry bath heating at 95°C for 10 minutes.

Adherent cells cultured on 6-well plates (Greiner 657160) were lysed by removing media, washed with 1X PBS, followed by adding 0.5 mL TrypLE^{TM} Express (Gibco 12605010) and incubated at 37°C for 5 minutes. TrypLE^{TM} was neutralized using 0.5 mL of media and cells were then transferred to a 1.5 mL Eppendorf tube spun down at 14,000 x g for 45 seconds. Supernatant was removed, and 1 mL of PBS was added to wash the cells. Cells were spun down at 14,000 x g for 45 seconds, supernatant was removed, and the cells were resuspended in 50 µL of AC lysis buffer. Freeze/thaw method was continued as described above.

For suspension cell lines, cells were centrifuged at 200 x g for 5 minutes and the supernatant removed. Cell pellet was resuspended in 1 mL of PBS and spun down at 14,000 x g for 45 seconds, supernatant was removed, and cells were resuspended in 50 µL of AC lysis buffer. Freeze/thaw method continued as above.

Cell Lysis Method 2 (MPER Extraction): Mammalian protein extraction reagent, MPER, (Thermo 78501) was used as an alternative lysis method for 10 cm^3 dishes. Media was removed from the cells, and 5 mL of 1X PBS was added to wash cells. 1 mL of MPER was added to the plate and was shaken in a room temperature (Innova 42 incubator) at 250 rpm for 5 minutes. The

solution was collected and spun down at 14,000 x g for 10 minutes. Supernatant was placed in a new tube and the protein concentration and sample preparation was conducted as described above.

2.6.5 Western Blotting

SDS-PAGE gels (8.5%) containing 25 µg of total protein per well were transferred to 0.45 µm nitrocellulose (Bio-Rad 1620115) using constant voltage (100V) for 1 hour at 4°C in 1X transfer buffer with 10% ethanol. After transferring, the nitrocellulose membrane was blocked with 5% milk 1X TBST at room temperature for 30 minutes. The membranes were then washed three times, five minutes each, with 1X TBST. Primary incubation with antibodies was done overnight at 4°C. After primary incubation, the blots were washed five times, five minutes each, with 1X TBST and then incubated in secondary antibody in 1% milk TBST for 30 minutes at room temperature. After secondary antibody incubation, the blots were washed five times, five minutes each, with 1X TBST and then once with 1X TBS for ten minutes. TBS was removed, and the blots were incubated in Clarity™ Western ECL substrate (Bio-Rad 1705061) and imaged on the Bio-Rad ChemiDoc™ Touch Imaging System using the chemiluminescence setting with 2x2 binning. Ladder images were taken using the colorimetric setting. After development, the membranes were washed with 1X TBST twice for five minutes each. 1:1000 β-actin HRP (Santa Cruz sc-47778 HRP) in 1% milk TBST was added and incubated for 1.5 hr at room temperature. Developing occurred the same as after secondary antibody incubation. Primary antibodies used were 1:500 OSBP A-5 (Santa Cruz sc-365771), 1:1000 OSBP2 B-1 (Santa Cruz sc-365922), 1:1000 OSBP1 1F2 (Novus NBP2-00935), and 1:1000 OSBP1 (Novus NBP2-47343). Secondary antibodies used were 1:3000 goat anti-mouse IgG1-HRP (Santa Cruz sc-2060) and 1:3000 goat anti-rabbit IgG-HRP (Santa Cruz sc-2004).

2.6.6 Washout Experiments

Cells were treated with 1 nM OSW-1, 1 nM Taxol, or DMSO media for 6 hours or the indicated time period. Media was removed, and the cells were gently washed with 5 mL of complete media 3 times and then 10 mL of fresh, OSW-1 compound free media was added back to the cells. Compound removal and washing for K562 cells utilized were centrifuged at 200 x g for 5 minutes for each step. The cells were then allowed to recover for the indicated times (0-72 hours) and were lysed as described above and analyzed by Western blot.

2.6.7 Immunofluorescence

50,000 cells were seeded onto sterile 18 mm cover slips in 12 well plates for treatments lasting (0-24 hours) or 25,000 cells for longer treatment. The cells rested for 24 hours before treatment to ensure attachment of the cells. Once treatments were completed media was aspirated and cells were washed with warm 1X PBS. PBS was removed and 0.5 mL of freshly prepared 4% paraformaldehyde in PBS was added. Coverslips were at 37°C for 20 mins and then the paraformaldehyde was removed followed by three 1X PBS washes. Permeabilization of the cells was done with 0.5 mL of 0.5% Triton X-100 in PBS at room temperature for 10 minutes. 1X PBS was used to wash the cells three times. Image-iT FX signal enhancer (Thermo I36933) was added onto the cover slips and incubate at room temperature for 30 minutes followed by three 1X PBS washes. Coverslips were blocked with 0.5 mL of 1% BSA in PBS at room temperature for 30 minutes followed by three washes with 1X PBS. Primary antibody was added, and the slips were incubated overnight at 4°C. The primary antibody solution was removed and washed slips three times with 1X PBS. Secondary antibody solution was incubated in darkness at room temperature for 1 hour. The secondary antibody solution was removed and washed three times with 1% BSA-PBS, three times with 1X PBS, and then soaked the cover slip in 300 nM DAPI (Thermo D1306)

solution for 10 minutes Mounted the slips onto glass slides using VECTASHEILD HardSet Antifade mounting media (VECTOR labs H-1400). Stored slides at -20°C until imaging was conducted. Primary antibodies used were 1:100 OSBP1 1F2 (Novus NBP2-00935) and 1:500 TGN46 (Novus NBP1-49643). Secondary antibodies used were 1:500 goat anti-mouse IgG H&L Alexa Fluor® 488 (Abcam ab150113) and donkey anti-rabbit IgG H&L Alexa Fluor® 594 (Abcam ab150076). Imaging was done with a Lecia SP8 using a 63x objective with 2x digital zoom. Images were analyzed with ImageJ software.

2.6.8 Trypan Blue Staining

HEK293 and HCT116 cells were seeded out at 0.85 x 10^5 cells/mL into 10 cm^3 dishes and left to recover for 20 hours. Cells were treated with 1 nM OSW-1, 1 nM Taxol, or DMSO for 6 hours, followed by washout procedure and recovery for 0-72 hours. After recovery time, cells were washed with 1X PBS and then incubated in 2.5 mL TrypLE™ for 5 minutes at 37°C. Reaction was neutralized using 7.5 mL of fresh media and cells were counted and viability analyzed on a TC20™ Automated Cell Counter (BioRad) by combining 10 µL of cell solution with 10 µL Trypan Blue stain (Thermo 15250061).

2.6.9 Calcein AM and Hoechst Staining

HEK293 cells were seeded out at 10,000 cells per well into a 24-well plate and left to recover for 20 hrs. Half the plate of cells was treated with 1 nM OSW-1, 1 nM Taxol, or DMSO for 6 hours, followed by washout while the other half was treated with the same concentration continuously. Washout and continual time points were 0, 24, 48, and 72 hours, with the cells being treated on subsequent days, therefore, all time points ended collectively. Once the treatments were finished, the media was removed and a solution of 5 µM Calcein AM (Thermo C1430) and 5.5 mg/mL Hoechst 33342 (Thermo H1399) was added to the cells and incubated at 37°C for 1 hour. Plate

was imaged using an Operetta High-Content Imaging System (PerkinElmer) using brightfield, 488, and Hoechst settings.

2.6.10 Intracellular OSW-1 Quantification Using LC-MS and Single Cell MS Methods

nano-UPLC/MS: HCT-116 cells ($1.5x10^5$) were seeded in a 6-well plate. Upon 60% confluency, cell lysate was created following a 1 hour treatment of 100 nM OSW-1, with or without a 24 hour post wash recovery. Trypsin (0.5 mL) was used to detach the cells, with additional McCoy's media (0.5 mL) to stop digestion. Cell count was performed using a Bio-Rad TC20™ Automated Cell Counter with trypan blue viability staining. Cells were spun at 500 x g for 5 min followed by a 1-mL PBS wash. The cell pellet was lysed using 1 mL of 50 nM d-OSW-1 dissolved in cold acetonitrile and methanol (1:1) with brief vortexing on ice for 10 min. The cell pellet was spun at 15000 x g at 4°C for 15 min. The supernatant was transferred to a new tube and dried using a speed vacuum (Savant SPD11V, Thermo Scientific) at 70°C. Prior to analysis, cells are resuspended in 150 µL of ACN: H2O (1:10). Analysis was performed using a Waters nanoAQUITY BEH C-18 column (100 µm x 100 mm, 1.7 µm) coupled with a mass spectrometer (Thermo LTQ Orbitrap XL, Waltham, MA) using a flow rate of 0.3 uL/min. Mobile phase A is ACN with 0.1% formic acid, and mobile phase B is H2O with 0.1% formic acid. The time/%A are as follows: 0/0, 1/50, 2/100, 3/100, and 4/0 for a total runtime of 5 minutes. Treatment of cells was done by Mr. Ryan Bensen and analysis of sample was done by Ms. Shawna Standke of Dr. Zhibo Yang's lab in the Department of Chemistry and Biochemistry, Univ. of Oklahoma.

2.6.11 Single Cell Mass Spectrometry

HCT-116 cells ($1.5x10^5$) were seeded on to a glass microchip (18 mm diameter) with chemically-etched microwells (55 µm diameter; 25 µm deep) placed into each well of a 6-well plate. Upon 60% cell confluency, cells were treated as described for nano-UPLC/MS. Following

treatment, the microchip was washed with 5 mL of FBS-free McCoy's media and placed on an X, Y, Z-translational stage for quantification. MS analysis was performed as previously described(206). Briefly, singleprobes were coupled to the mass spectrometer by using a flexible arm clamp to position the nano-ESI emitter in front of the inlet. The solvent-providing capillary was connected to the solvent through the conductive union. For quantification, 50 nM d-OSW-1 was added into the solvent. High voltage (~4.5 kV) was used for SCMS experiments in the positive ion mode with a mass resolution (m/Δm) of 60,000. A flow rate of ~5 nL/s was used (the actual flowrate is optimized for each Single-probe). Data was collected using Xcaliber software and exported into Excel for analysis. Treatment of cells was done by Mr. Ryan Bensen and analysis of sample was done by Ms. Shawna Standke of Dr. Zhibo Yang's lab in the Department of Chemistry and Biochemistry, Univ. of Oklahoma.

2.6.12 Mass Spec label-free 2D OSBP quantification

The first-dimension high-pH (pH=10) separation was performed on a Thermo Accela HPLC system (Thermo Scientific, Hanover Park, IL) with an ACQUITY UPLC BEH300 C18 column (50mm, Waters, Milford, MA, USA). The mobile phase A (MPA) was 20 mM ammonium formate in water and the mobile phase B (MPB) was 20 mM ammonium formate in acetonitrile. The mobile phases were adjusted to pH 10. A 60-min gradient from 3% to 70% (3% to 10% in a minute) mobile phase B was applied for peptide separation, and 60 fractions were collected (one minute per fraction). Fraction concatenation was performed following Yang's paper(213). A total of 12 fractions were obtained for the second-dimension low-pH LC-MS/MS analysis. Cell treatments were performed by Mr. Zachary Sevarance and the analysis was performed by Ms. Hongyan Ma of Dr. Si Wu's lab in the Department of Chemistry and Biochemistry, Univ. of Oklahoma.

2.6.13 Anti-Viral Experiments

HeLa cells were grown to <75% confluency (healthy log phase cells) in complete media, DMEM (Hyclone SH30081.0) with 10% FBS (Atlanta Biological S11550) and 1% penicillin-streptomycin (Gibco 15140-122). For experiments, cells were trypsinized, counted using a hemocytometer and seeded into 20 wells of two 24-well trays (Falcon 3047) with 2.0 x 10^5 cells per well, in 1.0 mL complete media. Each treatment is performed using quadruplicate wells (n=4) and each virus was on a separate plate. After seeding, cells were incubated 20 hours at 37 ºC, 5% CO2, at which point cells have grown to a near confluent monolayer.

For the OSW-1 compound continual treatment experiments, (**Figure 24A**), the media was gently removed from each well, and 1mL of media was added with the desired OSW1-compound concentration to each well, without disturbing the cells. Cells were incubated for 6 hours, after which time the media was removed and cells were gently washed three times with 1.0 mL of FBS-free DMEM media. After the media was removed, CoxA9-01 or Echo2-01 viruses, diluted in serum-free DMEM with a M.O.I. of 1.0 was added to the culture. The 2.0 x 10^5 cells per well was assumed to double during incubation so 4.0 x 10^5 pfu/well of virus was used for an M.O.I. of 1.0. The virus and cells were incubated for 30 minutes at 37 ºC 5% CO2. Then, the virus inoculum was removed, and the culture washed one time with 1.0 mL of serum-free media per well. Then, 1.0 mL of complete media with the indicated concentration of OSW-1 was added to the well, and the infected cells were then incubated for 10 hours at 37 ºC, 5% CO2. After 10 hours the plate was stored at -80 ºC until the TCID-50 titration. The experiment reported in the **Figure 24A** was repeated independently three times.

For the OSW-1 compound washout treatment experiments, (**Figure 24B**), cells were seeded as above. After 20 hours incubation the media was gently removed from each well, and

1mL of media was added with the desired OSW-1 compound concentration to each well, without disturbing the cells. Cells were incubated for 6 hours, after which time the media was removed and cells were gently washed three times with 1.0 mL of FBS-free DMEM media. This was replaced with complete media and cells allowed to incubate for 20 hours. After the media was removed, CoxA9-01 or Echo2-01 viruses, diluted in serum-free DMEM with a M.O.I. of 1.0 was added to the culture. The 2.0 x 10^5 cells per well was assumed to double and double again during incubation so 8.0 x 10^5 pfu/well of virus was used for an M.O.I. of 1.0. The virus and cells were incubated for 30 minutes at 37 ºC 5% CO2. Then, the virus inoculum was removed, and the culture washed one time with 1.0 mL of serum-free media per well. Then, 1.0 mL of complete media was added to the well, and the infected cells were then incubated for 10 hours at 37 ºC, 5% CO2. After 10 hours incubation, the plate was stored at -80 ºC until processing. Then, the plates were rapidly thawed, the cells in media were scrapped from the wells into sterile 1.5 mL centrifuge tubes and the suspension then centrifuged at 10,000 g at 4ºC to produce the virus containing supernatant, which is assayed for TCID-50 titration on sub-confluent RD cells. The experiment reported in the **Figure 24B** was repeated independently three times. The TCID-50 titration was performed according to the protocol described by Reed et al(210). This experiment was performed independently three times to generate the data in the Figure. All viral work was done by Dr. Earl Blewett.

2.6.14 Plasmid and Cloning

Human OSBP cDNA was obtained in a pOTB7 vector from the Mammalian Gene Collection (Thermo). PCR using 5'-GCTAGCATGGCGGCGACGGAG-3' forward and 5'AAGCTTGAAAATGTCCGGGCATGAGC-3' reverse primers amplified a 2.44 kb Nhe IHindIII fragment containing a full-length hOSBP cDNA, which was subcloned into pJET1.1

(Thermo) and sequence verified. The fragment was then cloned into the pcDNA™ 3.1/myc-His(-) C mammalian expression vector (Sigma) Nhe I-Hind III doublecut sites. The reverse primer does not include an additional nucleotide between HindIII cut site and the last OSBP codon resulting in an OSBP-tagless protein. ORP4L was cloned from HCT-116 with cDNA with a NheI forward primer 5'-GCTAGCATGGGGAAAGCG-3' and a HindIII reverse primer 5'-AAGCTTCGAAGATGTTGGGGCACATATG-3'. LacZ was PCR amplified from K-12 E. coli with NotI forward 5'- GCGGCCGCATGCCCG TCGTTTTA-3' and BamHI reverse primer 5'-GGGCGGATCCTTTTTGAC ACCAGACCAA-3'. To generate the proteins expressing tags, the MCS of the completed vector was changed through site-directed mutagenesis with a forward 5'-AAGCTTACGTACGAACAAAAACTCATCTCAGAAGAG3' and reverse 5'-CTCTTCTGAGATGAGTTTTTGTTCGTACGTAAGCTT-3'. The plasmid was expanded in E. Coli DH5α, and isolated through miniprep and maxiprep kits (Thermo). Gene and plasmid MCS were sequence verified through Oklahoma Medical Research Foundation (OMRF). This work was done by Dr. Juan Nuñez.

2.6.15 ([3H]-25-OHC) Charcoal/Dextran Binding Assay

The [3H]-25-OHC binding assay was run according to the protocol outlined in Burgett et al(46) by Mr. Zachary Severance and Mr. Ryan Bensen.

2.6.16 Statistical Analysis

Results are expressed as mean ± s.d. and are n=3 unless otherwise stated. All statistical tests were performed using GraphPad Prism 7.0. Comparison between groups were made by using a one-way ANOVA with a follow up Dunnett's test. The p values are reported using GraphPad Prism * values: * is $p \leq 0.05$, ** is $p \leq 0.01$ *** is $p \leq 0.001$, and **** is $p \leq 0.0001$.

Chapter 3: OSW-1 compound treatment induced OSBP loss occurs through an unknown mechanism

The following chapter is partially taken from the publication in ACS Chemical Biology by the author of this dissertation: Persistent, Multi-Generational Reduction of Oxysterol-Binding Protein Caused by Compound Treatment Induces Prophylactic Anti-Viral Activity. This was a collaborative work that consists of the following authors: Brett L. Roberts, Zachary C. Severance, Ryan C. Bensen, Anh T. Le, Naga Rama Kothapalli, Juan I. Nuñez, Hongyan Ma, Si Wu, Shawna J. Standke, Zhibo Yang, William J. Reddig, Earl L. Blewett, Anthony W. G. Burgett.

Mr. Zachary Severance conducted the authophagy experiment in **Figure 26** and iTRAQ experiment in **Figure 28**.

Mr. Ryan Bensen conducted the ALLN experiments in **Figure 25**.

Ms. Hongyan Ma conducted the iTRAQ experiment in **Figure 28**.

3.1 Abstract

The natural product OSW-1 causes proteasomal dependent degradation of the oxysterol-binding proteins OSBP and ORP4. Treatment with short non-toxic doses of OSW-1 compound, followed by removal, leads to prolonged reduction of OSBP levels, but not ORP4 (see **Chapter 2**: Persistent Reduction of Oxysterol-binding Protein Caused by Compound Treatment Induces Prophylactic Anti-Viral Activity). The compound-triggered repression of OSBP results in a prophylactic anti-viral response in cells to clinical isolates of *Enteroviruses*. The cellular mechanism through which short term, lose dose treatment with the OSW-1 compound induced a long-term repression of OSBP level in cells is unknown. Here we report that the long-term OSBP repression does not occur through a cellular mechanism of OSBP transcription repression, proteasomal degradation, or autophagy-induced proteolysis. The half-life of OSBP was

determined to be greater than 24 hours, and this result shows the rapid loss of OSBP upon OSW-1 compound treatment is not due to normal protein turnover. Global analysis of protein levels using iTRAQ analysis showed no wide-spread reduction of protein levels similar to the rapid loss of OSBP. This result suggests the cellular mechanism triggered by the OSW-1 compound is specific to OSBP and not a general effect reducing cellular proteins. Future research is required to identify the cellular mechanism through which OSBP levels are repressed upon OSW-1 treatment.

3.2 Introduction

The long-term repression of OSBP levels triggered by OSW-1 compound is an unusual response of cellular regulation of a protein (see **Chapter 2**: Persistent Reduction of Oxysterol-binding Protein Caused by Compound Treatment Induces Prophylactic Anti-Viral Activity). Proteins expression levels can be repressed by various cellular mechanism such as transcriptional, translational, post-translational or a combination of the three(214, 215). Transcriptional regulation can occur from multiple sources within a cell that will lead to the downregulation of mRNA production(214, 216). Repression of transcription can occur due to repressor proteins binding to silencer DNA sequences that inhibit RNA polymerase from binding the gene, or disrupting protein-protein interactions in the transcriptional machinery(216). Transcriptional repression can also occur through the methylation of DNA or histones(216). One mechanism of inhibiting translation is through microRNA (miRNA) binding to the mRNA which will lead to either destruction or sequestration of the mRNA target(217). Protein repression can occur in other forms, such as autophagy induction (see section 1.6.4 **Autophagy Overview**). Post-translational modifications such as ubiquitin can target a protein for destruction (see section 1.6.1 **Proteasome Overview**).

OSBP is a member of a highly conserved protein family found among all eukaryotes and evidence indicates it has roles in cholesterol transport and lipid sensing(1, 5). OSBP transports cholesterol from the ER to the Golgi and counter-transports PI4P(35, 36). OSBP can act as a sterol/lipid sensor and interact with cellular signaling pathways involved in proliferation and transcription(39, 40). The half-life and post-translational regulation of OSBP is not known. OSW-1 treatment induces a disruption of the trans-Golgi network, presumably through OSBP inhibition.OSW-1 treatment has also been shown to induce significant changes in the expression profiles of tumor related miRNAs(218). To investigate this mechanism of reduction we utilized approaches to determine at which step in the central dogma the reduction was occurring. Our results demonstrate that long-term reduction of OSBP does occur through a mRNA transcriptional repression, proteasomal degradation, or autophagy-induced proteolysis.

3.3 Results

3.3.1 OSW-1 "washout effect" is not due to prolonged proteasomal degradation

Continual OSW-1 treatment leads to proteasomal dependent degradation of OSBP(46) and calpain dependent degradation of the ER stress protein, glucose-regulated protein 78 (GRP78) (130). To confirm the previously reported results and to determine if calpains degrade OSBP, we utilized various proteasome inhibitors and the calpain inhibitor ALLN (**Figure 25A**). We found that using any proteasome inhibitor or ALLN leads to a significant protection of OSBP in the presence of OSW-1, confirming that OSBPs initial degradation is proteasomal dependent. To determine if long-term reduction of OSBP was proteasomal dependent, we induced the OSW-1 "washout effect" in HCT116 cells and allowed recovery for 24 hours to ensure OSBP reduction. After the 24 hour recovery, the cells were treated with proteasome inhibitors or ALLN for an additional 24 hours and the OSBP proteins levels were compared to washout cells that recovered

for 48 hours without additional treatment (**Figure 25B**). The proteasome inhibitors were not able to rescue the OSBP levels at 24 hours post-washout administration (**Figure 25B**). Only bortezomib was able to partially recover OSBP levels up to (~35%) compared to untreated OSW-1 washout cells (**Figure 25B**). Similar results were obtained with ALLN treatment in HeLa cells. The ALLn inhibitor restored ~25% of OSBP levels compared to untreated OSW-1 washout cells (**Figure 25B**).

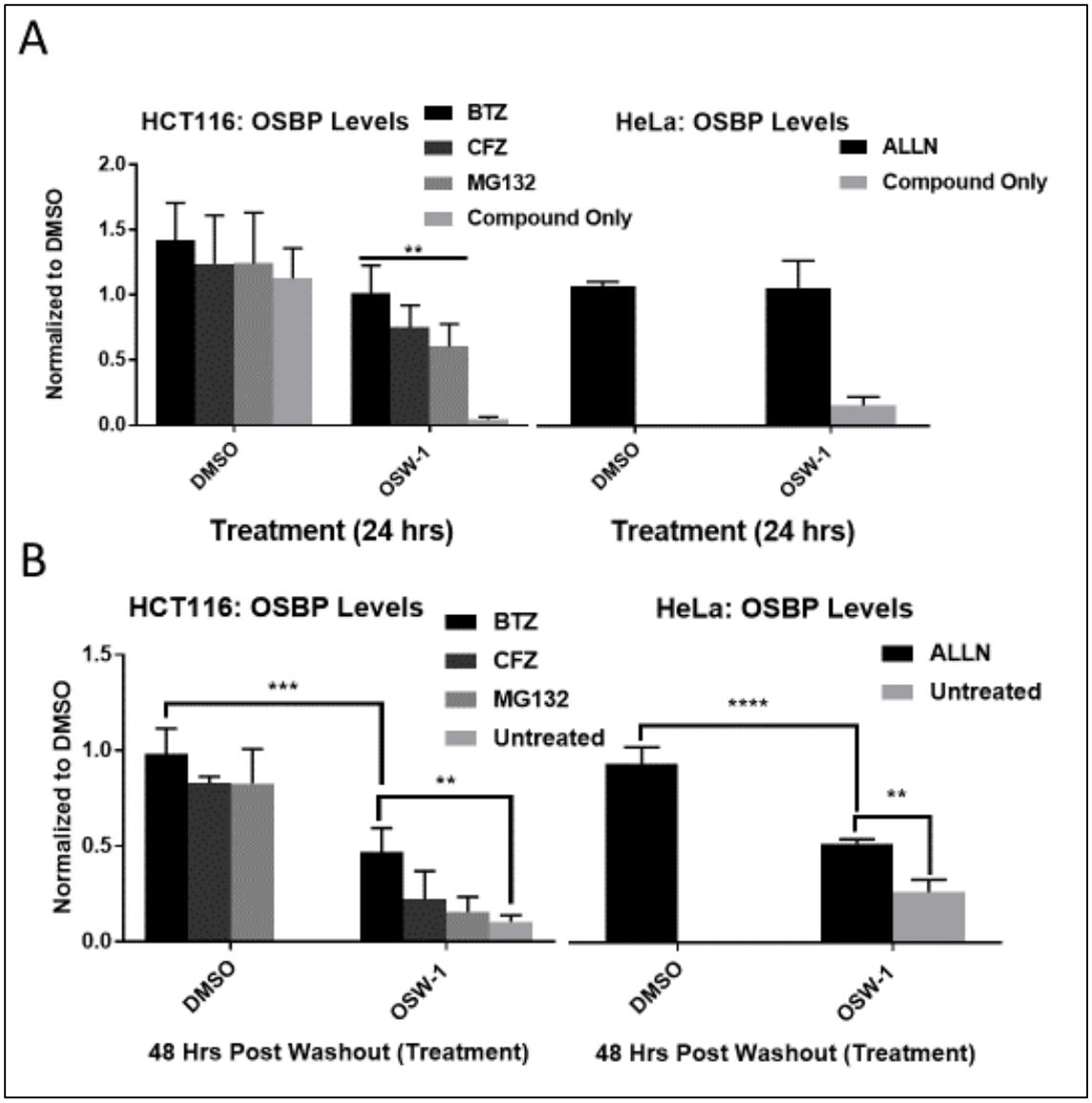

Figure 25: OSW-1 "washout effect" is not due to prolonged proteasomal degradation. (A)Continuous 1nM OSW-1 treatment in HCT-116 or HeLa with proteasome inhibitors (25 nM Bortezomib= BTZ, 25 nM Carfilzomib = CFZ, and 170 nM MG132) or calpain inhibitor (ALLN) results in significant protection of OSBP levels after 24 hours. (B) OSW-1 compound washout experiment (6-hour treatment, recovery time of 48 hours) with 1nM OSW-1 treatment results in long term repression of OSBP and addition of select proteasome inhibitors or ALLN at 24 hr pWo show partial recovery of OSBP. ALLN results collected by Mr. Ryan Bensen. (Full blots in **Figure 55**). The author had no contribution to the ALLN results.

3.3.2 OSW-1 "washout effect" induces autophagy, but autophagy is not the cause of long-term OSBP repression.

With proteasome degradation eliminated as the mechanism of long-term OSBP repression in OSW-1 washout cells, we then determined if the repression of OSBP could be due to autophagy proteolysis. The OSBP-binding natural product compound Schweinfurthin G (see 1.5.2 **Schweinfurthins**) was shown to disrupt AKT signaling and to induce autophagy (135). We found that OSW-1 washout treatment induces autophagy in HEK293 cells by monitoring the known markers of induced autophagy: LC3A/B and p62 (**Figure 26A** & **B**) (see 1.6.5 **Autophagy Induces and Inhibitors**). Chloroquine (CQ) is a chemical inhibitor of the proteolysis of autophagic substrates, and therefore co-administration of CQ is required to measure LC3B levels during autophagy. Rapamycin (Rap) is a mTORC1 inhibitor that induces autophagy in cells. Similar to Rap/CQ treatment, OSW-1 compound/CQ treatment causes a noticeable increase in LC3B levels relative to CQ treatment alone in HEK-293 cells over the time course observed (**Figure 26A**, lower band), indicating the induction of autophagy (**Figure 26A**). Additionally, 1 nM OSW-1 compound treatment for 6 hours resulted in ~60% reduction in p62 levels (**Figure 26B**). The p62 levels returned to normal 24 hours post-washout, indicating that the autophagy triggered by the OSW-1 compound washout treatment is transient. (**Figure 26A** & **B**). Despite this transient autophagy that is induced, co-incubation with 25 μM CQ and 1 nM OSW-1 for 6 hours, followed by compound washout and replacement of 25 μM CQ for 24 hours does not result in OSBP rescue (**Figure 26C**). Confirming autophagy is not involved in OSBP reduction, cell splitting and cell dilution do not rescue OSBP levels despite increased nutrient availability that

would inhibit autophagy(219) (**Figure 59**). These results confirm that long-term OSBP reduction is not due to sustained autophagy or proteasome induced degradation.

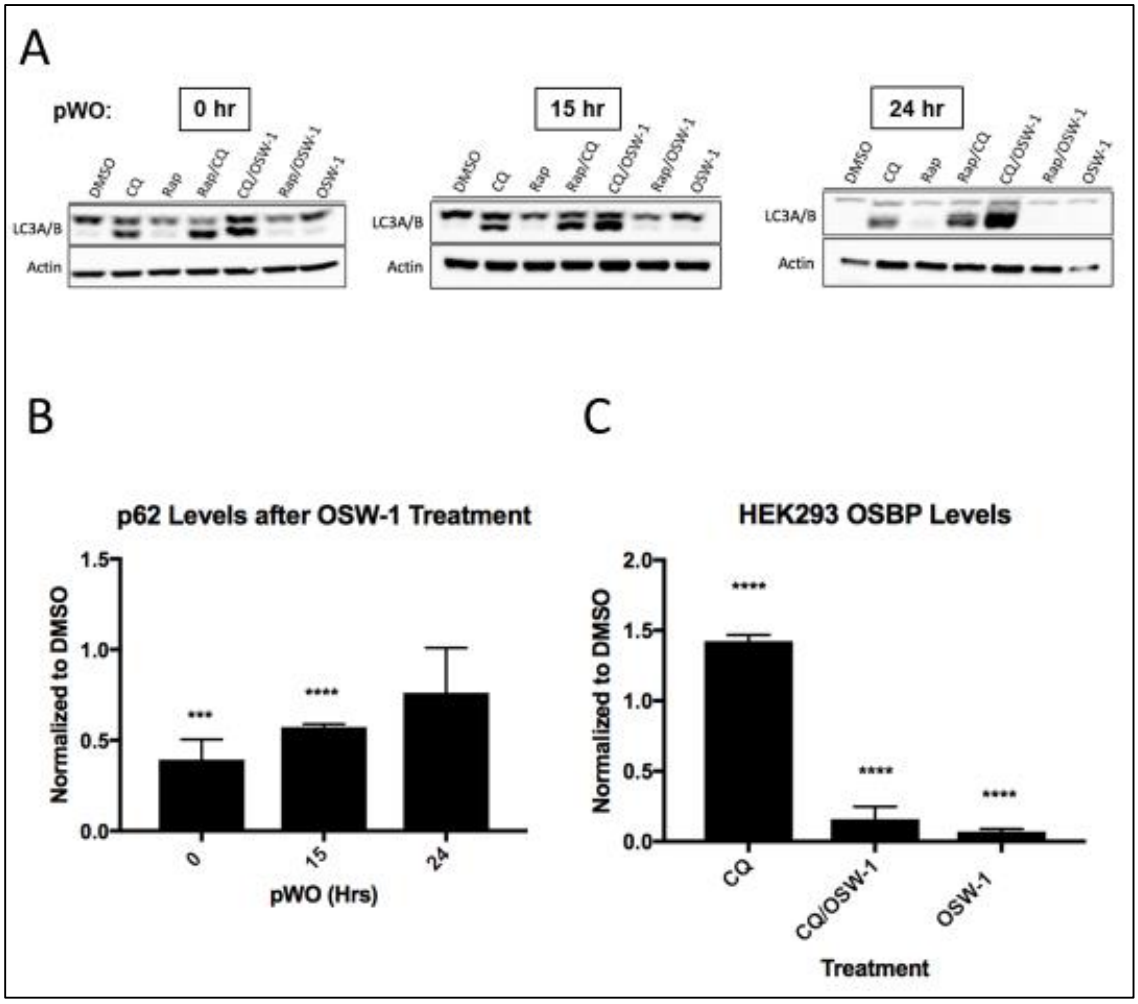

Figure 26: OSW-1 "washout effect" induces autophagy, but autophagy is not the cause of long-term OSBP repression. Treatment of HEK-293 cells for 6 hours with 1 nM OSW-1 decreases (A) p62 and (B) increases LC3B (lower band on Western blot), which are markers of cellular autophagy. Rap= Rapamycin, a known autophagy inducing compound and CQ= chloroquine, a known autophagy inhibitor. (C) Inhibition of autophagy-induced proteolysis using 25 µM CQ in HEK-293 cells does not rescue OSBP levels in OSW-1 washout experiment (i.e., 6-hour, 1 nM OSW-1 treatment, followed by compound washout and 24-hour recovery). CQ treatment increases OSBP levels compared to DMSO vehicle control in cells. Work was completed by Mr. Zachary Severance. (Full blots in **Figure 56**, **Figure 57** & **Figure 58**). The author had no contribution to the autophagy results.

3.3.3 Sustained OSBP loss is not due to rapid protein turnover

We next determined if translational repression could be responsible for the compound-triggered sustained reduction of OSBP levels. To identify if translational repression was occurring we determined the half-life of OSBP by using the translational inhibitor cycloheximide (CHX). CHX blocks the translocation step in protein synthesis, leading to inhibition of translational elongation. If OSW-1 treatment causes translational repression of OSBP, the protein half-life should overlap with the degradation of the protein under continual treatment with OSW-1 (**Figure 17B**). HCT116 cells were treated with 178 μM CHX for the indicated time and OSBP protein levels were determined by Western blotting. The results show that the half-life of the control protein, p21, is ~2 hours which is consistent with previous reports(220–222) (**Figure 27B**). OSBP has a half-life of longer than 24 hours; at 24 hours, the CHX-induced protein translation block begins to be toxic to the cells. The half-life of OSBP was also determined in the HEK293 cell line and showed similar results (**Figure 61A**) Similarly, ORP4 half-life correlates with OSBP, in that it is over 24 hours in the HCT116 cell line (**Figure 61B**). This is the first reported protein turnover rate of OSBP and ORP4. The long lifespan of OSBP in cells indicates that the long-term, compound induced reduction of OSBP levels is not due to rapid cycling of the protein under normal conditions (**Figure 27A**). The rapid reduction of OSBP upon OSW-1 treatment is not a standard cellular process, but instead the compound treatment causes a different process of OSBP regulation to become activated.

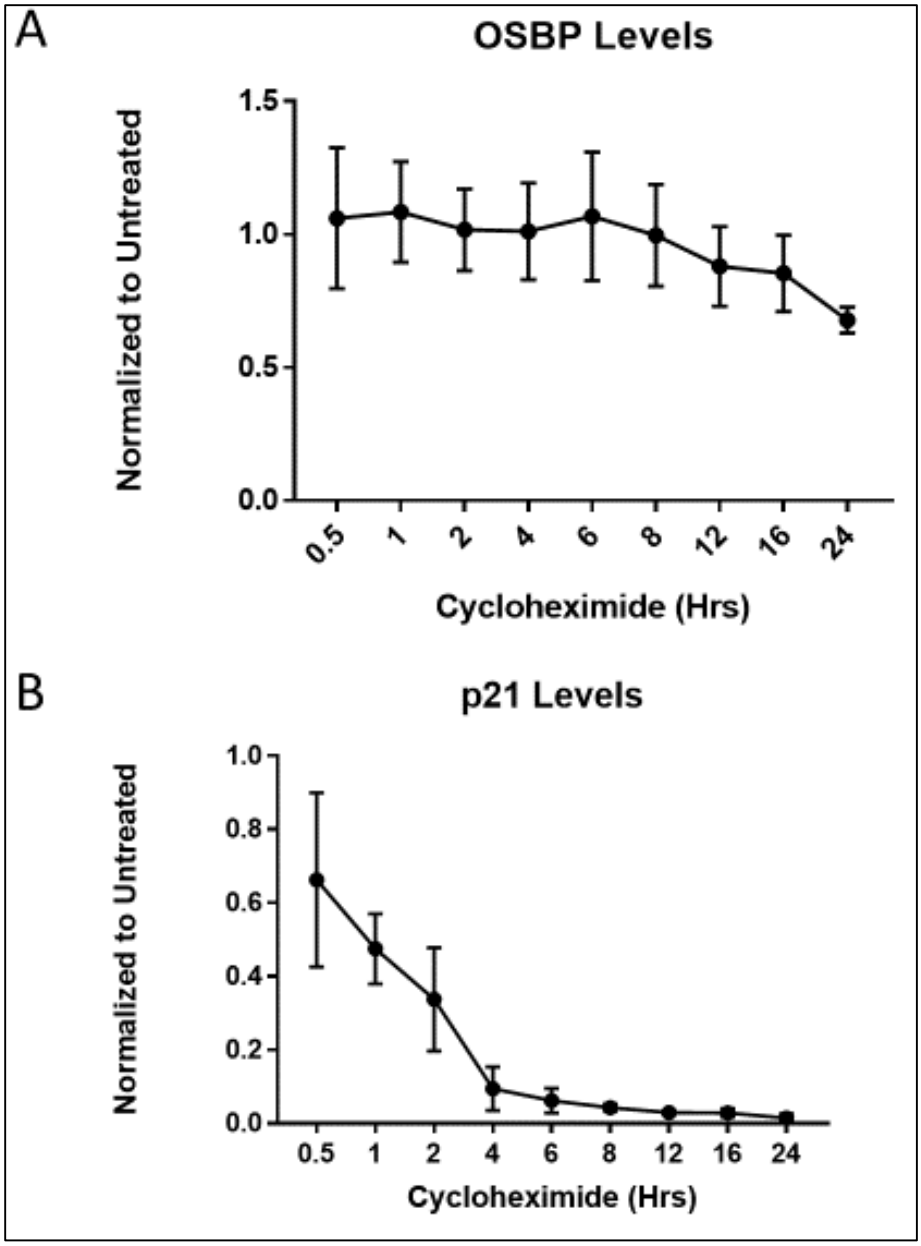

Figure 27: Sustained OSBP loss is not due to rapid protein turnover. (A) OSBP half-life is over 24 hrs as determined by 178 μM cycloheximide while (B) p21 has a relatively short protein half-life and serves as a control. (Full blots in **Figure 60**).

3.3.4 OSBP mRNA transcript remains stable throughout washout recovery.

Since post-translational and translational repression are not responsible for the long-term repression of OSBP upon OSW-1 compound treatment, the effect of OSW-1 compound treatment on OSBP mRNA levels was determined. RT-PCR analysis using intron spanning primers of the

OSBP mRNA of OSW-1 compound washout treated cells show that OSBP mRNA levels were are not changed relative to the DMSO vehicle control from 0-72 hours post washout (**Figure 28A**). This result clearly shows that transcriptional repression of OSBP mRNA levels is not responsible for the long-term reduction of OSBP protein levels triggered by OSW-1 treatment.

3.3.5 OSW-1 Compound Triggered Long-term Reduction of OSBP Levels is Specific for OSBP and Not a General Proteome Reduction

Cellular iTRAQ proteomic analysis demonstrates that the OSW-1 compound washout treatment in HEK293 cells does not induce broad degradation of cellular proteins (**Figure 28B & C**). Only a few of the (469) proteins confidently identified and quantified in the iTRAQ experiment showed significant changes in measured level ($p < 0.05$) at 24-hour post-washout, and the expression levels for these proteins return to levels similar to the vehicle control at 72-hour post-washout. The top three most significantly changed proteins are: PEBP1 (phosphatidylethanolamine-binding protein 1), a negative regulator of autophagy and RAF kinase inhibitor; RPL13 (60s Ribosomal Protein L13), a component of the large ribosome; and EIF4G1, a eukaryotic translation initiation scaffold protein. At the 24-hour recovery time point post-washout, many of the quantified proteins exhibit a small non-significant ($p > 0.05$) reduction in expression levels (**Figure 28C & D**), which might indicate a possible decrease in translation rate. The statistically significant ($p < 0.05$) decrease in the proteins RPL13, EIF4G1, EEF1A2, DARS2, which are involved in multiple levels of protein translation, could contribute to the general, non-significant reduction of many identified proteins 24 hours post-washout. The iTRAQ results, in combination with the lack of cytotoxicity and growth arrest in the OSW-1 compound washout experiment (**Figure 21**), indicate that the reduction of OSBP is targeted for that specific protein and is not the result of a widespread reduction of

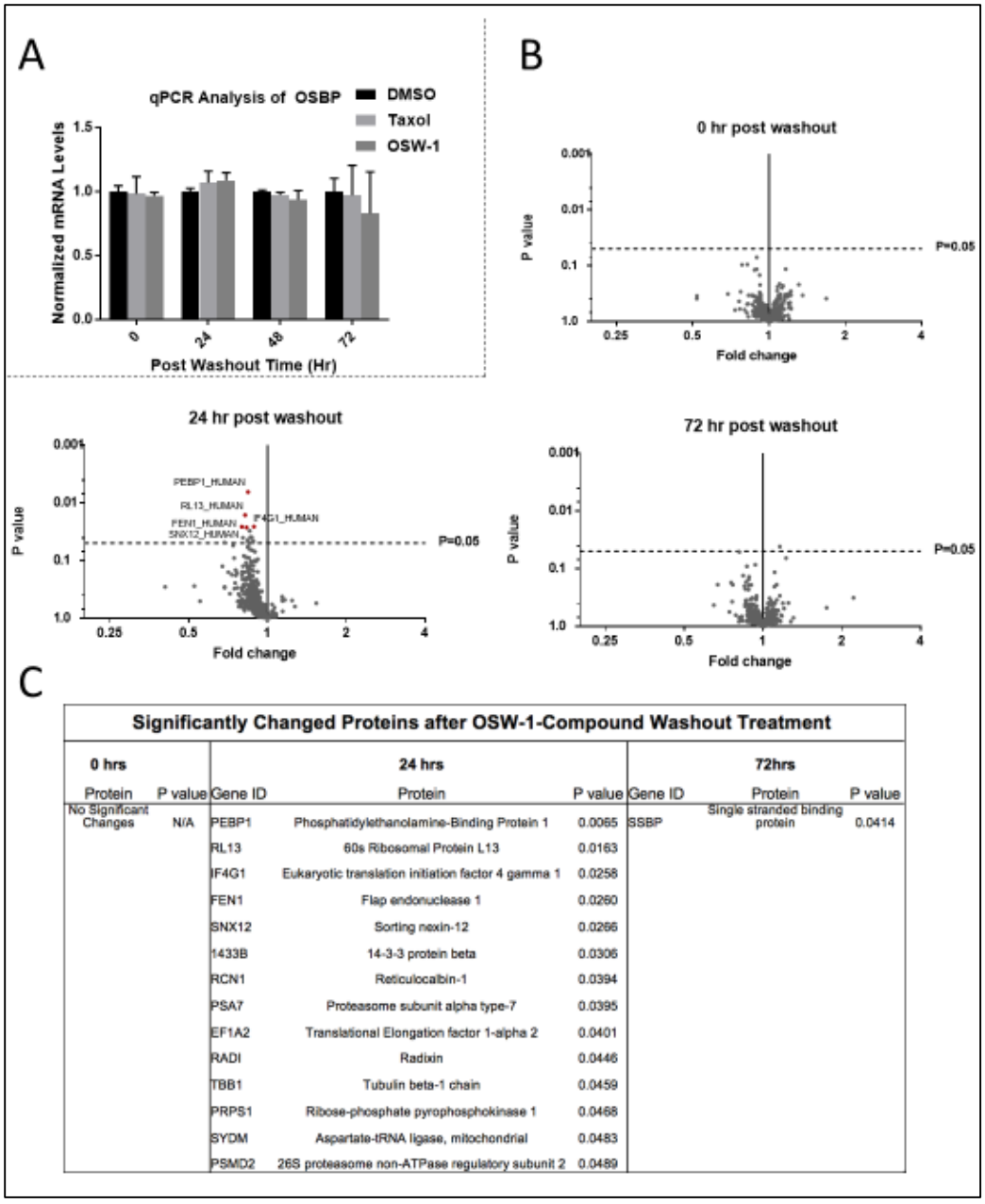

C

Significantly Changed Proteins after OSW-1-Compound Washout Treatment

0 hrs		24 hrs			72hrs		
Protein	P value	Gene ID	Protein	P value	Gene ID	Protein	P value
No Significant Changes	N/A	PEBP1	Phosphatidylethanolamine-Binding Protein 1	0.0065	SSBP	Single stranded binding protein	0.0414
		RL13	60s Ribosomal Protein L13	0.0163			
		IF4G1	Eukaryotic translation initiation factor 4 gamma 1	0.0258			
		FEN1	Flap endonuclease 1	0.0260			
		SNX12	Sorting nexin-12	0.0266			
		1433B	14-3-3 protein beta	0.0306			
		RCN1	Reticulocalbin-1	0.0394			
		PSA7	Proteasome subunit alpha type-7	0.0395			
		EF1A2	Translational Elongation factor 1-alpha 2	0.0401			
		RADI	Radixin	0.0446			
		TBB1	Tubulin beta-1 chain	0.0459			
		PRPS1	Ribose-phosphate pyrophosphokinase 1	0.0468			
		SYDM	Aspartate-tRNA ligase, mitochondrial	0.0483			
		PSMD2	26S proteasome non-ATPase regulatory subunit 2	0.0489			

Figure 28: OSW-1 compound washout does not induce OSBP transcript loss or wide-spread protein loss. (A) RT-PCR quantification of OSBP mRNA levels shows no reduction in transcript up to 72-hour pWO during the OSW-1 washout experiment (6-hour, 1 nM treatment) in HCT116 cells. (B) iTRAQ LC/MS/MS analysis (n=3) of OSW-1 compound treated lysates relative to vehicle control. All significantly changed proteins were decreased (24-hour pWO), except for SSBP1 (Single Stranded Binding Protein 1), which showed a slight increase in protein levels 72-hour pWO. (C) Table of proteins with significant changes (<0.05). Trend shows significant deviation from vehicle control protein levels after 24-hour pWO and begin to return to control levels 72-hour pWO. iTRAQ analysis was conducted by Mr. Zachery Severance and analyzed by Dr. Si Wu's lab. The author had no contribution to producing the iTRAQ results.

cellular proteins. Taken together, these results suggest a possible unique method of long-term protein reduction that cannot be fully explained by a single mechanism.

3.4 Discussion

The initial degradation of OSBP due to OSW-1 treatment is proteasome dependent as suggested by the protection afforded by the proteasome and calpain inhibitors (**Figure 25A**). While the initial loss of the protein is by the proteasome, the reduction seen during the post-washout recovery cannot be fully explained by these mechanisms. Addition of proteasome and calpain inhibitors during the recovery phase after OSW-1 compound washout did not rescue OSBP levels completely, but did show some protective effects resulting in more accumulation of OSBP during recovery (**Figure 25B**). This suggests that either the proteasome is only partially responsible for the long-term OSBP reduction, or the OSW-1 induced cellular mechanism is disrupted by these compounds and triggers small amounts of expression. The calpain inhibitor ALLN protects OSBP to the same extent as the proteasome inhibitor bortezomib during continual treatment which is potentially due the promiscuity of the compound. ALLN can inhibit most major proteases and has a Ki of 6 μM for the proteasome(168). The treatment concentration of 10 μM could inhibit not only calpain activity but also that of the proteasome. This overlap of inhibition helps to reconfirm the idea that neither proteolysis method is responsible for the long-term loss of OSBP.

Cycloheximide chase experiments found that the half-life of OSBP is over 24 hours (**Figure 27A**), which is considered standard because most of the proteome has a half-life between 20 and 40 hours(223). The initial loss of OSBP upon OSW-1 treatment (**Figure 17B**) appears to be an active process that occurs relatively quickly compared to the natural turn-over of the protein

(**Figure 27A**). Despite the quick degradation and prolonged loss of the protein, the mRNA of OSBP stays at a constant level throughout the recovery period (**Figure 28A**).

Interestingly, thapsigargin treatment in INS-1E cells has a similar effect on GRP78 protein as OSW-1 washout treatment has on OSBP(224). Thapsigargin treatment usually causes an increase in GRP78, but in INS-1E cells GRP78 protein levels decrease(224). mRNA levels are increased throughout treatment time and proteasomal degradation of GRP78 is only partially responsible for reduction(224). Similarly, treatment of macrophages with the trichothecene mycotoxin deoxynivalenol also led to degradation of GRP78 protein but not mRNA levels, resulting in an ER stress response(225). Continual treatment of OSW-1 has also been shown to decrease GRP78 levels after 24 hours(130), suggesting a possible overlap of response to the compounds through an ER induced stress mechanism. More studies need to be conducted to determine if ER stress is induced during the washout treatment.

Despite the possibility of ER stress induced reduction of OSBP, it is highly unlikely that the stress response could be sustained for multiple days without loss of viability. An alternative explanation for the reduction could be due to mRNA sequestration into p-bodies because of a stress event(226), which could be supported by the fact that the mRNA level of OSBP does not change throughout the recovery period. mRNA sequestration or a specific inhibition of OSBP mRNA translation through micro RNA (miRNA) are possible routes to explain the observed OSBP repression. ORP6(64), ORP8(227), and ORP9(228), close relatives of OSBP, are targeted by certain miRNAs to regulate homeostasis of cholesterol, insulin-mediated AKT activation, and lipid uptake respectively(64, 227, 228). Additionally, OSBP mRNA is reportedly targeted by a brain-specific miRNA during neurite elongation(229). However, it is currently unclear how the OSW-1 compound binding to and inducing the degradation of OSBP would then trigger a specific

suppression of subsequent OSBP levels, through miRNA targeting or any other mechanism. Additional experiments need to be performed to determine the exact mechanism of long-term OSBP reduction by OSW-1 treatment.

3.5 Conclusion

These results show the OSW-1 compound induced repression of OSBP proceeds through an unknown but non-typical cellular regulatory mechanism. This OSW-1 induced repression of OSBP is specific for OSBP and does not cause a global or wide spread change of protein levels. The OSW-1 compound induces a rapid loss of OSBP through proteasomal degradation, but the long-term repression of OSBP levels is not due to the proteasome. OSW-1 compound treatment is shown to induce autophagy for the first time, but the long-term reduction of OSBP levels triggered by the OSW-1 washout condition is not due to autophagy-induced proteolysis. The previously unknown half-lives of OSBP and ORP4 were established to be over 24 hours in cells. This shows that OSBP is not a short lived, rapidly-turned over protein, but has a longevity similar to the majority of cellular proteins(223). The rapid OSW-1 induced reduction of OSBP levels, and the long-term repression of OSBP caused by the compound in the washout condition clearly indicate a different cellular regulation of OSBP is being triggered. The OSBP mRNA transcript levels are not affected by OSW-1 compound treatment, including up to 48 and 72 hours post-washout. Future research is needed to identify the cellular mechanisms responsible for the long-term OSBP reduction triggered by OSW-1 compound treatment. A possible mechanism could be miRNA targeting of OSBP mRNA in OSW-1 compound treated cells.

3.6 Methods

3.6.1 Cell Culture

HEK293 STF (ATCC CRL-3249) and HeLa (ATCC CCL-2) were cultured in DMEM (Thermo 11995073) supplemented with 10% Hyclone (Fisher Sci SH3006603) and 1% penicillin-streptomycin (Thermo 15140122). HCT116 (ATCC CCL-247) was cultured in McCoy 5A media (Thermo 16600108) supplemented with 10% Hyclone and 1% penicillin streptomycin. HCT116 p21-/- cells were a gift from the Vogelstein Laboratory (Johns Hopkins University) and cultured in McCoy 5A media (Thermo 16600108) supplemented with 10% Hyclone and 1% penicillin streptomycin.

3.6.2 General Cell Culture

All mammalian cell lines were cultured at 37 ºC in 5% CO2. All handling of the mammalian cell culture was performed in a standard tissue culture hood using standard aseptic technique. Cell lines were cultured in the complete media described above. Cell culture stocks were aliquoted in complete media with 10% DMSO in 2 mL cryogenic vials (Corning 430659) and stored in liquid nitrogen vapor phase. Before beginning a new culture, the freezer stocks were thawed, diluted in 9 mL complete media and plated in Nunclon Delta 10 cm^3 dishes (VWR 10171744). After allowing ~16 hours for the revived cells to attach, the DMSO containing media was replaced with DMSO free complete media. All revived cultures were split at least twice prior to use in an experiment. Cell cultures were restarted approximately every 3-4 weeks. All cell-based experiments reported used multiple restarted cell cultures in the independent experiments that make up the replicate results. For experiments, cell cultures were used with a confluency of ~70%. The cell cultures were not allowed to ever become superconfluent, and the cellular morphology and proliferation rate of the cell culture was carefully tracked to identify any abnormalities; any

cell culture showing the slightest abnormalities were discard and the cell line restarted from frozen stocks. For experiments, cells were allowed to recover from splitting and replating a minimum of 16 hr prior to the start of an experiment.

The adherent mammalian cell lines are split every ~3 days with the following general procedure: the complete media is removed via aspiration and the cells are gently washed with 5 mL of 1X PBS. TrypLE trypsin reagent (2.5 mL for 10 cm^3 plate) is added and incubated for approximately 10 min at 37 ºC. After 10 mins 7.5 mL of the complete culture media is added to inactivate the TrypLE reagent. Cells were counted using a TC20™ Automated Cell Counter (BioRad), by combining 10 µL of cell solution with 10 µL Trypan Blue stain (Thermo 15250061).

3.6.3 OSW-1 Compound

The OSW-1 compound used was obtained through total synthesis in the Burgett lab or from isolation from the natural source. OSW-1 used in the experiments was of >95% purity as determined with ^{1}H-NMR and LCMS analysis. Solid OSW-1 compound was dissolved in analytical grade DMSO solution to produce 10mM stocks for experimentation. The 10 mM OSW-1 stock solution was aliquoted into Eppendorf brand 1.5 mL centrifuge tubes; Each individual 10 mM OSW-1 aliquots were thawed no more than three times. Additional cycles of freeze/thaws caused partial loss of OSW-1 compound in the aliquots.

3.6.4 Cell Lysis

Cells were cultured in Nunclon Delta 10 cm^3 dishes (VWR 10171744) and prepared for lysis by removing the media, washing with 1X PBS, followed by addition of 1 mL PBS and scraping. Cells were collected in a 1.5 mL Eppendorf brand centrifuge tubes and centrifuged at 14,000 x g for 45 seconds. Supernatant was removed, and the cells were resuspended in 50 µL of AC Lysis buffer (150 mM NaCl, 1.5 mM $MgCl_2$, 5% glycerol, 0.8% NP40, 1mM DTT, 50 mM

HEPES, 25 mM NaF, 1 mM Na_3PO_4) with 3X HALT/EDTA protease inhibitor (Thermo 78438) and 0.2 mM phenylmethanesulfonylfluoride (Goldbio). Cell lysis was performed by freezing cells in liquid nitrogen and thawing in a 37°C bead bath three times, followed by a 14,000 x g centrifugation for 15 minutes. Supernatant was transferred to a new tube and a portion was taken for protein quantification using a Bradford assay (Bio-Rad Protein Assay Dye Reagent Concentrate #5000006, BSA-Santa Cruz sc-2323). After protein quantification, the lysates were diluted to the desired concentration using AC lysis buffer and a final concentration of 1X Laemmli buffer (1 M Tris pH 6.8, 8% SDS, 40% glycerol, 20% β-mercaptoethanol, and 0.2% bromophenol blue), followed by dry bath heating at 95°C for 10 minutes.

Cells cultured on 6-well plates (Greiner 657160) were prepared for lysis by removing media, washing with 1X PBS, followed by adding 0.5 mL TrypLE™ Express (Gibco 12605010) and incubated at 37°C for 5 minutes. TrypLE™ was neutralized using 0.5 mL of media and cells were then transferred to a 1.5 mL Eppendorf tube and centrifuged at 14,000 x g for 45 seconds. Supernatant was removed, and 1 mL of PBS was added to wash the cells. Cells were centrifuged at 14,000 x g for 45 seconds, supernatant was removed, and the cells were resuspended in 50 µL of AC lysis buffer. Freeze/thaw lysis method was continued as described above.

3.6.5 Western Blotting

SDS-PAGE gels (8.5 or 12%) containing 25 µg of total protein per well were transferred to 0.45 µm nitrocellulose (Bio-Rad 1620115) using constant voltage (100V) for 1 hour at 4°C in 1X transfer buffer with 10% ethanol. After transferring, the nitrocellulose membrane was blocked with 5% milk 1X TBST at room temperature for 30 minutes. The membranes were then washed three times, five minutes each, with 1X TBST. Primary incubation with antibodies was done overnight at 4°C. After primary incubation, the blots were washed five times, five minutes each,

with 1X TBST and then incubated in secondary antibody in 1% milk TBST for thirty minutes at room temperature. After secondary antibody incubation, the blots were washed five times, five minutes each, with 1X TBST and then once with 1X TBS for ten minutes. TBS was removed, and the blots were incubated in Clarity™ Western ECL substrate (Bio-Rad 1705061) and imaged on the Bio-Rad ChemiDoc™ Touch Imaging System using the chemiluminescence setting with 2x2 binning. Ladder images were taken using the colorimetric setting. After development, the membranes were washed with 1X TBST twice for five minutes each. 1:1000 β-actin HRP (Santa Cruz sc-47778 HRP) in 1% milk TBST was added and incubated for 1.5 hours at room temperature. Developing occurred the same as after secondary antibody incubation. Primary antibodies used were 1:500 OSBP A-5 (Santa Cruz sc-365771), 1:500 p21 C-19 (Santa Cruz sc-397), 1:1000 OSBP2 B-1 (Santa Cruz sc-365922), 1:100 SQSTM1 (p62) D-3 (Santa Cruz sc-28359) and 1:1000 LC3A/B D3U4C XP® (Cell Signaling 12741). Secondary antibodies used were 1:1000-1:3000 goat anti-mouse IgG_1-HRP (Santa Cruz sc-2060), 1:3000 goat anti-rabbit IgG-HRP (Santa Cruz sc-2004) and 1:2000 goat antirabbit IgG-HRP (Cell Signaling 7074S).

3.6.6 Cycloheximide Chase Experiments

HCT116 and HEK293 cells were seeded at $1.6x10^5$ cell per well into six well plates (Greiner 657160) and left to rest for 20 hours. Media containing 177 μM cycloheximide (Sigma C7698-1G) was added to the plates and the cells were incubated for the times indicated before the cells were lysed and analyzed by Western blotting.

3.6.7 Proteasome Inhibitor Assays

HCT116 cells were seeded out into plates and left to rest for 20 hours. For the co-incubation experiments, the cells were treated with DMSO (Sigma 472301), 1 nM OSW-1, 25 nM Bortezomib (Sigma 5043140001), 25 nM Carfilzomib (AdooQ Bioscience A11278), 170 nM MG-132 (Sigma

474787), or a combination of treatments for 24 hours. Cells were lysed and analyzed by western blotting. For the washout experiments, the cells were treated with media containing DMSO or 1 nM OSW-1 for 6 hours, washed 3 times with 5 mL of media, and then allowed to recover for 24 hours. After the 24-hour recovery, one set of treatments were lysed as a control to ensure OSPB loss while the other cells were treated with media containing 25 nM Bortezomib, 25 nM Carfilzomib, 170 nM MG-132, or DMSO for 24 hours. Cells were lysed and analyzed by western blot.

3.6.8 Calpain Anaysis

For the continual treatment, HeLa cells were seeded out in a 6 well plate. Upon 70% confluency, cells were treated with DMSO, DMSO and ALLN (10µM), OSW-1 (1nM), or OSW-1 (1nM) and ALLN (10µM) for 24 hours. Cells were lysed and analyzed following the 6-well lysis method and the western blot protocol. Under the washout experimental conditions, cells were treated with DMSO or OSW-1 (1nM) for 6 hours. Cells were washed out according to the washout experimental method. After 24-hour recovery, one set of DMSO and one set of OSW-1 was lysed following the 6 well lysis method. At the same time (24 hours post-wash), ALLN (10µM) was added to one set of DMSO and one set of OSW-1. The cells continued to incubate until 48 hours post-wash, at which point they were lysed and analyzed using the western blot method. Experiments and analysis were performed by Mr. Ryan Bensen

3.6.9 RT-PCR Analysis

HCT116 and HEK293 cells were seeded at $0.85x10^5$ cells/mL into 10 cm^3 plates and left to rest for 20 hours. Cells were treated in the same manner as the washout with 1 nM Taxol, 1 nM OSW-1, and DMSO and left to recover for 0-72 hours. Once each time point was reached, media was removed from cell plates and 1 mL of TRIzol (Thermo 15596026) was added to the plates and

cells were scraped and collected in a 1.5 mL Eppendorf tube and incubated at room temperature for 5 minutes to ensure nucleoprotein complex dissociation. To each tube, 0.2 mL of chloroform was added and incubated for 2.5 minutes at room temperature. The samples were then spun down at 12,000 x g for 15 minutes at 4°C. After spinning the upper aqueous phase was transferred into a fresh 1.5 mL Eppendorf tube. 0.5 mL of 100% isopropanol was added and the tubes were mixed by inversion followed by a 10-minute incubation at room temperature. Samples were then spun down at 12,000 x g for 10 minutes at 4°C. Supernatant was discarded and 1 mL of 75% ethanol was added to the pellet to wash the RNA. The sample was vortexed briefly to dislodge pellet and then spun down at 7,500 x g for 5 minutes at 4°C. Supernatant was discarded and pellets were left to air dry for 5 minutes, after which 100 µL of MQ H_2O were added to resuspend the RNA. Samples were then heated at 60°C for 10 minutes. RNA concentration was taken using a nano-drop before being stored at -80°C. cDNA was made by using the Maxima First Strand cDNA Synthesis Kit (Thermo K1671). 4 µg of RNA was added to a PCR tube containing µ1 L of dsDNase, 1 µL of 10x dsDNase buffer, and MQ H_2O to 10 µL. PCR tube was then incubated at 37°C for 2 minutes, placed on ice, spun down briefly, and placed back on ice. 1 µL of 100 mM DTT was added to the tube and incubated at 55°C for 5 minutes, placed on ice, spun down briefly, and placed back on ice. 1 µL of 10 mM dNTPs, 1 µL random primers, and MQ H_2O to 15 µL. Tubes were briefly mixed and incubated at 65°C for 5 minutes, put on ice, spun down, and put back on ice. 4 µL of 5X RT buffer and 1 µL of Maxima enzyme were added to the tube and then incubated at 25°C for 20 minutes, 50° for 30 minutes, followed by an inactivation at 85°C for 5 minutes. cDNA was stored at -20°C. cDNA synthesis was confirmed by PCR with intron spanning β-Actin primers. Once verification was confirmed, RT-PCR was set up using Fast SYBR Green (Thermo 4385612) with intron spanning primers (OSBP, ORP4, and β-Actin). 10 µL of Fast SYBR

Green was mixed with 0.3 µL of 100 µmoles forward and reverse primer solution, 1 µL of cDNA, and MQ H_2O to 20 µL. Each gene was done in triplicate for each time point. The plate was then run on a Roche LightCycler480 using SYBR green protocol.

3.6.10 Autophagy Experiments

HEK293 cells were seeded into 10 cm^2 plates. Upon 70% confluency, cells were treated with DMSO as a vehicle control, 1 nM OSW-1, 25 µM chloroquine, or 100nM rapamycin, or a combination of treatments for 6 hours in 10 mL DMEM media for each 10cm^3 plate. After 6 hours, the media containing the OSW-1 compound was washed out with three separate 5 mL drug free media washes (same as the washout experimental protocol). Cells were then treated with either drug free media, 100 nM rapamycin, 25 µM chloroquine, or a combination of treatments, and allowed to recover from OSW-1 compound treatment for 6, 15, or 24 hours. After the indicated post washout time point, the cells were lysed using AC lysis buffer according to the cell lysis protocol described previously. Lysates were analyzed via Western blot using OSBP, SQSTM1 (p62), and LC3-A/B antibodies, with β-actin antibody used as a loading control for quantification (antibody information can be found in 'Western blotting' experimental methods). Experiments and analysis were performed by Mr. Zachary Severance

3.6.11 iTRAQ Experiments

HEK293 cells were seeded and treated according to the 0-72-hour recovery washout experimental procedure previously described (1nM OSW-1 or DMSO, 6-hour treatment). After the desired post washout time point, the cells were lysed according to the AC lysis protocol (lysis method 1) using modified AC lysis buffer. The modified AC lysis buffer contained no DTT and only 3X HALT (no EDTA or PMSF) for protease inhibitor. Free thiols can interfere with the

cysteine blocking step prior to iTRAQ tagging and protease inhibitors were kept to a minimum to avoid inhibiting trypsin during the digestion process.

Effective treatment was confirmed via Western blot using OSBP antibody and β-Actin antibody as a loading control. A Multiplex Buffer Kit (Sciex 4381664) was used for the denaturing, reducing, and blocking steps. Trypsin with $CaCl_2$ (Sciex 4352157) was used for digestion; and iTRAQ Reagent-8Plex Multiplex Kit (Sciex 4390812) was used for iTRAQ labeling. These kits were utilized according to the iTRAQ Reagents- 8plex Protocol. After tagging, the pH of the samples was lowered to approximately 3, using 1N Phosphoric Acid, and ran through a cation-exchange cartridge system (Sciex cationexchange cartridge 4326747, cartridge holder 4326688, outlet connector 4326690, and needleport adapter 4326689) to remove any substances that could interfere with LC/MS/MS analysis. The protein eluate was quantified using a NanoDrop One^C (Thermo). Samples were normalized to a "mixed" sample that contained 5.5 µg of protein from each sample. Only shared proteins in all 3 biological replicates were used to test for changes in different conditions. P-values were generated using multiple t-tests in GraphPad Prism 7 ($P<0.05$ for significantly changed proteins). Volcano plots were also generated in GraphPad Prism 7 to display P values against fold changes between the two treatment conditions. Cell treatments, lysate tagging, and protein quantification confirmation were performed by Mr. Zachary Sevarance and the LC/MS/MS experiments and analysis were performed by Ms. Hongyan Ma; Ms. Ma is a graduate student in the lab of Dr. Si Wu, Department of Chemistry and Biochemistry, Univ. of Oklahoma.

3.6.12 LC-MS/MS analysis of labeled peptides

Mixed peptide samples were analyzed using the LC-MS/MS following previously published protocol(203, 230). Peptide samples were desalted, dried in SpeedVac, and resuspended in buffer

A (0.1% formic acid in water). 1 µg of the digested sample was injected onto a custom-packed C18 RPLC column (75 µm i.d., 150 mm length, 2 µm C18 resin, Thermo) using a Waters (Milford, MA, USA) nano-Acquity UPLC system, which is online coupled with a LTQ Orbitrap Velos Pro mass spectrometer (Thermo) through a custom nano-ESI interface. For peptide separation, a 100-min gradient was applied from 3% buffer A to 35% buffer B (0.1% formic acid in acetonitrile). Full MS spectra were acquired at a resolution of 60K (m/z range between 350 and 2000). The data-dependent higher-energy collisional dissociation (HCD) based MS/MS spectra were acquired at a resolution of 15K with a normalized collisional energy of 33% using the ten most abundant parent ions. Peptides were identified using MSGF+ to search LC-MS/MS against the annotated Uniprot human protein database(231, 232). Peptide identifications were filtered with a MSGF cut-off score lower than the calculated FDR<1% at the unique peptide level against decoy database. The iTRAQ reporter ion intensities of each HCD scan were extracted and analyzed using in-house developed software. Experiments and analysis were performed by Ms. Hongyan Ma; Ms. Ma is a graduate student in the lab of Dr. Si Wu, Department of Chemistry and Biochemistry, Univ. of Oklahoma.

3.6.13 Cell Splitting and Density Experiment

HEK293 cells were cultured to ~70% confluency and then treated with either 1 nM OSW-1 compound or DMSO for 6 hours, followed by washout. Cells were split following protocol outlined in General Cell Culture. Cells were plated with placing back all of the cells (1:1), placing back half the cells (1:2), or placing back only 20% of the cells (1:5). All cells were allowed to recover for 24 hours before lysis and analysis by Western botting.

3.6.14 Statistical Analysis

Results are expressed as mean ± s.d. and are n=3 unless otherwise stated. All statistical tests were performed using GraphPad Prism 7.0. Comparison between groups were made by

using a one-way ANOVA with a follow up Dunnett's test. The p values are reported using GraphPad Prism * values: * is $p \leq 0.05$, ** is $p \leq 0.01$ *** is $p \leq 0.001$, and **** is $p \leq 0.0001$.

Chapter 4: The compound OSW-1 is a unique ORPphillin that has prophylactic anti-viral capabilities

The following chapter is partially taken from a previous unpublished prepared manuscript. This was a collaborative work that consists of the following authors: Brett L. Roberts, Zachary C. Severance, Ryan C. Bensen, Anh T. Le, Cori A. Malinky, Evan M. Mettenbrink, William J. Reddig, Earl L. Blewett, Anthony W. G. Burgett.

Mr. Zachary Severance conducted the radioactive binding assay in **Figure 32**

and the HeLa cell protein determination in **Figure 33**.

Mr. Ryan Bensen conducted the radioactive binding assay in **Figure 32**.

Dr. Earl Blewett conducted the anti-viral assays in **Figure 33**.

4.1 Abstract

The genus *Enterovirus* contains many important human pathogens (e.g. coxsackievirus, enteroviruses, human rhinovirus, polio virus) that cause a variety of diseases that currently lack approved therapy. Targeting host proteins that are hijacked for use in a conserved viral replication step in the early stages of infection enables broad-spectrum inhibition and provides fundamental knowledge about how these viruses hijack cells for replication. Currently the host protein OSBP is a desirable target due to its involvement in the formation of viral replication organelles where it supplies cholesterol to maintain efficient membrane lipid homeostasis required for viral genome replication. Compounds that target OSBP, which are called ORPphillins (OSW-1, Itraconazole, TTP-8307, and T-00127-HEV2), have been shown to have broad-spectrum anti-enteroviral activity. Here we show that of the ORPphillins tested, only OSW-1 can reduce OSBP protein levels with treatment. OSW-1 and T-00127-HEV2 show competitive binding to OSBP in a radioactive 25-OHC binding assay. T-00127-HEV2, but not oxysterols, can rescue OSBP levels in the

presence of OSW-1. Similarly, T-00127-HEV2 induces a ~2-fold change in the relative GI_{50} in the presence of OSW-1. All the compounds tested have anti-viral activity with continual treatment, but only OSW-1 induces an anti-viral response 24 hours after the compounds have been removed. Therefore, OSW-1 presents itself as the best candidate for further development as a broad spectrum anti-viral due to its prophylactic ability.

4.2 Introduction

Picornaviridae is a family of positive-sense RNA viruses with little therapeutic treatment, which includes many viruses that impact human health, one of the most notable being the *Enteroviruses* (see section 1.4.1.2 **Enteroviruses**). Oxysterol-binding protein (OSBP), a member of a highly conserved eukaryotic protein family, is associated with viral replication through its function as a lipid transport protein between the ER and Golgi (see section 1.4.1 **OSBP Function in Virus Replication**). The natural product OSW-1, is a high affinity ligand of OSBP and has broad-spectrum anti-enteroviral activity through inhibiting OSBP cellular functions (see section 1.5.1 **OSW-1**). Recent literature has identified other OSBP binding compounds that have anti-enteroviral activity, presumably through OSBP inhibition, but the cellular effects of these compounds on OSBP protein levels remain unknown (see section 1.5 **ORPphillins and OSBP/ORP4)**. We have previously shown that short low nanomolar doses of OSW-1 followed by removal of the compound from cells leads to reduction of OSBP up to 72 hours post compound removal. Cells treated with this OSW-1 washout were also resistant to enteroviral infections post compound removal.

In this study, we investigated a panel of OSBP targeting small molecules anti-viral abilities collectively as well determining their ability to produce a prophylactic anti-viral after compound washout. We show that OSW-1 is the only compound to produce a reduction in OSBP levels in a

panel of cell lines. Interestingly, co-incubation of THEV2, and to a lesser extent ITZ, with OSW-1 could rescue OSBP levels but TTP could not. Direct binding assays reveal that THEV2 has a similar Ki to OSW-1, while the other compounds were non-determinable. We provide evidence that continual treatment of all the compounds show anti-viral activity, but OSW-1 is the only compound to show anti-viral activity following pretreatment and removal of the compound. This provides evidence that OSW-1 has a unique effect on the cellular biology of OSBP, which makes it a promising compound for anti-viral pursuit.

4.3 Results

4.3.1 OSW-1, but no other ORPphillin, affects cell growth or OSBP protein expression

We found that none of the compounds, besides OSW-1, showed significant growth inhibition on HCT116 cells at the highest concentrations tested (**Figure 29A**). Treatment with OSW-1 and taxol gave GI_{50}s near previously reported values(46) (**Figure 29A**). Due to the solubility issues of ITZ and TTP, coupled with the lack of cytotoxicity, all compounds besides OSW-1 were tested at the highest soluble concentration (10μM). HCT116 cells were treated continual with the compounds for 24 hours to determine if they reduced OSBP levels similar to OSW-1 continual treatment. Only OSW-1 reduced OSBP protein levels in HCT116 cells (**Figure 29B**). Similar results were seen in HEK293 cells over the same time course and treatments (**Figure 64**).

4.3.2 ORPphillins show differential localization patterns of OSBP

To determine if the compounds affect OSBP cellular localization we utilized immunofluorescence microscopy in HCT116 cells. It is known that OSBP localizes to the trans-Golgi network upon the addition of various ligands(11, 46, 81, 156). The imagining experiments used the OSBP antibody and an antibody recognizing the trans Golgi marker TGN46, as well as a

nuclear stain. Treatment with 25-OHC caused a clustered localization of OSBP with the trans-Golgi marker TGN46 in HCT116 cells as previously reported(11, 46)(**Figure 30**). OSW-1 treated cells show a highly reduced signal, consistent with Western blotting, and show the remaining OSBP in a vesicle formation that is not associated with the TGN46 marker (**Figure 30**). The TGN46 signal in OSW-1 treated cells is also reduced and scattered, suggesting disruption of the Golgi-network due to loss of OSBP function. A phospho-memetic version of OSBP that is inactive was shown to have impaired Golgi localization which induced Golgi fragmentation(73). ITZ treatment shows a broader Golgi stain compared to DMSO but a vastly different OSBP staining (**Figure 30**). OSBP staining is very patchy but still mainly overlaps with the Golgi marker. TTP shows a very similar staining pattern to DMSO, but with intensified OSBP signal, which suggests that treatment causes more localization of OSBP to the Golgi in its native state (**Figure 30**). THEV2 is similar to 25-OHC staining, showing clustered OSBP and TGN46 signals (**Figure 30**).

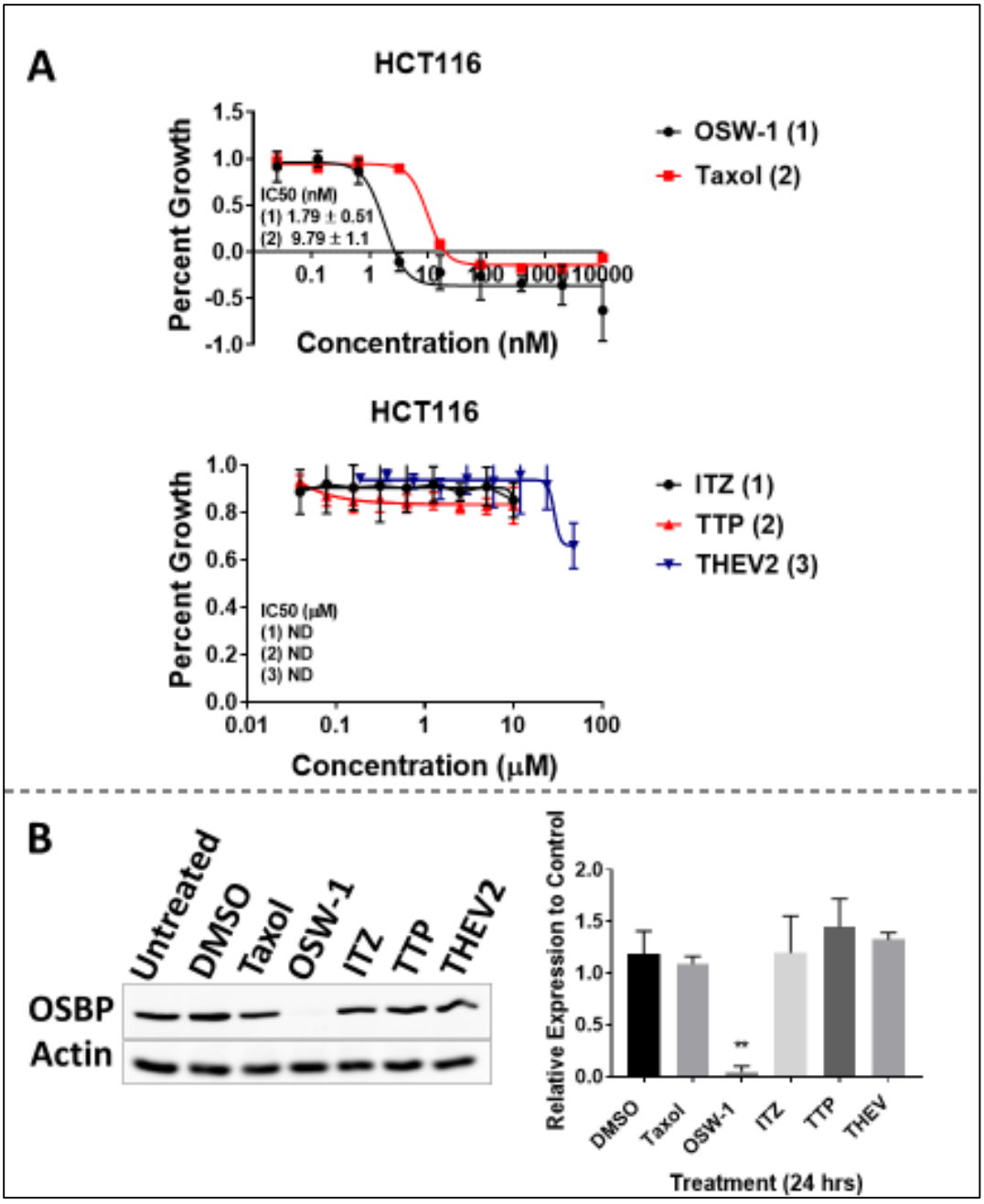

Figure 29: OSW-1, but no other ORPphillin, affects cell growth or OSBP protein expression. (A) Effect on 48-hour growth of OSW-1, Taxol, ITZ, TTP, or THEV2 in HCT116 cells. (B) OSBP levels are reduced with OSW-1 (1 nM) but not the other compounds (10 μM) after 24 hours of treatment in HCT116 as judged by western blotting analysis. (Full blot in **Figure 64**).

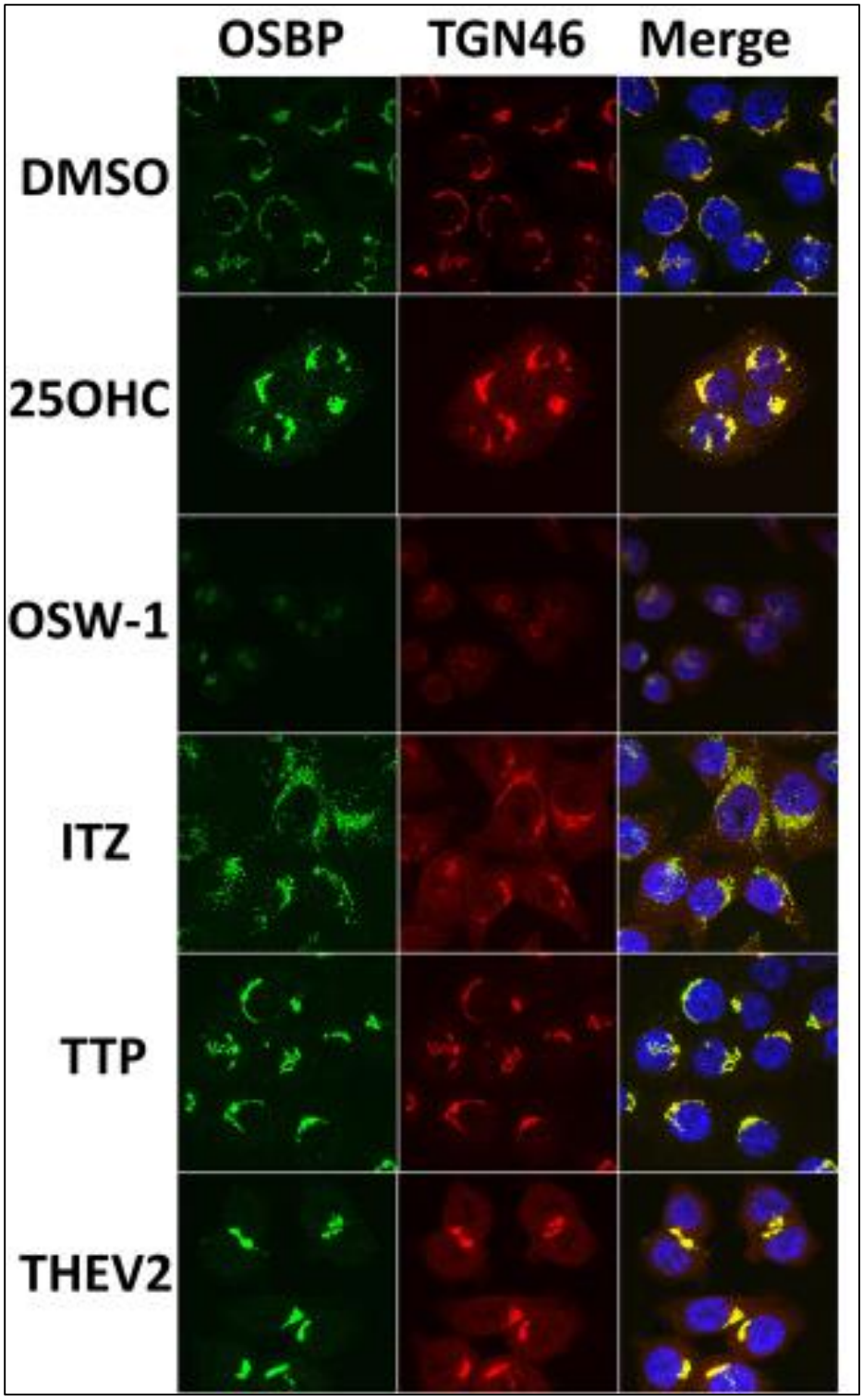

Figure 30: ORPphillins show differential localization patterns of OSBP. OSBP (green) and TGN46 (red) were visualized in HCT116 cells using indirect immunofluorescence. Cells were treated with DMSO, 1 nM OSW-1, or 10 μM of 25-OHC, ITZ, TTP, or THEV2 for 24 hours. Nuclei (blue) were stained with Hoescht 33342.

4.3.3 Co-incubation with THEV2 or ITZ, but not oxysterols, can rescue OSBP loss induced by OSW-1

We tested the compounds in tandem with OSW-1 to determine if any could rescue OSBP protein levels. It was previously reported that co-incubation of other OSBP ligands with OSW-1 could rescue the expression level of OSBP(46). We found that THEV2 and ITZ significantly rescued OSBP levels to around 70% and 40% respectively in HCT116 cells (**Figure 31A**). Interestingly, TTP co-incubation was not different than OSW-1 alone, suggesting it could not out compete OSW-1 (**Figure 31A**). Similar results were obtained in HEK293 cells.

Comparing the structures of the compounds (**Figure 9**, **Figure 12** & **Figure 13**), THEV2 is the most steroidal in structure and has the ability to localize OSBP similar to 25-OHC (**Figure 30**). It was previously reported that 25-OHC treatment could rescue OSBP levels when administered with OSW-1(46). We tested if OSW-1 treatment along with 25-OHC or 20-α-OHC, two naturally occurring oxysterols, could rescue OSBP levels in HCT116 cells. Interestingly, we found that neither oxysterol could protect OSBP levels with the addition of OSW-1 (**Figure 31B**).

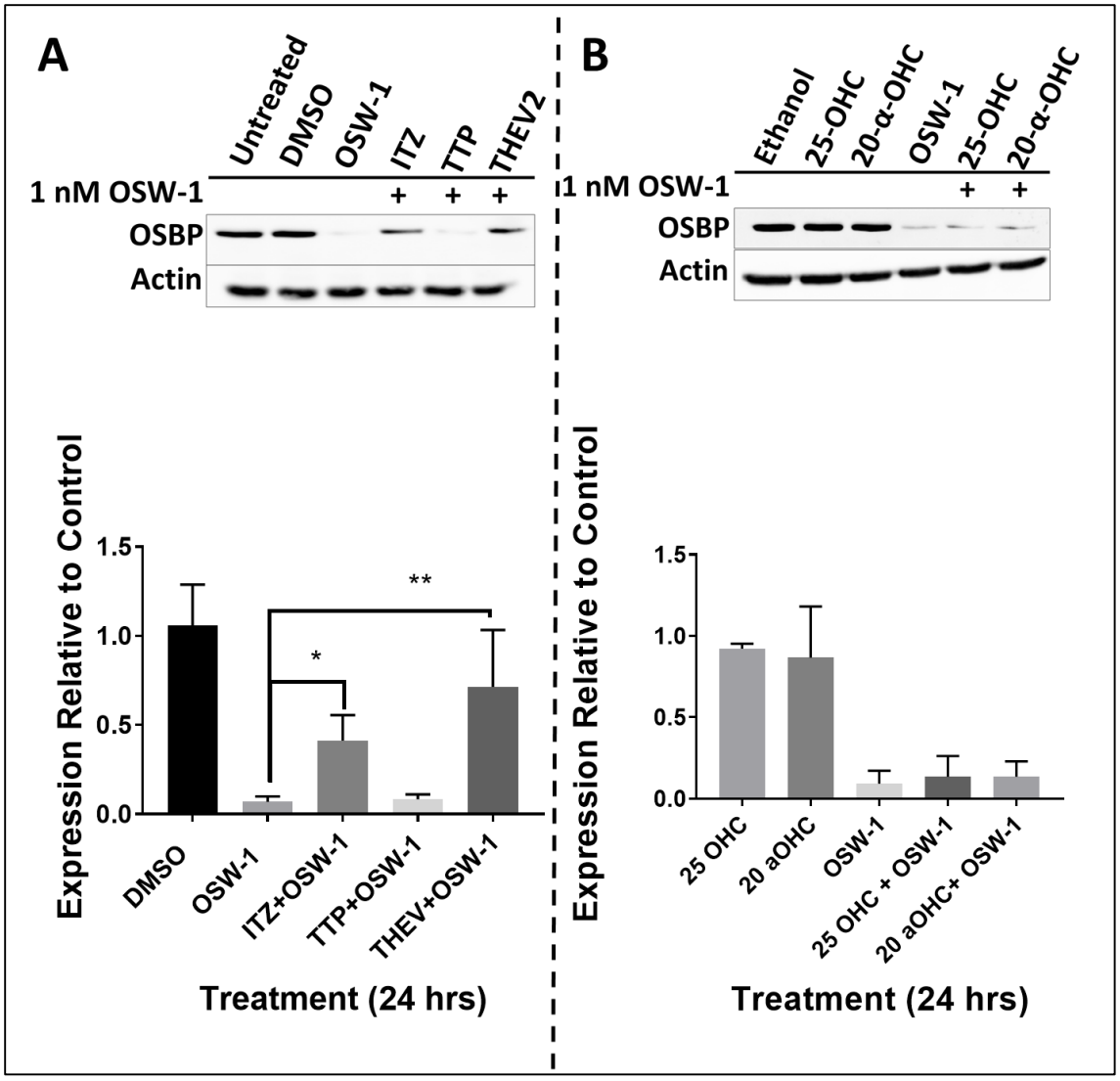

Figure 31: Co-incubation with THEV2 and ITZ, but not oxysterols, can rescue OSBP loss induced by OSW-1. HCT116 cells were treated with 1 nM OSW-1, DMSO, or a combination of 10 µM ITZ (A), TTP (A), THEV2 (A), 25-OHC (B), or 20-α-OHC in combination with 1 nM OSW-1 for 24 hours and then analyzed by western blot. (Full blots in **Figure 65**)

4.3.4 THEV2 binds OSBP competitively and suppresses OSW-1 cytotoxic activity.

Based on the mixed results of localization and co-incubation rescue data, we determined the ability of each compound to competitively bind to OSBP. Using a previously established *in vitro* competitive binding assay with [3H]-25-OHC(46), we found that THEV2 binds competitively with OSBP while ITZ and TTP did not (**Figure 32A** & **C**). THEV2 and 25-OHC

have comparable binding affinity to OSBP and show similar localization patterns, yet THEV2 has the ability to rescue OSBP during OSW-1 co-incubation while 25-OHC does not (**Figure 31**, **Figure 32A** & **C**). Interestingly, ITZ does not bind OSBP competitively but was shown to have some protective ability in the co-incubation experiments (**Figure 31A** & **Figure 32A**). The unusual localization induced by ITZ (**Figure 30**) could be a result of the lack of competitive binding (**Figure 32A**). Not surprisingly, TTP does not display competitive binding to OSBP (**Figure 32A**), which was expected due to the lack of protection against OSW-1 induced OSBP protein reduction (**Figure 31A**).

Our results from the co-incubation Western blot and cellular localization show mixed results for the compounds in terms of their competitive binding ability. Since the *in vitro* binding assay can only detect competitive binding, there is a possibility that ITZ and TTP can bind OSBP at a different site than OSW-1. To determine the effect of these compounds on OSBP *in vivo*, we conducted a 48-hour growth inhibition assay with co-incubations of OSW-1 and a set concentration of ITZ, TTP, or THEV in HeLa cells (**Figure 32B &C**). THEV2 co-incubation was able to significantly reduce OSW-1 growth inhibition by ~2 fold while ITZ and TTP co-incubation had little effect (**Figure 32B & C**). We also found that co-incubation with 1 nM OSW-1 and 10 µM of the compounds showed similar viability changes as the growth inhibition assay after 24 hours (**Figure 66**).

Immunofluorescence microscopy in HCT116 cells revealed that the localization of OSBP with co-incubation of the compounds has similar results as the *in vivo* binding and growth inhibition assays (**Figure 67**). Co-incubation with THEV2 and OSW-1 shows a split pattern of slightly reduced OSBP staining clustered to Golgi staining similar to THEV2 alone (**Figure 30** & **Figure 67**). There is also OSBP vesicle staining that is dissociated from the Golgi (**Figure 30** &

Figure 67). Co-incubation of ITZ and OSW-1 showed a more clustered OSBP staining to the Golgi than ITZ by itself (**Figure 30**), but more OSBP signal was in vesicles dissociated from the Golgi (**Figure 30** & **Figure 67**). TTP co-incubation resembles OSW-1 alone (**Figure 30**) with highly reduced OSBP signal in vesicles dissociated from the Golgi (**Figure 67**). These results suggest that competitive binding to OSBP is required to efficiently inhibit OSW-1 induced degradation.

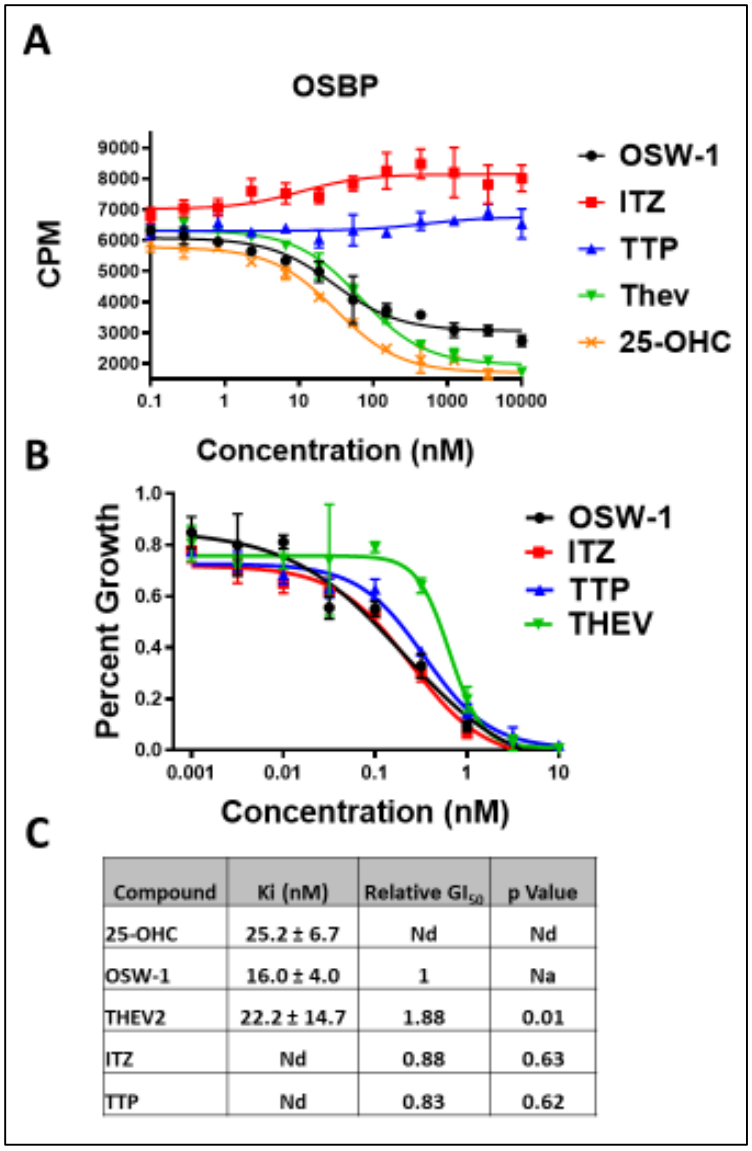

Compound	Ki (nM)	Relative GI_{50}	p Value
25-OHC	25.2 ± 6.7	Nd	Nd
OSW-1	16.0 ± 4.0	1	Na
THEV2	22.2 ± 14.7	1.88	0.01
ITZ	Nd	0.88	0.63
TTP	Nd	0.83	0.62

Figure 32: THEV2 binds OSBP competitively and suppresses OSW-1 cytotoxic activity. (A) THEV2 has a similar Ki values (C) as OSW-1 and 25-OHC while ITZ and TTP did not show competitive binding. (B) THEV shows significant protection against OSW-1 growth arrest (C) as determined by 48-hour co-incubation cell growth assay with OSW-1 and 10 µM of ORPphillins in HeLa cells. ITZ and TTP do not have any effect on cell growth when co-incubated with OSW-1. (C) Table showing the Ki generated from (A), the relative GI_{50} as compared to OSW-1 and p value from a two-tailed t-test from (B). Nd= not determined and Na= not applicable. Data collected by Mr. Zachary Severance and Mr. Ryan Bensen. The author had no contribution to the results of these experiments.

4.3.5 OSW-1 exerts anti-viral activity 24 hours after compound has been removed

We tested the ability of the ORPphillins to exert anti-viral activity against two clinically isolated *Enteroviruses* in Hela cells. The ORPphillins tested so far have been shown to exert anti-viral activity on various enteroviruses through disruption of OSBP function(81, 82, 155, 156). All of the compounds inhibited viral replication of the two clinically isolated *Enteroviruses* under continual treatment, but treatment with OSW-1 was the most effective (**Figure 33A**). We have previously shown that OSW-1 is able to induce the degradation of OSBP during straight treatment (**Figure 29B**), but it can also reduce the OSBP protein levels for multiple days after a short non-toxic treatment followed by removal of the compound we have termed washout experiments (

Figure 18). We conducted washout experiments with the compounds to determine if a similar anti-viral response to OSW-1 washout treatment could be induced (**Figure 24B**). In short, the cells were treated with compounds for six hours, followed by three rounds of washing with media and allowed to recover for 24 hours before being infected. We found that only OSW-1 could reduce OSBP protein levels in Hela cells under these conditions (**Figure 33C**) and was the only compound to still exert anti-viral activity 24 hours after the compound had been removed (**Figure 33B**).

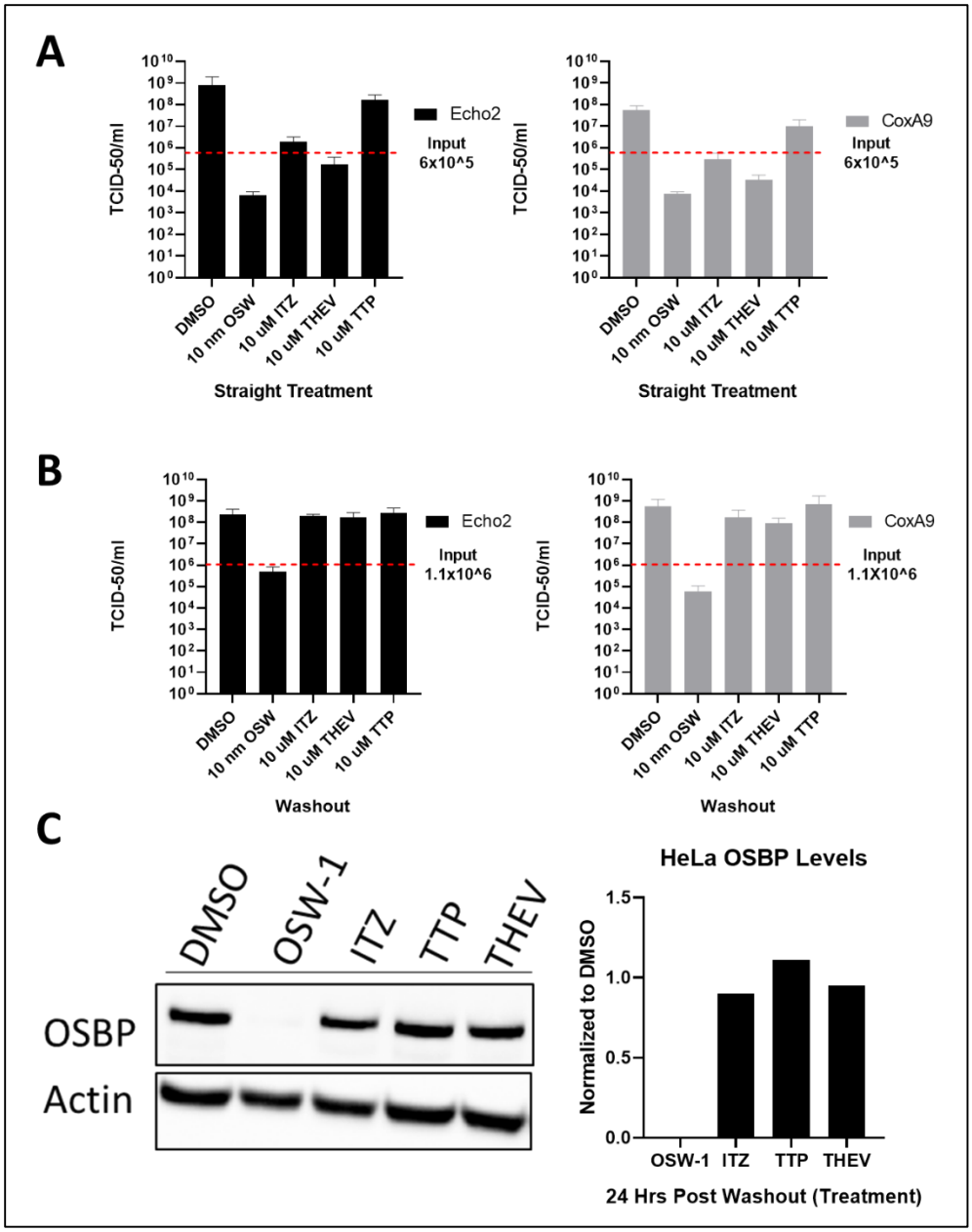

Figure 33:**OSW-1 exerts anti-viral activity 24 hours after compound has been removed.** (A) Viral titers of infected HeLa cells incubated in the presence of the compounds. Cells were treated with the indicated concentrations of compounds for 6 hours, followed by viral infection for 30 min (MOI of 1.0), followed by re-incubation for 10 hours with compounds (B) Viral titers in compound washout HeLa cells. Cells were treated with the indicated concentrations of compounds for 6 hours, compounds were removed, cells were allowed to recover for 24 hours in compound-free media. Then, cells were infected for 30 min with virus (M.O.I.=1.0) followed by 10-hour incubation in compound-free media. (C) OSBP protein levels of compound washout HeLa cells at the 24-hour recovery point before infection. All viral assays were done by Dr. Earl Blewett and OSBP determination was done by Mr. Zachary Severance. (Full blot in **Figure 68**). The author had no contribution to producing these results

4.4 Discussion

The biological effect of various anti-viral compounds targeting OSBP was assessed and of the compounds tested, only OSW-1 showed any cytotoxicity and could cause a reduction of OSBP levels at 1 nM of treatment. Treatment with the other compounds at 10 µM did not affect the protein level, which is not surprising since there was no cytotoxicity of the compounds in this range. These results reconfirm the idea that select OSBP ligands cause OSBP protein loss(46).

The co-incubation of the compounds with OSW-1 treatment showed that ITZ and THEV2 possess protective activity, but to different degrees. Although ITZ shows a modest protection of around 40%, the viability of cells treated with ITZ or ITZ+OSW-1 is similar to OSW-1 by itself (**Figure 66**). One of the possible reasons for the loss of viability during treatment with ITZ is due to its anti-cancer activity(148, 150, 233). THEV2 protects OSBP to around 70% and the viability with THEV2+OSW-1 is near that of untreated cells (**Figure 66**). This would suggest that THEV2 can out compete OSW-1 interactions with OSBP without the loss of viability due to other cellular interactions. The *in vitro* competitive binding assay confirms this binding interaction, showing that of the compounds tested, THEV2 is similar to 25-OHC in its Ki and OSBP localization pattern (**Figure 30** & **Figure 32A**). THEV2 is able to significantly increase the GI_{50} of OSW-1, suggesting the necessity to remove OSW-1 from the binding pocket to protect OSBP

Interestingly, 25-OHC did not protect OSBP in a similar manner as previously reported(46) (**Figure 31B**). A possible explanation for this discrepancy is the loss of potency of OSW-1 stocks after multiple freeze/thaw cycles that we witnessed in previous experiments. It is quite possible that the stock compound used in the original experiments was diluted due to the hydroscopic nature of the DMSO solvent during the freeze/thaw cycles. We have shown previously that OSBP loss due to OSW-1 treatment is both time and concentration dependent (**Figure 22B** & **Figure 46**), so

this could explain how 25-OHC treatment would be able to protect OSBP during OSW-1 treatments in the original experiments. For our experiments, we minimized the freeze/thaw cycle of aliquots to three times before discarding the aliquot for a new one. This experiment suggests that the protective effect of THEV2 is not solely due to the steroidal nature of the compound. Despite similar Ki values and localization patterns, there is a difference in the ability of THEV2 and 25-OHC to rescue OSBP levels. This might be due to the availability of the compounds within the cells because 25-OHC is a promiscuous ligand interacting with various proteins(234). Further testing of THEV2 needs to be performed to understand its full effect within the cell.

Although ITZ and TTP have no competitive binding, they demonstrate the ability to change the localization of OSBP, which suggests an alternative binding site. Previous studies have shown that ITZ binds to OSBP with a Kd of around 430 nM and that all eight stereoisomers of ITZ are able to induce OSBP re-localization and anti-viral activity (81, 235). This indicates a lose fitting interaction with OSBP(81, 235). This weak, non-competitive binding interaction could explain the slight rescue of OSBP witnessed during the co-incubation experiments. A previous study has shown that TTP inhibits the cholesterol and lipid transporting abilities of OSBP, but to a far lesser extent than ITZ(156). Based on the lack of competitive binding results, it might suggest that TTP binds to OSBP in a manner that allows for sterol binding but not transfer. TTP specific targeting of OSBP is questionable since overexpression of OSBP was not able to rescue viral replication, suggesting interaction with other targets that are involved in viral replication(156). It seems that both molecules have weak affinity for OSBP, but may interact with multiple targets within cells, calling their use as antivirals into question.

Unsurprisingly, all the compounds exhibited anti-viral activity when tested under continuous treatment conditions (**Figure 33A**). The log-fold inhibition of viral titers is highest

with OSW-1, despite being 1,000-fold less concentrated than the other compounds. This suggests OSW-1 is more specific for OSBP than THEV2, since the compounds have similar Ki values (**Figure 32C** & **Figure 33A**). Despite the differences in log-fold inhibition, all the compounds can inhibit replication to at least 20% compared to the control, suggesting a strong anti-viral response (**Figure 33A**). OSW-1 was the only compound to induce an anti-viral response 24-hours after the compound was removed from cells (**Figure 33B**). This anti-viral activity is presumably due to the ability of OSW-1 washout treatment to induce long-term reduction of OSBP (**Figure 33C**). This result is significant because initial treatment with OSW-1 was in the low nanomolar range for only a few hours before removal and the anti-viral effect persists for over 40 hours after the compound was first introduced to cells. This provides more evidence that OSW-1 is a specific inhibitor of OSBP with strong capabilities for prophylactic anti-viral treatment.

4.5 Conclusion

Taken together, these findings highlight the uniqueness of OSW-1 in the pool of OSBP targeting anti-viral compounds. ITZ and TTP do not seem to be ideal candidates for anti-viral treatment due to their lack of high specificity for OSBP and the increased dose needed to produce the anti-viral response. Our research has increased the anti-viral knowledge of the THEV2 compound by expanding the number of enteroviruses the compound has been tested against. THEV2 seems to be a unique compound, given its relatively low Ki for OSBP and ability to rescue OSBP expression in the company of OSW-1. Despite these characteristics, OSW-1 displays a stronger anti-viral replication response in the continual treatments with far less concentration. One of the potential reasons to deviate from using OSW-1 is the relatively high toxicity of the compound (~1 nM after 48 hours of continual treatment). We have shown that there is a way around this toxicity by removing the compound with the washout experiments and still retaining

the anti-viral response, which all the other anti-viral OSBP targeting compounds lack. These findings lead to potential of producing a prophylactic anti-viral treatment for a group of viruses which lack any current approved treatment options. Future research should focus on producing OSW-1 derivatives that preferentially target OSBP over ORP4 to fully optimize the potential of this finding.

4.6 Methods

4.6.1 Plasmids and Cloning

Human OSBP cDNA was obtained in a pOTB7 vector from the Mammalian Gene Collection (Thermo). PCR using 5'-GCTAGCATGGCGGCGACGGAG-3' forward and 5'AAGCTTGAAAATGTCCGGGCATGAGC-3' reverse primers amplified a 2.44 kb Nhe IHindIII fragment containing a full-length hOSBP cDNA, which was subcloned into pJET1.1 (Thermo) and sequence verified. The fragment was then cloned into the pcDNA™ 3.1/myc-His(-) C mammalian expression vector (Sigma) Nhe I-Hind III doublecut sites. The reverse primer does not include an additional nucleotide between HindIII cut site and the last OSBP codon resulting in an OSBP-tagless protein. ORP4L was cloned from HCT-116 with cDNA with a NheI forward primer 5'-GCTAGCATGGGGAAAGCG-3' and a HindIII reverse primer 5'-AAGCTTCGAAGATGTTGGGGCACATATG-3'. LacZ was PCR amplified from K-12 E. coli with NotI forward 5'- GCGGCCGCATGCCCG TCGTTTTA-3' and BamHI reverse primer 5'-GGGCGGATCCTTTTTGAC ACCAGACCAA-3'. To generate the proteins expressing tags, the MCS of the completed vector was changed through site-directed mutagenesis with a forward 5'-AAGCTTACGTACGAACAAAAACTCATCTCAGAAGAG3' and reverse 5'-CTCTTCTGAGATGAGTTTTTGTTCGTACGTAAGCTT-3'. The plasmid was expanded in E.

Coli DH5α, and isolated through miniprep and maxiprep kits (Thermo). Gene and plasmid MCS were sequence verified through Oklahoma Medical Research Foundation (OMRF).

4.6.2 Cell Lines and Viruses

HEK293 STF (ATCC CRL-3249) and HeLa (ATCC CCL-2) were cultured in DMEM (Thermo 11995073) supplemented with 10% Hyclone (Fisher Sci SH3006603) and 1% penicillin-streptomycin (Thermo 15140122). HCT116 (ATCC CCL-247) was cultured in McCoy 5A media (Thermo 16600108) supplemented with 10% Hyclone and 1% penicillin streptomycin. RD, (rhabdomyosarcoma) cells (ATCC-CCL-136) were cultured in DMEM (Fisher Sci SH30081.0) with 10% FBS (Atlanta Biological S11550) and 1% penicillin-streptomycin (Gibco 15140-122). Coxsackievirus A9 (strain CoxA9-01) and Echovirus 2 (strain Echo201) were obtained from the Oklahoma State Department of Health Laboratory. They are clinical isolates, obtained from OK residents and typed by the OK State Department of Health and/or the Center for Disease Control and Prevention. All other identifiers have been stripped off. These viruses were passaged twice in RD cells, aliquoted in 1.0 mL amounts and stored in complete medium at -80 ºC. Each virus was titered on RD cells using a TCID-50 assay(210). To allow M.O.I . to be determined a conversion factor of 0.7 was used to change TCID-50 to pfu/ml.

4.6.3 General Cell Culture

All mammalian cell lines were cultured at 37 ºC in 5% CO_2. All handling of the mammalian cell culture was performed in a standard tissue culture hood using standard aseptic technique. Cell lines were cultured in the complete media described above. Cell culture stocks were aliquoted in complete media with 10% DMSO in 2 mL cryogenic vials (Corning 430659) and stored in liquid nitrogen vapor phase. Before beginning a new culture, the freezer stocks were thawed, diluted in 9 mL complete media and plated in Nunclon Delta 10 cm^3 dishes (VWR 10171744). After allowing

~16 hours for the revived cells to attach, the DMSO containing media was replaced with DMSO free complete media. All revived cultures were split at least twice prior to use in an experiment. Cell cultures were restarted approximately every 3-4 weeks. All cell based experiments reported used multiple restarted cell cultures in the independent experiments that make up the replicate results. For experiments, cell cultures were used with a confluency of ~70%. The cell cultures were not allowed to ever become superconfluent, and the cellular morphology and proliferation rate of the cell culture was carefully tracked to identify any abnormalities; any cell culture showing the slightest abnormalities were discard and the cell line restarted from frozen stocks. For experiments, cells were allowed to recover from splitting and replating a minimum of 16 hour prior to the start of an experiment.

Cell lines are split every ~3 days with the following general procedure: the complete media is removed via aspiration and the cells are gently washed with 5 mL of 1X PBS. TrypLE trypsin reagent (2.5 mL for 10 cm^3 plate) is added and incubated for approximately 10 minutes at 37 ºC. After 10 minutes, 7.5 mL of the complete culture media is added to inactivate the TrypLE reagent. Cells were counted using a TC20™ Automated Cell Counter (BioRad), by combining 10 µL of cell solution with 10 µL Trypan Blue stain (Thermo 15250061).

4.6.4 Compounds

The OSW-1 compound used was obtained through total synthesis in the Burgett lab or from isolation from the natural source. OSW-1 used in the experiments was of >95% purity as determined with ^{1}H-NMR and LCMS analysis. Solid OSW-1 compound was dissolved in analytical grade DMSO solution to produce 10mM stocks for experimentation. The 10 mM OSW-1 stock solution was aliquoted into Eppendorf brand 1.5 mL centrifuge tubes; Each individual 10

mM OSW-1 aliquots were thawed no more than three times. Additional cycles of freeze/thaws caused partial loss of OSW-1 compound in the aliquots.

4.6.5 Cell Lysis

Cells were cultured in Nunclon Delta 10 cm^3 dishes (VWR 10171744) and prepared for lysis by removing the media, washing with 1X PBS, followed by addition of 1 mL PBS and scraping. Cells were collected in a 1.5 mL Eppendorf brand centrifuge tubes and centrifuged at 14,000 x g for 45 seconds. Supernatant was removed, and the cells were resuspended in 50 µL of AC Lysis buffer (150 mM NaCl, 1.5 mM $MgCl_2$, 5% glycerol, 0.8% NP40, 1mM DTT, 50 mM HEPES, 25 mM NaF, 1 mM Na_3PO_4) with 3X HALT/EDTA protease inhibitor (Thermo 78438) and 0.2 mM phenylmethanesulfonylfluoride (Goldbio). Cells were lysed by freezing in liquid nitrogen and thawing in a 37°C bead bath three times, followed by a 14,000 x g centrifugation for 15 minutes. Supernatant was transferred to a new tube and a portion was taken for protein quantification using a Bradford assay (Bio-Rad Protein Assay Dye Reagent Concentrate #5000006, BSA-Santa Cruz sc-2323). After protein quantification, the lysates were diluted to the desired concentration using AC lysis buffer and a final concentration of 1X Laemmli buffer (1 M Tris pH 6.8, 8% SDS, 40% glycerol, 20% β-mercaptoethanol, and 0.2% bromophenol blue), followed by dry bath heating at 95°C for 10 minutes.

Cells cultured on 6-well plates (Greiner 657160) were prepared for lysis by removing media, washing with 1X PBS, followed by adding 0.5 mL TrypLE™ Express (Gibco 12605010) and incubated at 37°C for 5 minutes. TrypLE™ was neutralized using 0.5 mL of media and cells were then transferred to a 1.5 mL Eppendorf tube and centrifuged at 14,000 x g for 45 seconds. Supernatant was removed, and 1 mL of PBS was added to wash the cells. Cells were centrifuged

at 14,000 x g for 45 seconds, supernatant was removed, and the cells were resuspended in 50 µL of AC lysis buffer. Freeze/thaw lysis method was continued as described above.

4.6.6 Western Blotting

SDS-PAGE gels (8.5%) containing 25 µg of total protein per well were transferred to 0.45 µm nitrocellulose (Bio-Rad 1620115) using constant voltage (100V) for 1 hour at 4°C in 1X transfer buffer with 10% ethanol. After transferring, the nitrocellulose membrane was blocked with 5% milk 1X TBST at room temperature for 30 minutes. The membranes were then washed three times, five minutes each, with 1X TBST. Primary incubation with antibodies was done overnight at 4°C. After primary incubation, the blots were washed five times, five minutes each, with 1X TBST and then incubated in secondary antibody in 1% milk TBST for thirty minutes at room temperature. After secondary antibody incubation, the blots were washed five times, five minutes each, with 1X TBST and then once with 1X TBS for ten minutes. TBS was removed, and the blots were incubated in ClarityTM Western ECL substrate (Bio-Rad 1705061) and imaged on the Bio-Rad ChemiDocTM Touch Imaging System using the chemiluminescence setting with 2x2 binning. Ladder images were taken using the colorimetric setting. After development, the membranes were washed with 1X TBST twice for five minutes each. 1:1000 β-actin HRP (Santa Cruz sc-47778 HRP) in 1% milk TBST was added and incubated for 1.5 hours at room temperature. Developing occurred the same as after secondary antibody incubation. Primary antibody used was 1:500 OSBP A-5 (Santa Cruz sc-365771). Secondary antibody used was 1:1000-1:3000 goat anti-mouse IgG1-HRP (Santa Cruz sc-2060).

4.6.7 ORPphillin Compound Treatments and Cell Viability Assay

HCT116 and HEK293 cells were seeded out $5x10^5$ into 6 well plates and left to rest for 20 hours. For the co-incubation experiments the cells were treated with DMSO (Sigma 472301), 1

nM OSW-1, 1 nM Taxol, 10µM Itraconazole (Sigma I6657), 10µM TTP, 10µM T-00127-HEV2, or a combination of treatments for 24 hours. Cells were washed with 1X PBS and then incubated in 0.5 mL TrypLE^{TM} for five minutes at 37°C. Reaction was neutralized using 0.5 mL of fresh media and cells were counted on a TC20™ Automated Cell Counter (BioRad) by combining 10 µL of cell solution with 10 µL Trypan Blue stain (Thermo 15250061). The rest of the cell solution was lysed and analyzed by western blotting.

4.6.8 Sterol Treatments

HCT116 cells were seeded out 5x10^5 into 6 well plates and left to rest for 20 hours. For the co-incubation experiments the cells were treated with 100% Ethanol, 1 nM OSW-1, 10 µM 25-hydroxycholsterol (Cayman Chemical 11097), 10 µM 20-α-hydroxycholesterol (Cayman Chemical 20103), or a mixture for 24 hours. Cells were lysed and analyzed by western blotting.

4.6.9 Immunofluorescence

HCT116 cells were seeded at 50,000 cells onto sterile 18 mm cover slips in 12 well plates for treatments lasting 24 hrs. The cells rested for 24 hours before treatment to ensure attachment of the cells. Once treatments were completed, media was removed and cells were washed with warm 1X PBS. PBS was removed and 0.5 mL of freshly prepared 4% paraformaldehyde in PBS was added. Cover slips were at 37°C for 20 minutes and then the paraformaldehyde was removed followed by three 1X PBS washes. Permeabilization of the cells was done with 0.5 mL of 0.5% Triton X-100 in PBS at room temperature for 10 minutes. 1X PBS was used to wash the cells three times. Image-iT FX signal enhancer (Thermo I36933) was added onto the cover slips, and incubate at room temperature for 30 minutes followed by three 1X PBS washes. Coverslips were blocked with 0.5 mL of 1% BSA in PBS at room temperature for 30 minutes followed by three washes with 1X PBS. Primary antibody was added and the slips were incubated overnight at 4°C. The

primary antibody solution was removed and the cover slips were washed three times with 1X PBS. Secondary antibody was incubated in darkness at room temperature for one hour. Removed the secondary antibody solution and washed three times with 1% BSA-PBS, three times with 1X PBS, and then soaked the cover slip in 300 nM DAPI (Thermo D1306) solution for 10 minutes Mounted the slips onto glass slides using VECTASHEILD HardSet Antifade mounting media (VECTOR labs H-1400). Stored slides at -20°C until imaging was conducted. Primary antibodies used were 1:100 OSBP1 1F2 (Novus NBP2-00935) and 1:500 TGN46 (Novus NBP1-49643). Secondary antibodies used were 1:500 goat anti-mouse IgG H&L Alexa Fluor® 488 (Abcam ab150113) and donkey anti-rabbit IgG H&L Alexa Fluor® 594 (Abcam ab150076). Imaging was done with a Lecia SP8 using a 63x objective with 2x digital zoom. Images were analyzed with ImageJ software.

4.6.10 Cytotoxicity Assay

HCT116 cells were seeded out at 2,000 cells per well into opaque 96 well Falcon plates (VWR 25382-208). Cells were allowed to rest for 20 hours before treatments. Day zero control plate was created by adding 25 µL of media containing either 0.1% DMSO or 1% DMSO and 20 µL of cell titer blue (Promega G8081) to each of the wells containing cells. Incubated at 37°C with 5% CO_2 for 1 hour and 30 minutes. Plates were read using a GloMax® Discover using the Cell Titer Blue protocol. Remaining plates with cells were treated with various dilutions of drugs and incubated at 37°C for 48 hours under 5% CO_2. After the incubation time, 20 µL of cell titer blue was added to the wells and the plates were incubated and read as incubated above. Control plate was subtracted from the treatment plate and the values were analyzed using GraphPad Prism software.

Co-incubation experiments were done using the same protocol above by Mr. Zachary Severance with HeLa cells seeded out at 5,000 cells per well. 10µM of ITZ, TTP, or THEV2 were

added to all the wells during the 48-hour treatment and the OSW-1 concentration was varied between wells.

4.6.11 ([3H]-25-OHC) Charcoal/Dextran Binding Assay

The [3H]-25-OHC binding assay was run according to the protocol outlined in Burgett et al(46) by Mr. Zachary Severance and Mr. Ryan Bensen.

4.6.12 Antiviral Experiments

HeLa cells were grown to <75% confluency (healthy log phase cells) in complete media, DMEM (Hyclone SH30081.0) with 10% FBS (Atlanta Biological S11550) and 1% penicillin-streptomycin (Gibco 15140-122). For experiments, cells were trypsinized, counted using a hemocytometer and seeded into 20 wells of two 24-well trays (Falcon 3047) with 2.0 x 10^5 cells per well, in 1.0 mL complete media. Each treatment is performed using quadruplicate wells (n=4) and each virus was on a separate plate. After seeding, cells were incubated 20 hour at 37 ºC, 5% CO_2, at which point cells have grown to a near confluent monolayer.

For the continual compound treatment experiments, (**Figure 33A**), the media was gently removed from each well, and 1mL of media was added with the desired compound concentration to each well, without disturbing the cells. Cells were incubated for 6 hours, after which time the media was removed and cells were gently washed three times with 1.0 mL of FBS-free DMEM media. After the media was removed, CoxA9-01 or Echo2-01 viruses, diluted in serum-free DMEM with a M.O.I. of 1.0 was added to the culture. The 2.0 x 10^5 cells per well was assumed to double during incubation so 4.0 x 10^5 pfu/well of virus was used for an M.O.I. of 1.0. The virus and cells were incubated for 30 minutes at 37 ºC 5% CO_2. Then, the virus inoculum was removed, and the culture washed one time with 1.0 mL of serum-free media per well. Then, 1.0 mL of complete media with the indicated concentration of compound was added to the well, and the

infected cells were then incubated for 10 hours at 37 ºC, 5% CO_2. After 10 hours the plate was stored at -80 ºC until the TCID-50 titration. The experiment reported in the **Figure 33A** was repeated independently three times.

For the compound washout treatment experiments, (**Figure 33B**), cells were seeded as above and a 6 well plate was seeded with $4.5x10^5$ cells per well. After 20 hours of incubation the media was gently removed from each well, and 1mL of media was added to each well for the 24 well plate and 3 mL of media for the 6 well plate with the desired compound concentration to each well, without disturbing the cells. Cells were incubated for 6 hours, after which time the media was removed and cells were gently washed three times with 1.0 mL of FBS-free DMEM media. This was replaced with complete media and cells allowed to incubate for 20 hours, after which time the 6 well plate was lysed to quantify OSBP protein levels. After the media was removed, CoxA9-01 or Echo2-01 viruses, diluted in serum-free DMEM with a M.O.I. of 1.0 was added to the culture. The 2.0×10^5 cells per well was assumed to double and double again during incubation so 8.0×10^5 pfu/well of virus was used for an M.O.I. of 1.0. The virus and cells were incubated for 30 minutes at 37 ºC 5% CO2. Then, the virus inoculum was removed, and the culture washed one time with 1.0 mL of serum-free media per well. Then, 1.0 mL of complete media was added to the well, and the infected cells were then incubated for 10 hours at 37 ºC, 5% CO_2. After 10-hour incubation, the plate was stored at -80 ºC until processing.

Then, the plates were rapidly thawed, the cells in media were scrapped from the wells into sterile 1.5 mL centrifuge tubes and the suspension then centrifuged at 10,000 g at 4ºC to produce the virus containing supernatant, which is assayed for TCID-50 titration on sub-confluent RD cells. This experiment was performed independently three times to generate the data in the Figure. The TCID-50 titration was performed according to the protocol described by Reed et al.(210) The

experiment reported in the **Figure 33B** was repeated independently three times. Viral work was performed by Dr. Earl Blewett and analysis of OSBP protein level was done by Mr. Zachary Severance.

4.6.13 Statistical Analysis

Results are expressed as mean ± s.d. and are n=3 unless otherwise stated. All statistical tests were performed using GraphPad Prism 7.0. Comparison between groups were made by using a one-way ANOVA with a follow up Dunnett's test. The p values are reported using GraphPad Prism * values: * is $p \leq 0.05$, ** is $p \leq 0.01$ *** is $p \leq 0.001$, and **** is $p \leq 0.0001$.

Chapter 5: Conclusions and Future Outlook

The work outlined in this dissertation has uncovered a potentially significant cellular effect induced by OSW-1 compound treatment that can occur in a variety of cell lines quickly and at non-toxic levels. We have shown that ORP4, not only OSBP, is targeted for degradation through OSW-1 treatment, which in itself is a new discovery that has implications for the anti-cancer avenue of the drug. The degradation of these proteins has a distinct pattern with OSBP being degraded to a higher degree and faster than ORP4 in a time dependent manner This finding suggests it is possible to preferentially target OSBP over ORP4 with short doses of OSW-1. These short doses followed by removal (washouts) lead to multi-day OSBP repression within all human cell lines tested, and the viability of washout cells is similar to control cells. The "washout effect" can occur in under an hour of treatment at near sub-nanomolar concentrations. We show that washout cells have anti-viral activity against two clinical isolates of *Enteroviruses*, which gives rise to the potential of not only a therapy for a virus genus that currently does not have any approved treatment, but the potential for a prophylactic therapy.

The "washout effect" occurs through a currently unidentified cellular mechanism that is only caused by OSW-1 treatment and not any other ORPphillin with anti-viral activity. Through our experiments we show for the first time that both OSBP and ORP4 are long-lived proteins with half-lives of at least 24 hours, and the "washout effect" causes active degradation of OSBP through a proteasomal mechanism. This initial degradation by the proteasome does not account for the long-term repression of OSBP induced in response to OSW-1 washout treatment. OSW-1 treatment induces transient autophagy, but OSBP induced reduction by OSW-1 treatment does not occur through autophagy-induced proteolysis. We show that the mRNA transcript of OSBP is

stable throughout the washout condition and that the global proteome is also largely unaffected as a result of these washout conditions.

Our results also provide insight into other small molecule OSBP inhibitors that have not previously had their effects analyzed with respect to OSBP protein levels. We show that of the known OSBP inhibitors that have anti-viral activities towards the same viruses as OSW-1, only the THEV2 compound binds competitively with a similar Ki. Previous research has showed that ITZ and TTP inhibit OSBP sterol/PI4P transport, which is presumably through the LBD, but we show that these compounds do not inhibit this function in a competitive manner. There may be an alternative binding sites that allow for sterol/PI4P ligands to bind in the LBD but ORPphillin binding could inhibit the the transport between membranes. These compounds could also bind in a way that prevents sterol binding entirely, more in depth studies need to be performed on ligand binding. Regardless of binding ability, none of the compounds besides OSW-1 can induce degradation of OSBP, which calls in to question the exact mechanism of the "washout effect".

Future work will need to focus on determining the exact repression mechanism by which OSW-1 induces OSBP repression for multiple days. As mentioned previously, thapsigargin treatment in INS-1E cells appears to have a similar mechanism targeting GRP78. Treatment leads to ER stress and repression of GRP78 protein levels that cannot be explained completely through proteasomal degradation and overall mRNA levels are increased throughout treatment time(224). Similarly, Macrophages treated with deoxynivalenol also lead to degradation of GRP78 protein but not mRNA levels, resulting in an ER stress response(225). Prolonged OSW-1 treatment was shown to cause degradation of GRP78 through calpain dependent mechanism(130). GRP78 is a crucial component of the unfolded protein response (UPR) which is induced under ER stress. ER stress was shown to lead to global mRNA stabilization due to the formation of stress granules that

can inhibit translation by sequestering mRNA for stabilization or degradation(236). This could be a potential mechanism by which OSBP is repressed due to the result of the OSBP mRNA transcript being stably expressed throughout the OSW-1 washout recovery period. Prolonged ER stress can lead to cell death(237), meaning that the likelihood of ER stress being the sole responsible source of repression is unlikely. We have briefly tested the ability of an inhibitor to inositol-requiring enzyme 1 (STF-083010)(238), which is involved with ER stress through the UPR, to protect OSBP during OSW-1 treatment. The inhibitor failed to rescue OSBP protein levels (**Figure 69**), which provides evidence that OSBP repression goes beyond prolonged ER stress, which is also supported by the fact that cells are viable (**Figure 21**) and the Golgi returns to a normal state during washout(**Figure 20B**).

Another possible mechanism for prolonged repression is through targeted translational repression of the mRNA transcript. Our cycloheximide results show that the half-life of OSBP is over 24 hours (**Figure 27A**) which means the initial degradation is an active process and not due to translational inhibition during OSW-1 treatment. Based on the stable OSBP mRNA levels throughout the washout, we are unable to rule out that the OSBP mRNA transcript is not being translated throughout the recovery process. In order to answer this question, the use of polysome profiling with puromycin controls to determine active versus stalled ribosomes(239, 240) could determine if the OSBP mRNA transcript in DMSO washout cells is actively being translated throughout the entire recovery period, or if the long half-life of OSBP is the result of repression. Using the polysome profiling technique(239), we would be able to not only determine the translational status of OSBP, but also look at the global translation to see if there are differences between the treatments that correspond with our iTRAQ data (**Figure 28B** & **C**).

If there is a differential pattern in the translation of OSW-1 washout cells, then RNA sequencing (RNA-seq), specifically small RNA-seq, could be used to identify differences in the transcriptome. It has previously been reported that OSBP and other members of the OSBP/ORP family have been targeted by miRNAs(64, 227–229). Identification of miRNA repression through RNA-seq could be confirmed by using a target protecting morpholino oligo that binds to the mRNA of OSBP to determine if OSBP expression returns. Alternatively, the mRNA transcript could be sequestered into p-bodies which can be induced during stress events. In order to determine the subcellular localization of the OSBP transcript during washout conditions, using either *in situ* hybridization coupled to immunofluorescence (FISH-IF)(241) or MS2 mRNA-targeting(242) to determine where the transcript is located and if it is inside of a p-body. Knowing the exact mechanism of OSW-1 induced OSBP repression will advance the potential therapeutic aspect of the compound.

Despite the capacity of the "washout effect", the fact that OSW-1 is not specific to OSBP is concerning. Future research needs to be invested in developing OSW-1 analogs that are specific to OSBP which can also induce the "washout effect". Our results show that there is something specific about how OSW-1 binds that induces OSBP degradation. It also seems that only specific competitive binding ligands are able to rescue OSBP from this degradation(46)(**Figure 31** & **Figure 32**). We have tested the scarce Schweinfurthin A in efforts to determine its effect on OSBP protein level during washout conditions and found that it induces the "washout effect" but to a much lesser extent and recovers quicker than OSW-1 (**Figure 70**). Taken with the results presented earlier, more research needs to be done to determine the exact mechanism induced by OSW-1 treatment and what specifically about the OSW-1 compound induces the "washout effect". Regardless of these obstacles, we have

demonstrated that as of now, OSW-1 treatment for short periods of time is non-toxic and induces a prophylactic antiviral response against a genus of viruses that is a public health menace without currently approved treatments(243). With the “washout effect” being inducible in all tissues types tested so far, and the fact that OSBP is utilized by a plethora of viruses, the application of this research has great potential moving forward.

References

1. Olkkonen VM, Zhou Y, Yan D, Vihervaara T. 2012. Oxysterol-binding proteins-emerging roles in cell regulation. Eur J Lipid Sci Technol 114:634–643.
2. Pietrangelo A, Ridgway ND. 2018. Bridging the molecular and biological functions of the oxysterol-binding protein family. Cell Mol Life Sci 75:3079–3098.
3. Olkkonen VM, Li S. 2013. Oxysterol-binding proteins: Sterol and phosphoinositide sensors coordinating transport, signaling and metabolism. Prog Lipid Res 52:529–538.
4. Yan D, Olkkonen VM. 2008. Characteristics of Oxysterol Binding Proteins. Int Rev Cytol. Elsevier Masson SAS.
5. Kentala H, Weber-Boyvat M, Olkkonen VM. 2016. OSBP-Related Protein Family: Mediators of Lipid Transport and Signaling at Membrane Contact Sites, p. 299–340. *In* International Review of Cell and Molecular Biology. Elsevier Inc.
6. Olkkonen VM, Beaslas O, Nissila E. 2012. Oxysterols and their cellular effectors. Biomolecules 2:76–103.
7. Kulig W, Cwiklik L, Jurkiewicz P, Rog T, Vattulainen I. 2016. Cholesterol oxidation products and their biological importance. Chem Phys Lipids 199:144–160.
8. Vihervaara T, Jansen M, Uronen RL, Ohsaki Y, Ikonen E, Olkkonen VM. 2011. Cytoplasmic oxysterol-binding proteins: Sterol sensors or transporters? Chem Phys Lipids. Elsevier Ireland Ltd.
9. Weber-Boyvat M, Zhong W, Yan D, Olkkonen VM. 2013. Oxysterol-binding proteins: Functions in cell regulation beyond lipid metabolism. Biochem Pharmacol 86:89–95.
10. Dawson PA, Ridgway ND, Slaughter CA, Brown MS, Goldstein JL. 1989. cDNA cloning and expression of oxysterol-binding protein, an oligomer with a potential leucine zipper. J

Biol Chem 264:16798–16803.

11. Ridgway ND, Dawson P a, Ho YK, Brown MS, Goldstein JL. 1992. Translocation of oxysterol binding protein to Golgi apparatus triggered by ligand binding. J Cell Biol 116:307–19.

12. WANG C, JeBAILEY L, RIDGWAY ND. 2002. Oxysterol-binding-protein (OSBP)-related protein 4 binds25-hydroxycholesterol and interacts with vimentin intermediate filaments. Biochem J 361:461.

13. Zhao K, Ridgway ND. 2017. Oxysterol-Binding Protein-Related Protein 1L Regulates Cholesterol Egress from the Endo-Lysosomal System. Cell Rep 19:1807–1818.

14. Suchanek M, Hynynen R, Wohlfahrt G, Lehto M, Johansson M, Saarinen H, Radzikowska A, Thiele C, Olkkonen VM. 2007. The mammalian oxysterol-binding protein-related proteins (ORPs) bind 25-hydroxycholesterol in an evolutionarily conserved pocket. Biochem J 405:473–480.

15. Du X, Kumar J, Ferguson C, Schulz TA, Ong YS, Hong W, Prinz WA, Parton RG, Brown AJ, Yang H. 2011. A role for oxysterol-binding protein-related protein 5 in endosomal cholesterol trafficking. J Cell Biol 192:121–135.

16. Ngo M, Ridgway ND. 2009. Oxysterol Binding Protein–related Protein 9 (ORP9) Is a Cholesterol Transfer Protein That Regulates Golgi Structure and Function. Mol Biol Cell 20:1388–1399.

17. Charman M, Colbourne TR, Pietrangelo A, Kreplak L, Ridgway ND. 2014. Oxysterol-binding protein (OSBP)-related protein 4 (ORP4) is essential for cell proliferation and survival. J Biol Chem 289:15705–15717.

18. Ghai R, Du X, Wang H, Dong J, Ferguson C, Brown AJ, Parton RG, Wu JW, Yang H.

2017. ORP5 and ORP8 bind phosphatidylinositol-4, 5-biphosphate (PtdIns(4,5)P2) and regulate its level at the plasma membrane. Nat Commun 8.

19. Mesmin B, Bigay J, Moser Von Filseck J, Lacas-Gervais S, Drin G, Antonny B. 2013. A four-step cycle driven by PI(4)P hydrolysis directs sterol/PI(4)P exchange by the ER-Golgi Tether OSBP. Cell 155.

20. Im YJ, Raychaudhuri S, Prinz WA, Hurley JH. 2005. Structural mechanism for sterol sensing and transport by OSBP-related proteins. Nature 437:154–158.

21. de Saint-Jean M, Delfosse V, Douguet D, Chicanne G, Payrastre B, Bourguet W, Antonny B, Drin G. 2011. Osh4p exchanges sterols for phosphatidylinositol 4-phosphate between lipid bilayers. J Cell Biol 195:965–978.

22. Loewen CJR, Roy A, Levine TP. 2003. A conserved ER targeting motif in three families of lipid binding proteins and in Opi1p binds VAP. EMBO J 22:2025–2035.

23. Nissilä E, Ohsaki Y, Weber-Boyvat M, Perttilä J, Ikonen E, Olkkonen VM. 2012. ORP10, a cholesterol binding protein associated with microtubules, regulates apolipoprotein B-100 secretion. Biochim Biophys Acta - Mol Cell Biol Lipids 1821:1472–1484.

24. Levine TP, Munro S. 1998. The pleckstrin homology domain of oxysterol-binding protein recognises a determinant specific to Golgi membranes. Curr Biol 8:729–739.

25. Johansson M, Lehto M, Tanhuanpää K, Cover TL, Olkkonen VM. 2005. The Oxysterol-binding Protein Homologue ORP1L Interacts with Rab7 and Alters Functional Properties of Late Endocytic Compartments. Mol Biol Cell 16:5480–5492.

26. Lehto M, Hynynen R, Karjalainen K, Kuismanen E, Hyvärinen K, Olkkonen VM. 2005. Targeting of OSBP-related protein 3 (ORP3) to endoplasmic reticulum and plasma membrane is controlled by multiple determinants. Exp Cell Res 310:445–462.

27. Taylor FR, Saucier SE, Shown EP, Parish EJ, Kandutsch AA. 1984. Correlation between oxysterol binding to a cytosolic binding protein and potency in the repression of hydroxymethylglutaryl coenzyme A reductase. J Biol Chem 259:12382–12387.

28. Taylor FR, Kandutsch AA. 1985. Oxysterol binding protein. Chem Phys Lipids 38:187–194.

29. Dawson PA, Van Der Westhuyzen DR, Goldstein JL, Brown MS. 1989. Purification of oxysterol binding protein from hamster liver cytosol. J Biol Chem 264:9046–9052.

30. Levanon D, Hsieh CL, Francke U, Dawson PA, Ridgway ND, Brown MS, Goldstein JL. 1990. cDNA cloning of human oxysterol-binding protein and localization of the gene to human chromosome 11 and mouse chromosome 19. Genomics 7:65–74.

31. Jaworski CJ, Moreira E, Li A, Lee R, Rodriguez IR. 2001. A family of 12 human genes containing oxysterol-binding domains. Genomics 78:185–196.

32. Laitinen S, Olkkonen VM, Ehnholm C, Ikonen E. 1999. Family of human oxysterol binding protein (OSBP) homologues. A novel member implicated in brain sterol metabolism. J Lipid Res 40:2204–11.

33. Levine TP, Munro S. 2002. Targeting of Golgi-specific pleckstrin homology domains involves both {PtdIns} 4-kinase-dependent and -independent components. Curr Biol 12:695–704.

34. Wyles JP, McMaster CR, Ridgway ND. 2002. Vesicle-associated membrane protein-associated protein-A (VAP-A) interacts with the oxysterol-binding protein to modify export from the endoplasmic reticulum. J Biol Chem 277:29908–29918.

35. Mesmin B, Bigay J, Moser Von Filseck J, Lacas-Gervais S, Drin G, Antonny B. 2013. A four-step cycle driven by PI(4)P hydrolysis directs sterol/PI(4)P exchange by the ER-

Golgi Tether OSBP. Cell 155.

36. Mesmin B, Bigay J, Polidori J, Jamecna D, Lacas-Gervais S, Antonny B. 2017. Sterol transfer, PI4P consumption, and control of membrane lipid order by endogenous OSBP. EMBO J 36:e201796687.

37. Nhek S., Ngo M., Yang X., Ng M.M., Field J. S., Asara J.M., Ridgway N.D., A. T. 2010. Regulation of Oxysterol-binding Protein Golgi Localization through Protein Kinase D-mediated Phosphorylation. Mol Biol Cell 21:2327–2337.

38. Perry RJ, Ridgway ND. 2006. Oxysterol-binding Protein and Vesicle-associated Membrane Protein–associated Protein Are Required for Sterol-dependent Activation of the Ceramide Transport Protein. Mol Biol Cell 17:2604–2616.

39. Wang P-Y, Weng J, Anderson RGW. 2005. OSBP is a cholesterol-regulated scaffolding protein in control of ERK 1/2 activation. Science 307:1472–1476.

40. Romeo GR, Kazlauskas A. 2008. Oxysterol and diabetes activate STAT3 and control endothelial expression of profilin-1 via OSBP1. J Biol Chem 283:9595–9605.

41. Zeghouf M, Guibert B, Zeeh J-C, Cherfils J. 2005. Arf, Sec7 and Brefeldin A: a model towards the therapeutic inhibition of guanine nucleotide-exchange factors. Biochem Soc Trans 33:1265–1268.

42. Hausser A, Märtens S, Link G, Pfizenmaier K. 2006. Protein kinase D regulates vesicular transport by phosphorylation and activation of phosphatidylinositol-4 kinase III β at the Golgi complex 7:880–886.

43. Fugmann T, Hausser A, Schöffler P, Schmid S, Pfizenmaier K, Olayioye MA. 2007. Regulation of secretory transport by protein kinase D-mediated phosphorylation of the ceramide transfer protein. J Cell Biol 178:15–22.

44. Moreira EF, Jaworski C, Li A, Rodriguez IR. 2001. Molecular and Biochemical Characterization of a Novel Oxysterol-binding Protein (OSBP2) Highly Expressed in Retina. J Biol Chem 276:18570–18578.

45. Silva N, Fournier M V, Pimenta G, Pulcheri WA, Spector N, Carvalho MG. 2003. HLMOSBP2 is expressed in chronic myeloid leukemia. Int J Mol Med 12:663–666.

46. Burgett AWG, Poulsen TB, Wangkanont K, Anderson DR, Kikuchi C, Shimada K, Okubo S, Fortner KC, Mimaki Y, Kuroda M, Murphy JP, Schwalb DJ, Petrella EC, Cornella- I, Schirle M, Tallarico JA, Shair MD. 2011. Natural products reveal cancer cell dependence on oxysterol- binding proteins 7:639–647.

47. Wyles JP, Perry RJ, Ridgway ND. 2007. Characterization of the sterol-binding domain of oxysterol-binding protein (OSBP)-related protein 4 reveals a novel role in vimentin organization. Exp Cell Res 313:1426–1437.

48. Zhong W, Pan G, Wang L, Li S, Ou J, Xu M, Li J, Zhu B, Cao X, Ma H, Li C, Xu J, Olkkonen VM, Staels B, Yan D. 2016. ORP4L Facilitates Macrophage Survival via G-Protein-Coupled Signaling. Circ Res 119:1296–1312.

49. Pietrangelo A, Ridgway ND. 2018. Golgi localization of oxysterol binding protein-related protein 4L (ORP4L) is regulated by ligand binding. J Cell Sci 131:jcs215335.

50. Sarria AJ, Panini SR, Evans RM. 1992. A functional role for vimentin intermediate filaments in the metabolism of lipoprotein-derived cholesterol in human SW-13 cells. J Biol Chem 267:19455–19463.

51. Gillard BK, Harrell RG, Marcus DM. 1996. Pathways of glycosphingolipid biosynthesis in SW13 cells in the presence and absence of vimentin intermediate filaments. Glycobiology 6:33–42.

52. Heidenthal AK, Weber PC, Lottspeich F, Hrboticky N. 2000. The binding in vitro of modified LDL to the intermediate filament protein vimentin. Biochem Biophys Res Commun 267:49–53.

53. Udagawa O, Ito C, Ogonuki N, Sato H, Lee S, Tripvanuntakul P, Ichi I, Uchida Y, Nishimura T, Murakami M, Ogura A, Inoue T, Toshimori K, Arai H. 2014. Oligo-astheno-teratozoospermia in mice lacking ORP4, a sterol-binding protein in the OSBP-related protein family. Genes to Cells 19:13–27.

54. Zhong W, Yi Q, Xu B, Li S, Wang T, Liu F, Zhu B, Hoffmann PR, Ji G, Lei P, Li G, Li J, Li J, Olkkonen VM, Yan D. 2016. ORP4L is essential for T-cell acute lymphoblastic leukemia cell survival. Nat Commun 7:1–14.

55. Johansson M, Bocher V, Lehto M, Chinetti G, Kuismanen E, Ehnholm C, Staels B, Olkkonen VM. 2003. The Two Variants of Oxysterol Binding Protein-related Protein-1 Display Different Tissue Expression Patterns, Have Different Intracellular Localization, and Are Functionally Distinct. Mol Biol Cell 14:903–915.

56. Lee S, Wang P-Y, Jeong Y, Mangelsdorf DJ, Anderson RGW, Michaely P. 2012. Sterol-dependent nuclear import of ORP1S promotes LXR regulated trans-activation of apoE. Exp Cell Res 318:2128–2142.

57. Laitinen S, Lehto M, Lehtonen S, Hyvarinen K, Heino S, Lehtonen E, Ehnholm C, Ikonen E, Olkkonen VM. 2002. ORP2, a homolog of oxysterol binding protein, regulates cellular cholesterol metabolism. J Lipid Res 43:245–255.

58. Hynynen R, Suchanek M, Spandl J, Bäck N, Thiele C, Olkkonen VM. 2009. OSBP-related protein 2 is a sterol receptor on lipid droplets that regulates the metabolism of neutral lipids. J Lipid Res 50:1305–1315.

59. Murphy S, Martin S, Parton RG. 2009. Lipid droplet-organelle interactions; sharing the fats. Biochim Biophys Acta - Mol Cell Biol Lipids 1791:441–447.

60. Escajadillo T, Wang H, Li L, Li D, Sewer MB. 2016. Oxysterol-related-binding-protein related Protein-2 (ORP2) regulates cortisol biosynthesis and cholesterol homeostasis. Mol Cell Endocrinol 427:73–85.

61. Lehto M, Tienari J, Lehtonen S, Lehtonen E, Olkkonen VM. 2004. Subfamily III of mammalian oxysterol-binding protein (OSBP) homologues: The and intracellular localization of ORP3, ORP6, and ORP7. Cell Tissue Res 315:39–57.

62. Lehto M, Mayranpaa MI, Pellinen T, Ihalmo P, Lehtonen S, Kovanen PT, Groop P-H, Ivaska J, Olkkonen VM. 2008. The R-Ras interaction partner ORP3 regulates cell adhesion. J Cell Sci 121:695–705.

63. Weber-Boyvat M, Kentala H, Lilja J, Vihervaara T, Hanninen R, Zhou Y, Peränen J, Nyman TA, Ivaska J, Olkkonen VM. 2015. OSBP-related protein 3 (ORP3) coupling with VAMP-associated protein A regulates R-Ras activity. Exp Cell Res 331:278–291.

64. Ouimet M, Hennessy EJ, Van Solingen C, Koelwyn GJ, Hussein MA, Ramkhelawon B, Rayner KJ, Temel RE, Perisic L, Hedin U, Maegdefessel L, Garabedian MJ, Holdt LM, Teupser D, Moore KJ. 2016. MiRNA targeting of oxysterol-binding protein-like 6 regulates cholesterol trafficking and efflux. Arterioscler Thromb Vasc Biol 36:942–951.

65. Mochizuki S, Miki H, Zhou R, Kido Y, Nishimura W, Kikuchi M, Noda Y. 2018. Oxysterol-binding protein-related protein (ORP) 6 localizes to the ER and ER-plasma membrane contact sites and is involved in the turnover of PI4P in cerebellar granule neurons. Exp Cell Res 370:601–612.

66. Zhong W, Zhou Y, Li S, Zhou T, Ma H, Wei K, Li H, Olkkonen VM, Yan D. 2011.

OSBP-related protein 7 interacts with GATE-16 and negatively regulates GS28 protein stability. Exp Cell Res 317:2353–2363.

67. Teslovich TM, Musunuru K, Smith A V., Edmondson AC, Stylianou IM, Koseki M, Pirruccello JP, Ripatti S, Chasman DI, Willer CJ, Johansen CT, Fouchier SW, Isaacs A, Peloso GM, Barbalic M, Ricketts SL, Bis JC, Aulchenko YS, Thorleifsson G, Feitosa MF, Chambers J, Orho-Melander M, Melander O, Johnson T, Li X, Guo X, Li M, Shin Cho Y, Jin Go M, Jin Kim Y, Lee JY, Park T, Kim K, Sim X, Twee-Hee Ong R, Croteau-Chonka DC, Lange LA, Smith JD, Song K, Hua Zhao J, Yuan X, Luan J, Lamina C, Ziegler A, Zhang W, Zee RYL, Wright AF, Witteman JCM, Wilson JF, Willemsen G, Wichmann HE, Whitfield JB, Waterworth DM, Wareham NJ, Waeber G, Vollenweider P, Voight BF, Vitart V, Uitterlinden AG, Uda M, Tuomilehto J, Thompson JR, Tanaka T, Surakka I, Stringham HM, Spector TD, Soranzo N, Smit JH, Sinisalo J, Silander K, Sijbrands EJG, Scuteri A, Scott J, Schlessinger D, Sanna S, Salomaa V, Saharinen J, Sabatti C, Ruokonen A, Rudan I, Rose LM, Roberts R, Rieder M, Psaty BM, Pramstaller PP, Pichler I, Perola M, Penninx BWJH, Pedersen NL, Pattaro C, Parker AN, Pare G, Oostra BA, O'donnell CJ, Nieminen MS, Nickerson DA, Montgomery GW, Meitinger T, Mcpherson R, Mccarthy MI, Mcardle W, Masson D, Martin NG, Marroni F, Mangino M, Magnusson PKE, Lucas G, Luben R, Loos RJF, Lokki ML, Lettre G, Langenberg C, Launer LJ, Lakatta EG, Laaksonen R, Kyvik KO, Kronenberg F, König IR, Khaw KT, Kaprio J, Kaplan LM, Johansson Å, Jarvelin MR, Cecile A, Ingelsson E, Igl W, Kees Hovingh G, Hottenga JJ, Hofman A, Hicks AA, Hengstenberg C, Heid IM, Hayward C, Havulinna AS, Hastie ND, Harris TB, Haritunians T, Hall AS, Gyllensten U, Guiducci C, Groop LC, Gonzalez E, Gieger C, Freimer NB, Ferrucci L, Erdmann J, Elliott P, Ejebe KG, Döring

A, Dominiczak AF, Demissie S, Deloukas P, De Geus EJC, De Faire U, Crawford G, Collins FS, Chen YDI, Caulfield MJ, Campbell H, Burtt NP, Bonnycastle LL, Boomsma DI, Boekholdt SM, Bergman RN, Barroso I, Bandinelli S, Ballantyne CM, Assimes TL, Quertermous T, Altshuler D, Seielstad M, Wong TY, Tai ES, Feranil AB, Kuzawa CW, Adair LS, Taylor HA, Borecki IB, Gabriel SB, Wilson JG, Holm H, Thorsteinsdottir U, Gudnason V, Krauss RM, Mohlke KL, Ordovas JM, Munroe PB, Kooner JS, Tall AR, Hegele RA, Kastelein JJP, Schadt EE, Rotter JI, Boerwinkle E, Strachan DP, Mooser V, Stefansson K, Reilly MP, Samani NJ, Schunkert H, Cupples LA, Sandhu MS, Ridker PM, Rader DJ, Van Duijn CM, Peltonen L, Abecasis GR, Boehnke M, Kathiresan S. 2010. Biological, clinical and population relevance of 95 loci for blood lipids. Nature 466:707–713.

68. Chung J, Torta F, Masai K, Lucast L, Czapla H, Tanner LB, Narayanaswamy P, Wenk MR, Nakatsu F, De Camilli P. 2015. PI4P/phosphatidylserine countertransport at ORP5- and ORP8-mediated ER-plasma membrane contacts. Science (80-) 349:428–432.

69. Galmes R, Houcine A, van Vliet AR, Agostinis P, Jackson CL, Giordano F. 2016. ORP5/ORP8 localize to endoplasmic reticulum–mitochondria contacts and are involved in mitochondrial function. EMBO Rep 17:800–810.

70. Du X, Zadoorian A, Lukmantara IE, Qi Y, Brown AJ, Yang H. 2018. Oxysterol-binding protein–related protein 5 (ORP5) promotes cell proliferation by activation of MTORC1 signaling. J Biol Chem 293:3806–3818.

71. Zhou T, Li S, Zhong W, Vihervaara T, Béaslas O, Perttilä J, Luo W, Jiang Y, Lehto M, Olkkonen VM, Yan D. 2011. Osbp-related protein 8 (ORP8) regulates plasma and liver tissue lipid levels and interacts with the nucleoporin Nup62. PLoS One 6.

72. Wyles JP, Ridgway ND. 2004. VAMP-associated protein-A regulates partitioning of oxysterol-binding protein-related protein-9 between the endoplasmic reticulum and Golgi apparatus. Exp Cell Res 297:533–547.

73. Nhek S., Ngo M., Yang X., Ng M.M., Field J. S., Asara J.M., Ridgway N.D. and TA. 2010. Regulation of Oxysterol-binding Protein Golgi Localization through Protein Kinase D-mediated Phosphorylation. Mol Biol Cell 21:2327–2337.

74. Liu X, Ridgway ND. 2014. Characterization of the sterol and phosphatidylinositol 4-Phosphate binding properties of golgi-associated OSBP-related protein 9 (ORP9). PLoS One 9:1–12.

75. Lessmann E, Ngo M, Leitges M, Minguet S, Ridgway ND, Huber M. 2007. Oxysterol-binding protein-related protein (ORP) 9 is a PDK-2 substrate and regulates Akt phosphorylation. Cell Signal 19:384–392.

76. Fairn GD, McMaster CR. 2005. The roles of the human lipid-binding proteins ORP9S and ORP10S in vesicular transport. Biochem Cell Biol 83:631–636.

77. Li D, Dammer EB, Lucki NC, Sewer MB. 2013. cAMP-stimulated phosphorylation of diaphanous 1 regulates protein stability and interaction with binding partners in adrenocortical cells. Mol Biol Cell 24:848–857.

78. Zhou Y, Li S, Mäyränpää MI, Wenbin Z, Bäck N, Yan D, Olkkonen VM. 2010. OSBP-related protein 11 (ORP11) dimerizes with ORP9 and localizes at the Golgi—late endosome interface. Chem Phys Lipids 163:S55.

79. Amako Y, Sarkeshik A, Hotta H, Yates J, Siddiqui A. 2009. Role of oxysterol binding protein in hepatitis C virus infection. J Virol 83:9237–46.

80. Arita M, Kojima H, Nagano T, Okabe T, Wakita T, Shimizu H. 2013. Oxysterol-Binding

Protein Family I Is the Target of Minor Enviroxime-Like Compounds. J Virol 87:4252–4260.

81. Strating JRPM. 2015. ITRACONAZOLE INHIBITS ENTEROVIRUS REPLICATION BY TARGETING THE OXYSTEROL-BINDING PROTEIN 25:1–30.

82. Albulescu L, Strating JRPM, Thibaut HJ, Linden L Van Der, Shair MD, Neyts J, van Kuppeveld FJM. 2015. Broad-range inhibition of enterovirus replication by OSW-1, a natural compound targeting OSBP. Antiviral Res 117:110–114.

83. Dorobantu CM, Albulescu L, Lyoo H, van Kampen M, De Francesco R, Lohmann V, Harak C, van der Schaar HM, Strating JRPM, Gorbalenya AE, van Kuppeveld FJM. 2016. Mutations in Encephalomyocarditis Virus 3A Protein Uncouple the Dependency of Genome Replication on Host Factors Phosphatidylinositol 4-Kinase IIIα and Oxysterol-Binding Protein. mSphere 1:e00068-16.

84. Meutiawati F, Bezemer B, Strating JRPM, Overheul GJ, Žusinaite E, van Kuppeveld FJM, van Cleef KWR, van Rij RP. 2018. Posaconazole inhibits dengue virus replication by targeting oxysterol-binding protein. Antiviral Res 157:68–79.

85. Munir S, Saleem S, Idrees M, Tariq A, Butt S, Rauff B, Hussain A, Badar S, Naudhani M, Fatima Z, Ali M, Ali L, Akram M, Aftab M, Khubaib B, Awan Z. 2010. Hepatitis C Treatment: Current and future perspectives. Virol J 7:1–6.

86. Strating JR, van Kuppeveld FJ. 2017. Viral rewiring of cellular lipid metabolism to create membranous replication compartments. Curr Opin Cell Biol 47:24–33.

87. van der Schaar HM, Dorobantu CM, Albulescu L, Strating JRPM, van Kuppeveld FJM. 2016. Fat(al) attraction: Picornaviruses Usurp Lipid Transfer at Membrane Contact Sites to Create Replication Organelles. Trends Microbiol 24:535–546.

88. Nagy PD, Strating JRPM, van Kuppeveld FJM. 2016. Building Viral Replication Organelles: Close Encounters of the Membrane Types. PLoS Pathog 12:6–11.

89. Lim YS, Hwang SB. 2011. Hepatitis C virus NS5A protein interacts with phosphatidylinositol 4-kinase type III?? and regulates viral propagation. J Biol Chem 286:11290–11298.

90. Tai AW, Salloum S. 2011. The role of the phosphatidylinositol 4-kinase PI4KA in hepatitis C virus-induced host membrane rearrangement. PLoS One 6:1–12.

91. Amako Y, Syed GH, Siddiqui A. 2011. Protein kinase D negatively regulates hepatitis C virus secretion through phosphorylation of oxysterol-binding protein and ceramide transfer protein. J Biol Chem 286:11265–74.

92. Wang H, Perry JW, Lauring AS, Neddermann P, De Francesco R, Tai AW. 2014. Oxysterol-binding protein is a phosphatidylinositol 4-kinase effector required for HCV replication membrane integrity and cholesterol trafficking. Gastroenterology 146:1373–1385.e11.

93. Bishé B, Syed G, Siddiqui A. 2012. Phosphoinositides in the hepatitis C virus life cycle. Viruses 4:2340–2358.

94. Bishé B, Syed GH, Field SJ, Siddiqui A. 2012. Role of phosphatidylinositol 4-phosphate (PI4P) and its binding protein GOLPH3 in hepatitis C virus secretion. J Biol Chem 287:27637–27647.

95. Aizaki H, Morikawa K, Fukasawa M, Hara H, Inoue Y, Tani H, Saito K, Nishijima M, Hanada K, Matsuura Y, Lai MMC, Miyamura T, Wakita T, Suzuki T. 2008. Critical Role of Virion-Associated Cholesterol and Sphingolipid in Hepatitis C Virus Infection. J Virol 82:5715–5724.

96. Nielsen SU, Bassendine MF, Burt AD, Martin C, Pumeechockchai W, Geoffrey L, Toms GL. 2006. Association between Hepatitis C Virus and Very-Low-Density Lipoprotein (VLDL)/ LDL Analyzed in Iodixanol Density Gradients Association between Hepatitis C Virus and Very-Low-Density Lipoprotein (VLDL)/ LDL Analyzed in Iodixanol Density Gradients. J Virol 80:2418–2428.

97. Albecka A, Belouzard S, de Beeck AO, Descamps V, Goueslain L, Bertrand-Michel J, Tercé F, Duverlie G, Rouillé Y, Dubuisson J. 2012. Role of low-density lipoprotein receptor in the hepatitis C virus life cycle. Hepatology 55:998–1007.

98. Syed GH, Tang H, Khan M, Hassanein T, Liu J, Siddiqui A, Diamond MS. 2014. Hepatitis C Virus Stimulates Low-Density Lipoprotein Receptor Expression To Facilitate Viral Propagation. J Virol 88:2519–2529.

99. Yan D, Lehto M, Rasilainen L, Metso J, Ehnholm C, Ylä-Herttuala S, Jauhiainen M, Olkkonen VM. 2007. Oxysterol binding protein induces upregulation of SREBP-1c and enhances hepatic lipogenesis. Arterioscler Thromb Vasc Biol 27:1108–1114.

100. Polio Global Eradication Initiative. Polio Now – GPEI.

101. Hawken J, Troy SB. 2012. Adjuvants and inactivated polio vaccine: A systematic review. Vaccine.

102. Non-Polio Enterovirus | Symptoms Non-Polio Enterovirus Infection | Picornavirus | CDC.

103. Arden KE, Mackay IM. 2009. Human rhinoviruses: Coming in from the cold. Genome Med 1:1–5.

104. Mackay IM. 2010. Human rhinoviruses. PCR Clin Microbiol An Aust Int Perspect 26:299–301.

105. Lugo D, Krogstad P. 2016. Enteroviruses in the early 21st century. Curr Opin Pediatr

28:107–113.

106. Lee KY. 2016. Enterovirus 71 infection and neurological complications. Korean J Pediatr 59:395–401.

107. Holm-Hansen CC, Midgley SE, Fischer TK. 2016. Global emergence of enterovirus D68: A systematic review. Lancet Infect Dis 16:e64–e75.

108. Reading F. 2008. Echoviruses, p. 65–71. *In* Brian W.J. Mahy and Marc H.V. Van Regenmortel (ed.), Encyclopedia of Virology, 3rd ed. Academic Press.

109. Strating JRPM, van Kuppeveld FJM. 2017. Viral rewiring of cellular lipid metabolism to create membranous replication compartments. Curr Opin Cell Biol 47:24–33.

110. Belov GA, Van Kuppeveld FJ. 2012. (+)RNA viruses rewire cellular pathways to build replication organelles. Curr Opin Virol 2:734–741.

111. Belov GA, Altan-Bonnet N, Kovtunovych G, Jackson CL, Lippincott-Schwartz J, Ehrenfeld E. 2007. Hijacking Components of the Cellular Secretory Pathway for Replication of Poliovirus RNA. J Virol 81:558–567.

112. Hsu NY, Ilnytska O, Belov G, Santiana M, Chen YH, Takvorian PM, Pau C, van der Schaar H, Kaushik-Basu N, Balla T, Cameron CE, Ehrenfeld E, van Kuppeveld FJM, Altan-Bonnet N. 2010. Viral reorganization of the secretory pathway generates distinct organelles for RNA replication. Cell 141:799–811.

113. Arita M. 2014. Phosphatidylinositol-4 kinase III beta and oxysterol-binding protein accumulate unesterified cholesterol on poliovirus-induced membrane structure. Microbiol Immunol 58:239–256.

114. Dorobantu CM, Albulescu L, Harak C, Feng Q, van Kampen M, Strating JRPM, Gorbalenya AE, Lohmann V, van der Schaar HM, van Kuppeveld FJM. 2015. Modulation

of the Host Lipid Landscape to Promote RNA Virus Replication: The Picornavirus Encephalomyocarditis Virus Converges on the Pathway Used by Hepatitis C Virus. PLoS Pathog 11:1–27.

115. Ilnytska O, Santiana M, Hsu NY, Du WL, Chen YH, Viktorova EG, Belov G, Brinker A, Storch J, Moore C, Dixon JL, Altan-Bonnet N. 2013. Enteroviruses harness the cellular endocytic machinery to remodel the host cell cholesterol landscape for effective viral replication. Cell Host Microbe 14:281–293.

116. Albulescu L, Wubbolts R, van Kuppeveld FJM, Strating JRPM. 2015. Cholesterol shuttling is important for RNA replication of coxsackievirus B3 and encephalomyocarditis virus. Cell Microbiol 17:1144–1156.

117. Carocci M, Bakkali-Kassimi L. 2012. The encephalomyocarditis virus. Virulence 3:351–367.

118. Dorobantu CM, Albulescu L, Lyoo H, van Kampen M, De Francesco R, Lohmann V, Harak C, van der Schaar HM, Strating JRPM, Gorbalenya AE, van Kuppeveld FJM. 2016. Mutations in Encephalomyocarditis Virus 3A Protein Uncouple the Dependency of Genome Replication on Host Factors Phosphatidylinositol 4-Kinase IIIα and Oxysterol-Binding Protein. mSphere 1:1–17.

119. Murrell S, Wu SC, Butler M. 2011. Review of dengue virus and the development of a vaccine. Biotechnol Adv 29:239–247.

120. Vaughn DW, Green S, Kalayanarooj S, Innis BL, Nimmannitya S, Suntayakorn S, Endy TP, Raengsakulrach B, Rothman AL, Ennis FA, Nisalak A. 2000. Dengue viremia titer, antibody response pattern, and virus serotype correlate with disease severity. J Infect Dis 181:2–9.

121. Fried JR, Gibbons R V., Kalayanarooj S, Thomas SJ, Srikiatkhachorn A, Yoon IK, Jarman RG, Green S, Rothman AL, Cummings DAT. 2010. Serotype-specific differences in the risk of dengue hemorrhagic fever: An analysis of data collected in Bangkok, Thailand from 1994 to 2006. PLoS Negl Trop Dis 4:1–6.

122. Welsch S, Miller S, Romero-Brey I, Merz A, Bleck CKE, Walther P, Fuller SD, Antony C, Krijnse-Locker J, Bartenschlager R. 2009. Composition and Three-Dimensional Architecture of the Dengue Virus Replication and Assembly Sites. Cell Host Microbe 5:365–375.

123. Rothwell C, LeBreton A, Young Ng C, Lim JYH, Liu W, Vasudevan S, Labow M, Gu F, Gaither LA. 2009. Cholesterol biosynthesis modulation regulates dengue viral replication. Virology 389:8–19.

124. Fournier M V, Guimarães da Costa F, Paschoal ME, Ronco L V, Carvalho MG, Pardee a B, Giumaraes FC. 1999. Identification of a gene encoding a human oxysterol-binding protein-homologue: a potential general molecular marker for blood dissemination of solid tumors. Cancer Res 59:3748–53.

125. Albulescu L, Bigay J, Biswas B, Weber-Boyvat M, Dorobantu CM, Delang L, van der Schaar HM, Jung YS, Neyts J, Olkkonen VM, van Kuppeveld FJM, Strating JRPM. 2017. Uncovering oxysterol-binding protein (OSBP) as a target of the anti-enteroviral compound TTP-8307. Antiviral Res 140:37–44.

126. Kubo S, Mimaki Y, Terao M, Sashida Y. 1992. Acylated cholestane glycosides from the bulbs of. Phytochemistry 31:3969–3973.

127. Mimaki Y, Kuroda M, Kameyama A, Sashida Y, Hirano T, Oka K, Maekawa R, Wada T, Sugita K, Beutler JA. 1997. Cholestane glycosides with potent cytostatic activities on

various tumor cells from Ornithogalum saundersiae bulbs. Bioorganic Med Chem Lett 7:633–636.

128. Antonny B, Bigay J, Mesmin B. 2018. The Oxysterol-Binding Protein Cycle: Burning Off PI(4)P to Transport Cholesterol. Annu Rev Biochem 87:annurev-biochem-061516-044924.

129. Zhou Y, Garcia-Prieto C, Carney D a, Xu R, Pelicano H, Kang Y, Yu W, Lou C, Kondo S, Liu J, Harris DM, Estrov Z, Keating MJ, Jin Z, Huang P. 2005. OSW-1: a natural compound with potent anticancer activity and a novel mechanism of action. J Natl Cancer Inst 97:1781–5.

130. Garcia-Prieto C, Ahmed KBR, Chen Z, Zhou Y, Hammoudi N, Kang Y, Lou C, Mei Y, Jin Z, Huang P. 2013. Effective killing of leukemia cells by the natural product OSW-1 through disruption of cellular calcium homeostasis. J Biol Chem 288:3240–3250.

131. Beutler JA, Shoemaker RH, Johnson T, Boyd MR. 1998. Cytotoxic geranyl stilbenes from Macaranga schweinfurthii. J Nat Prod 61:1509–1512.

132. Beutler JA, Jato J, Cragg GM, Boyd MR. 2000. Schweinfurthin D, a cytotoxic stilbene from Macaranga schweinfurthii. Nat Prod Lett 14:399–404.

133. Klausmeyer P, Van Que N, Jato J, McCloud TG, Beutler JA. 2010. Schweinfurthins I and J from Macaranga schweinfurthii. J Nat Prod 73:479–481.

134. Harmalkar DS, Mali JR, Sivaraman A, Choi Y, Lee K. 2018. Schweinfurthins A-Q: Isolation, synthesis, and biochemical properties. RSC Adv 8:21191–21209.

135. Bao X, Zheng W, Sugi NH, Agarwala KL, Xu Q, Wang Z, Tendyke K, Lee W, Parent L, Li W, Cheng H, Shen Y, Taylor N, Dezso Z, Du H, Kotake Y, Zhao N, Wang J, Postema M, Woodall-Jappe M, Takase Y, Uenaka T, Kingston DGI, Nomoto K. 2015. Small

molecule schweinfurthins selectively inhibit cancer cell proliferation and mTOR/AKT signaling by interfering with trans-Golgi-network trafficking. Cancer Biol Ther 16:589–601.

136. Beutler JA, Jato JG, Cragg G, Wiemer DF, Neighbors JD, Salnikova M, Hollingshead M, Scudiero DA, Mccloud TG. 2006. Chapter 22 the Schweinfurthins. Med Aromat Plants Agric Commerical, Ecol Leg Pharmalogical Soc Asp 301–309.

137. Pettit GR, Inoue M, Kamano Y, Herald DL, Arm C, Dufresne C, Christie ND, Schmidt JM, Doubek DL, Krupa TS. 1988. Isolation and structure of the powerful cell growth inhibitor cephalostatin 1. J Am Chem Soc 110:2006–2007.

138. Dirsch VM, Vollmar AM. 2005. Cephalostatin 1-induced apoptosis in tumor cells: Selective induction of Smac/DIABLO Release, p. 209–221. *In* Application of Apoptosis to Cancer Treatment. Springer-Verlag, Berlin/Heidelberg.

139. Fukuzawa S, Matsunaga S, Fusetani N. 1995. Isolation and structure elucidation of ritterazines B and C, highly cytotoxic dimeric steroidal alkaloids, from the tunicate Ritterella tokioka. J Org Chem 60:608–614.

140. Knölker H-J. 2018. Cephalostatins and Ritterazines, p. 175. *In* The Alkaloids, 16th ed. Elsevier Science.

141. Gryszkiewicz-Wojtkielewicz A, Jastrzebska I, Morzycki J, Romanowska D. 2003. Approaches Towards the Synthesis of Cephalostatins, Ritterazines and Saponins from Ornithogalum saundersiae - New Natural Products With Cytostatic Activity. Curr Org Chem 7:1257–1277.

142. DELESCLUSE J, CAUWENBERGH G, DEGREEF H. 1986. Itraconazole, a new orally active antifungal, in the treatment of pityriasis versicolor. Br J Dermatol 114:701–703.

143. Van Cutsem J, Van Gerven F, Van de Ven MA. 1984. Itraconazole, a new triazole that is orally active in aspergillosis. Antimicrob Agents Chemother 26:527–534.

144. Lestner J, Hope WW. 2013. Itraconazole: an update on pharmacology and clinical use for treatment of invasive and allergic fungal infections. Expert Opin Drug Metab Toxicol 9:911–926.

145. U.S. Food & Drug Administration. Drug Approval Package.

146. Pounds R, Leonard S, Dawson C, Kehoe S. 2017. Repurposing itraconazole for the treatment of cancer (review). Oncol Lett 14:2587–2597.

147. Gao Q, Yuan S, Zhang C, Wang Y, Wang Y, He G, Zhang S, Altmeyer R, Zou G. 2015. Discovery of itraconazole with broad-spectrum in vitro antienterovirus activity that targets nonstructural protein 3A. Antimicrob Agents Chemother 59:2654–2665.

148. Xu J, Dang Y, Ren YR, Liu JO. 2010. Cholesterol trafficking is required for mTOR activation in endothelial cells. Proc Natl Acad Sci 107:4764–4769.

149. Nacev BA, Grassi P, Dell A, Haslam SM, Liu JO. 2011. The antifungal drug itraconazole inhibits Vascular Endothelial Growth Factor Receptor 2 (VEGFR2) glycosylation, trafficking, and signaling in endothelial cells. J Biol Chem 286:44045–44056.

150. Kim J, Tang JY, Gong R, Kim J, Lee JJ, Clemons K V., Chong CR, Chang KS, Fereshteh M, Gardner D, Reya T, Liu JO, Epstein EH, Stevens DA, Beachy PA. 2010. Itraconazole, a Commonly Used Antifungal that Inhibits Hedgehog Pathway Activity and Cancer Growth. Cancer Cell 17:388–399.

151. Mellaerts R, Mols R, Jammaer JAG, Aerts CA, Annaert P, Van Humbeeck J, Van den Mooter G, Augustijns P, Martens JA. 2008. Increasing the oral bioavailability of the poorly water soluble drug itraconazole with ordered mesoporous silica. Eur J Pharm

Biopharm 69:223–230.

152. Heinz BA, Vance LM. 1995. The antiviral compound enviroxime targets the 3A coding region of rhinovirus and poliovirus. J Virol 69:4189–4197.

153. Brown-Augsburger P, Vance LM, Malcolm SK, Hsiung H, Smith DP, Heinz BA. 1999. Evidence that enviroxime targets multiple components of the rhinovirus 14 replication complex. Arch Virol 144:1569–1585.

154. Arita M, Kojima H, Nagano T, Okabe T, Wakita T, Shimizu H. 2011. Phosphatidylinositol 4-Kinase III Beta Is a Target of Enviroxime-Like Compounds for Antipoliovirus Activity. J Virol 85:2364–2372.

155. Arita M, Kojima H, Nagano T, Okabe T, Wakita T, Shimizu H. 2013. Oxysterol-binding protein family I is the target of minor enviroxime-like compounds. J Virol 87:4252–4260.

156. Albulescu L, Bigay J, Biswas B, Weber-Boyvat M, Dorobantu CM, Delang L, van der Schaar HM, Jung YS, Neyts J, Olkkonen VM, van Kuppeveld FJM, Strating JRPM. 2017. Uncovering oxysterol-binding protein (OSBP) as a target of the anti-enteroviral compound TTP-8307. Antiviral Res 140:37–44.

157. Statistics - DrugBank.

158. Aberle N, Crews CM. 2012. Exploring biology with small organic molecules. Chem Genomics 432:10–25.

159. Ravid T, Hochstrasser M. 2008. Diversity of degradation signals in the ubiquitin-proteasome system. Nat Rev Mol Cell Biol 9:679–689.

160. Nalepa G, Rolfe M, Harper JW. 2006. Drug discovery in the ubiquitin - Proteasome system. Nat Rev Drug Discov 5:596–613.

161. Tanaka K. 2009. The proteasome: overview of structure and functions. Proc Jpn Acad Ser

B Phys Biol Sci 85:12–36.

162. Aiken CT, Kaake RM, Wang X, Huang L. 2011. Oxidative Stress-Mediated Regulation of Proteasome Complexes. Mol Cell Proteomics 10:R110.006924.

163. Kammerl IE, Meiners S. 2016. Proteasome function shapes innate and adaptive immune responses. Am J Physiol - Lung Cell Mol Physiol ajplung.00156.2016.

164. Adams J. 2004. The Proteasome in Cell-Cycle Regulation, p. 77–84. *In* Proteasome Inhibitors in Cancer Therapy. Humana Press, Totowa, NJ.

165. Leonard JP, Furman RR, Coleman M. 2006. Proteasome inhibition with bortezomib: A new therapeutic strategy for non-Hodgkin's lymphoma. Int J Cancer 119:971–979.

166. Elliott PJ, Zollner TM, Boehncke WH. 2003. Proteasome inhibition: A new anti-inflammatory strategy. J Mol Med 81:235–245.

167. Goldberg AL. 2012. Development of proteasome inhibitors as research tools and cancer drugs. J Cell Biol 199:583–588.

168. Kisselev AF, Goldberg AL. 2001. Proteasome inhibitors: from research tools to drug candidates. Chem Biol 8:739–758.

169. Vinitsky A, Michaud C, Orlowski M, Powers JC. 1992. Inhibition of the Chymotrypsin-like Activity of the Pituitary Multicatalytic Proteinase Complex. Biochemistry 31:9421–9428.

170. Lee DH, Goldberg AL. 1996. Selective inhibitors of the proteasome-dependent and vacuolar pathways of protein degradation in Saccharomyces cerevisiae. J Biol Chem 271:27280–27284.

171. Wang KK, Yuen PW. 1994. Calpain inhibition: an overview of its therapeutic potential. Trends Pharmacol Sci 15:412–9.

172. Rock KL, Gramm C, Rothstein L, Clark K, Stein R, Dick L, Hwang D, Goldberg AL. 1994. Inhibitors of the proteasome block the degradation of most cell proteins and the generation of peptides presented on MHC class I molecules. Cell 78:761–71.

173. Palombella VJ, Rando OJ, Goldberg AL, Maniatis T. 1994. The ubiquitin-proteasome pathway is required for processing the NF-kappa B1 precursor protein and the activation of NF-kappa B. Cell 78:773–85.

174. Tsubuki S, Saito Y, Tomioka M, Ito H, Kawashima S. 1996. Differential inhibition of calpain and proteasome activities by peptidyl aldehydes of di-leucine and tri-leucine. J Biochem 119:572–6.

175. Kane RC, Bross PF, Farrell AT, Pazdur R. 2003. Velcade: U.S. FDA Approval for the Treatment of Multiple Myeloma Progressing on Prior Therapy. Oncologist 8:508–513.

176. Groll M, Berkers CR, Ploegh HL, Ovaa H. 2006. Crystal Structure of the Boronic Acid-Based Proteasome Inhibitor Bortezomib in Complex with the Yeast 20S Proteasome. Structure 14:451–456.

177. Accardi F, Toscani D, Bolzoni M, Dalla Palma B, Aversa F, Giuliani N. 2015. Mechanism of action of bortezomib and the new proteasome inhibitors on myeloma cells and the bone microenvironment: Impact on myeloma-induced alterations of bone remodeling. Biomed Res Int 2015.

178. Perel G, Bliss J, Thomas CM. 2016. Carfilzomib (Kyprolis): A Novel Proteasome Inhibitor for Relapsed And/or Refractory Multiple Myeloma. Pharm Ther 41:303–7.

179. Schneekloth AR, Pucheault M, Tae HS, Crews CM. 2008. Targeted intracellular protein degradation induced by a small molecule: En route to chemical proteomics. Bioorg Med Chem Lett 18:5904–5908.

180. Cromm PM, Crews CM. 2017. Targeted Protein Degradation: from Chemical Biology to Drug Discovery. Cell Chem Biol 24:1181–1190.

181. Tonelli F, Lim KG, Loveridge C, Long J, Pitson SM, Tigyi G, Bittman R, Pyne S, Pyne NJ. 2010. FTY720 and (S)-FTY720 vinylphosphonate inhibit sphingosine kinase 1 and promote its proteasomal degradation in human pulmonary artery smooth muscle, breast cancer and androgen-independent prostate cancer cells. Cell Signal 22:1536–1542.

182. Myat LO, Thangada S, Wu MT, Liu CH, Macdonald TL, Lynch KR, Lin CY, Hla T. 2007. Immunosuppressive and anti-angiogenic sphingosine 1-phosphate receptor-1 agonists induce ubiquitinylation and proteasomal degradation of the receptor. J Biol Chem 282:9082–9089.

183. Chiosis G, Timaul MN, Lucas B, Munster PN, Zheng FF, Sepp-Lorenzino L, Rosen N. 2001. A small molecule designed to bind to the adenine nucleotide pocket of Hsp90 causes Her2 degradation and the growth arrest and differentiation of breast cancer cells. Chem Biol 8:289–299.

184. Bondeson DP, Mares A, Smith IED, Ko E, Campos S, Miah AH, Mulholland KE, Routly N, Buckley DL, Gustafson JL, Zinn N, Grandi P, Shimamura S, Bergamini G, Faelth-Savitski M, Bantscheff M, Cox C, Gordon DA, Willard RR, Flanagan JJ, Casillas LN, Votta BJ, den Besten W, Famm K, Kruidenier L, Carter PS, Harling JD, Churcher I, Crews CM. 2015. Catalytic in vivo protein knockdown by small-molecule PROTACs. Nat Chem Biol 11:611–617.

185. Yang Z, Klionsky DJ. 2010. Mammalian autophagy: core molecular machinery and signaling regulation. Curr Opin Cell Biol 22:124–131.

186. Yorimitsu T, Klionsky DJ. 2005. Autophagy: molecular machinery for self-eating. Cell

Death Differ 12:1542–1552.

187. Parzych KR, Klionsky DJ. 2014. An Overview of Autophagy: Morphology, Mechanism, and Regulation. Antioxid Redox Signal 20:460–473.

188. Zachari M, Ganley IG. 2017. The mammalian ULK1 complex and autophagy initiation. Essays Biochem 61:585–596.

189. SEHGAL SN, BAKER H, VÉZINA C. 1975. Rapamycin (AY-22,989), a new antifungal antibiotic. II. Fermentation, isolation and characterization. J Antibiot (Tokyo) 28:727–732.

190. Abraham RT, Wiederrecht GJ. 1996. Immunopharmacology of Rapamycin. Annu Rev Immunol 14:483–510.

191. Seto B. 2012. Rapamycin and mTOR: a serendipitous discovery and implications for breast cancer. Clin Transl Med 1:29.

192. Mizushima N, Yoshimori T, Levine B. 2010. Methods in Mammalian Autophagy Research. Cell 140:313–326.

193. Thoreen CC, Sabatini DM. 2009. Rapamycin inhibits mTORC1, but not completely. Autophagy 5:725–726.

194. Tanida I, Ueno T, Kominami E. 2008. LC3 and Autophagy, p. 77–88. *In* Methods in molecular biology (Clifton, N.J.).

195. Mauthe M, Orhon I, Rocchi C, Zhou X, Luhr M, Hijlkema KJ, Coppes RP, Engedal N, Mari M, Reggiori F. 2018. Chloroquine inhibits autophagic flux by decreasing autophagosome-lysosome fusion. Autophagy 14:1435–1455.

196. Schneider-Poetsch T, Ju J, Eyler DE, Dang Y, Bhat S, Merrick WC, Green R, Shen B, Liu JO. 2010. Inhibition of eukaryotic translation elongation by cycloheximide and lactimidomycin. Nat Chem Biol 6:209–217.

197. Obrig TG, Culp WJ, McKeehan WL, Hardesty B. 1971. The mechanism by which cycloheximide and related glutarimide antibiotics inhibit peptide synthesis on reticulocyte ribosomes. J Biol Chem 246:174–81.

198. Pestova T V., Hellen CUT. 2003. Translation elongation after assembly of ribosomes on the Cricket paralysis virus internal ribosomal entry site without initiation factors or initiator tRNA. Genes Dev 17:181–186.

199. Buchanan BW, Lloyd ME, Engle SM, Rubenstein EM. 2016. Cycloheximide Chase Analysis of Protein Degradation in Saccharomyces cerevisiae J Vis Exp 1–9.

200. JIN J, JIN X, QIAN C, RUAN Y, JIANG H. 2013. Signaling network of OSW-1-induced apoptosis and necroptosis in hepatocellular carcinoma. Mol Med Rep 7:1646–1650.

201. Zhu J, Xiong L, Yu B, Wu J. 2005. Apoptosis induced by a new member of saponin family is mediated through caspase-8-dependent cleavage of Bcl-2. Mol Pharmacol 68:1831–1838.

202. M-PER Mammalian Protein Extraction Reagent - Thermo Fisher Scientific.

203. Wang Z, Ma H, Smith K, Wu S. 2018. Two-dimensional separation using high-pH and low-pH reversed phase liquid chromatography for top-down proteomics. Int J Mass Spectrom 427:43–51.

204. Goto A, Charman M, Ridgway ND. 2016. Oxysterol-binding protein activation at endoplasmic reticulum-golgi contact sites reorganizes phosphatidylinositol 4-phosphate pools. J Biol Chem 291:1336–1347.

205. MRC-5 ATCC ® CCL-171^{TM} Homo sapiens lung Normal.

206. Pan N, Rao W, Kothapalli NR, Liu R, Burgett AWG, Yang Z. 2014. The Single-Probe: A

Miniaturized Multifunctional Device for Single Cell Mass Spectrometry Analysis. Anal Chem 86:9376–9380.

207. Rao W, Pan N, Yang Z. 2016. Applications of the Single-probe: Mass Spectrometry Imaging and Single Cell Analysis under Ambient Conditions. J Vis Exp 1–9.

208. Newman CF, Havelund R, Passarelli MK, Marshall PS, Francis I, West A, Alexander MR, Gilmore IS, Dollery CT. 2017. Intracellular Drug Uptake—A Comparison of Single Cell Measurements Using ToF-SIMS Imaging and Quantification from Cell Populations with LC/MS/MS. Anal Chem 89:11944–11953.

209. Passarelli MK, Newman CF, Marshall PS, West A, Gilmore IS, Bunch J, Alexander MR, Dollery CT. 2015. Single-Cell Analysis: Visualizing Pharmaceutical and Metabolite Uptake in Cells with Label-Free 3D Mass Spectrometry Imaging. Anal Chem 87:6696–6702.

210. REED LJ, MUENCH H. 1938. A SIMPLE METHOD OF ESTIMATING FIFTY PER CENT ENDPOINTS12. Am J Epidemiol 27:493–497.

211. Jie Xue, Peng Liu, Yanbin Pan and, Guo* Z. 2007. A Total Synthesis of OSW-1.

212. Deng S, Yu B, Lou Y, Hui Y. 1999. First total synthesis of an exceptionally potent antitumor saponin, OSW- 1. J Org Chem 64:202–208.

213. Yang F, Shen Y, Camp Ii DG, Smith RD. 2012. High pH reversed-phase chromatography with fraction concatenation as an alternative to strong-cation exchange chromatography for two-dimensional proteomic analysis 9:129–134.

214. Rojo F. 2001. Mechanisms of transcriptional repression. Curr Opin Microbiol 4:145–51.

215. Iwakawa H oki, Tomari Y. 2015. The Functions of MicroRNAs: mRNA Decay and Translational Repression. Trends Cell Biol 25:651–665.

216. Levine M, Tjian R. 2003. Transcription regulation and animal diversity. Nature 424:147–151.

217. Orang AV, Safaralizadeh R, Kazemzadeh-Bavili M. 2014. Mechanisms of miRNA-mediated gene regulation from common downregulation to mRNA-specific upregulation. Int J Genomics 2014.

218. Jin JC, Jin XL, Zhang X, Piao YS, Liu SP. 2013. Effect of OSW-1 on microRNA expression profiles of hepatoma cells and functions of novel microRNAs. Mol Med Rep 7:1831–1837.

219. He C, Klionsky DJ. 2009. Regulation Mechanisms and Signaling Pathways of Autophagy. Annu Rev Genet 43:67–93.

220. Rousseau D, Cannella D, Boulaire J, Fitzgerald P, Fotedar A, Fotedar R. 1999. Growth inhibition by CDK-cyclin and PCNA binding domains of p21 occurs by distinct mechanisms and is regulated by ubiquitin-proteasome pathway. Oncogene 18:4313–4325.

221. Bloom J, Amador V, Bartolini F, DeMartino G, Pagano M. 2003. Proteasome-mediated degradation of p21 via N-terminal ubiquitinylation. Cell 115:71–82.

222. Lin PY, Fosmire SP, Park SH, Park JY, Baksh S, Modiano JF, Weiss RH. 2007. Attenuation of PTEN increases p21 stability and cytosolic localization in kidney cancer cells: A potential mechanism of apoptosis resistance. Mol Cancer 6:1–14.

223. Cambridge SB, Gnad F, Nguyen C, Bermejo JL, Krüger M, Mann M. 2011. Systems-wide proteomic analysis in mammalian cells reveals conserved, functional protein turnover. J Proteome Res 10:5275–5284.

224. Rosengren V, Johansson H, Lehtiö J, Fransson L, Sjöholm Å, Ortsäter H. 2012. Thapsigargin down-regulates protein levels of GRP78/BiP in INS-1E cells. J Cell

Biochem 113:1635–1644.

225. Shi Y, Porter K, Parameswaran N, Bae HK, Pestka JJ. 2009. Role of GRP78/BiP degradation and ER stress in deoxynivalenol-induced interleukin-6 upregulation in the macrophage. Toxicol Sci 109:247–255.

226. Decker CJ, Parker R. 2012. P-Bodies and Stress Granules: Possible Roles in the Control of Translation and mRNA Degradation. Cold Spring Harb Perspect Biol 4:a012286–a012286.

227. Jordan SD, Krüger M, Willmes DM, Redemann N, Wunderlich FT, Brönneke HS, Merkwirth C, Kashkar H, Olkkonen VM, Böttger T, Braun T, Seibler J, Brüning JC. 2011. Obesity-induced overexpression of miRNA-143 inhibits insulin-stimulated AKT activation and impairs glucose metabolism. Nat Cell Biol 13:434–446.

228. Chen T, Huang Z, Wang L, Wang Y, Wu F, Meng S, Wang C. 2009. MicroRNA-125a-5p partly regulates the inflammatory response, lipid uptake, and ORP9 expression in oxLDL-stimulated monocyte/macrophages. Cardiovasc Res 83:131–139.

229. Gu X, Li A, Liu S, Lin L, Xu S, Zhang P, Li S, Li X, Tian B, Zhu X, Wang X. 2016. MicroRNA124 Regulated Neurite Elongation by Targeting OSBP. Mol Neurobiol 53:6388–6396.

230. Ma H, Delafield DG, Wang Z, You J, Wu S. 2017. Finding Biomass Degrading Enzymes Through an Activity-Correlated Quantitative Proteomics Platform (ACPP). J Am Soc Mass Spectrom 28:655–663.

231. Chen C, Huang H, Wu CH. 2017. Protein Bioinformatics Databases and Resources, p. 3–39. *In* .

232. Kim S, Pevzner PA. 2014. MS-GF+ makes progress towards a universal database search

tool for proteomics. Nat Commun 5:1–10.

233. Head SA, Shi W, Zhao L, Gorshkov K, Pasunooti K, Chen Y, Deng Z, Li R, Shim JS, Tan W, Hartung T, Zhang J, Zhao Y, Colombini M, Liu JO. 2015. Antifungal drug itraconazole targets VDAC1 to modulate the AMPK/mTOR signaling axis in endothelial cells. Proc Natl Acad Sci 112:E7276–E7285.

234. Lathe R, Kotelevtsev Y. 2014. Steroid signaling: Ligand-binding promiscuity, molecular symmetry, and the need for gating. Steroids 82:14–22.

235. Bauer L, Ferla S, Head SA, Bhat S, Pasunooti KK, Shi WQ, Albulescu L, Liu JO, Brancale A, van Kuppeveld FJM, Strating JRPM. 2018. Structure-activity relationship study of itraconazole, a broad-range inhibitor of picornavirus replication that targets oxysterol-binding protein (OSBP). Antiviral Res 156:55–63.

236. Kawai T, Fan J, Mazan-Mamczarz K, Gorospe M. 2004. Global mRNA Stabilization Preferentially Linked to Translational Repression during the Endoplasmic Reticulum Stress Response. Mol Cell Biol 24:6773–6787.

237. Maurel M, Chevet E, Tavernier J, Gerlo S. 2014. Getting RIDD of RNA: IRE1 in cell fate regulation. Trends Biochem Sci 39:245–254.

238. Papandreou I, Denko NC, Olson M, Van Melckebeke H, Lust S, Tam A, Solow-Cordero DE, Bouley DM, Offner F, Niwa M, Koong AC. 2011. Identification of an Ire1alpha endonuclease specific inhibitor with cytotoxic activity against human multiple myeloma. Blood 117:1311–1314.

239. Panda A, Martindale J, Gorospe M. 2017. Polysome Fractionation to Analyze mRNA Distribution Profiles. Bio-Protocol 7.

240. Chassé H, Boulben S, Costache V, Cormier P, Morales J. 2017. Analysis of translation

using polysome profiling. Nucleic Acids Res 45:e15.

241. Wang C, Schmich F, Srivatsa S, Weidner J, Beerenwinkel N, Spang A. 2018. Context-dependent deposition and regulation of mRNAs in P-bodies. Elife 7:1–25.

242. Aizer A, Kalo A, Kafri P, Shraga A, Ben-Yishay R, Jacob A, Kinor N, Shav-Tal Y. 2014. Quantifying mRNA targeting to P-bodies in living human cells reveals their dual role in mRNA decay and storage. J Cell Sci 127:4443–4456.

243. Baggen J, Thibaut HJ, Strating JRPM, van Kuppeveld FJM. 2018. The life cycle of non-polio enteroviruses and how to target it. Nat Rev Microbiol 16:368–381.

Appendix 1: Chapter 2 Supplemental

Protein	Full Length	OSBP	ORP4	
Identities	OSBP		77%	Positives
	ORP4	64%		
DNA	Full Length	OSBP	ORP4	
Identities	OSBP		57.8%	Positives
	ORP4	57.8%		

Protein	LBD	OSBP	ORP4	
Identities	OSBP		80%	Positives
	ORP4	68%		
DNA	LBD	OSBP	ORP4	
Identities	OSBP		65.1%	Positives
	ORP4	65.1%		

Figure 34: OSBP and ORP4 Sequence Homology. Protein and DNA Identities and Positives for Full length and LBD sequences of OSBP and ORP4.

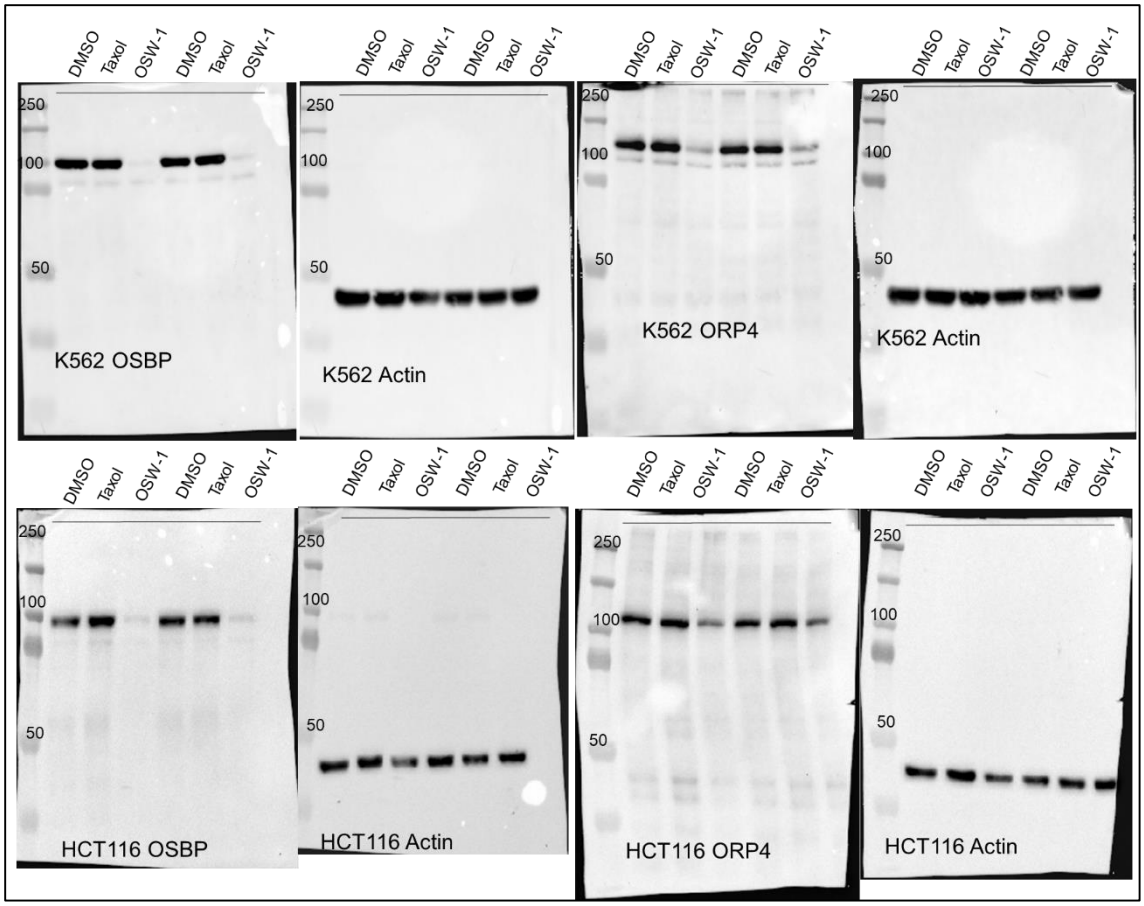

Figure 35: Full blots of Figure 17A

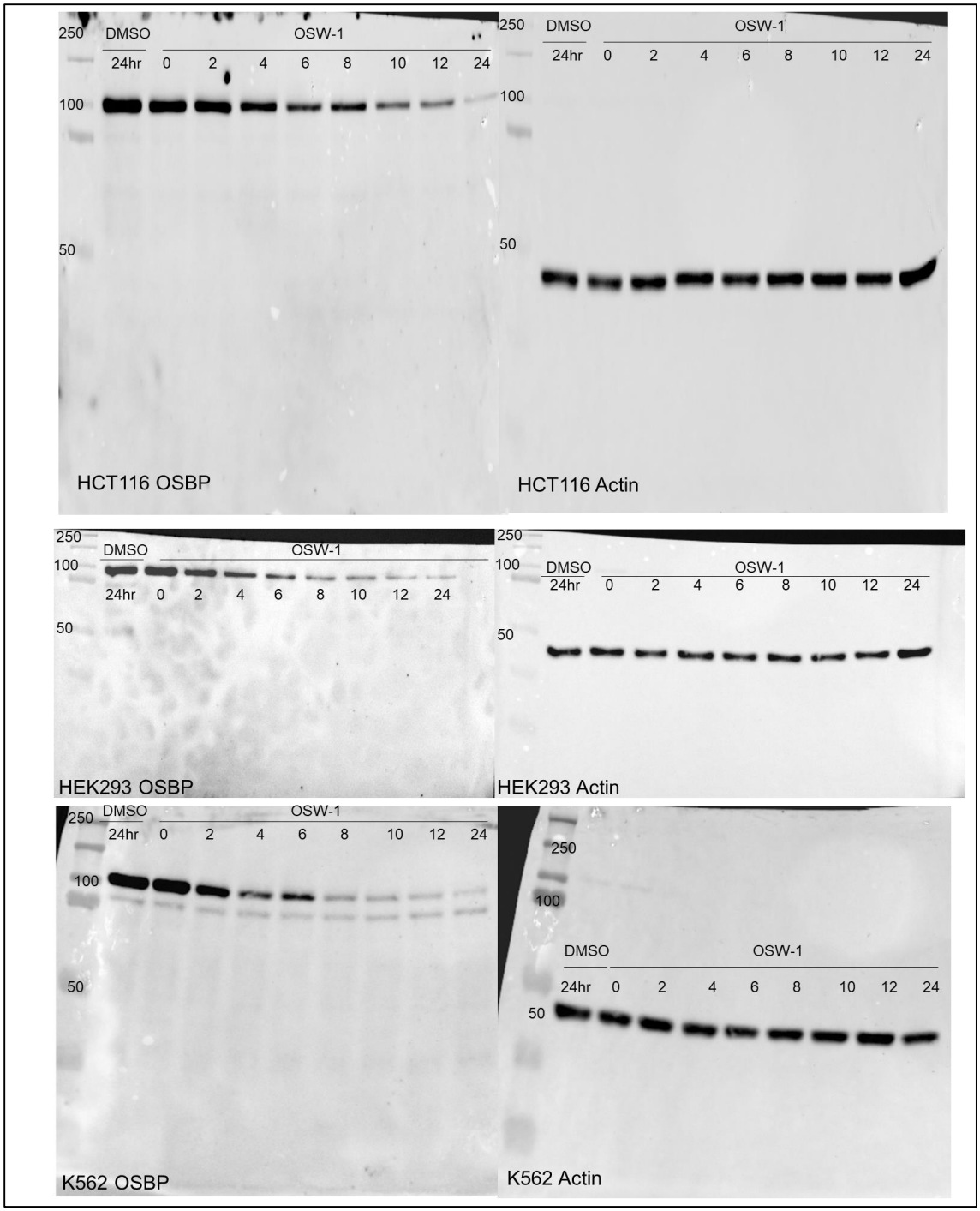

Figure 36: Full OSBP blots of Figure 17B.

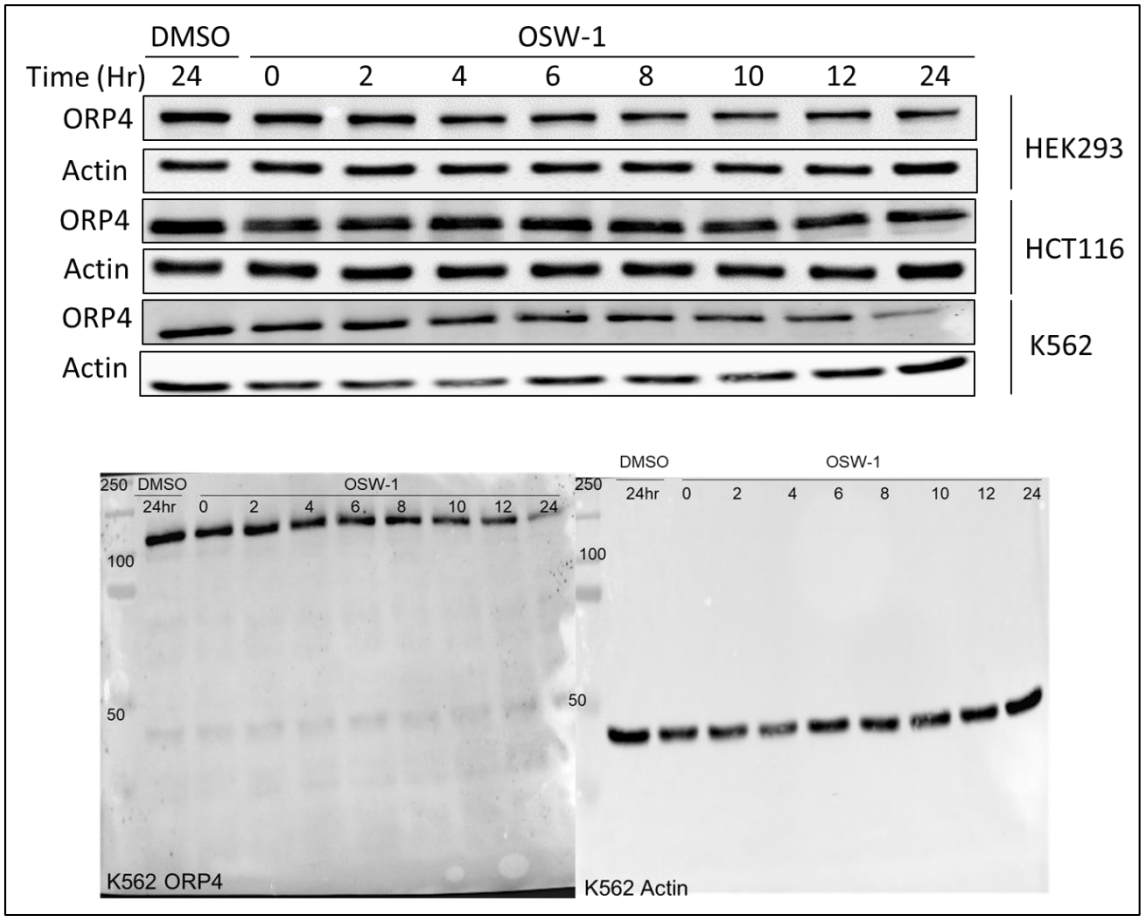

Figure 37: Full ORP4 blots of Figure 17B

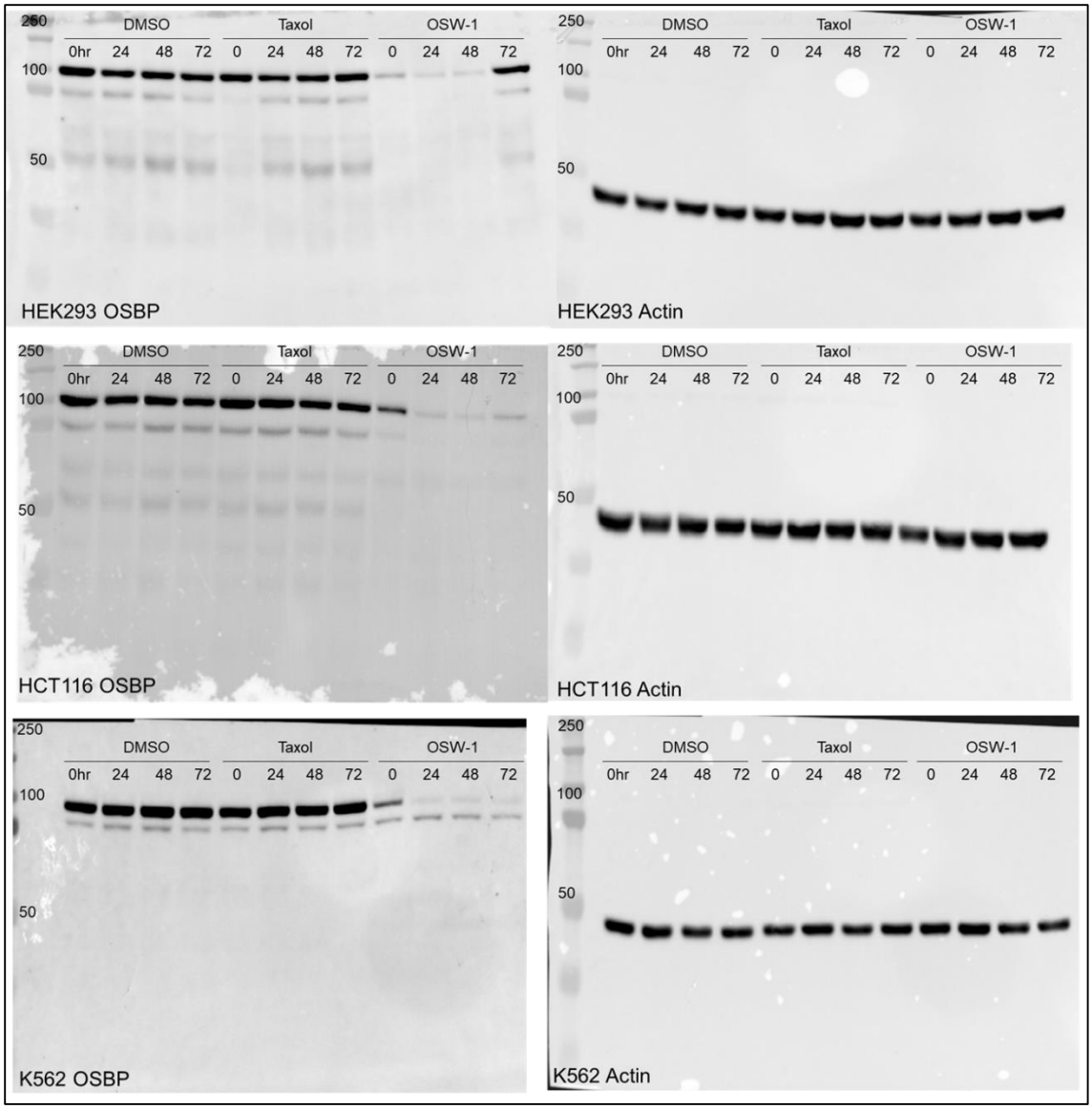

Figure 38: Full blots of Figure 18.

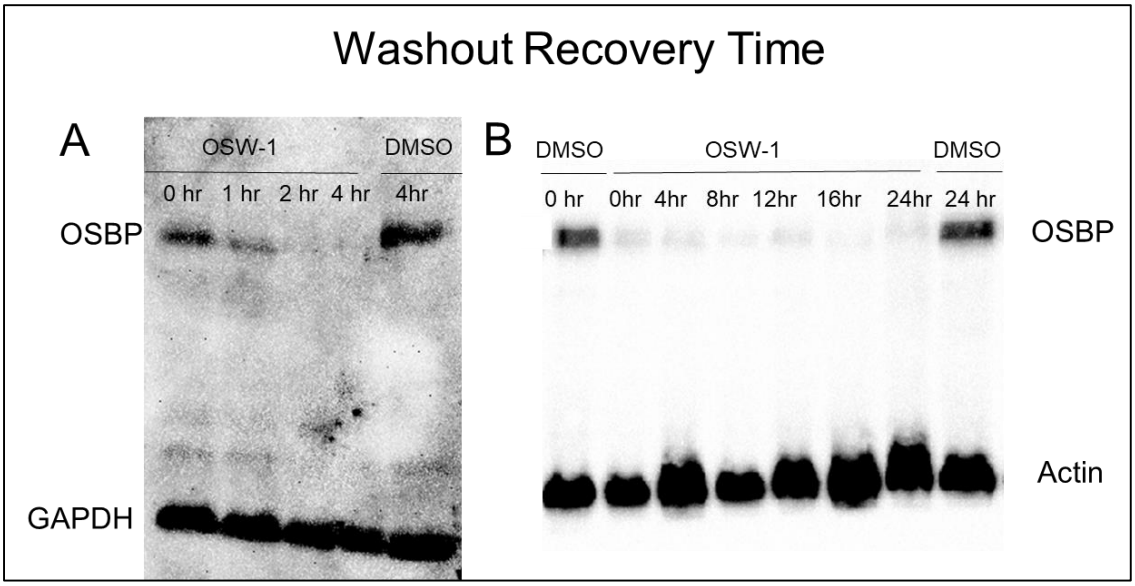

Figure 39: OSW-1 compound washout shows reduction of OSBP up to 24 hours. Cells were treated with 1 nM OSW-1 or DMSO for 6 hours and then the media was replaced and cells were allowed to recover for the indicated time before cell lysis and analysis by western blot.

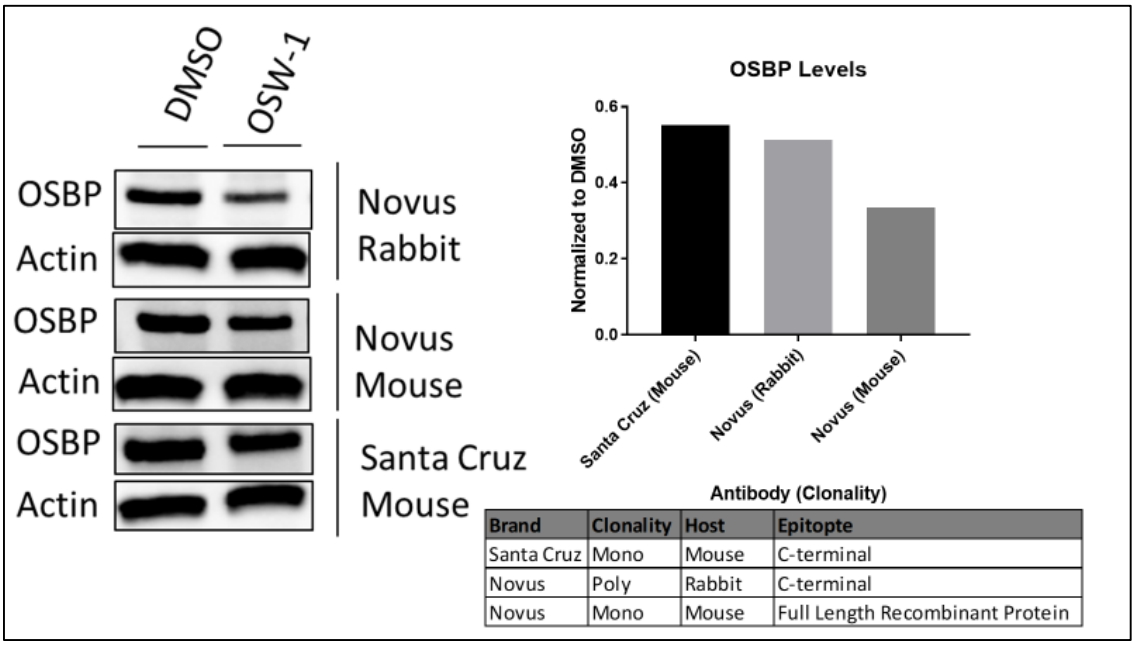

Brand	Clonality	Host	Epitopte
Santa Cruz	Mono	Mouse	C-terminal
Novus	Poly	Rabbit	C-terminal
Novus	Mono	Mouse	Full Length Recombinant Protein

Figure 40: Confirmation of OSBP loss by multiple antibodies. A combination of different clonalities from various hosts with distinct epitopes shows similar OSBP expression in both DMSO and 1 nM OSW-1 0 hr washout recovery treated HCT116 lysates. (Full blots in **Figure** 52).

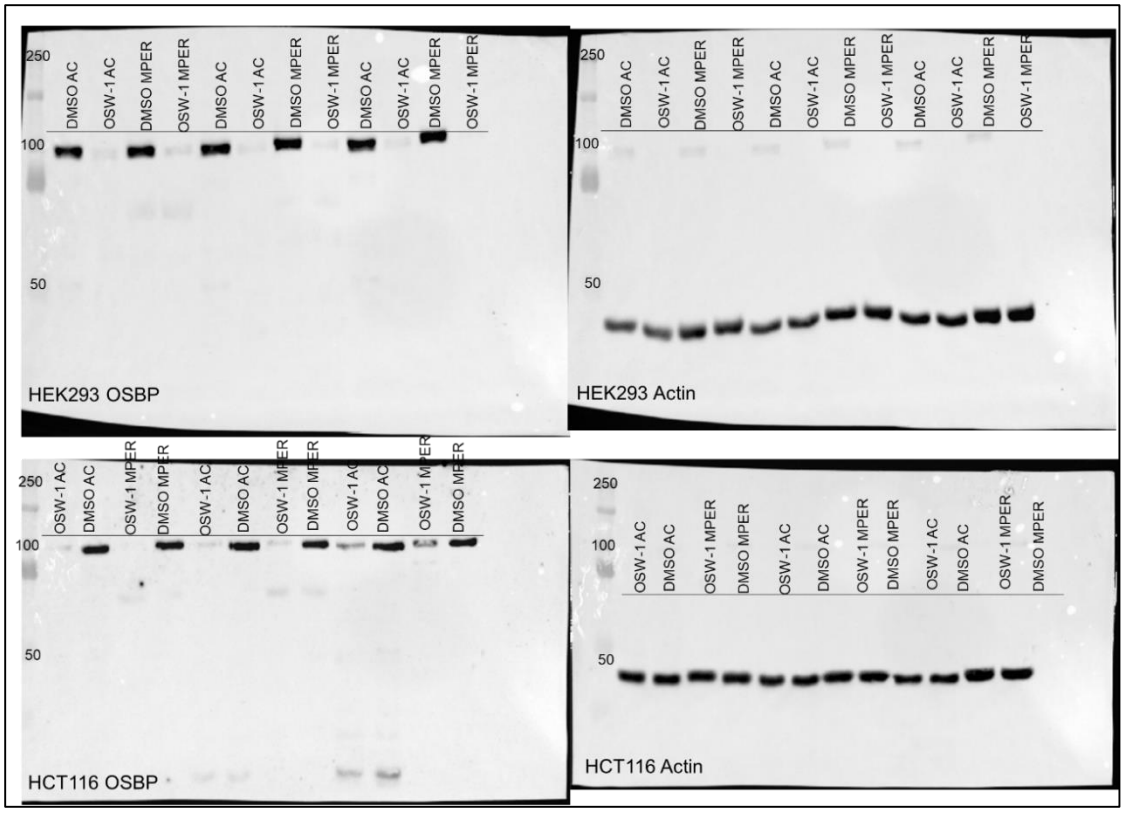

Figure 41:Full blots of Figure 19.

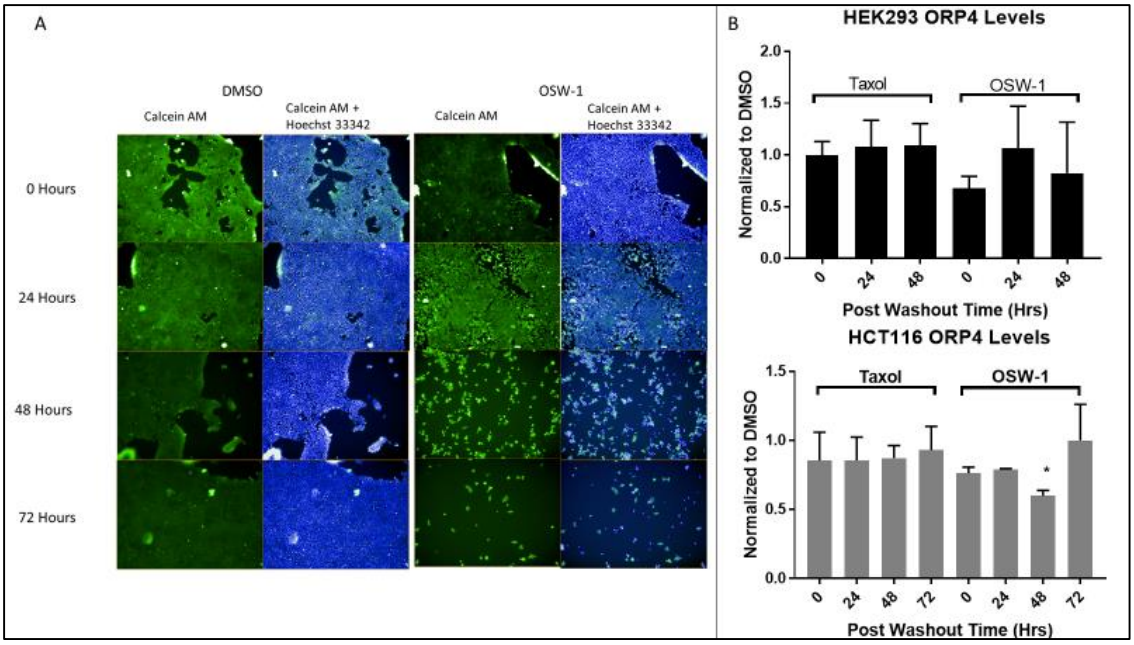

Figure 42: Continual OSW-1 compound treatment is cytotoxic but OSW-1 compound washout cells do not show ORP4 loss similar to OSBP. (A) Calcein AM and Hoechst 33342 staining of 0-72 hours of 1 nM OSW-1 or DMSO in HEK293 cells using Operetta High-Content Imaging System that shows cytotoxicity in OSW-1 treated cells by 24 hours. (B) Western blot analysis reveals that ORP4 levels do not experience the same change as OSBP during 1 nM OSW-1 washout recovery (Full blots in **Figure** 53).

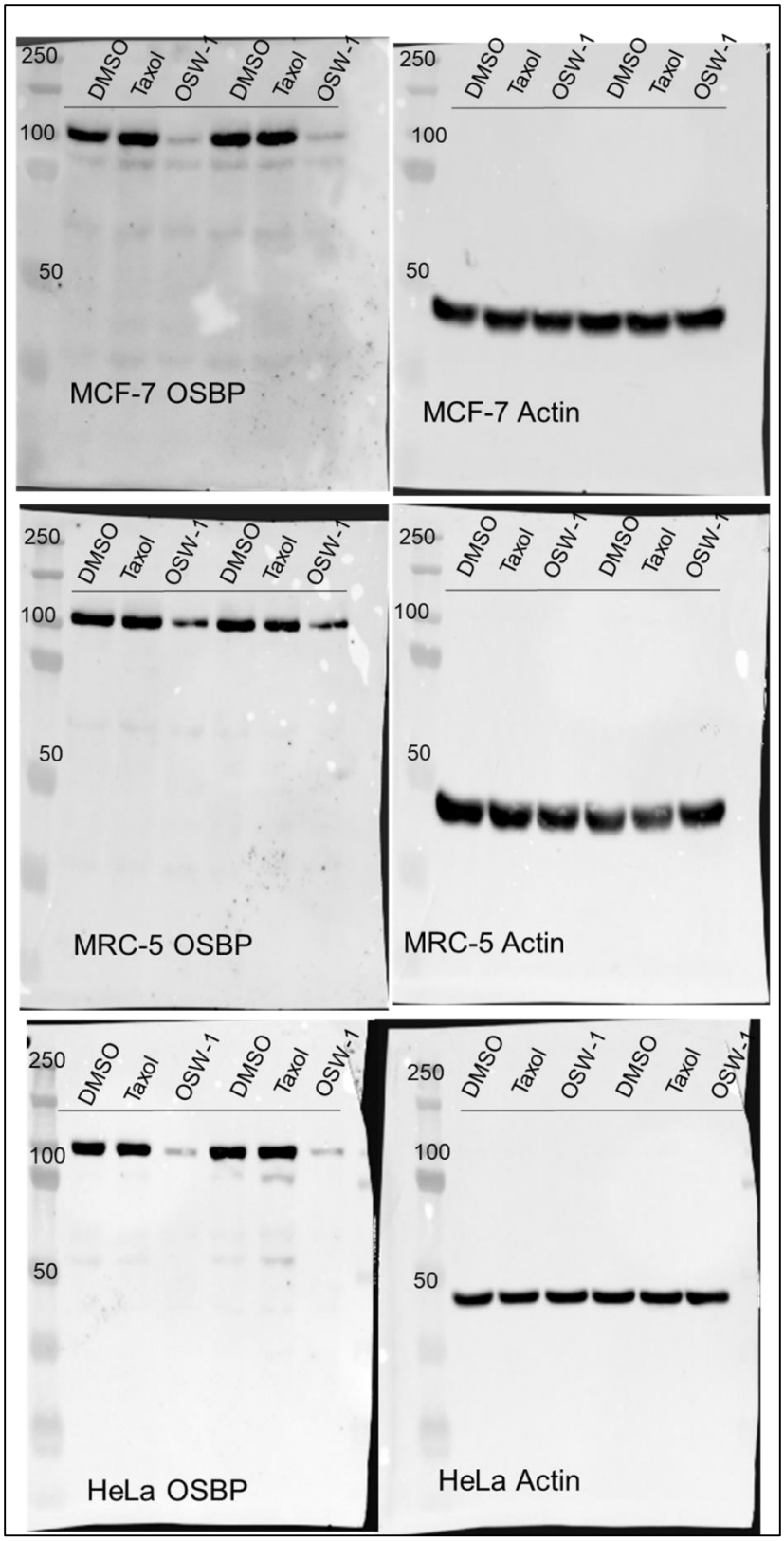

Figure 43: Full blots of Figure 22A

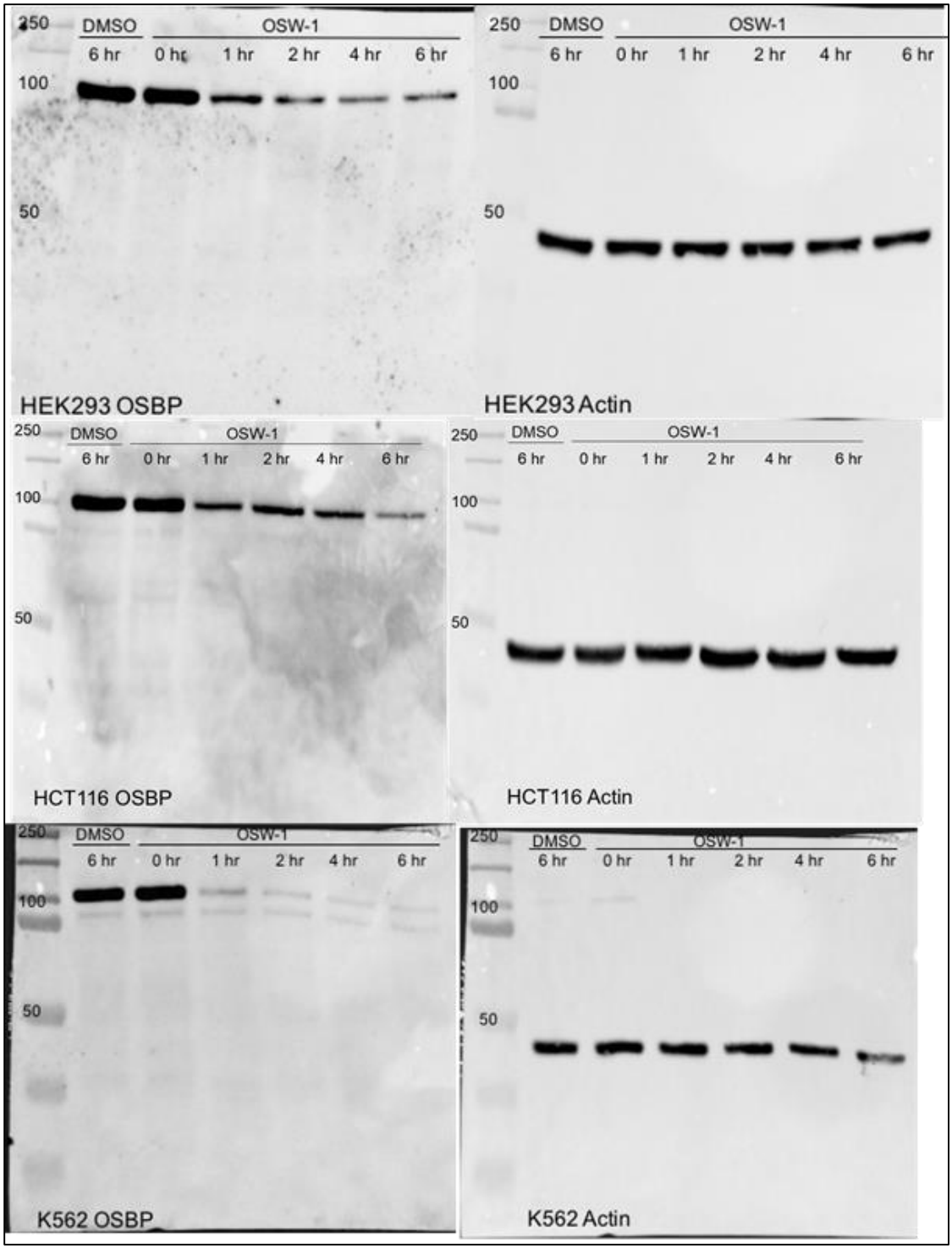

Figure 44: Full blots of Figure 22B.

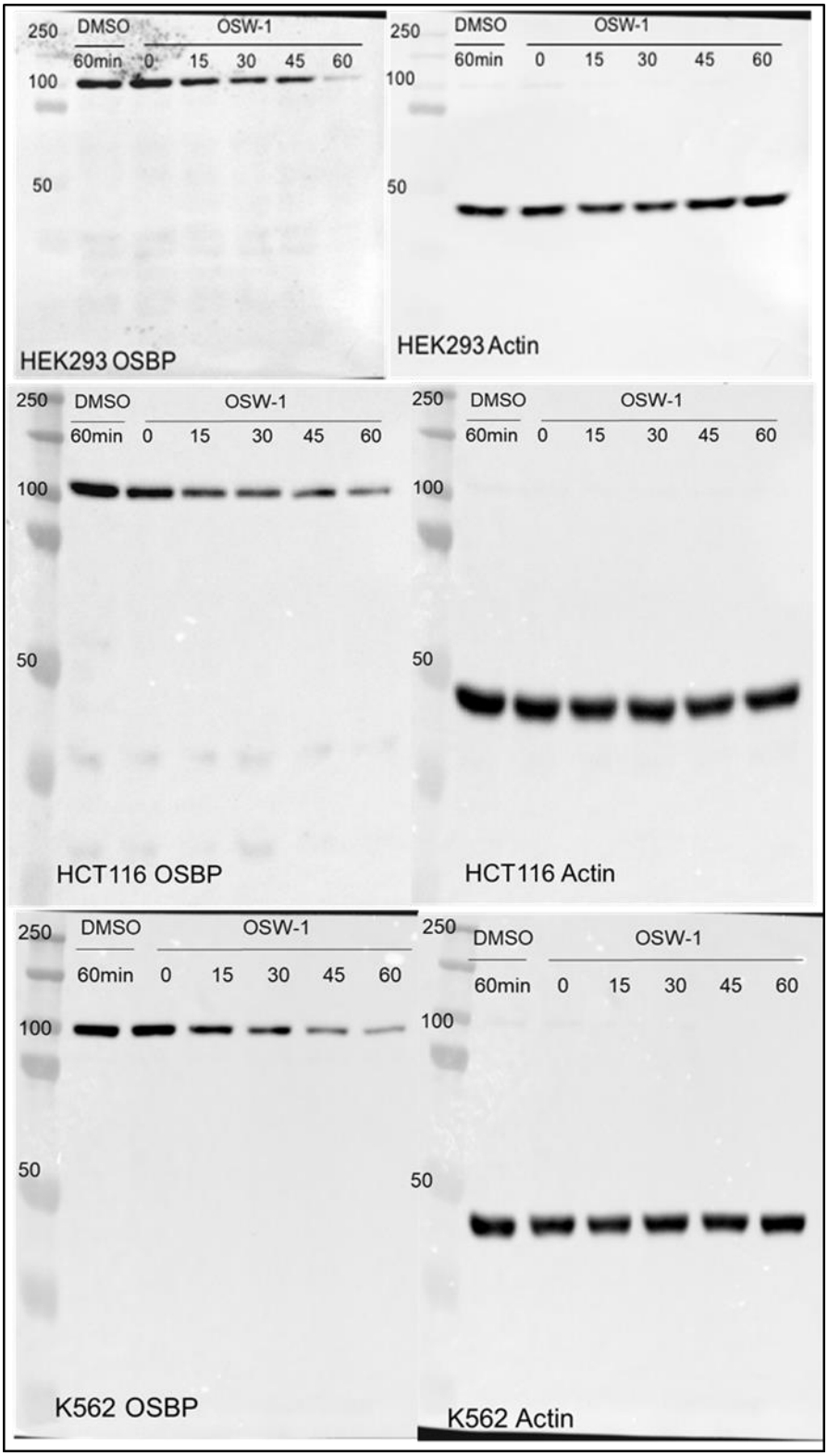

Figure 45: Full blots of Figure 22C.

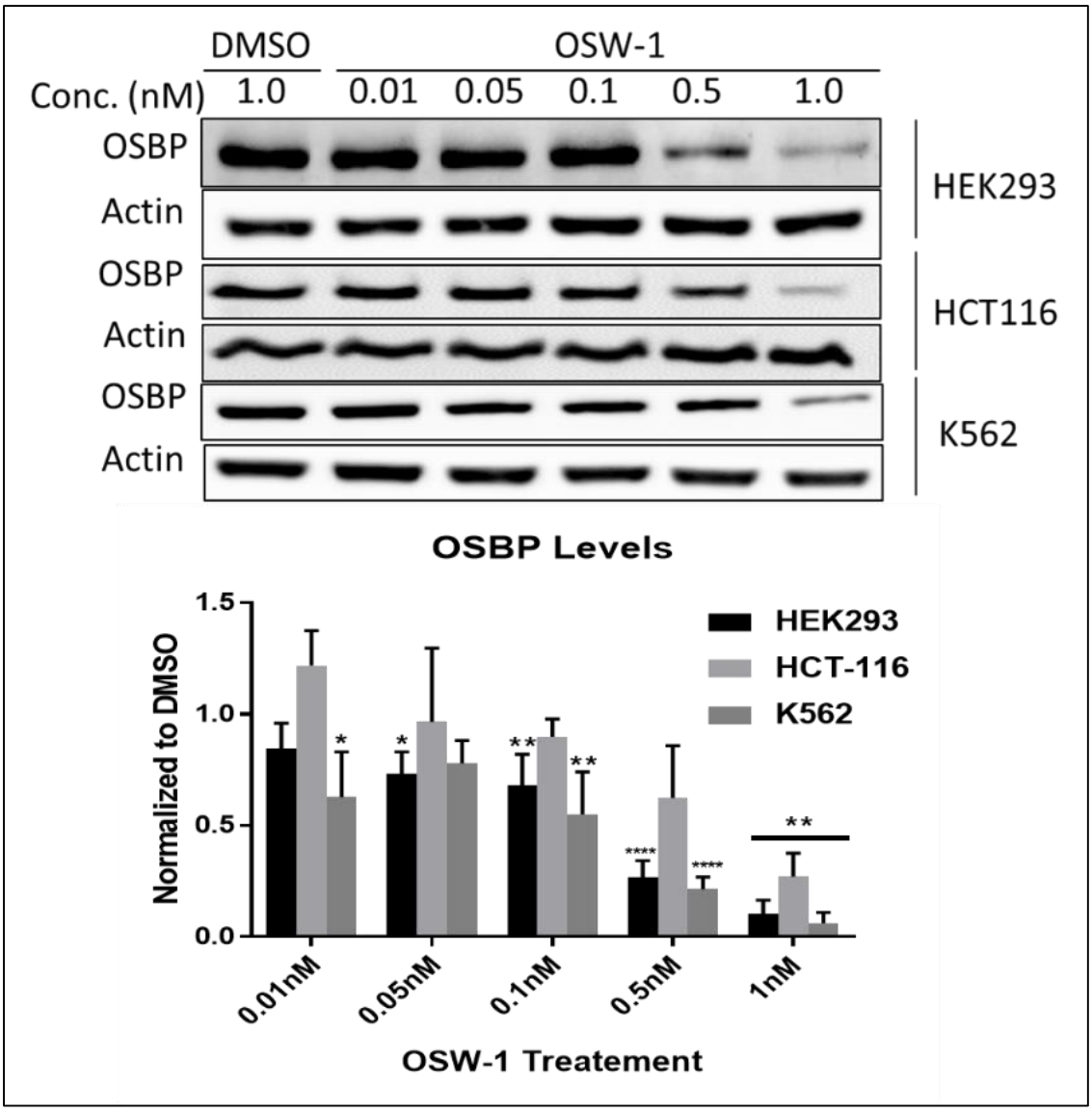

Figure 46: Sub-nanomolar OSW-1 compound washout treatments lead to significant OSBP reduction.

Cell lines were treated with the indicated concentration of OSW-1 compound for 6 hours and then recovered for 24 hours before being analyzed by western blot. Values are mean ± sd (n=3). HEK293 results were collected by Mr. Zachary Severance and HCT116 results were collected by Mr. Ryan Bensen. (Full western blots in **Figure** 54)

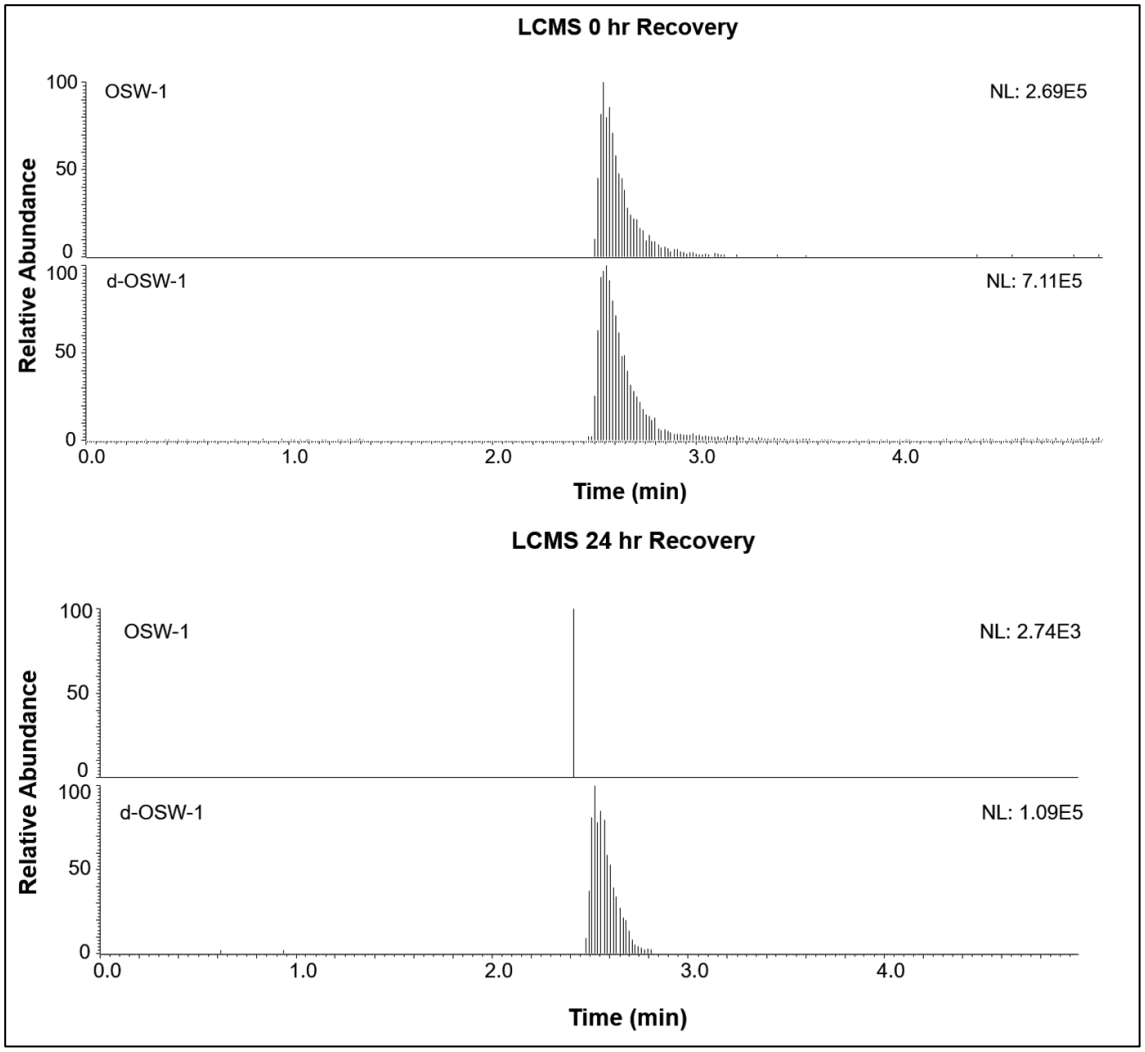

Figure 47: Full Chromatogram of LCMS 100 nM OSW-1 Treatment. Chromatogram of Liquid Chromatography Mass Spectrometry (LCMS) quantification of OSW-1 via an internal standard of 50nM deuterated OSW-1 following a 1hr 100nM treatment of OSW-1 with 0 or 24hr recovery.

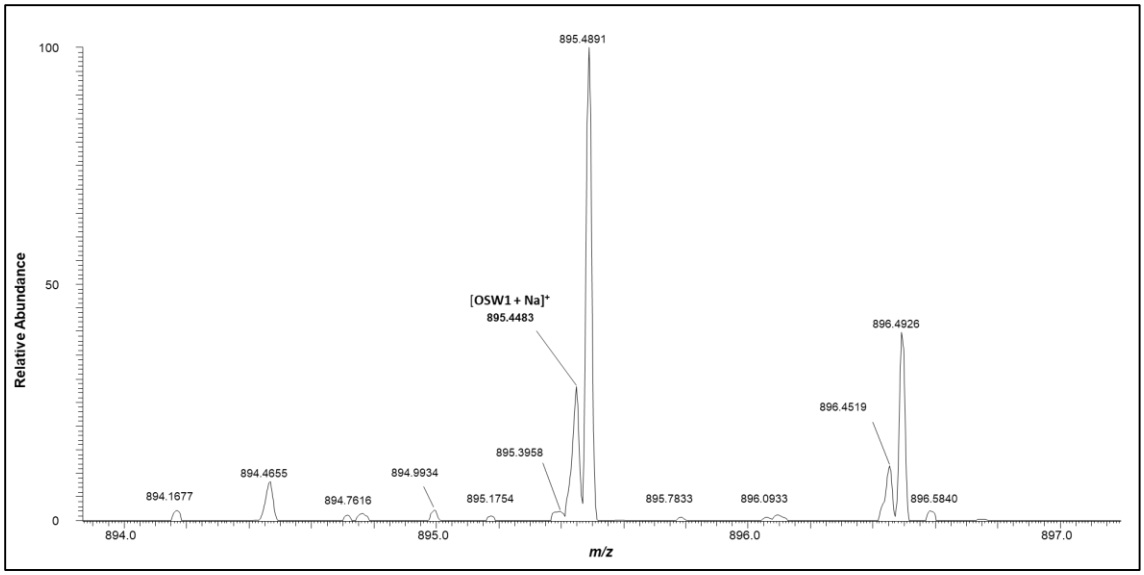

Figure 48: LCMS Limit of Quantification.
Spectra of LCMS 100pM OSW-1 spiked lysate sample for limit of quantification. 100pM OSW-1 signified ~4 fold ratio between signal to noise. Experiment was run in two independent replicates (n=2).

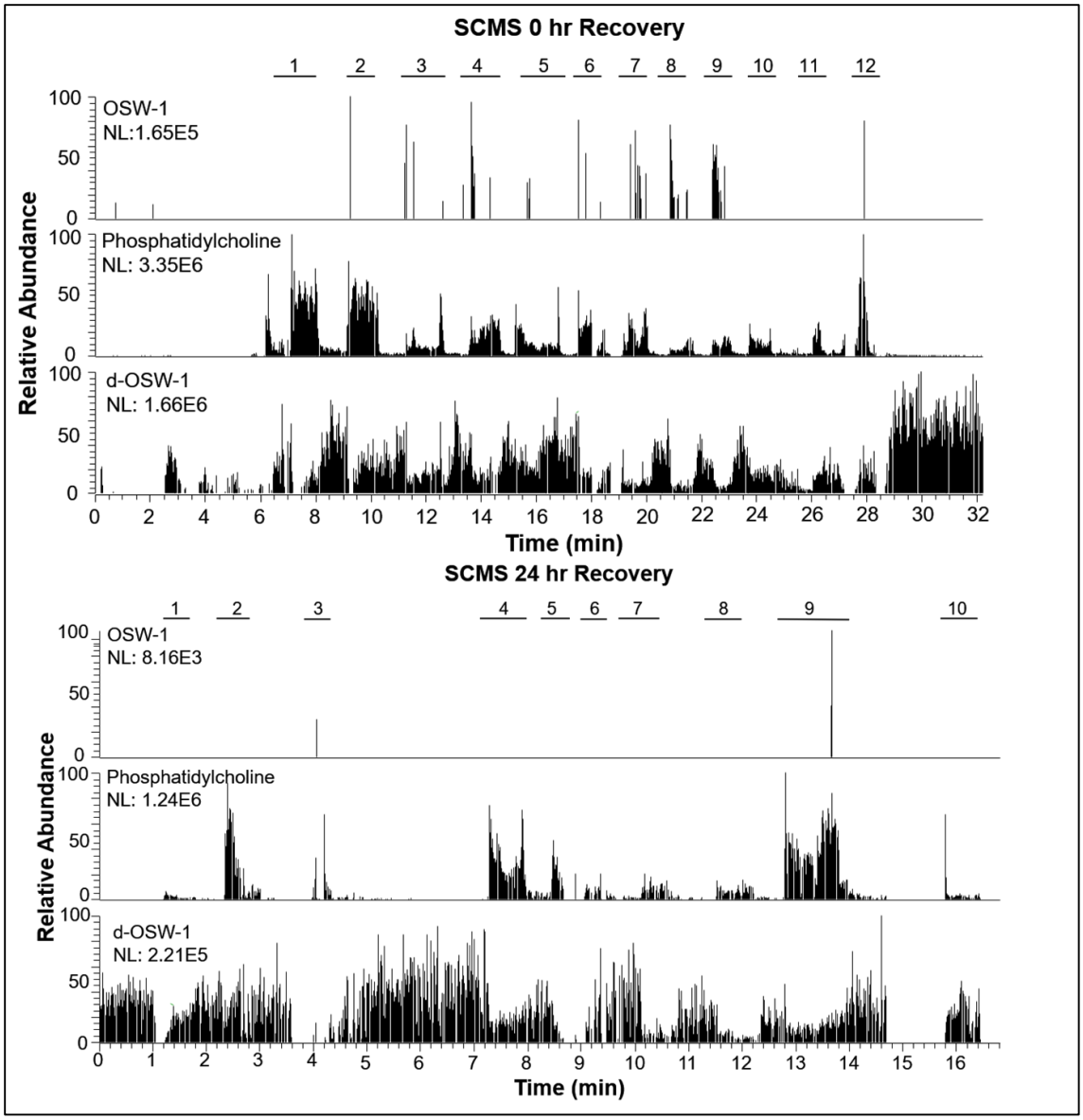

Figure 49: Full Chromatogram of SCMS 100 nM OSW-1 Treatment. Chromatogram of Single Cell Mass Spectrometry (SCMS) quantification of OSW-1 utilizing a constant flow of d-OSW-1. Individual cells were analyzed with the Single-Probe upon detection of the intracellular lipid, phosphatidylcholine, and depicted as specified.

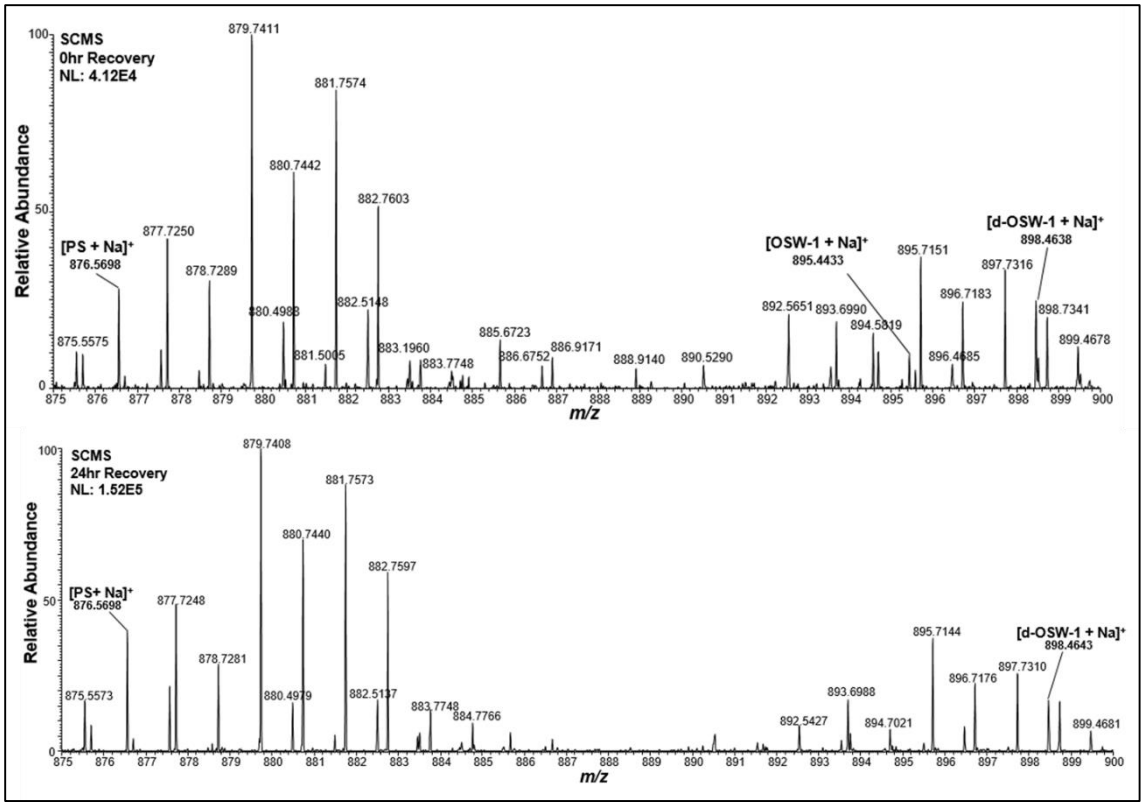

Figure 50: Spectra of SCMS at 0 and 24 hr Recovery

Zoomed out spectra of **Figure** 2 Single Cell Mass Spectrometry (SCMS) detecting Phosphatidylserine (PS). PS lipid detection signifies cellular content is being analyzed with either the detection (0hr recovery) or absence (24hr recovery) of OSW-1.

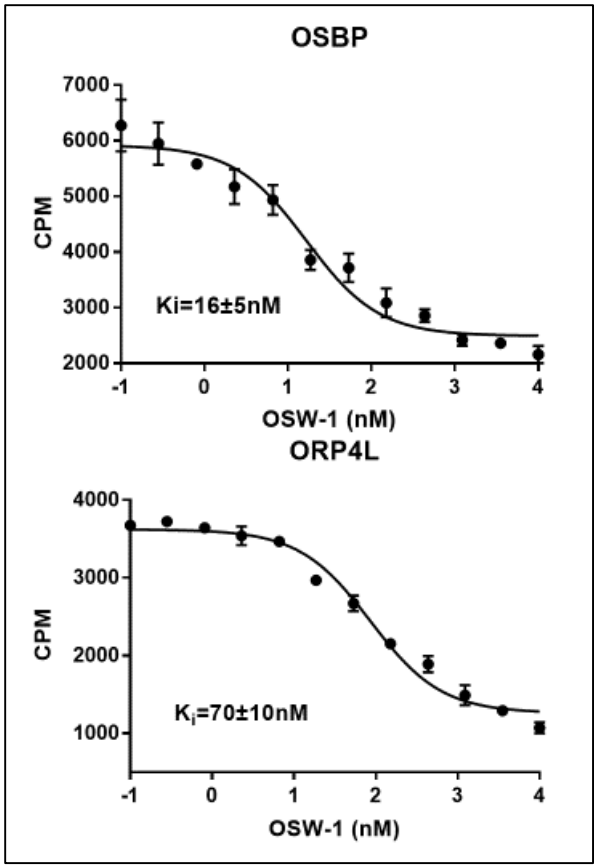

Figure 51: Binding curves of OSW-1 to OSBP and ORP4

Representative binding curves for OSW-1 to overexpressed OSBP and ORP4L in HEK293T cells using a competition radioactivity assay against [3H]-25-OHC. Ki values indicated are the average between each replicate. The error comprises of standard deviation between the replicates. A minimum of n=2 was used. Work done by Dr. Juan Nuñez.

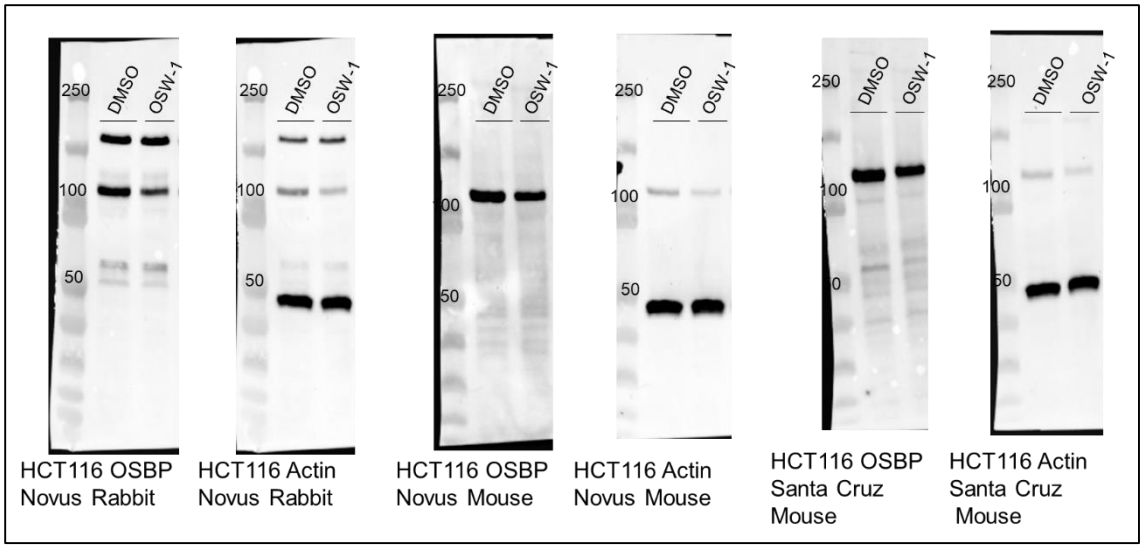

Figure 52: Full western blots of Figure 40.

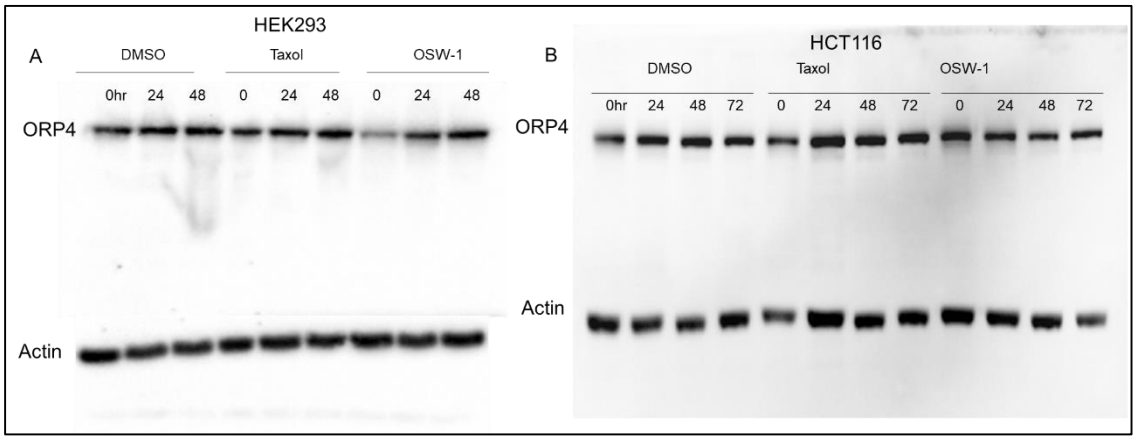

Figure 53: Full western blots of Figure 42. (A) HEK293 and (B) HCT116 cells were treated with DMSO, 1 nM Taxol, or 1nM OSW-1 for 6 hours followed by compound washout and recovered for the times indicated before lysis and analysis by western blot.

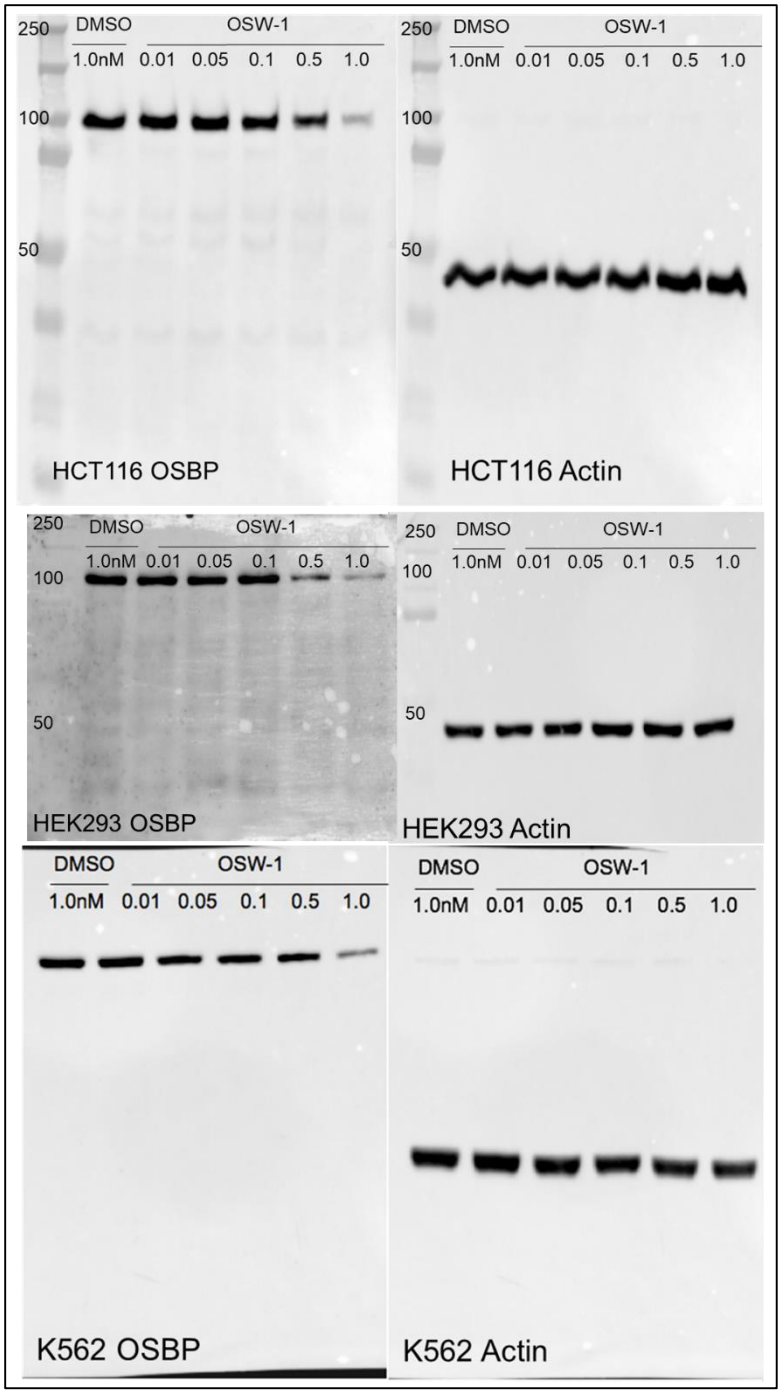

Figure 54: Full blots of Figure 46

Appendix 2: Chapter 3 Supplemental

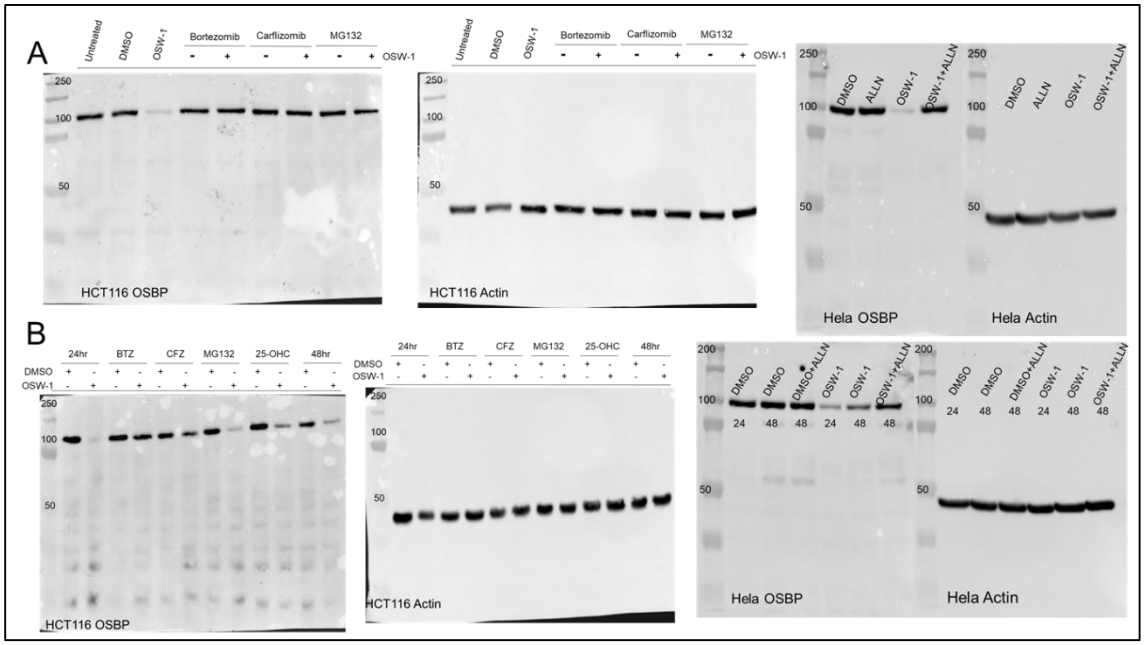

Figure 55:Full blots of Figure 25. (A) Co-incubation blots correspond to (A) and (B) washout blots correspond to (B).

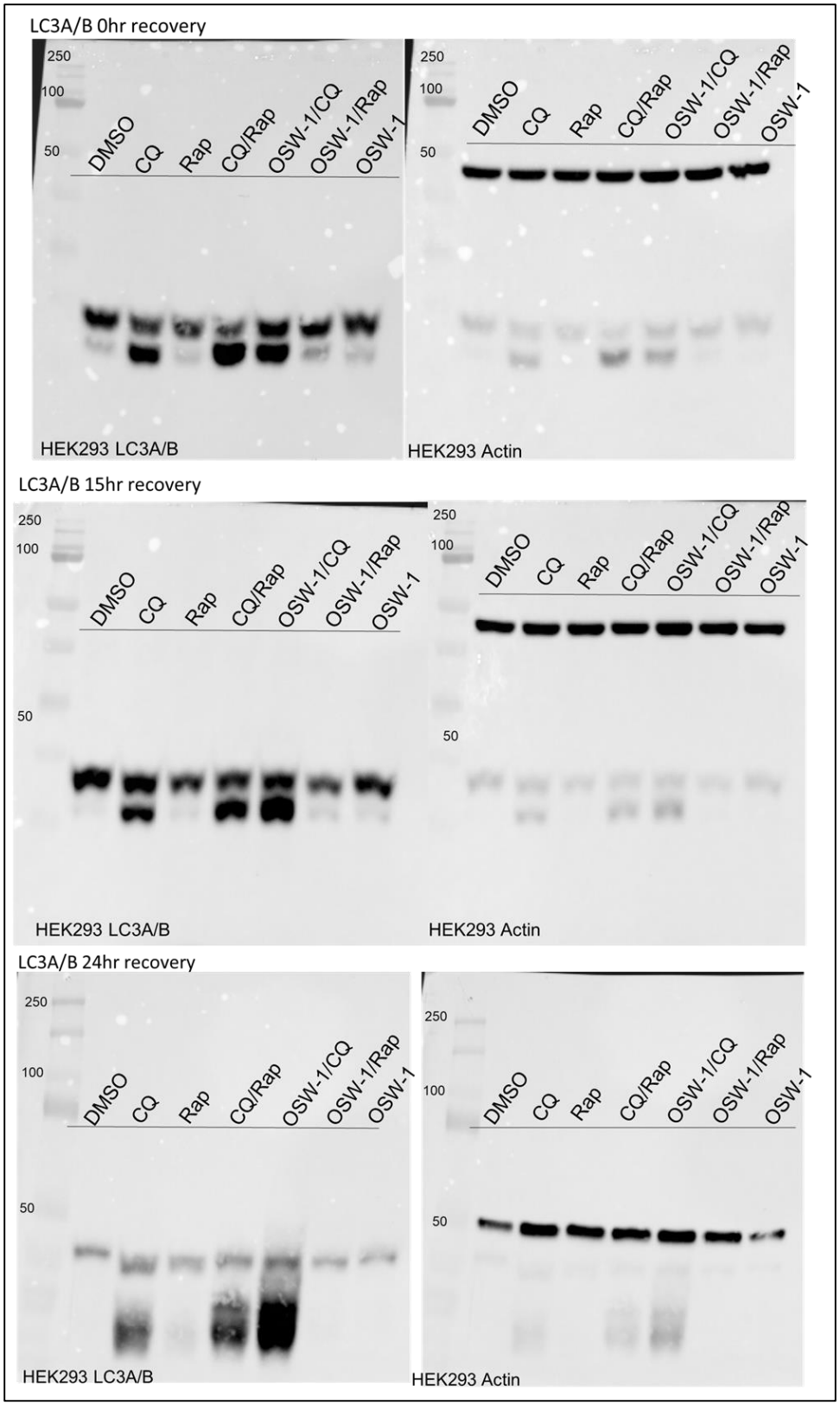

Figure 56:Full blots of LC3A/B from Figure 26

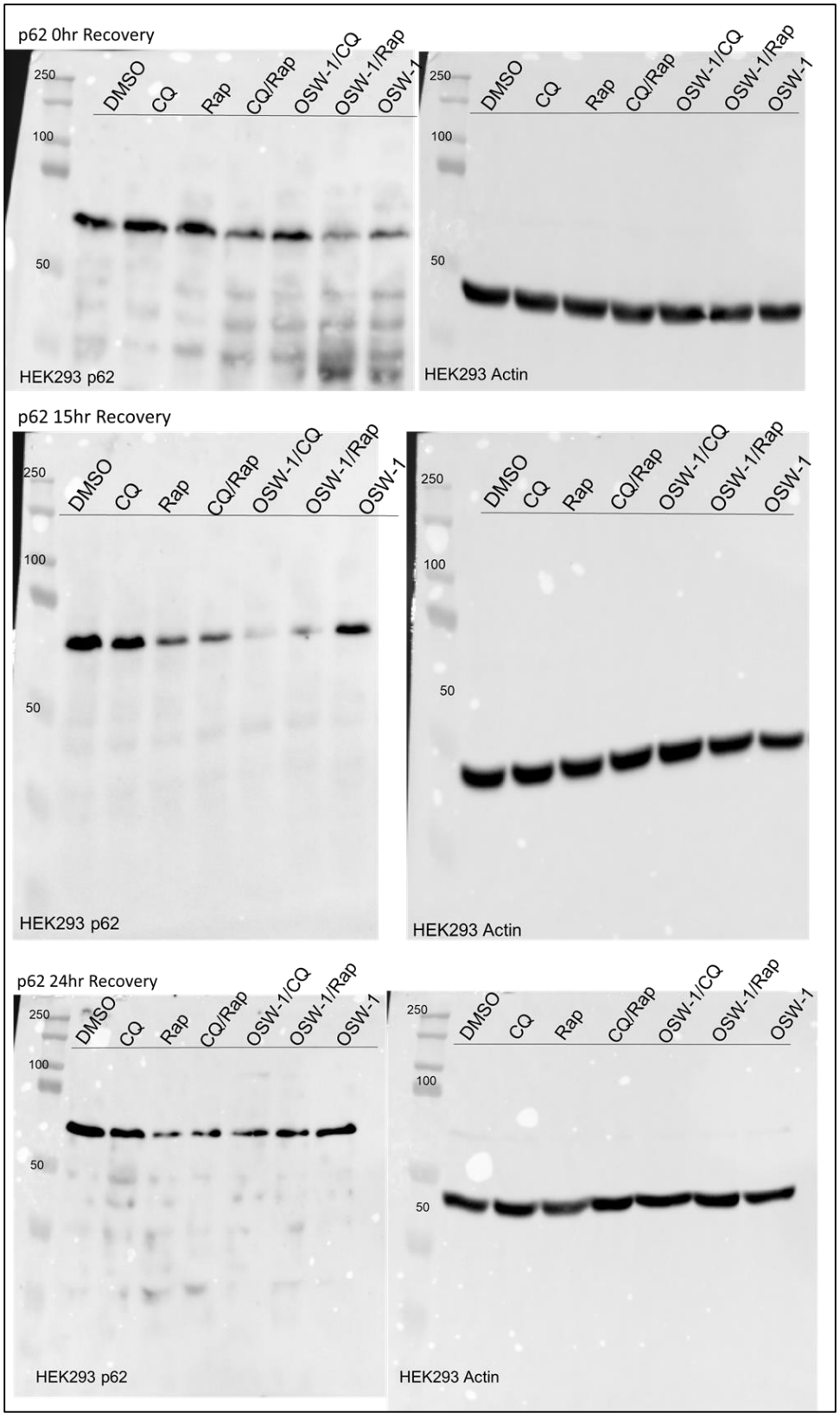

Figure 57: Full blots of p62 from Figure 26

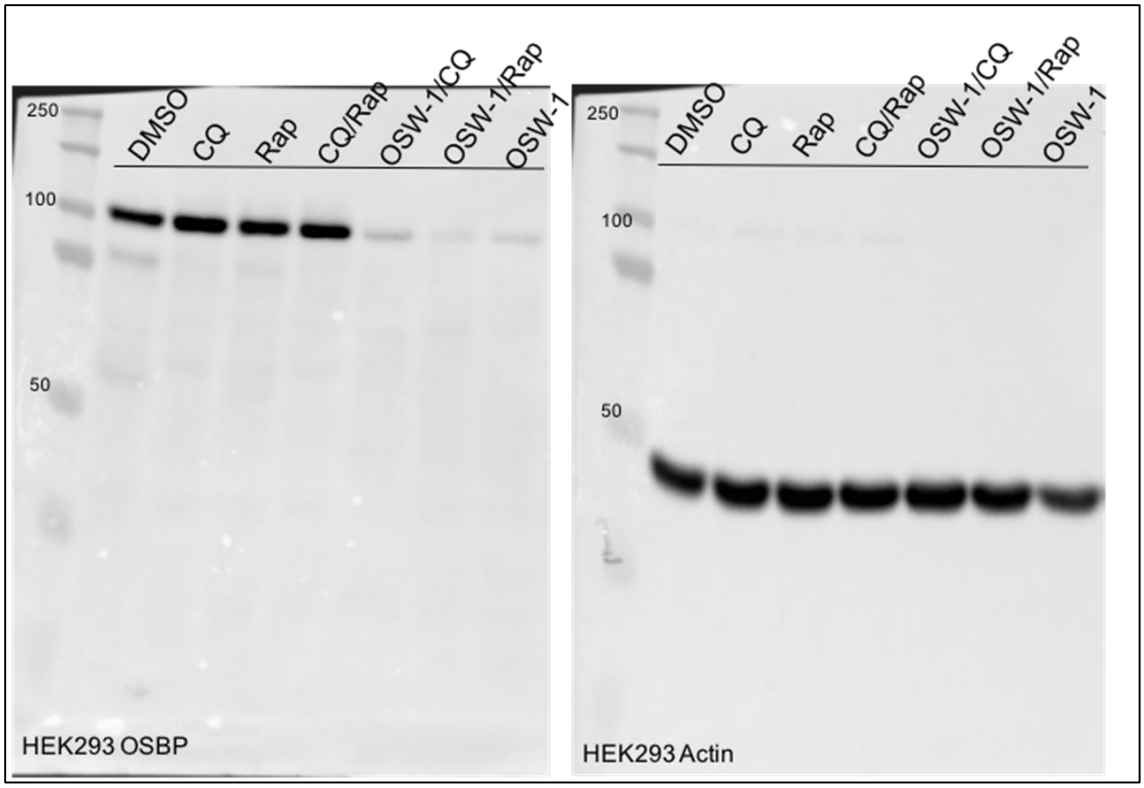

Figure 58:Full OSBP blot from Figure 26

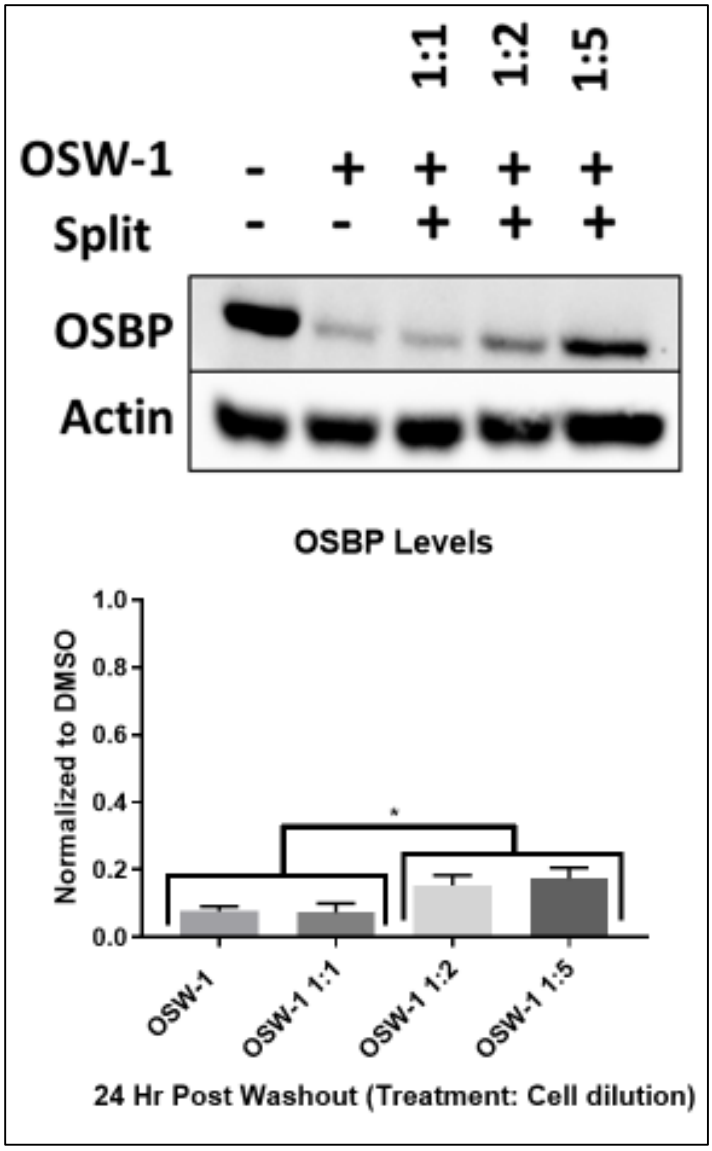

Figure 59: Cell splitting and cell density do not recover OSBP. HEK293 cells were treated with 1nM OSW-1 for 6 hours and then washed out. Following washout cells were split and then diluted as indicated and recovered for 24 hours before lysis. Results are mean ± sd (n=3). (Full blot in **Figure** 62)

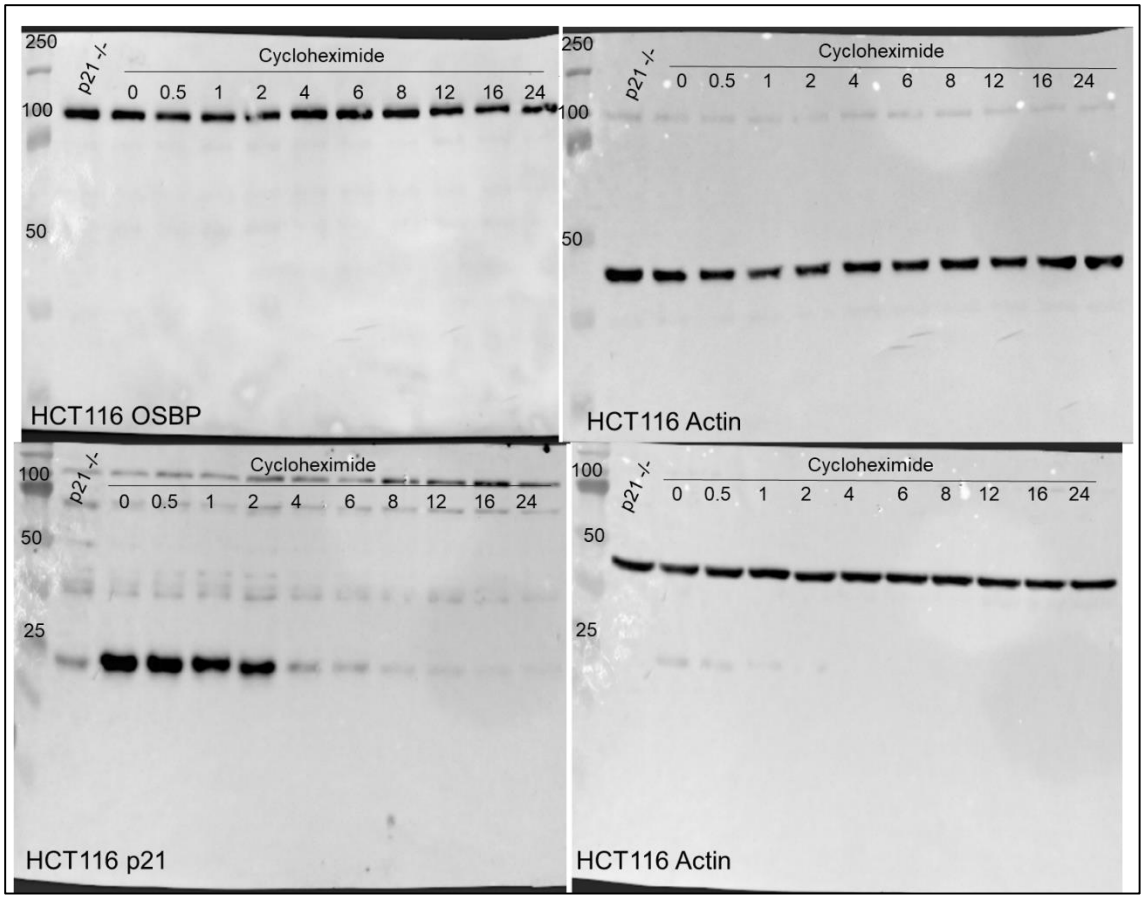

Figure 60: Full blots of Figure 27

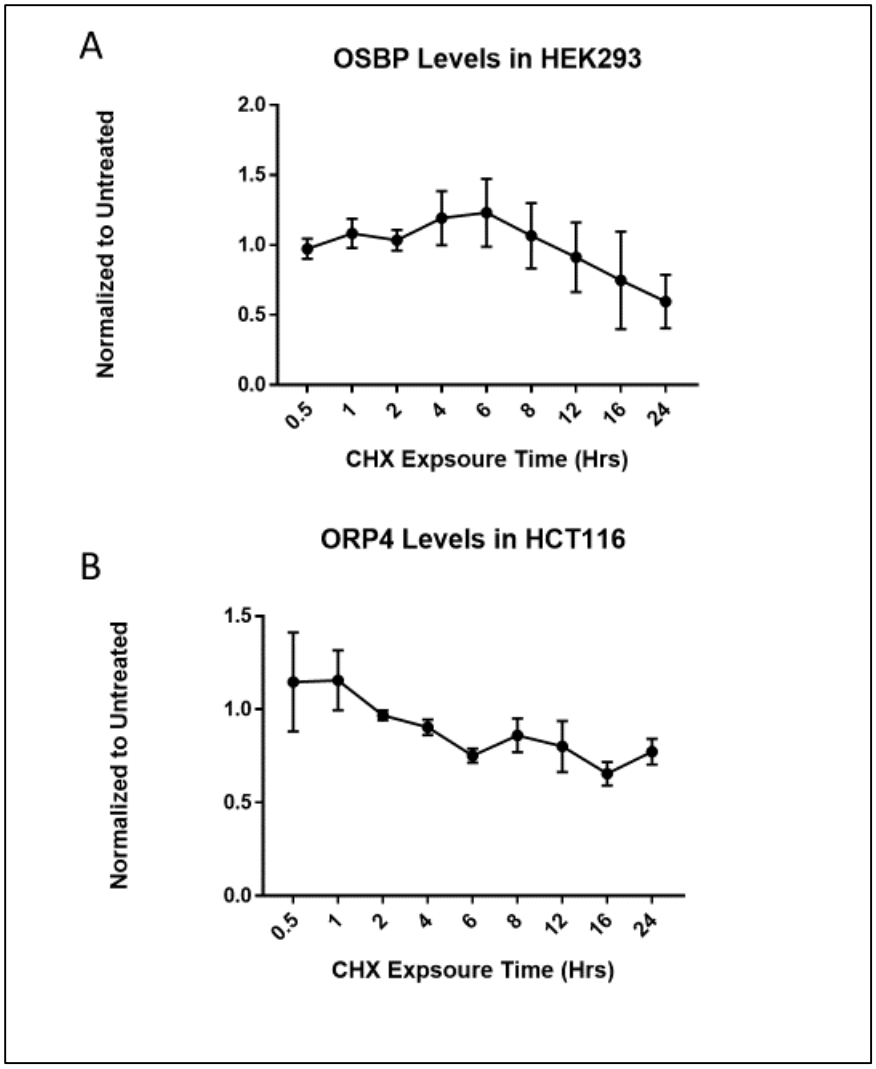

Figure 61: OSBP and ORP4 are long lived proteins. (A) OSBP levels in HEK293 and (B) ORP4 levels in HCT116 show that the half-life of OSBP is over 24 hours. 178 μM Cycloheximide (CHX) was used throughout the experiment. Results are mean ± sd (n=3). (Full blots in **Figure** 63)

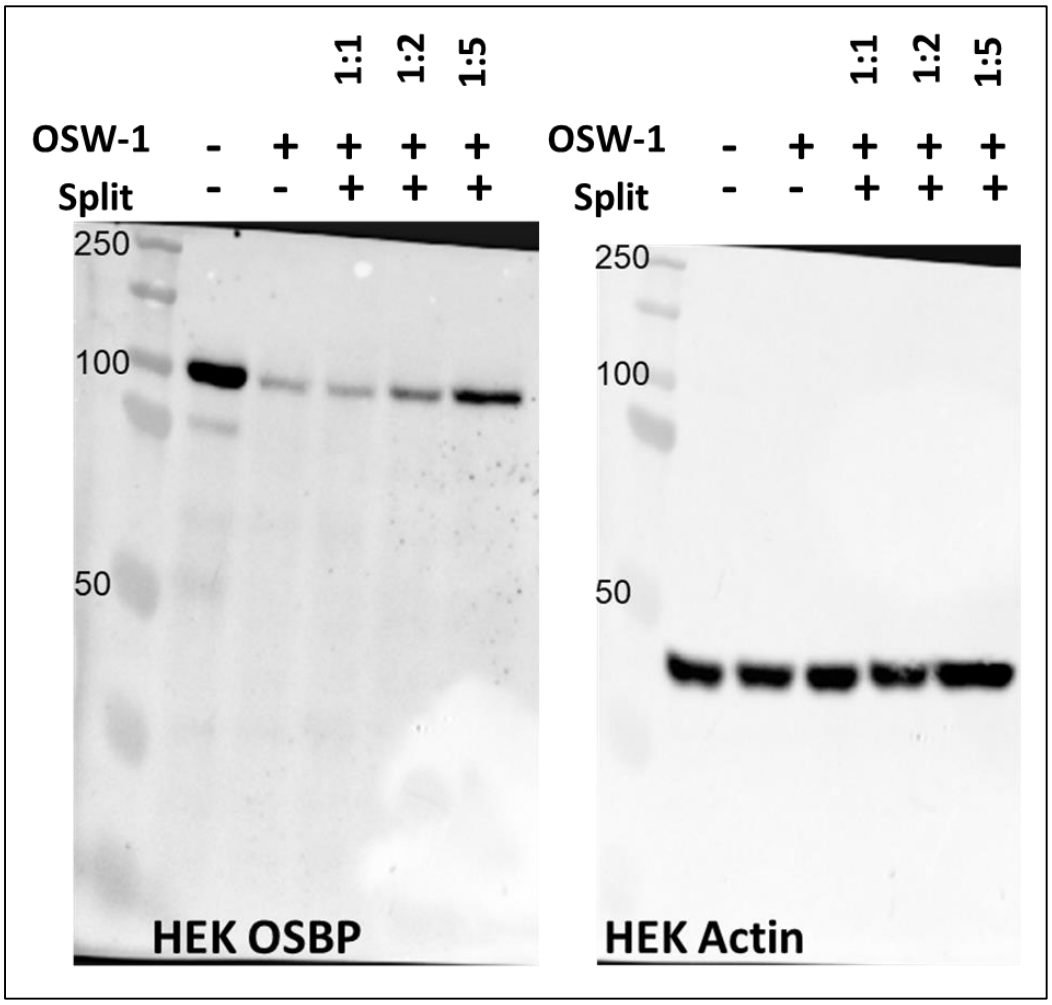

Figure 62: Full blots of Figure 59

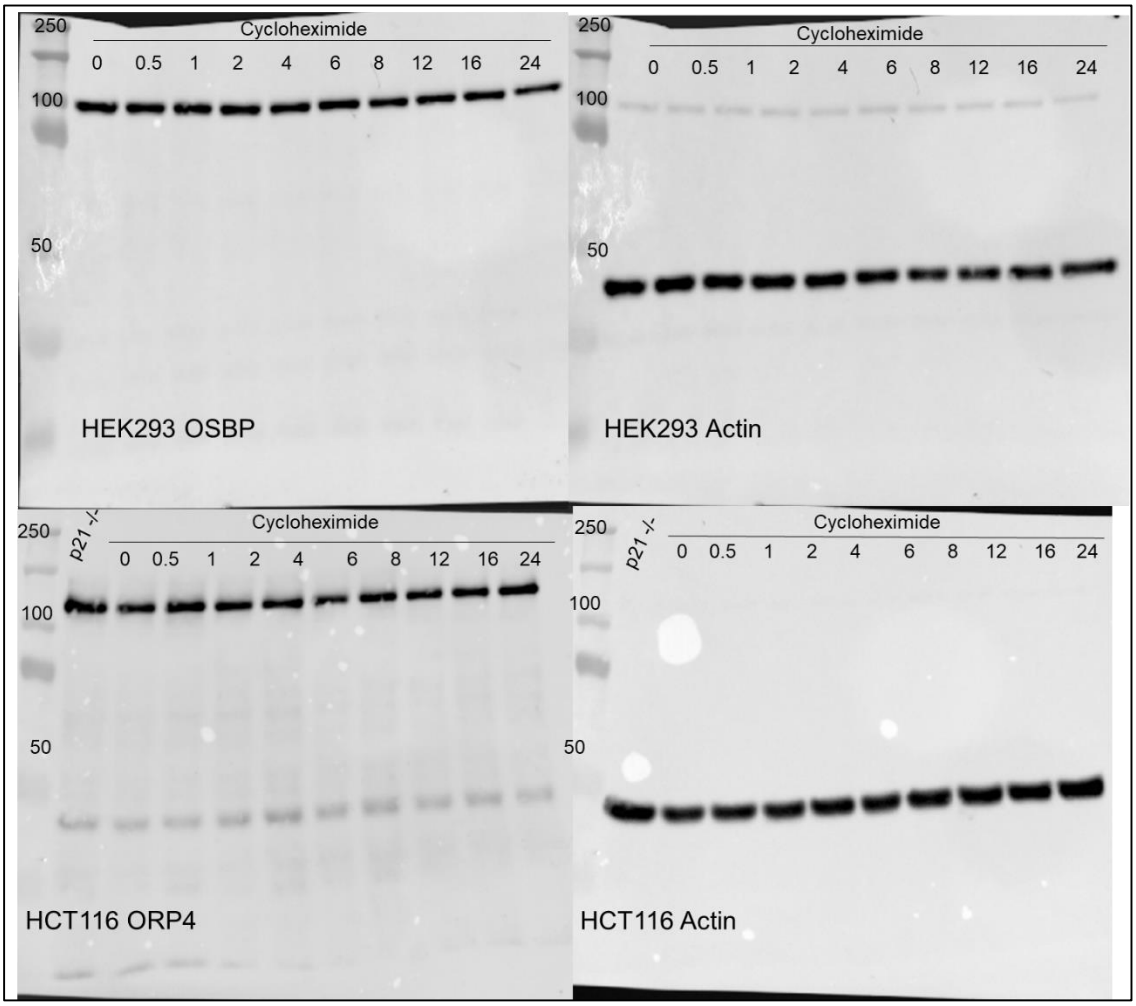

Figure 63: Full blots from Figure 61.

Appendix 3: Chapter 4 Supplemental

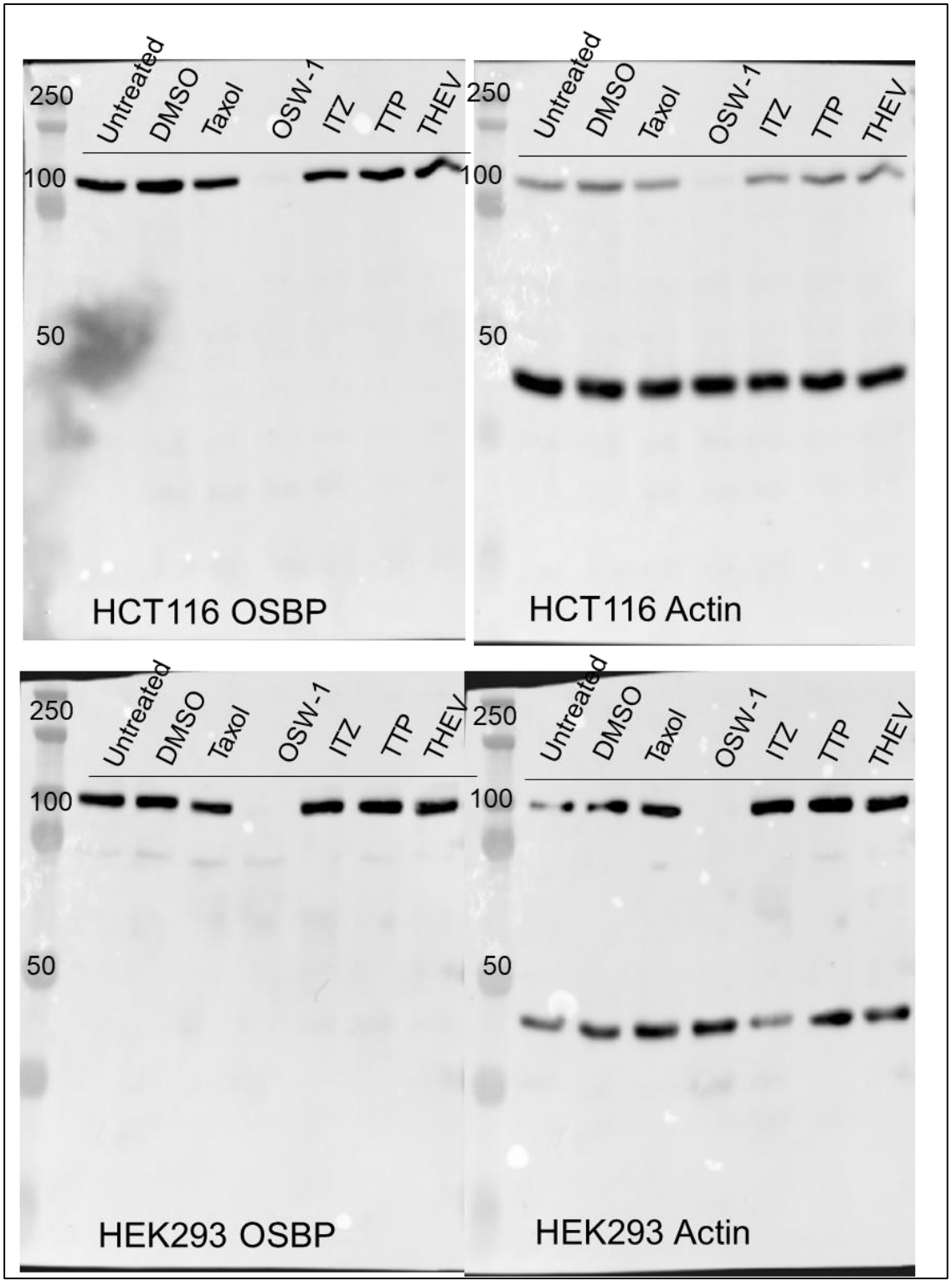

Figure 64: Full blots of Figure 29

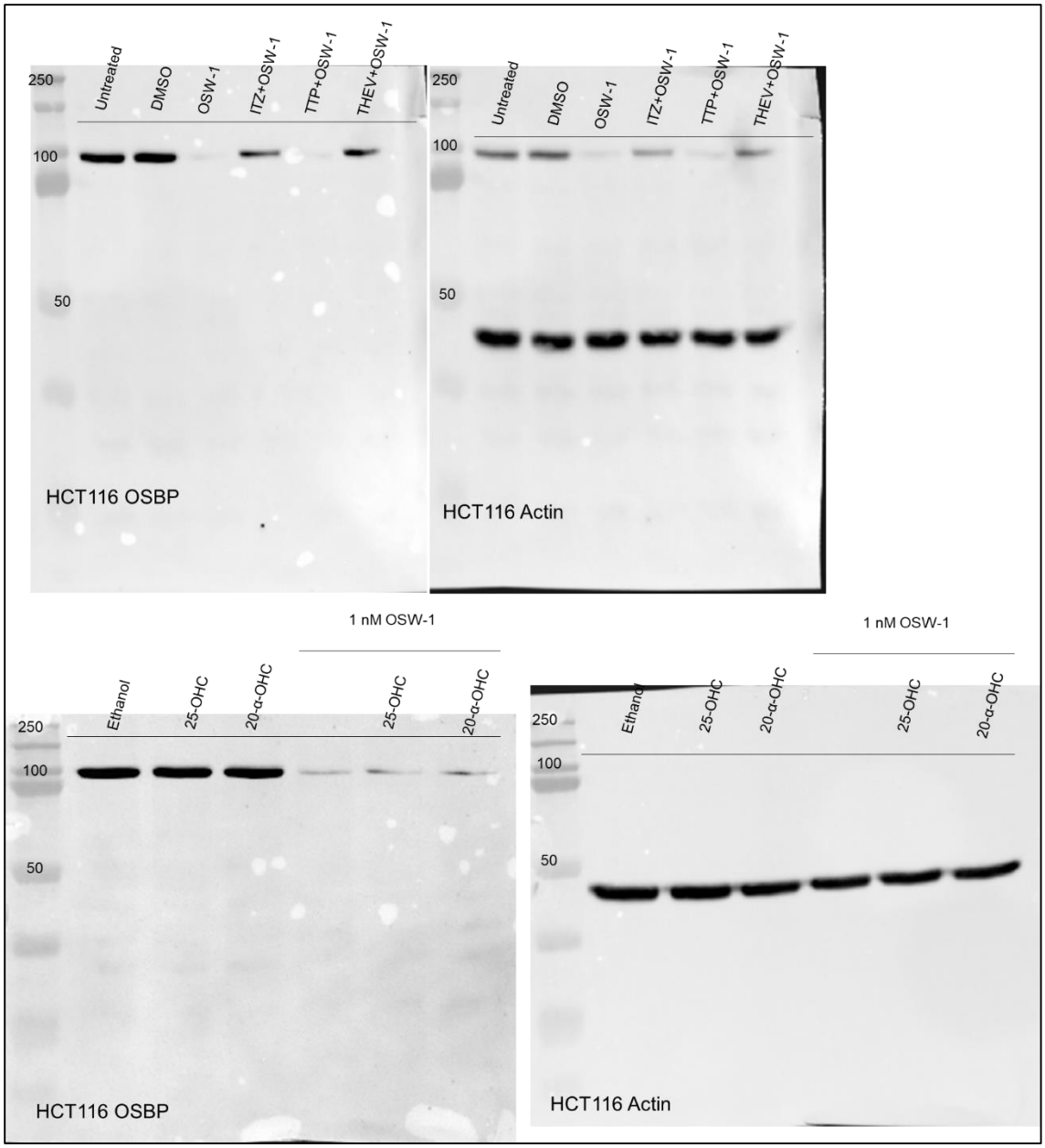

Figure 65: Full blots of Figure 31.

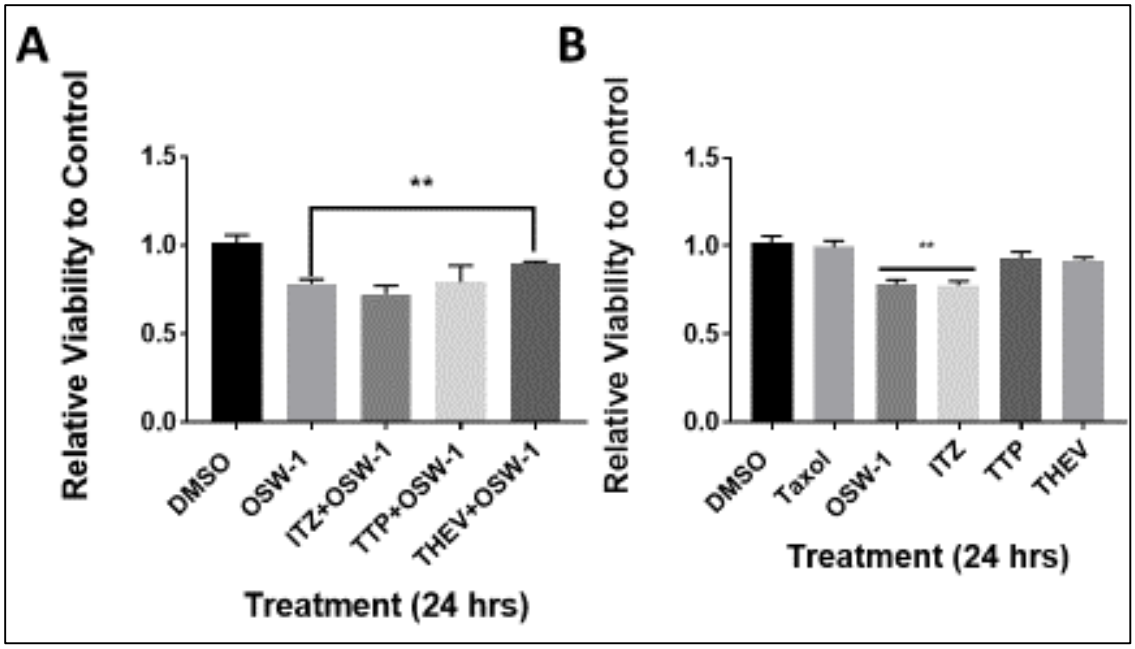

Figure 66: THEV2 attenuates OSW-1 induced viability loss. (A) HCT116 cells were treated with DMSO, 1 nM OSW-1, or a combination of OSW-1 and 10µM of the indicated compound for 24 hours after which cell viability was determined by Cell Titer Blue method. (B) HCT116 cells were treated with DMSO, 1 nM Taxol, 1 nM OSW-1 or 10µM of the indicated compound for 24 hours after which cell viability was determined by Cell Titer Blue method.

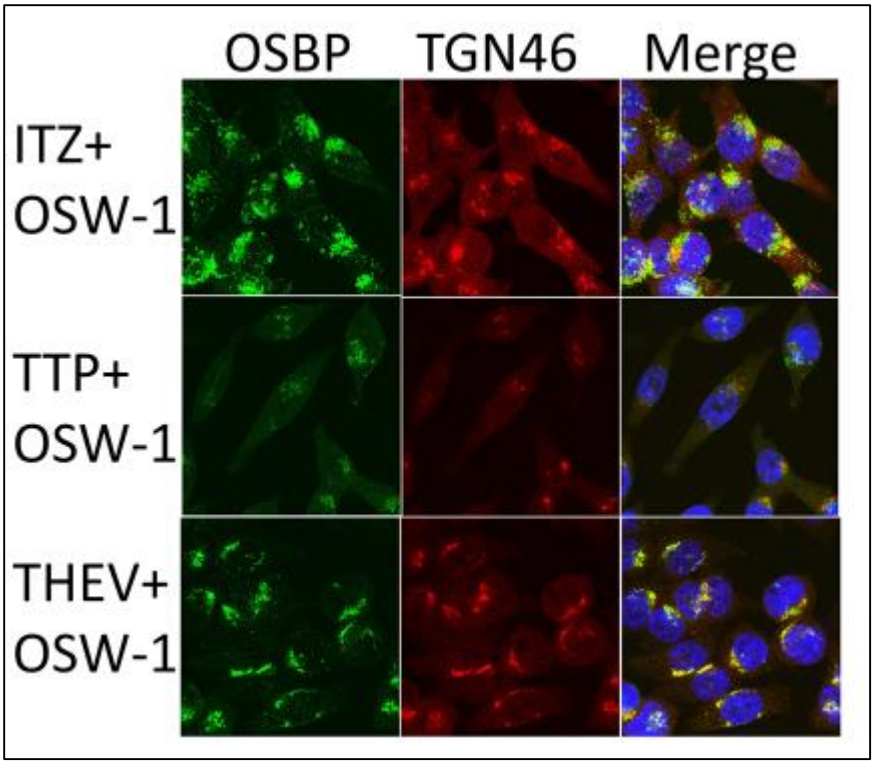

Figure 67: Co-incubation of OSW-1 and ORPphillins cause variable OSBP localization. Indirect immunofluorescence was used to determine localization of OSBP (green) and TGN46 (red) when incubated with 1 nM OSW-1 and 10 µM of an ORPphillin for 24 hours. Nuclei (blue) were stained with Hoescht 33342.

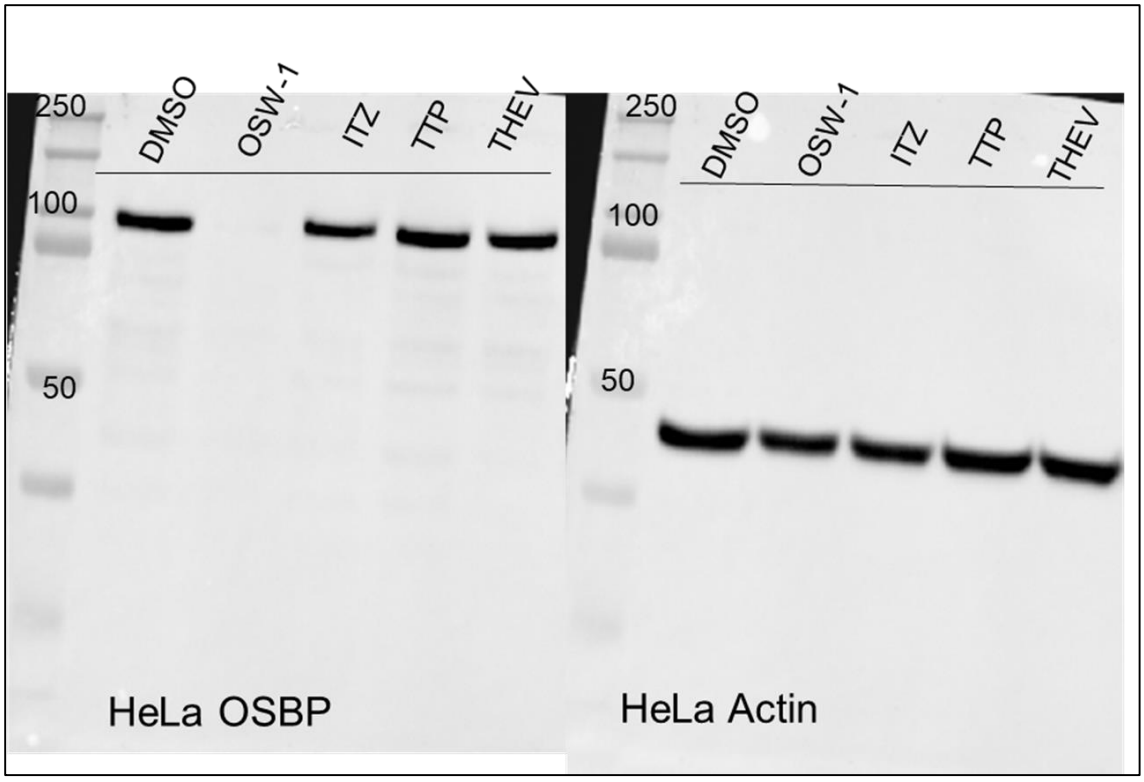

Figure 68: Full blot of Figure 33.

Appendix 4: Chapter 5 Supplemental

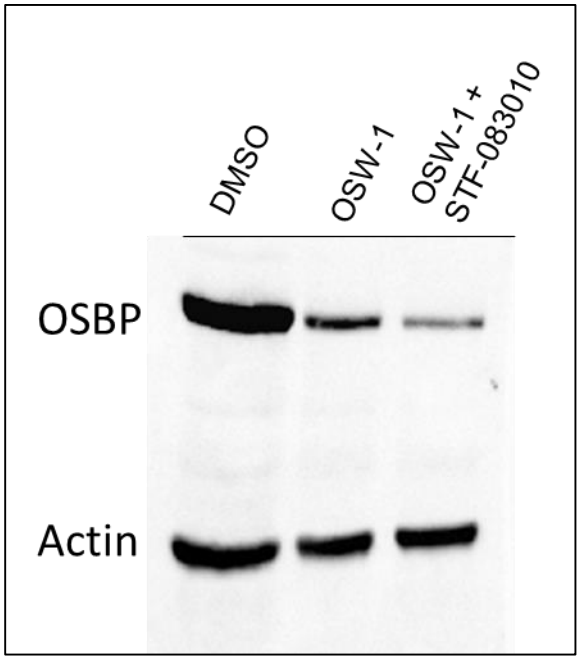

Figure 69: An ER-Stress inhibitor does not rescue OSBP induced OSW-1 degradation. HEK293 cells were treated with DMSO, 1 nM OSW-1, or 1 nM OSW-1 with 50 µM STF-0803010 for 24 hours and analyzed by western blot.

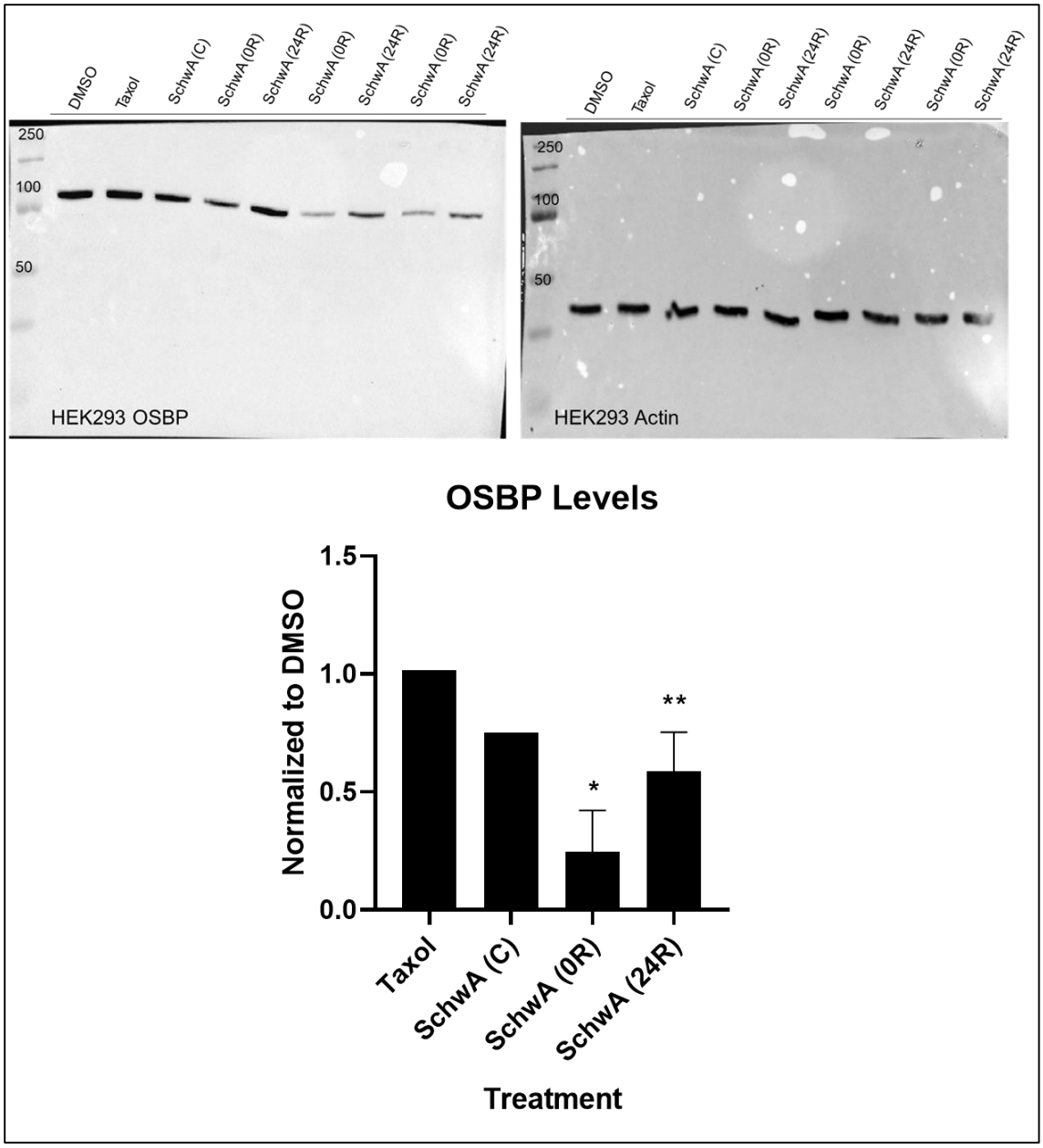

Figure 70: Schweinfurthin A induces OSBP washout, but to a lesser extent than OSW-1. Continual 500 nM Schweinfurthin A (SchwA (C), n=1) causes a slight drop of OSBP levels in HEK293. 6-hour treatment of 500 nM SchwA followed by washout leads to a significant drop of OSBP levels in HEK293 at 0-hour and 24-hour recovery (SchwA (0R) and SchwA (24R), n=3).